



School of Chemical Sciences  
Dublin City University  
Glasnevin, Dublin 9.

**Development of Chiral and Achiral Supercritical Fluid  
Chromatographic methods for the characterisation of ophthalmic  
drug substances and drug products.**

**Adrian Michael Marley, B.Sc.**

Under the supervision of:

Dr. Damian Connolly, Pharmaceutical and Molecular Biotechnology Research Centre  
(PMBRC), Department of Science, Waterford Institute of Technology.

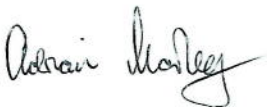
Prof. Apryll M. Stalcup, Irish Separation Science Cluster (ISSC), National Centre for  
Sensor Research, Dublin City University, Glasnevin, Dublin 9, Ireland.

A thesis submitted to Dublin City University for consideration for the degree of:  
Master of Science.

September 2016

**Declaration**

I hereby certify that this material, which I now submit for assessment on the programme of study leading the award of *Master of Science* is entirely my own work, that I have exercised reasonable care to ensure that the work is original, and does not to the best of my knowledge breach any law of copyright, and has not been taken from the work of others save and to the extent that such work has been cited and acknowledged within the text of my work.

Signed:  Student No: 10118489 Date: 08 / Sept / 2016

## Table of Contents

<b>List of Publications</b> .....	7
<b>List of Tables</b> .....	9
<b>List of Figures</b> .....	10
<b>Acknowledgments</b> .....	13
<b>Abstract</b> .....	14
<b>1.0 Chapter 1: Introduction to Supercritical Fluid Chromatography</b> .....	15
1.1 What is Supercritical Fluid Chromatography (SFC)? .....	15
1.2 Supercritical Fluids (SFs) .....	15
1.3 Properties of SFs.....	18
1.4 Historical development of SFC .....	20
1.5 pSFC Applications.....	24
1.6 pSFC Instrumentation.....	24
1.6.1 Gas supply .....	24
1.6.2 Pumps .....	25
1.6.2.1 Compressible fluid pump.....	25
1.6.3 Mobile Phases used in pSFC .....	28
1.6.4 pSFC Injector.....	29
1.6.5 pSFC Columns and Stationary Phases.....	30
1.6.6 Column oven.....	31
1.6.7 Detectors .....	32
1.6.8 Backpressure Regulator (BPR).....	33
1.7 SFC versus LC.....	35
1.8 Green Chromatography .....	36
1.9 Project outline.....	38

<b>2.0 Chapter 2: Determination of (R)-timolol in (S)-timolol maleate active pharmaceutical ingredient: Validation of a new pSFC method with an established NP-HPLC method.</b> .....	40
2.1 Introduction .....	40
2.1.1 Properties of Timolol Maleate .....	40
2.1.2 Analysis of Timolol Maleate by HPLC .....	41
2.1.3 Analysis of Timolol Maleate by Capillary Electrophoresis (CE).....	46
2.1.4 Chiral analysis by SFC .....	50
2.2 Experimental.....	53
2.2.1 Instrumentation and Software.....	53
2.2.2 Materials and Reagents.....	54
2.2.3 Solution preparation for Timolol NP-HPLC analysis .....	54
2.2.4 Solution preparation for Timolol pSFC analysis .....	55
2.2.5 Solution preparation for evaluation of Timolol pSFC Specificity .....	55
2.3 Results and discussion .....	55
2.3.1 Timolol pSFC Method Development .....	55
2.3.2 Timolol pSFC Method Validation.....	62
2.3.2.1 Validation of Timolol pSFC Method as a Limit Test – Specificity and LOD ...	62
2.3.2.2 Investigation of Timolol pSFC Method as a potential Quantitative Impurities Assay .....	63
2.3.2.3 Timolol pSFC Precision studies: Repeatability and Intermediate Precision .....	63
2.3.2.4 Timolol pSFC Robustness .....	64
2.3.2.5 Timolol pSFC Accuracy .....	65
2.3.3 Analytical Performance Comparison: pSFC versus NP-HPLC .....	66
2.4 Conclusion .....	70
<b>3.0 Chapter 3: Development and Validation of a new stability indicating Reversed Phase liquid chromatographic method for the determination of Prednisolone acetate and impurities in an ophthalmic suspension.</b> .....	71

3.1	Introduction .....	71
3.2	Experimental.....	74
3.2.1	Instrumentation and Software.....	74
3.2.2	Materials and Reagents.....	74
3.2.3	Solution preparation for PAC RP-HPLC analysis.....	75
3.3	Results and discussion .....	77
3.3.1	PAC RP-HPLC Method Development.....	77
3.3.2	PAC RP-HPLC Method Validation.....	80
3.3.2.1	PAC RP-HPLC Accuracy/Linearity studies.....	80
3.3.2.2	PAC RP-HPLC Precision .....	84
3.3.2.3	PAC RP-HPLC Specificity and Solution Stability.....	85
3.3.2.4	PAC RP-HPLC Method Detection Limits and Acceptance Criteria.....	86
3.3.2.5	PAC RP-HPLC Robustness.....	87
3.4	Conclusion.....	92
<b>4.0</b>	<b>Chapter 4: Development of an orthogonal method for the determination of Prednisolone acetate and impurities in an ophthalmic suspension using supercritical fluid chromatography: Validation based on the Total Error Approach with Accuracy Profiles. ....</b>	<b>93</b>
4.1	Introduction .....	93
4.1.1	Analysis of Steroids by SFC.....	93
4.1.2	Method Validation using the Total Error Approach.....	97
4.2	Experimental.....	113
4.2.1	Instrumentation and Software.....	113
4.2.2	Materials and Reagents.....	114
4.2.3	Solution preparation for PAC pSFC analysis .....	114
4.2.3.1	pSFC PAC Matrix Placebo solution preparation.....	114
4.2.3.2	pSFC PAC Column Screening Study Standard Preparation .....	114
4.2.3.3	pSFC PAC Calibration and Validation Standard Preparations .....	114

4.2.3.4	pSFC PAC Impurity Calibration and Validation Standard Preparations .....	115
4.2.3.5	pSFC PAC Real Sample Preparation.....	115
4.3	Results and discussion .....	115
4.3.1	PAC pSFC Method Development .....	115
4.3.2	Method Transfer onto an Ultra Performance SFC (UPSFC) system.....	124
4.3.3	PAC Method Development on UPSFC system .....	130
4.3.4	PAC UPSFC Robustness .....	134
4.3.5	PAC UPSFC Method Validation.....	138
4.3.5.1	PAC UPSFC Specificity/Stability Indication and Solution Stability .....	139
4.3.5.2	PAC UPSFC Trueness and Precision .....	141
4.3.5.3	PAC UPSFC Accuracy .....	141
4.3.5.4	PAC UPSFC Impurity Accuracy and LOQ/LOD limits .....	142
4.3.5.5	PAC UPSFC Linearity.....	144
4.3.6	Selection of Appropriate Response Function for PAC UPSFC Quantitative Analysis .....	145
4.3.7	Analytical Performance Comparison; UPSFC versus RP-HPLC.....	146
4.4	Conclusion .....	149
<b>5.0</b>	<b>Conclusions and future work.....</b>	<b>150</b>
<b>6.0</b>	<b>References .....</b>	<b>152</b>

## List of Publications

- A. Marley, D. Connolly, Determination of (R)-timolol in (S)-timolol maleate active pharmaceutical ingredient: Validation of a new supercritical fluid chromatography method with an established normal phase liquid chromatography method, *Journal of Chromatography A*, Volume 1325, 17 January 2014, Pages 213-220. (Chapter 2)

Journal of Chromatography A, 1325 (2014) 213–220



Contents lists available at ScienceDirect

Journal of Chromatography A

journal homepage: [www.elsevier.com/locate/chroma](http://www.elsevier.com/locate/chroma)



## Determination of (R)-timolol in (S)-timolol maleate active pharmaceutical ingredient: Validation of a new supercritical fluid chromatography method with an established normal phase liquid chromatography method



Adrian Marley<sup>a,b</sup>, Damian Connolly<sup>c,\*</sup>

<sup>a</sup>Allergan Pharmaceuticals, Westport, Mayo, Ireland

<sup>b</sup>Irish Separation Science Cluster (ISSC), National Centre for Sensor Research, Dublin City University, Glasnevin, Dublin 9, Ireland

<sup>c</sup>Pharmaceutical and Molecular Biotechnology Research Centre (PMBRC), Department of Chemical and Life Sciences, Waterford Institute of Technology, Waterford, Ireland

### ARTICLE INFO

#### Article history:

Received 26 July 2013

Received in revised form 27 October 2013

Accepted 4 December 2013

Available online 14 December 2013

#### Keywords:

Supercritical fluid chromatography

Drug substance

R-timolol impurity limit test

Method validation

Timolol maleate

### ABSTRACT

An enantioselective supercritical fluid chromatography (SFC) method was developed and validated to meet the current European Pharmacopoeia requirements of a limit test for the determination of S-timolol maleate enantiomeric purity in timolol maleate drug substance. The developed method is presented as an alternative to the current normal phase high performance liquid chromatography (NP-HPLC) method described in the European Pharmacopoeia (Timolol Maleate Monograph). Using a 4.6 mm × 250 mm Chiralcel OD-H ( $d_p$ : 5  $\mu$ m) column and a mobile phase of (93:7) CO<sub>2</sub>/0.1% (v/v) TEA in MeOH delivered at 4.0 mL min<sup>-1</sup> resolution of 2.0 was achieved within 5 min, representing a 3-fold reduction in run-time and an 11-fold reduction in solvent consumption relative to the NP-HPLC method. Method robustness was examined by the variation of flow rate ( $\pm 0.5$  mL min<sup>-1</sup>), column temperature ( $\pm 5$  °C) and column back-pressure ( $\pm 10$  bar) and resolution was maintained at  $\geq 1.9$  in all cases. R-timolol was resolved from all potential impurities and the limit of detection was improved by increasing the sample concentration threefold compared to the NP-HPLC method such that the method could detect the R-timolol enantiomer at 0.5% (w/w) with respect to S-timolol maleate. Additional validation parameters demonstrated that the potential of the method to be used for routine release testing of timolol maleate raw material for drug product manufacturing in which the quantitation of R-timolol impurity in S-timolol maleate drug substance would be a requirement.

© 2013 Elsevier B.V. All rights reserved.

### 1. Introduction

The chromatographic separation of enantiomers presents significant challenges in analytical chemistry. Since amino acids and carbohydrates contain chiral centres, chirality is a fundamental characteristic of all living organisms. All essential physiological processes display enantioselectivity, where one enantiomer interacts more strongly with a certain target site than the other due to differences in its spatial configuration [1]. While it is well known that substantial pharmacological differences exist between enantiomeric pharmaceuticals, it was not until after the thalidomide disaster in the 1960s that research activity increased in the field

of chirality. Today the United States Food and Drug Administration (USFDA) requires enantiomeric studies to be performed on all new racemic drugs as described below [2] as do the European and Japanese regulatory authorities. These guidelines include the development of enantioselective identification and quantification methods for each active pharmaceutical ingredient with chiral properties. In addition pharmacokinetic and toxicological assays should be executed using both pure enantiomers and with the racemate. Furthermore, there is accumulating evidence demonstrating the medicinal advantage of using pure enantiomers over racemates as active drug substances. As a result, numerous methods have recently been adopted to replace existing racemates with single enantiomeric drugs [3].

Beta adrenergic receptor blocking agents, commonly called  $\beta$ -blockers [4,5], are a group of drugs used to treat high blood pressure, heart failure and myocardial ischaemia diseases [6]. Most  $\beta$ -blockers are available as racemates with

\* Corresponding author. Tel.: +353 51 845509.

E-mail addresses: [marley\\_adrian@allergan.com](mailto:marley_adrian@allergan.com) (A. Marley), [dconnolly@wit.ie](mailto:dconnolly@wit.ie) (D. Connolly).

- A. Marley, A.M. Stalcup, D. Connolly, Development and validation of a new stability indicating reversed phase liquid chromatographic method for the determination of prednisolone acetate and impurities in an ophthalmic suspension, *Journal of Pharmaceutical and Biomedical Analysis*, Volume 102, 5 January 2015, Pages 261-266. (Chapter 3)



## Development and validation of a new stability indicating reversed phase liquid chromatographic method for the determination of prednisolone acetate and impurities in an ophthalmic suspension



Adrian Marley<sup>a,b</sup>, Apyrll M. Stalcup<sup>b</sup>, Damian Connolly<sup>c,\*</sup>

<sup>a</sup> Allergan Pharmaceuticals, Westport, Mayo, Ireland

<sup>b</sup> Irish Separation Science Cluster (ISSC), National Centre for Sensor Research, Dublin City University, Glasnevin, Dublin 9, Ireland

<sup>c</sup> Pharmaceutical and Molecular Biotechnology Research Centre (PMBRC), Department of Chemical and Life Sciences, Waterford Institute of Technology, Waterford, Ireland

### ARTICLE INFO

#### Article history:

Received 28 June 2014

Received in revised form 9 September 2014

Accepted 16 September 2014

Available online 28 September 2014

#### Keywords:

Prednisolone acetate

Ophthalmic suspension

Reversed-phase high performance liquid chromatography

Impurity analysis

Core-shell particles

### ABSTRACT

A new stability indicating reversed phase high performance liquid chromatography (RP-HPLC) method was developed and validated under current International Conference of Harmonisation (ICH) guidance for the determination of prednisolone acetate (PAC) and impurities in an ophthalmic suspension. The developed method is presented as an alternative to a modified version of the current RP-HPLC method described in the USP monograph for the assay of PAC in an ophthalmic suspension. Along with the assay of PAC, the new method is also capable of identifying and quantifying eight selected PAC impurities and degradation products in an ophthalmic suspension. Using an Agilent Poroshell 120 EC-C18 100 mm × 4.6 mm ( $d_p$ : 2.7  $\mu$ m) column set to 60 °C with step gradient elution generated using mobile phase A: acetonitrile/water (10:90) (v/v) and mobile phase B: acetonitrile delivered at 1.2 mL min<sup>-1</sup>, all peaks of interest are eluted in 33 min with resolution of 1.5 between the critical pairs. The developed method was validated for PAC and impurities to ICH recommendations for accuracy, linearity, precision (repeatability), limit of detection, limit of quantitation, robustness and specificity.

© 2014 Elsevier B.V. All rights reserved.

### 1. Introduction

It is a technical requirement of the International Conference on Harmonization (ICH) for registration of pharmaceuticals for human use [1] that impurities present in an active pharmaceutical ingredient (API) as well as the final drug product be quantified and/or identified. Impurities may be derived from the API and/or final drug product manufacturing process or may be generated over time due to poor stability of either the API or drug product. Many process-related impurities have similar chemical structures as the API or can often co-elute with components of the drug product sample matrix, such that method specificity is a key analytical performance criterion for any chromatographic method used for drug product release testing or stability indicating assays.

Prednisolone acetate (PAC) is a synthetic glucocorticoid steroid which is used as the API either alone or in combination with an

additional API in several commercial ophthalmic suspensions used for the treatment of a wide range of inflammatory conditions of the eye. PAC is produced by the esterification of prednisolone and is defined as a pro-drug with modified pharmacokinetic properties compared to prednisolone [2,3]. The usefulness of pro-drugs in ophthalmic drug delivery has been comprehensively discussed in a number of reviews [4,5]. Acetate ester pro-drugs such as PAC have been designed to increase the lipophilicity and the corneal absorption of the parent steroid [6–9]. Enzymatic transformation of pro-drugs in ocular tissues is often utilised for releasing the active drug. In fact, PAC hydrolyses completely to prednisolone in vitro and in vivo, and the enzymatic conversion is assumed to occur in the cornea [10,11]. Although ester pro-drugs are usually more stable in vitro than in vivo, they may exhibit chemical instability in aqueous eye-drop formulations [12]. Since PAC is vulnerable to enzymatic and chemical hydrolysis [13] it is important to monitor the concentration of PAC and related substances in such suspensions over time. Fig. 1 shows the molecular structure of PAC along with its eight known impurities (and potential degradants).

There have been numerous publications reporting on the chromatographic determination of either prednisolone or PAC in tissue

\* Corresponding author. Tel.: +353 51 845509.  
E-mail addresses: [marley\\_adrian@allergan.com](mailto:marley_adrian@allergan.com) (A. Marley),  
[dconnolly@wit.ie](mailto:dconnolly@wit.ie) (D. Connolly).

## List of Tables

<b>Table 1.1:</b>	Comparison of Gases, Supercritical Fluids and Liquids.....	20
<b>Table 1.2:</b>	The twelve principles of green chemistry.....	37
<b>Table 2.1:</b>	Solution preparation for NP-HPLC and pSFC analysis.....	58
<b>Table 2.2:</b>	Analytical performance for determination of R-timolol impurity in S-timolol maleate.....	68
<b>Table 2.3:</b>	Comparison between HPLC and pSFC analytical conditions and performance.....	69
<b>Table 3.1:</b>	Solution preparation for validation of RP-HPLC method.....	76
<b>Table 3.2:</b>	RP-HPLC PAC method optimisation.....	82
<b>Table 3.3:</b>	Analytical performance for determination of PAC and selected impurities in a spiked ophthalmic suspension.....	89
<b>Table 3.4:</b>	Comparison between HPLC analytical conditions and performance.....	92
<b>Table 4.1:</b>	Solution preparation for validation of UPSFC method.....	117
<b>Table 4.2:</b>	Summary of column screening results from the Thar Method Station.....	119
<b>Table 4.3:</b>	Impurity level accuracy and LOQ/LOD limits based on accuracy profiles...	142
<b>Table 4.4:</b>	Comparison between RP-HPLC and UPSFC analytical conditions and performance.....	148

## List of Figures

<b>Figure 1.1:</b> Phase diagram for a pure substance.....	16
<b>Figure 1.2:</b> Demonstration of the formation of supercritical CO <sub>2</sub> .....	18
<b>Figure 1.3:</b> Left: Giddings eluotropic series .....	21
<b>Figure 1.4:</b> Schematic overview of typical pSFC system .....	22
<b>Figure 1.5:</b> Diagram demonstrating the operation of the compressible fluid pump.....	27
<b>Figure 1.6:</b> Relationship between the calculated critical temperature, pressure and concentration of the organic modifier .....	29
<b>Figure 2.1:</b> Molecular structure of S-timolol maleate .....	42
<b>Figure 2.2:</b> Molecular structure of the Chiracel OD chiral stationary phase .....	43
<b>Figure 2.3:</b> HPLC separation of timolol maleate enantiomers.....	44
<b>Figure 2.4:</b> Typical chromatograms of a solution containing S-timolol, R-timolol.....	47
<b>Figure 2.5:</b> Enantio-separation of a reconstituted racemic mixture of timolol maleate.....	48
<b>Figure 2.6:</b> Typical electropherogram of a mixture solution containing the main timolol impurities .....	49
<b>Figure 2.7:</b> Peak sharpening of S-timolol .....	51
<b>Figure 2.8:</b> Separation of R-timolol and S-timolol via pSFC .....	59
<b>Figure 2.9:</b> Plot of retention factor ( <i>k</i> ) of R-timolol (red) and S-timolol (green) along with resolution ( <i>R<sub>s</sub></i> ) between R-timolol and S-timolol (purple).....	60
<b>Figure 2.10:</b> Comparison of optimised pSFC separation (a) and normal phase separation (b) of timolol enantiomers .....	61
<b>Figure 2.11:</b> Chromatograms of (a), pSFC sample containing R-timolol at the LOD .....	63
<b>Figure 2.12:</b> Chromatograms of (a) EP timolol for system suitability CRS .....	64
<b>Figure 2.13:</b> Typical chromatograms of the CRM containing R-timolol and S-timolol .....	65
<b>Figure 2.14:</b> Typical chromatograms comparing pSFC (a,b) and NP-HPLC (c,d) .....	67
<b>Figure 3.1:</b> Molecular structure of prednisolone acetate (PAC) and impurities.....	72
<b>Figure 3.2:</b> (a): Separation of eight selected PAC impurities.....	78
<b>Figure 3.3:</b> Representative chromatograms of development injections .....	81
<b>Figure 3.4:</b> Chromatogram of PAC impurity standard mixture containing the eight selected PAC impurities.....	85
<b>Figure 3.5:</b> Top: (a) Chromatogram of 0.20 mg.mL <sup>-1</sup> PAC spiked with eight selected PAC impurities .....	87

<b>Figure 3.6:</b> Overlaid chromatograms of 0.20 mg.mL <sup>-1</sup> PAC spiked with eight selected PAC impurities. ....	88
<b>Figure 4.1:</b> Lifecycle of an analytical method.....	98
<b>Figure 4.2:</b> Example of an accuracy profile .....	99
<b>Figure 4.3:</b> Accuracy profile obtained for the validation of the quantification amoxicilline in pharmaceutical formulation.....	112
<b>Figure 4.4:</b> Representative chromatograms of development injections conducted on the Thar method station.....	121
<b>Figure 4.5:</b> (a) Overlaid chromatograms of PAC standard at 200 mg.L <sup>-1</sup> and impurity stock standards at 40 mg.L <sup>-1</sup> ). ....	122
<b>Figure 4.6:</b> Overlaid chromatograms (expanded view to show baseline detail) of spiked sample containing PAC at 600 mg.L <sup>-1</sup> and impurities 3 mg.L <sup>-1</sup> .....	123
<b>Figure 4.7:</b> Expanded chromatogram of spiked sample containing PAC at 600 mg.L <sup>-1</sup> and impurities 12 mg.L <sup>-1</sup> conducted on the Waters UPC2 system.....	125
<b>Figure 4.8:</b> Expanded chromatogram of spiked sample under the geometric transfer conditions.....	127
<b>Figure 4.9:</b> Expanded chromatogram of spiked sample under the geometric transfer conditions described in Figure 4.7 with the following exceptions; Back-pressure regulation: 220 bar.....	127
<b>Figure 4.10:</b> Expanded chromatogram of spiked sample under the geometric transfer conditions described in Figure 4.7 with the following exceptions; Column temperature: 45 °C. ....	128
<b>Figure 4.11:</b> Expanded chromatogram of spiked sample under the geometric transfer conditions described in Figure 4.7 with the following exceptions; Column temperature: 55 °C.....	129
<b>Figure 4.12:</b> Expanded chromatogram of spiked sample under conditions described in Figure 4.7 with the following exceptions Mobile phase: 10 to 20 % MeOH over 15 min. ...	130
<b>Figure 4.13:</b> Expanded overlaid chromatograms of spiked sample containing PAC at 600 mg.L <sup>-1</sup> and impurities 6 mg.L <sup>-1</sup> (black) .....	132
<b>Figure 4.14:</b> Chromatogram of spiked sample containing PAC at 600 mg.L <sup>-1</sup> and impurities 6 mg.L <sup>-1</sup> . Chromatographic conditions; Column: DEA.....	133
<b>Figure 4.15:</b> Expanded overlaid chromatograms of spiked sample containing PAC at 600 mg.L <sup>-1</sup> and impurities 6 mg.L <sup>-1</sup> .....	134

<b>Figure 4.16:</b> <i>Plot of retention time (Rt) and resolution (Rs) versus column temperature. Chromatographic conditions as per Figure 4.14 with temperatures of 40, 45, 50, 55 and 60 °C.</i> .....	136
<b>Figure 4.17:</b> <i>Plot of retention time (Rt) and resolution (Rs) versus back pressure (bar). Chromatographic conditions as per Figure 4.14 with back pressures of 110, 120, 138, 150 and 160 bar.</i> .....	137
<b>Figure 4.18:</b> <i>Plot of retention time (Rt) and resolution (Rs) versus flow rate (mL.min<sup>-1</sup>). Chromatographic conditions as per Figure 4.14 with flow rates of 2.3, 2.4, 2.5, 2.6 and 2.7 mL.min<sup>-1</sup>.</i> .....	138
<b>Figure 4.19:</b> <i>Overlaid chromatograms of MeOH blank (blue), placebo blank (red), PAC standard at 600 mg.L<sup>-1</sup> (green) and spiked sample</i> .....	140
<b>Figure 4.20:</b> <i>Plots of relative bias (%) and repeatability RSD (%) for PAC and impurity results generated using the L and Lo response functions</i> .....	143
<b>Figure 4.21:</b> <i>Overlaid chromatograms of MeOH blank (blue), placebo blank (red) and spiked placebo containing PAC and impurities at 0.3 mg.L<sup>-1</sup>(black)</i> .....	144
<b>Figure 4.22:</b> <i>(a) Chromatogram of spiked sample containing PAC at 200 mg.L<sup>-1</sup> and impurities 1.2 mg.L<sup>-1</sup> under RP-HPLC conditions</i> .....	147
<b>Figure 4.23:</b> <i>Comparison of relative retention times (vs matrix peak) in UPSFC method and in RP-HPLC method.</i> .....	148

## **Acknowledgments**

I would like to take this opportunity to thank Professor Apryll Stalcup (DCU/ISSC), Dr. Damian Connolly (WIT) and Dr. Aoife Hennessy (WIT) for their guidance and advice over the duration of this Masters project. I would also like to thank the management of Allergan Pharmaceuticals Westport for giving me the opportunity to undertake this Masters project and for their continuous support and financial sponsorship throughout. Many thanks also go to the technical staff of the School of Chemical Sciences in DCU, particularly to Stephen Fuller for his invaluable assistance. To the members of the Waters Corporation who assisted in this project by securing the loan of instrumentation which enabled the completion of the work detailed in Chapter 4. Without their willingness to assist in this project, the completion of this work would not have been possible. Finally, I would like to thank my work colleagues, friends and most of all, my family, for their constant support and encouragement throughout this journey.

## **Abstract**

### **Development of Chiral and Achiral Supercritical Fluid Chromatographic methods for the characterisation of ophthalmic drug substances and drug products.**

**Adrian Michael Marley, B.Sc.**

With the global drive for faster, more environmentally friendly separation techniques, the aim of this research was to demonstrate the potential of Supercritical Fluid Chromatography (SFC) as a viable alternative or complementary technique to High Performance Liquid Chromatography (HPLC) in the highly regulated world of the Quality Control (QC) laboratory. SFC methods capable of meeting QC method performance expectations in accordance with current guidance were therefore developed and validated under current International Conference of Harmonisation (ICH) guidance.

Firstly, an enantioselective pSFC method was developed and validated to meet the current European Pharmacopoeia requirements of a limit test for the determination of S-timolol maleate enantiomeric purity in timolol maleate drug substance. The newly developed pSFC method achieved a resolution of 2.0 within 5 min, representing a 3-fold reduction in run-time and an 11-fold reduction in solvent consumption relative to the normal phase HPLC method described in the European Pharmacopoeia.

Secondly, a stability-indicating Reversed Phase (RP-HPLC) method was developed and validated for the determination of prednisolone acetate (PAC) and eight selected PAC impurities and degradation products in an ophthalmic suspension using a superficially porous “*core-shell*” stationary phase. Using an Agilent Poroshell column with step gradient elution, all peaks of interest were eluted in 33 min with resolution of 1.5 between the critical pairs. With core-shell stationary phases being considered the most efficient technology currently available for packed column HPLC applications, this RP-HPLC method was developed to enable a direct comparison to be made between RP-HPLC and SFC in terms of orthogonality, efficiency, selectivity, sensitivity and reproducibility.

Finally, an orthogonal achiral pSFC method was developed and validated for the same PAC sample described above. For the pSFC method, validation was carried out using the total error approach to generate accuracy profiles for two regression models, based on  $\beta$ -expectation tolerance intervals. Successful completion of the method validation demonstrated that the new pSFC method was a viable complementary or alternative to the previously developed RP-HPLC method for use in the highly regulated QC laboratory environment.

## **1.0 Chapter 1: Introduction to Supercritical Fluid Chromatography**

### **1.1 What is Supercritical Fluid Chromatography (SFC)?**

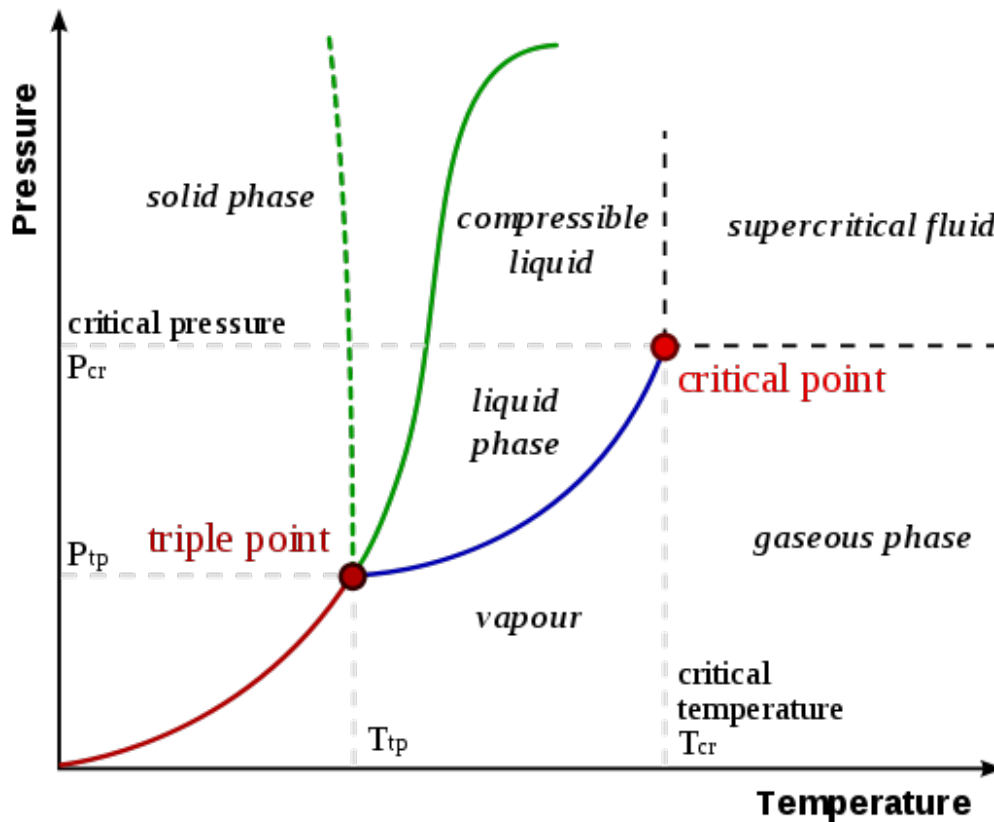
Supercritical fluid chromatography (SFC) has been described by Berger as a chromatographic technique with properties that place it somewhere between liquid chromatography (LC) and gas chromatography (GC) [1]. As with LC and GC, separation of solutes is achieved in SFC through physicochemical interactions of solute molecules with a stationary phase and a mobile phase. In SFC, the mobile phase primarily consists of a highly compressible dense fluid which is often in the supercritical state. However, for many applications involving binary or tertiary mobile phases, the mobile phase is not maintained in the supercritical state but rather at “*near-critical*” or so called “*subcritical*” states. Over the course of its development as a separations technique, this fact has led to some confusion over the correct naming of this technique, with alternative names such as “*dense gas chromatography*” and in more recent times “*convergence chromatography*” being proposed. However, to date, SFC remains the popular description regardless of the defined state of the mobile phase. Probably the most practical description of the mobile phase used in SFC would be as a dense compressed fluid which due to the lack of intermolecular forces, will dramatically expand if the external pressure is removed [1].

### **1.2 Supercritical Fluids (SFs)**

Before one begins any discussion of SFC, it is important to gain some appreciation of the properties of supercritical fluids (SFs). To put SFs in context one must first consider the three possible states of matter; i.e. solids, liquids and gases. Pressure and temperature are the parameters that determine the thermodynamically distinct phase in which matter will exist. Transitioning from one phase to another is known as phase transition and can take place when the conditions of pressure and temperature are altered so that the conditions favour the existence of a particular phase, e.g. when a solid is heated it may become a liquid or when a gas is compressed it may become a liquid.

Phase diagrams are a type of two-dimensional graph used to show the conditions in which thermodynamically distinct phases can occur and can be used to demonstrate supercritical conditions for a given substance. In Figure 1.1, the x-axis of the phase diagram corresponds to temperature, while the y-axis corresponds to pressure. The phase diagram

shows, in pressure-temperature space, the lines of equilibrium, known as phase boundaries between the three phases of matter for a given substance [1].



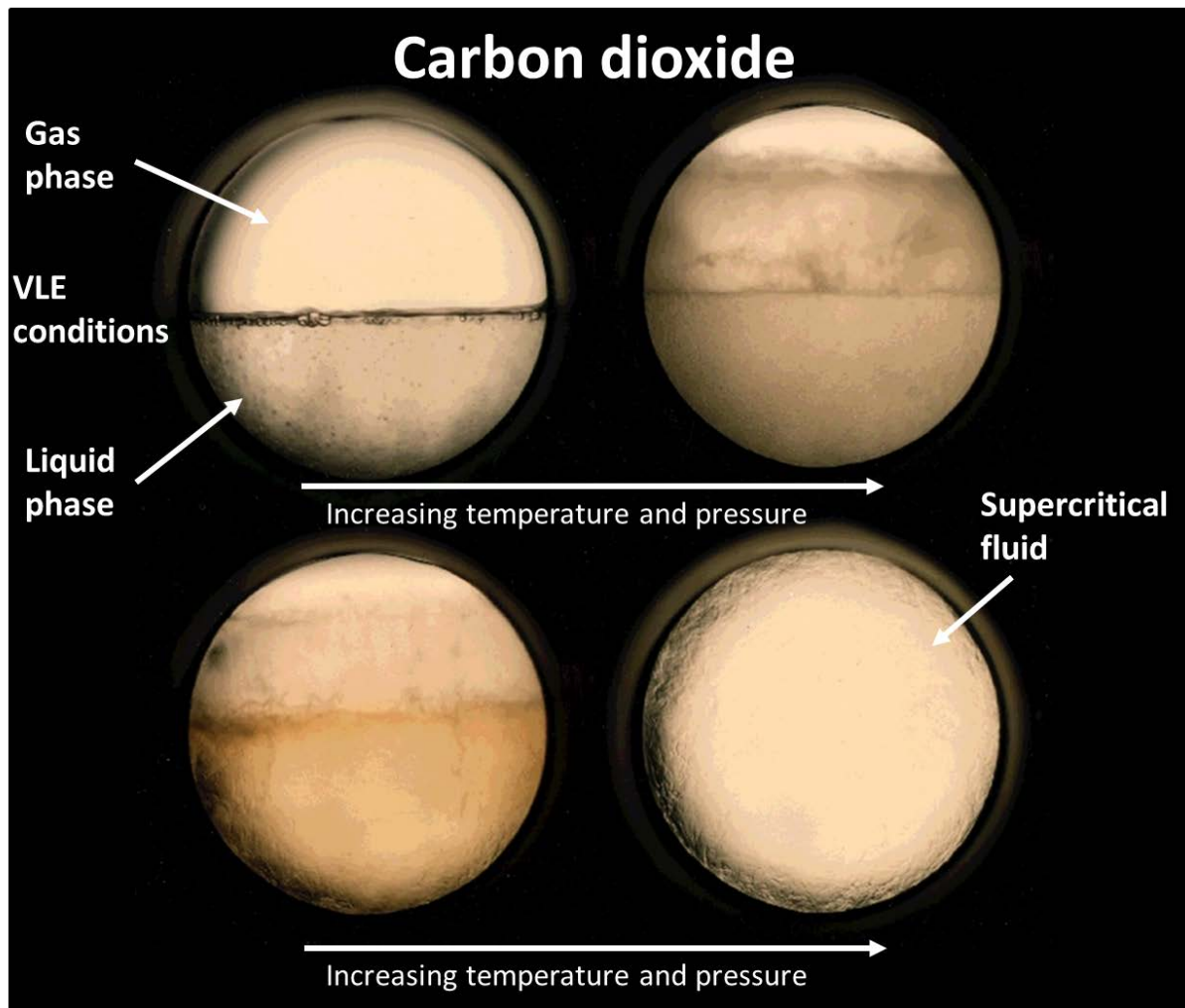
**Figure 1.1:** Phase diagram for a pure substance. Reproduced from [2].

Figure 1.1 illustrates a typical phase diagram for a pure substance. The red line emerging from the lower left-hand corner separates the solid phase from the gaseous phase. Crossing this line from left to right represents sublimation of the solid to the gas [3]. The “triple point” is the point in the diagram where all three phases; i.e. solid, liquid and gas, exist in equilibrium. The solid green vertical line emerging from the triple point separates the solid phase from the liquid phase. The line itself represents a phase boundary and defines the conditions where equilibrium exists between solid and liquid. The blue line that continues diagonally from the triple point towards the upper right of the diagram separates the liquid phase from the gaseous phase. Above and to the left of the line only liquid exists, while below and to the right, only gas exists. As is the case for the solid/liquid boundary, this line represents the phase boundary between the liquid and gaseous phases. Directly on the liquid/gas boundary, both liquid and gases exists in equilibrium. This line is sometimes called

the boiling line or the vapour-liquid equilibrium line (VLE) [1]. This VLE line continues to a point on the diagram known as the “*critical point*”.

The idea of a critical point was developed by Andrews in 1896 [3]. It was proposed that for all substances, there is a temperature above which it can no longer exist as a liquid, no matter how much pressure is applied. This temperature is called the critical temperature ( $T_c$ ) of the substance. Likewise, there is a pressure above which the substance can no longer exist as a gas no matter how high the temperature is increased. This pressure value is called the critical pressure ( $P_c$ ) of the substance. Therefore, the critical point can be described as the point where both the  $T_c$  and the  $P_c$  of the substance in question are reached. Thus,  $T_c$  and  $P_c$  are the defining boundaries on a phase diagram for the critical point for a pure substance. Above both  $T_c$  and  $P_c$ , no increase in temperature or pressure can cause two phases to form and the substance is said to exist in the supercritical state or as a SF. However, below either  $T_c$  or  $P_c$  or both, the substance is said to be in a subcritical state.

The most important point to note with respect to phase diagrams is that while moving from one phase to another; i.e. crossing a phase boundary represents a phase transition, moving from so called subcritical conditions to supercritical conditions, does not constitute a phase transition. The dashed lines emerging horizontally and vertically from the critical point in the phase diagram shown in Figure 1.1 are only included for illustrative purposes to highlight the supercritical region. Some would argue that these lines should not be included as there is no phase transition between a liquid and a SF or between a gas and a SF and the inclusion of such lines only results in confusion [1]. SFs are not a separate state of matter and should never be considered as such as they do not possess any unique physical characteristics that would deem them to be a distinct phase [1]. Therefore, being supercritical is about being in a defined state; i.e. defining the conditions of pressure and temperature in which a substance finds itself, rather than being a distinct phase. It should be emphasised that for a substance to be truly in the supercritical state, it must be maintained in conditions above both its  $P_c$  and  $T_c$ . Thus, for SFs with the word “super” only intended to indicate “above”. Figure 1.2 demonstrates the formation of supercritical  $\text{CO}_2$  where the conditions of pressure and temperature are increased to a point where the substance becomes supercritical. Note that below the critical point, two phases can exist in equilibrium; i.e. on the VLE line of a phase diagram.



**Figure 1.2:** *Demonstration of the formation of supercritical CO<sub>2</sub> by increasing temperature and pressure to reach the critical point. Modified from [4].*

### 1.3 Properties of SFs

All molecules can be described as having both kinetic and potential energies. The kinetic energy is related to the motion of the molecules, while the potential energy relates to the attractive forces between the molecules [5]. For liquids, the molecules condense to form the liquid because the interactions between the molecules are more intense than the thermal energy of the system; i.e. the force of attraction between the molecules prevents them from expanding into a gas. Increasing the temperature of a liquid can increase the kinetic or thermal energy between the molecules enough to disrupt these forces which allow the molecules to separate from each other; i.e. expand to become a gas.

SFs lack the adequate intermolecular interactions to allow them to condense into liquids [1] and are maintained in the fluid state due to the presence of an external pressure source. With SFs, this pressure can be increased, forcing the molecules as close together as the molecules in a condensed liquid; thus increasing the density of the fluid. This enforced molecular closeness results in high collision frequency between molecules which makes the fluids reasonable solvents for many solutes [1]. This property of SFs was first demonstrated by Hannay and Hogarth in 1879 when they successfully dissolved inorganic salts in supercritical ethanol and re-precipitated them by decreasing the temperature [3]. This ability of SFs to solvate solute molecules is the key to SFs being used in chromatographic separations.

Altering the amount of pressure applied to the fluid has the effect of changing the density of the fluid and hence its ability to dissolve solutes by making the fluid either more gas like or more liquid like. Temperature also has an effect on the density of the SF. Increasing temperature at a constant pressure has the effect of reducing the density of the SF and hence the solvent strength of the SF. These properties of SFs enables the solvent strength of the fluid to be manipulated by altering physical parameters; i.e. temperature and pressure which, as will be discussed later, can be exploited to fine tune chromatographic separations involving the use of SFs as the mobile phase.

It should be noted that the forcing together of molecules in SFs results in more extensive molecular interactions, but does not force more intense molecular interactions [1]. Having low inherent intermolecular interactions, SFs have lower viscosities and higher diffusivity of solutes in the fluids compared to normal liquids. The intermolecular forces that cause liquid molecules to “stick” together give rise to surface tension, higher viscosity, and slower diffusion for normal liquids compared to supercritical fluids. Such properties can hinder the solvation because the molecules do not mix or diffuse well. In the case of SFs, when above a solvent’s  $T_c$ , the kinetic energy overcomes the potential energy effect and the molecules no longer “stick” together. As a consequence, surface tension and viscosity are lower, and diffusion rates increase for supercritical fluids compared to normal liquids [5]. Thus, SFs have properties that lie between those of gases and liquids. Table 1.1 compares the properties of gases, SFs and liquids in terms of density, viscosity and diffusivity.

**Table 1.1:** Comparison of Gases, Supercritical Fluids and Liquids. Reproduced from [6].

	Density (kg/m <sup>3</sup> )	Viscosity (μPa·s)	Diffusivity (mm <sup>2</sup> /s)
<b>Gases</b>	1	10	1–10
<b>Supercritical Fluids</b>	100–1000	50–100	0.01–0.1
<b>Liquids</b>	1000	500–1000	0.001

#### 1.4 Historical development of SFC

A number of articles have been published charting the development and theory of SFC from its beginnings up to the present day [3,7-9]. Klesper *et al.* are credited with discovering SFC in 1962 when they described the separation of thermo-labile porphyrin derivatives on a packed column using supercritical chlorofluorocarbon as the mobile phase [10]. From that first reported separation, many separation scientists recognised the potential of SFC and attempted to exploit the properties of SFs as mobile phases to generate faster, more efficient chromatographic separations. Throughout the late 1960's, Calvin Giddings dominated the theoretical development of SFC. His work focused on using pure SFs as mobile phases including various gases such as He, N<sub>2</sub>, CO<sub>2</sub> and NH<sub>3</sub> [8]. However, over the course of time, CO<sub>2</sub> was to become the default choice of fluid for use as SFC mobile phases due to its low critical temperature (31.1 °C) and pressure (74 bar) respectively along with being non-toxic, non-flammable and inexpensive [8]. In 1968, Giddings proposed an eluotropic series in which supercritical CO<sub>2</sub> was placed next to isopropanol in terms of solvent polarity [11]. According to Giddings' series, the polarity of CO<sub>2</sub> could be changed from hydrocarbon-like to alcohol-like simply by altering the density of the fluid; i.e. by adjusting a physical parameter such as pressure. This wide range of polarity would have eliminated the need for binary mobile phases and allowed the separation of solutes with wide ranging polarities using pure SF CO<sub>2</sub> as the mobile phase coupled with density programming. Unfortunately, Giddings eluotropic series turned out not to be correct and it was later shown that the polarity of SF CO<sub>2</sub> was actually closer to that of pentane rather than isopropanol [12]. However, Giddings series was left unchallenged for almost 30 years and greatly influenced the course of SFC development as separation technique during this time.

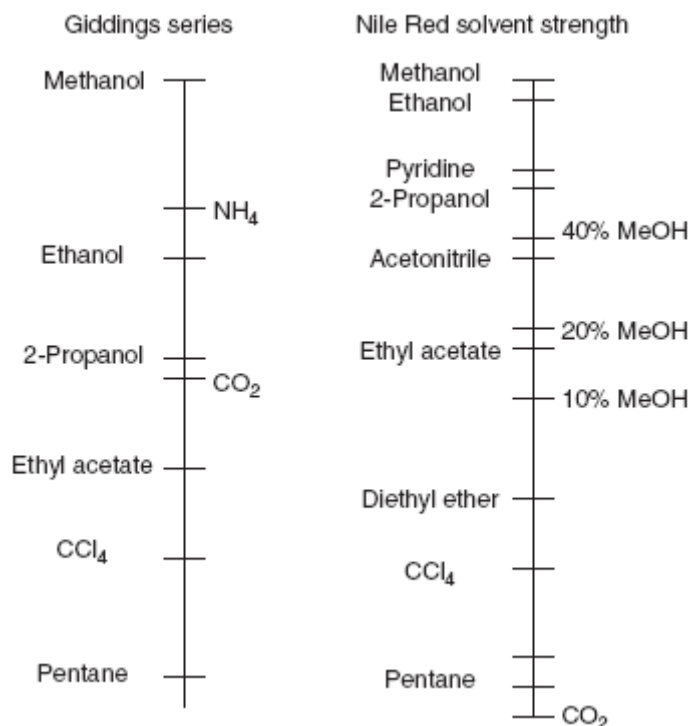


**Figure 1.3:** Left: Giddings eluotropic series [11], based on calculated Hildebrand solubility parameters. Right: Dyes Nile Red energy scale indicating the relative solvent polarity of CO<sub>2</sub> as a pure fluid, or in combination with MeOH [12]. Reproduced from [1].

From the 1960's to the 1980's, SFC development attracted only sporadic interest from the separation scientist community. Reasons for this included that this time period coincided with the tremendous period of development in high performance liquid chromatography (HPLC) technology. Also, the lack of dedicated commercially available SFC systems meant that most SFC applications were being performed on modified HPLC or gas chromatography (GC) instruments. As discussed later in this chapter, these modified systems were not capable of providing reproducible chromatographic separations as at this time, the operators were unaware of many of the fundamental differences between SFC and HPLC and hence failed to modify the systems adequately. Over time, SFC split into two separate entities, namely packed column SFC (pSFC) and capillary column SFC (cSFC). pSFC, as the name suggests, involves the use of packed columns and closely resembles traditional HPLC in terms of instrumentation used (See Figure 1.4). cSFC uses either packed or open tubular columns and closely resembles traditional GC. One of the major differences between pSFC and cSFC is that for cSFC, the use of a fixed restrictor means that it is the pressure generated from the system pump in terms of set flow rate that generates the supercritical state of the

mobile phase. In the case of pSFC, a dynamic back pressure regulator (BPR) is used instead of a fixed restrictor. The BPR can respond to changes in system pressure and maintain the fluid in the supercritical/subcritical state thus removing this function from the system pumps [8]

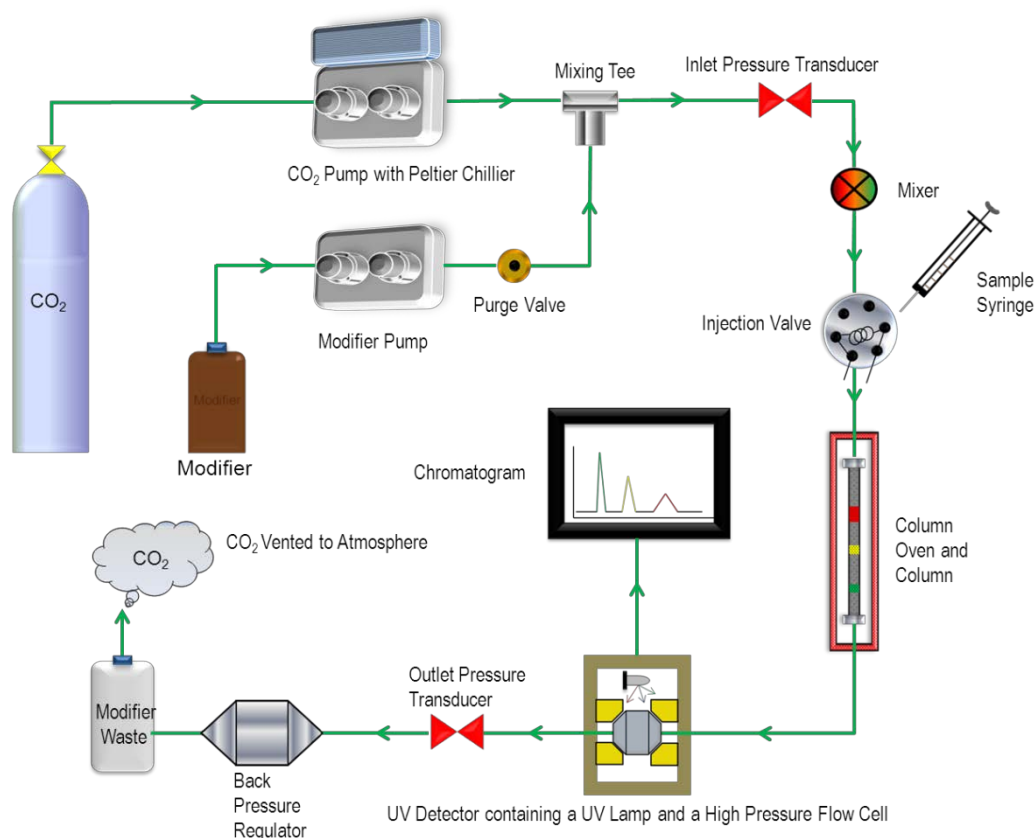


**Figure 1.4:** Schematic overview of typical pSFC system. Modified from [13].

The 1980's saw the focus shift to the use of cSFC with the introduction of the first commercial SFC systems. Open tubular capillary columns were preferred as packed columns using pure CO<sub>2</sub> as the mobile phase were found to be too retentive to allow for solute elution when used without the addition of a modifier. In SFC, a modifier is the term given to a more polar organic solvent which is blended with the SF CO<sub>2</sub> to increase the overall solvent strength and compound solubility of the mobile phase. It was widely believed that the presence of the modifier in the binary mobile phase only served to increase the density of the mixture and did not noticeably change the polarity. If this was the case, then the density of the mobile phase could have been increased by simply increasing the pressure of the system. This would result in increasing the polarity of the mobile phase and eliminating the need for

the modifier thus reducing the need for a second modifier pump. This unchallenged belief, based on Giddings eluotropic series, that the polarity of CO<sub>2</sub> could be altered to that close to isopropanol simply by increasing the pressure of the system led to practitioners persisting with the use of pure fluids in the supercritical state on packed columns. This resulted in a very limited success rate for packed column separations with most applications being confined to very non-polar solutes [3].

Berger and Deye [12] went on to disprove the theory that the function of the modifier in the binary mixture acting solely as a means to increase the density of the mixture. They did this by measuring the density of CO<sub>2</sub>-methanol mixtures and proved that even at a constant density, altering the concentration of the modifier had a major effect on solute retention. They later went on to prove that Giddings eluotropic series was incorrect and that CO<sub>2</sub> was in fact non-polar and more closely related to pentane in terms of solvent polarity. Their findings along with the fact that the addition of modifiers can greatly increase the polarity of binary mixtures led to a renewed interest in the 1990's for pSFC coupled with composition programming rather than pressure programming [3]. Over time, alcohols were found to be the most universal modifiers being able to provide good overall efficiency [14,15] with methanol now being considered the first choice for the elution of polar compounds in pSFC [16].

Due to the type and quality of packed column stationary phases that were available in the late 1980's, many polar solutes still failed to elute, or eluted with poor peak shapes when pSFC was employed with binary mobile phases. This prompted investigation into the use of additives as part of the mobile phase. Berger, Deye and Taylor were among the first to publish work on the role of additives in pSFC [17]. Additives can be described as very polar substances, usually strong acids or bases, which are added to the modifier in small concentrations and can greatly improve peak shape and resolution. The addition of additives shifted the emphasis of pSFC towards the analysis of small drug-like molecules during the 1990's. Additives and modifiers had the effect of changing pSFC from a largely lipophilic technique to a small, polar molecule technique [3]. This new found potential range of application shifted the focus of SFC development towards pSFC applications and signalled the decline in interest for cSFC.

## 1.5 pSFC Applications

One of the first major areas of success for pSFC application was in the separation of chiral compounds. A key factor in this success was the development of a number of highly efficient and versatile chiral stationary phases (CSPs) in the 1980's by Okamoto *et al.* [18,19] which were later commercialised by the Daicel Corporation, Osaka, Japan. The availability of such stationary phases combined with the practical advantages of pSFC over liquid chromatography (LC) in terms of fast method development times, high sample throughput and ease of solute recovery resulted in many successful pSFC chiral applications being reported [20,21]. This success has made pSFC the preferred option for chiral separations at both the analytical and preparative scale.

pSFC has also been successfully employed for both chiral and achiral applications in different fields including; pharmaceutical [22,23], bioanalysis [24,25] and biomolecules [26,27], agrochemicals and environmental applications [28,29], polymer additives [30,31], food science [32,33] and natural products [34,35]. This ever increasing range of application demonstrates that all applications that are relevant to HPLC analysis of small molecules should also be applicable to SFC.

## 1.6 pSFC Instrumentation

Figure 1.4 shows a schematic overview of a typical pSFC system. While the overall picture may closely resemble that of a traditional HPLC system, there are a number of modifications that must be made in order to achieve reproducible chromatography using pSFC. Berger, who has been described by as the father of modern SFC [7], based on his contribution to SFC instrumental design, provided a detailed description of the practical aspects of SFC hardware [1]. Due to the important role instrumentation plays in generating reproducible chromatography in SFC applications, the following sections provide detail on some of the functional requirements of SFC hardware and the challenges that must be overcome compared to conventional HPLC.

### 1.6.1 Gas supply

For most pSFC applications, food grade CO<sub>2</sub> is of sufficient purity to give acceptable chromatographic performance. pSFC systems require that CO<sub>2</sub> be supplied to the pump in liquid form. To achieve this, high pressure gas cylinders are used in which the majority of the CO<sub>2</sub> in the cylinder exists as a liquid with the remaining head space being filled with CO<sub>2</sub>

gas. The liquid CO<sub>2</sub> is supplied to the pSFC pump using a dip-tube feed which takes the liquid CO<sub>2</sub> from the bottom of the cylinder where it is under greatest pressure. The headspace pressure within the cylinder is used to force the liquid CO<sub>2</sub> up through the dip tube and into the pSFC pump. To achieve consistent and reproducible chromatography in pSFC, the relationship between cylinder temperature and cylinder pressure is extremely important. Any fluctuations in temperature between the gas supply and the pump head can have detrimental effects on chromatographic performance [1]. The best option to avoid problems associated with the CO<sub>2</sub> supply to the pSFC system is to have the cylinder as close to the pSFC system as possible. This will ensure that there are no temperature fluctuations during the transport of the CO<sub>2</sub> from the cylinder to the pSFC system, while ensuring that the supply line is short enough to avoid any large pressure differences between the cylinder and the pump heads. For these reasons, it is always best to have the CO<sub>2</sub> cylinder in the same room and as close as possible to the pSFC system.

## **1.6.2 Pumps**

The pumps used in modern pSFC systems are similar to those used in HPLC systems in that they are both positive displacement reciprocating piston pumps which can operate up to 600 bar pressure and flow rates up to 10 mL.min<sup>-1</sup>. As pSFC often requires a modifier to ensure solute elution from the column, pSFC systems contain two separate reciprocating pumps, one to deliver the pressurized CO<sub>2</sub>, which is known as the compressible fluid pump and the other to deliver the liquid modifier, which is known as the modifier pump. The modifier pump used is identical to those used in traditional HPLC systems. However, a number of modifications are required for the compressible fluid pump to ensure a consistent flow rate is maintained.

### **1.6.2.1 Compressible fluid pump**

The compressible fluid pump is probably the most important component of the pSFC system. It must be able to deliver a precise amount of a compressible fluid independently of the column temperature or pressure, to ensure consistent and reproducible chromatography. The first issue this pump has to deal with is that although the CO<sub>2</sub> supplied from the cylinder is defined as a liquid, it will readily expand to form a low density gas if the external pressure source is removed. Therefore, the pump must be capable of maintaining pressure at all times, even during the filling stroke. This is to ensure that the CO<sub>2</sub> doesn't expand and separate into two phases due to the pressure drop when the CO<sub>2</sub> enters the pump cylinder [1].

The first major modification of the compressible fluid pump compared to the modifier pump is the presence of a chilling unit attached to the pump head. Chilling the CO<sub>2</sub> as it enters the pump ensures that it remains in the liquid form and reduces the possibility of phase separation due to an increase in temperature within the pump head. To ensure adequate heat transfer, most modern pSFC systems are fitted with electronically controlled Peltier coolers which are directly attached to the pump head. This type of cooling system allows accurate temperature control of the pump and reduces the risk of phase separation within the pump due to inadequate heat transfer. However, chilling the CO<sub>2</sub> to ensure that it remains in the liquid form as it enters the pump is only part of the solution to providing an accurate flow from the compressible fluid pump. Even in its liquid form, CO<sub>2</sub> remains relatively compressible. Therefore, this compressibility factor must be taken into account by the pump to ensure that the correct flow from the pump is achieved at all times.

On completion of the fill stroke, the pump is filled with the liquid CO<sub>2</sub> at the same pressure as the supply cylinder. It is at this point that compressibility compensation comes into play to ensure accurate and precise CO<sub>2</sub> delivery from the pump. As the pump piston moves forward it will continue to compress the fluid within the pump. However, the outlet check valve will not open and hence there will be no flow to the column until the pressure within the pump exceeds that of the column pressure. As the CO<sub>2</sub> is compressible, it may take up to 12% of the pump delivery stroke just to increase the pump pressure enough to open the outlet check valve [1]. Without compressibility compensation, this would result in a 12% loss of flow from the pump compared to the set flow rate which could have a dramatic effect on the chromatographic results especially when binary mobile phases are used. Therefore, so called compressibility factors must be calculated and included in each delivery stroke in order to accurately achieve the desired flow rate. The distance the piston must travel in order to achieve adequate compression is dependent on the pressure at the head of the column. Greater compression is required with higher column pressure which results in greater loss of the delivery stroke.

Calculation of compressibility factors is dependent on factors including the volume of the pump head cylinder, the temperature and the pressure both in the piston and at the head of the column [1]. Pump control algorithms were developed to empirically optimise nominal compressibility compensation for any fluid and also to compensate for pump leaks. Such compensation also helped minimize baseline noise which improved the sensitivity of pSFC [36].

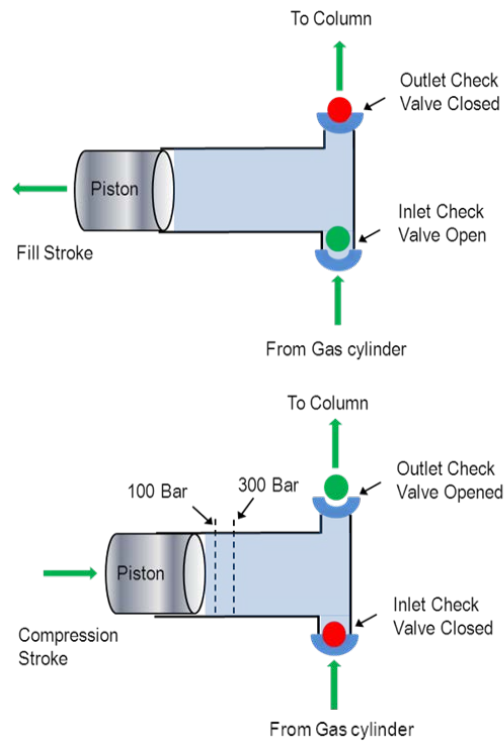


**Figure 1.5:** Diagram demonstrating the operation of the compressible fluid pump including compression compensation.

However, even if one knows the precise values required for accurate generation of the compressibility factor, there is still a further issue that can affect the fluid delivery from the pump. The factor in question is a rise in temperature during the compression stroke of the pump cycle; i.e. when liquids are compressed, there is an increase in temperature due to adiabatic heating [1]. The temperature of the fluid in the pump cylinder is at its highest just after the completion of the compression stroke. As there is no time for this heat to dissipate into the cylinder walls prior to delivery, this increase in temperature causes a net increase in the pressure within the pump cylinder which in turn can result in the premature opening of the outlet check valve. The premature opening of the outlet check valve results in more mass leaving the pump than expected. However, as the fluid cools, its density increases and the shrinking volume of the fluid negates part of the forward motion of the piston during the delivery stroke. This results in less mass than expected leaving the pump. Therefore, during each pump cycle, the delivery stroke repeats a cycle of first excessive flow followed by inadequate flow as a result of adiabatic heating. As there is no way of keeping the fluid isothermal during the compression stroke, the only way to ensure consistent flow is to vary the piston speed to compensate for the changing fluid densities. This has been made possible

as heat generation during compression can be accurately modelled so an algorithm can be written to vary the piston speed during delivery.

In summary, to ensure accurate and precise flow from the compressible fluid pump requires not only that the pump head be chilled to help maintain the CO<sub>2</sub> in the liquid form but also accurate calculation of the compressibility factor. In turn, further compensation factors must be generated by the system software to regulate the piston speed in order to negate the effects of adiabatic heating and to compensate for seal and check valve leaks. The sum of all these factors result in a complex challenge for the compressible fluid pump to ensure accurate flow and if any factor is over looked or underestimated; the results can be noisy chromatography with poor reproducibility.

### ***1.6.3 Mobile Phases used in pSFC***

Due to the low polarity of CO<sub>2</sub>, most mobile phases used in pSFC applications are binary mixtures of CO<sub>2</sub> and an organic modifier. It has been demonstrated that the composition of these binary mixtures is the most important factor in controlling SFC separations [37] with temperature and pressure being used for fine tuning separations. Methanol has emerged as the first choice when trying to elute polar compounds as it is completely miscible with CO<sub>2</sub> over a wide range of temperatures and pressures [16]. Saito and Nitta investigated the relationship between critical values of CO<sub>2</sub>/methanol mixtures and found that the addition of an organic modifier to the mobile phase can have a substantial effect on the critical point of the mobile phase with both T<sub>c</sub> and P<sub>c</sub> increasing proportionally to the amount of modifier present [8] (see Figure 1.6). However, the important point to note when using binary or tertiary mobile phases in pSFC is not whether or not the mobile phase is strictly maintained in the supercritical state, but rather that a single phase is maintained; i.e. that the mobile phase doesn't phase separate. It has been reported that all binary CO<sub>2</sub>/methanol mixtures form a single phase at 40 °C and with pressure set to 80 bar [38]. However, if the pressure is reduced below 80 bar, the mobile phase will separate into two phases. To ensure that this doesn't happen, it is recommended that the pressure be maintained above 100 bar when using CO<sub>2</sub> based binary mobile phases with pSFC.

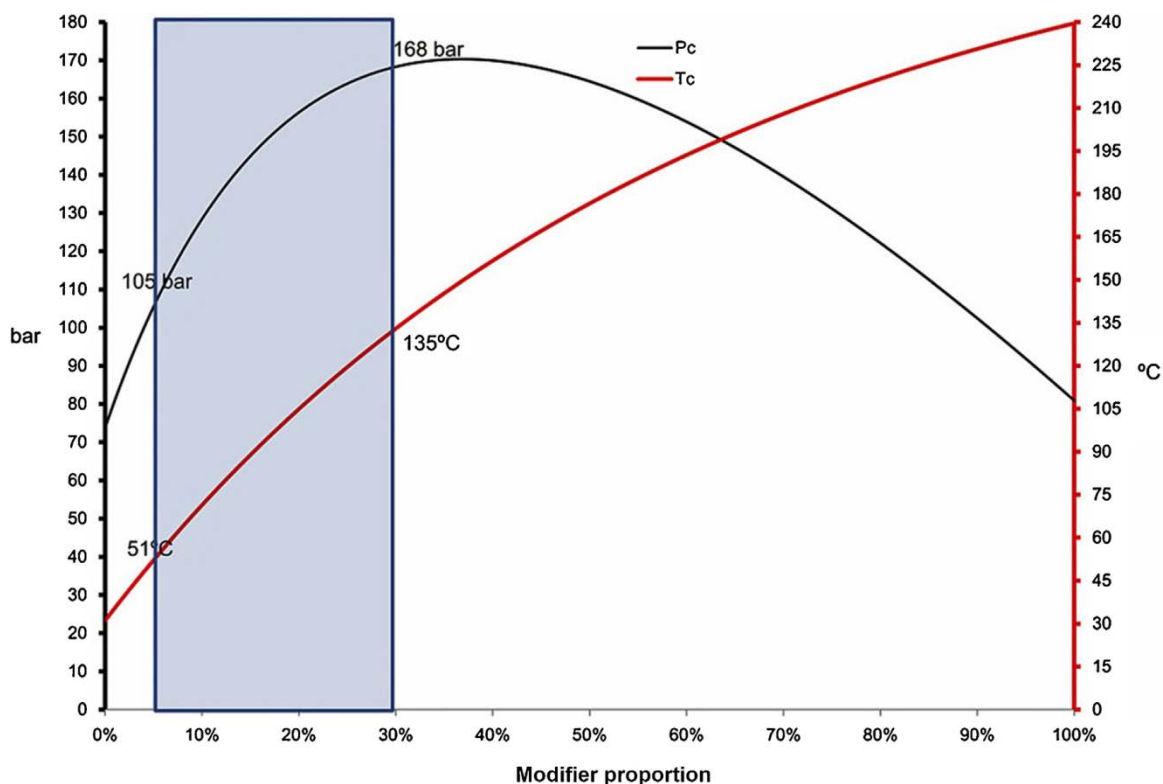


**Figure 1.6:** Relationship between the calculated critical temperature, pressure and concentration of the organic modifier. Reproduced from [8].

#### 1.6.4 pSFC Injector

Traditional external loop autosamplers are the best option to ensure accurate and reproducible injections in pSFC applications. The size of the injection loop used is extremely important in ensuring reproducible results are obtained. In HPLC, it can be common place to use large sample loops and vary the injection volumes. This results in what is known as partial loop injections in which part of the loop can remain filled with mobile phase. This does not work with pSFC as any mobile phase left in the sample loop will expand back into the syringe once the system pressure is removed. For this reason, it was always better to use small sample loops and carryout full loop injections in pSFC where the sample loop will be completely filled with sample. However, more recent advances in injector design now allow for partial loop injections to be carried out with pSFC; i.e. on the Waters Acquity UPC<sup>2</sup> system.

Along with the injection mode, the sample solvent composition and injection volume are also important factors in pSFC. Recent studies [39,40] detailing the influence of sample solvent composition in analytical SFC demonstrate that non-polar solvents such as heptane or hexane are best to deliver good peak shapes. The reason for this is due to the similar polarity

of these solvents is similar to that of CO<sub>2</sub>. However, there are drawbacks to using such solvents; firstly, due to their volatile nature they can evaporate quickly which could result in the sample being continually concentrated over the course of analysis. This has a detrimental effect on quantitative analysis. Secondly, they have limited dissolving power, particularly for ionisable compounds. Therefore, to achieve good solubility and acceptable peak shapes it is recommended to blend miscible polar and apolar solvents [39]. It is also recommended that the injection volume be kept as small as possible; i.e. without compromising injection repeatability or detection limits. In HPLC, the rule of thumb is that the injection volume be approximately 1% of the column volume [16]. However, in pSFC it is recommended that this be reduced to 0.1 – 0.5% of the column volume [16].

### ***1.6.5 pSFC Columns and Stationary Phases***

In the past, the most common column dimension used in pSFC were 4.6 mm i.d x 250 mm column packed with 5 µm or 3 µm particle size. Due to the lower viscosity of the pSFC mobile phase compared to normal liquids, the columns could be used at 3 to 5 times the maximum flow rate recommended by the column manufacturer without impacting the performance or lifetime of the column. It is this ability to operate at much higher flow rates that gives pSFC its advantage over HPLC in terms of speed of analysis. pSFC has also benefited from the development of stationary phases with smaller particle sizes; i.e. sub 2 µm, which were designed to improve efficiency and performance in LC separations. However, a study carried out to assess column performance on two modern pSFC systems, namely, the Waters Acquity UPC<sup>2</sup> and Agilent 1260 Infinity Analytical SFC systems, versus HPLC/ Ultra High Performance LC (UHPLC) systems suggests that not all sub 2 µm columns will provide improved performance on pSFC systems [16]. The study was based on the measurement of efficiency loss arising from instrumental contributions and found that when a standard column dimension for UHPLC, namely, 50 x 2.1 mm, 1.7µm. It was found that when such a column was used with modern SFC systems, the intrinsic column efficiency could be reduced by as much as 45%. Therefore, to keep the efficiency loss below the recommend 10% [41] level, the best compromise proposed is to use a 100 x 3.0 mm, 1.7µm column as this would only result in a 9% loss on the modern SFC systems studied.

SFC is described as a unified separation method as, due to the lack of water in the mobile phase, it allows the use of both polar and non-polar stationary phases with the same mobile phase [42,43]. Therefore, virtually all HPLC stationary phases can be used with SFC

from pure silica to octadecylsilyl-bonded silica (ODS) [16]. While these columns can also be used for pSFC applications, in recent years, manufacturers have started to develop and produce stationary phases specifically designed for pSFC applications. One of the first stationary phases to be specifically designed for pSFC achiral applications was the 2-ethylpyridine phase. This stationary phase was often recommended as the first choice for pSFC column screening because it offers good selectivity between acidic, neutral and basic compounds and offers reduced tailing for basic compounds [43-47]. With the addition of the pSFC specifically designed stationary phases, the analyst now has a wide array of possibilities when it comes to choosing the best one for a particular application. While having such an array of stationary phases to choose from provides pSFC with countless options for achiral applications, for the same reason it can make the method development process tricky in terms of choosing the best suited stationary for a given application. For this reason, a number of studies have been carried out to develop a classification system for stationary phases used in pSFC. Using the solvation parameter model and studying over 70 varied stationary phases, West *et al.* [48-55] graphically illustrated the functional distribution of the various stationary phases in the form of a spidergram. Such diagrams allow the analyst to select the most appropriate stationary phase options when it comes to method development, thus speeding up the process.

#### **1.6.6 Column oven**

In pSFC, changes in temperature can have a greater effect on selectivity among closely related compounds than on solute retention [56]. Therefore, in pSFC, ensuring precise temperature control is important for maintaining the quality and reproducibility of the separation. Column ovens used in pSFC are similar to those used in HPLC with most consisting of a temperature controlled metal block which is held in contact with the column. To insure adequate heat transfer to the column, most modern column ovens contain a pre-column heater, which consists of metal block with tubing passing through it. The block is set to the desired temperature and as the mobile phase passes through the tubing, it is heated to the desired temperature before it reaches the head of the column.

While pre-column heaters can help solve part of the problem of poor heat transfer from the column heating block to the column, there is another factor at play in pSFC that must be considered. The mobile phase passing through the column in pSFC is subject to a certain amount of pressure drop. As the pressure drops, the compressed fluid is able to

expand slightly on its journey through the column. This expansion results in localized adiabatic cooling within the column. Therefore, in pSFC, the column oven has to be capable of overcoming not only thermal contact and heat transfer issues, but also the fact that the column is being slightly cooled internally as the mobile phase is flowing through the column. Both of these effects can result in the temperature of the fluid being as much as 5 °C different from the set temperature. This could have a major effect on solute selectivity and depending on the column oven type used, could result in issues with method transfer. Therefore, some manufacturers recommend programming a temperature gradient within the column heater, with a higher temperature at the column outlet. This helps offset any temperature variations within the column, ensuring precise and accurate column temperature control. One drawback of column ovens which are used on modern SFC systems is that they are unable to perform column cooling. This results in a limited temperature range and prevents applications being carried out under sub-ambient conditions.

#### **1.6.7 Detectors**

SFC is compatible with a wide range of detector types including evaporative light-scattering (ELSD), corona charged aerosol detectors (CAD), Uv-vis and diode array detectors (PDA), mass spectrometry and flame ionization detectors (FID) detectors. However, as binary mobile phases are required for many pSFC applications, FID are not suitable due to the presence of carbon containing modifiers in the binary mobile phase which contributes to excessive baseline noise [1]. Therefore, the UV-Vis and PDA detectors are the most common type of detectors used in pSFC applications involving binary mobile phases.

The major difference between the UV detector used in HPLC and pSFC systems is that in pSFC, the detector cell must be capable of withstanding the high pressures resulting from the mobile phase being a compressed fluid. In some cases, the pressure can be as high as 400 bar. To prevent the cell from shattering under such pressures, a special design was developed in which the windows of the cell are bevelled at a 45 ° angle on both the front and back [1]. The design means that only small parts of the window surfaces remain parallel to each other and also that only a small portion of the window remains perpendicular to the cell axis. This unusual shape results in all of the forces within the cell being distributed towards the centre with the net result being that the forces cancel each other out. This design is similar to that used in the windows of submarines [56] and results in the detector cell being able to withstand the large forces experienced in pSFC.

Historically, pSFC with UV detection has suffered from a lack of sensitivity compared to HPLC due to the higher baseline noise observed in pSFC. Variations in mobile phase refractive index (RI) within the detector flow cell greatly impact the level of baseline noise observed in pSFC [57]. Such variations can be caused by fluctuations in the pumping system or the BPR, along with temperature changes in the detector cell which may arise from fluctuations in room temperature, or through heat generated from the detector itself which is intermittently transferred to the mobile phase before entering the cell. The RI is relative to the density of the fluid within the cell; i.e. The RI increases with increasing fluid density. Therefore, an increase in temperature within the detector cell will result in a decrease in the fluid density and thus a decrease in the RI of the fluid [58,59]. Keeping the detector temperature below the  $T_c$  helps minimise any density changes and thus RI variations within the cell [60]. It has also been reported that with back-pressures above 100 bar, fluctuations in RI are very similar whether operating at 40 °C or 90 °C [59]. This suggests that maintaining the back pressure well above  $P_c$  can help reduce RI effects as a result of temperature variations. The presence of a modifier in the mobile phase can also help reduce RI fluctuations and hence RI induced noise. Therefore, a combination of back pressures above 100 bar coupled with modifier composition of greater than 5% has been reported as an effective way to reduce detector noise and allow pSFC to be applied to low-level impurity analysis [57].

Another factor that must be considered in pSFC detectors has to do with the detector sampling rate. Due to the higher flow rates and faster analysis times found in pSFC compared to HPLC, the peak widths of pSFC peaks are often  $1/3^{\text{rd}}$  to  $1/5^{\text{th}}$  of those found in HPLC. This meant that in the past detectors designed for standard HPLC applications were simply not fast enough to detect the peaks in pSFC. This was also the major reason why smaller particle sized columns were not suitable for pSFC as their greater efficiency was lost in pSFC detection [1]. For this reason, the columns used in pSFC tend to be longer columns with larger particle sizes. However, with the development of UPLC, there are now detectors available with sample bandwidths up to 80 Hz which should make the advantages of smaller particle sizes available for exploitation in pSFC.

### **1.6.8 Backpressure Regulator (BPR)**

As mentioned previously, pSFC requires that the entire system be maintained at a particular pressure in order to maintain the integrity of the mobile phase as a fluid, from the supply

cylinder to the detector cell. This pressure control is achieved by a BPR, which is situated downstream from the detector cell. In the early days of pSFC, back pressure regulators were more akin to fixed restrictors in that they were passive mechanical devices which had to be adjusted manually. Such devices were cumbersome to use and required constant monitoring during the course of an analysis. However, fixed restrictors can still be a useful option to allow for example simple hyphenation of SFC with mass spectrometry (MS) [61]. The development of dynamic electronically controlled BPRs allowed for automatic dynamic control of system pressure which, coupled with inlet and outlet pressure transducers, enables the pSFC system to deliver a constant flow of mobile phase with constant pressure control which is unaffected by changes in fluid viscosity.

BPRs allow for the controlled expansion of the compressed mobile phase to waste. When using pure CO<sub>2</sub> as the mobile phase, this expansion can lead to the formation of dry ice due to adiabatic cooling of the gas as it expands. This dry ice can transiently plug the back pressure regulator outlet which can result in system pressure fluctuations resulting from erratic flow. The particles can also lead to a noisy baseline which in turn will affect the chromatography obtained. While binary mobile phases are less likely to form dry ice, the cooling on expansion can also cause pressure fluctuations. Such adiabatic cooling with subsequent dry ice formation and melting can also lead to issues with corrosion of the back pressure regulator. To prevent the issues of plugging and corrosion, the back pressure regulator should be heated. Just enough heat needs to be applied to prevent the formation of dry ice with temperatures of 40 °C to 80 °C being common. This ensures the prevention of dry ice formation while preventing the thermal destruction of solutes if peak collection is important. The dead volume of the regulator is also important for peak collection as low dead volumes ensure that excessive peak broadening is avoided.

In pSFC, once the binary mobile phase exits the back pressure regulator it breaks down into two phase. The majority of waste produced will be CO<sub>2</sub> gas with a small proportion being the modifier. Thus, the modifier waste volumes will be low compared to HPLC. This also offers SFC an advantage in terms of sample collection or fraction collection as the solute can be collected dissolved in the modifier solution.

## 1.7 SFC versus LC

Despite being compatible with a wide range of stationary phase types, unlike LC which can be described under a number of different modes, SFC is virtually always considered by definition to be a normal phase technique [1]. By simplest definition, normal phase chromatography occurs with a combination of a polar stationary phase with a non-polar mobile phase. In pSFC, when CO<sub>2</sub> is used as the mobile phase, adsorption of CO<sub>2</sub> onto the stationary phase occurs regardless of the type of stationary phase used. The adsorbed CO<sub>2</sub> is essentially a condensed fluid which has a density in the region of 1.0 g.cm<sup>-3</sup>, even when the density of the CO<sub>2</sub> in the mobile phase is in the region of 0.3 g.cm<sup>-3</sup> [1]. Therefore, for pSFC separations using pure CO<sub>2</sub> as the mobile phase, the adsorbed CO<sub>2</sub> layer on the stationary phase will always have a higher density than that of the CO<sub>2</sub> in the mobile phase. As solvent strength is proportional to the density of the fluid, the denser adsorbed layer should have a higher solvent strength than the less dense mobile phase. Therefore, the adsorbed layer not only modifies the volume of the stationary but also its polarity. This gives rise to the situation where the stationary phase becomes more polar than the mobile phase and thus, by definition pSFC with pure CO<sub>2</sub> is considered to be a normal phase technique. Therefore, SFC has the potential to replace many NP-HPLC methods and reduce the amount of harsh chemicals associated with this technique. Also, SFC can offer orthogonal selective compared to the widely used reversed phase HPLC (RP-HPLC) technique. Having such orthogonality can be useful in the drug development context or as a confirmation of method specificity of established RP-HPLC applications.

The kinetic advantages of SFC over LC are primarily due to the properties of the mobile phase used in SFC, the majority of which being composed of a sub or supercritical fluids which have higher diffusivity and lower viscosity compared to normal liquids. These advantages can be illustrated by plotting Van Deemter curves and pressure plots for SFC and LC applications to compare both techniques. Grand-Guillaume Perrenoud *et al.* [62] generated four such Van Deemter curves corresponding to HPLC, UPLC, SFC and Ultra High Performance SFC (UPSFC) to compare the kinetic performances of each technique. As one would expect, conventional HPLC was found to be the least efficient strategy with a low optimal liner velocity being reported. Compared to HPLC, SFC recorded a comparable H<sub>min</sub> value but with 5 times higher optimal liner velocity. UPLC gave the lowest H<sub>min</sub> value; three times lower than HPLC but only 1.2 times lower compared to UPSFC. However, UPSFC was able to operate at 4.6 times the optimal linear velocity of UPLC. It is this ability of SFC to

operate at much higher optimal linear velocities that gives it advantages in terms of sample throughput and reduced analysis times over LC. The authors also examined pressure drops across the column for the four different configurations listed above. The reported pressure drop for UPSFC was 1.7 times less than for UPLC (185 bar versus 322 bar) when operating at optimum linear velocities on columns packed with sub 2  $\mu\text{m}$  particles. Thus, the ability to operate at higher optimum linear velocities while generating lower column pressure drops gives UPSFC further potential advantages over conventional UPLC.

However, despite kinetic advantages of using sub or supercritical fluids as mobile phases, working with such compressible fluids results in SFC being far more complex than traditional LC. These issues have led to SFC being described by some as a “*rubber variant*” of LC where everything that can be considered as constant in LC, varies in SFC [63-65]. In pSFC, as the mobile phase travels through the column it is subject to a certain amount of pressure drop. This drop in pressure allows the fluid to expand somewhat which in turn allows for adiabatic cooling to take place within the column. The cooling results in both radial and axial density and temperature gradients within the column which in turn affects the thermodynamics of adsorption and cause a volumetric flow rate gradient through the column [66-68]. The practical consequences of this are that one cannot guarantee that the set operational conditions reflect the true conditions over the column like one can in LC separations [63], which has resulted in poor system-to-system reproducibility and method transfer to alternative systems for SFC applications. However, with modern holistically designed SFC instruments, the issues of poor system-to-system reproducibility could be reduced somewhat as these systems are manufactured and maintained to ensure that differences in system dwell volumes are kept to a minimum. Therefore, one would expect to see more successful SFC method transfers in the future and open the door to increased application of SFC in the analytical laboratory.

## **1.8 Green Chromatography**

Since the early 1990's there has been a focused attempt by a number of chemists to promote so-called “*green chemistry*” within academia and industry, in an attempt to reduce the risks of chemical exposure to both humans and the environment [69]. Green chemistry is based on 12 founding principles which are set out to improve upon all types of chemical products and processes by reducing impacts on human health and the environment relative to competing

technologies [69]. The 12 principles are broadly dominated by three themes; i.e. waste, hazard (health, environment and safety) and energy are outlined in Table 1.2.

Of the twelve principles listed in Table 1.2, numbers 1, 5, 6, 8, 11 and 12 are all directly applicable to analytical chemistry. Therefore, the goal of green analytical chemistry is to use procedures that generate less hazardous waste, are safer to use and are more benign to the environment [69].

**Table 1.2:** The twelve principles of green chemistry. Adapted from [70].

Number	Principle
1	Prevent waste
2	Maximize atom economy
3	Design less hazardous chemical syntheses
4	Design safer chemicals and products
5	Use safer solvents and reaction conditions
6	Increase energy efficiency
7	Use renewable feedstocks
8	Avoid chemical derivatives
9	Use catalysts, not stoichiometric reagents
10	Design chemicals and products that degrade
11	Analyse in real time to prevent pollution
12	Minimize the potential for accidents

In terms of fulfilling the principles of green chromatography, SFC performs well, especially at analytical scale. SFC can be considered environmentally friendly as it minimised the use of toxic organic solvents and additives thus reducing the contaminant risks to laboratory workers while reducing disposal issues post analysis [71]. Although CO<sub>2</sub> is not considered to be a toxic chemical, some may argue that it is a greenhouse gas and therefore, how can SFC be considered to be “green”? The answer to this is that the majority of CO<sub>2</sub> used in SFC applications is reclaimed from the atmosphere. Therefore, SFC is not a net producer of CO<sub>2</sub> and thus can be considered as a green analytical technique.

## 1.9 Project outline

With the global drive for faster, more environmentally friendly separation techniques, the aim of this research was to demonstrate the potential of SFC to be used as a viable alternative or complementary technique to HPLC in the highly regulated world of the Pharma Quality Control (QC) laboratory. This was achieved in the present work through the development and more importantly, the validation of selected applications to showcase the strengths, while at the same time dispelling some of the historically perceived weaknesses (e.g. poor sensitivity, reproducibility), associated with analytical SFC. To do this, any SFC application had to be capable of meeting, if not exceeding the performance levels of the current established LC applications for QC testing of pharmaceutical drug substance (DS) and drug product (DP) formulations.

Chapter 2 focuses on exploiting one of the recognised and established strengths of SFC (i.e. chiral separations). In this chapter, a new enantioselective pSFC method was developed and validated under International Conference of Harmonisation (ICH) guidance to meet the current European Pharmacopoeia requirements of a limit test for the determination of S-timolol enantiomeric purity in timolol maleate DS. The developed pSFC method is presented as an alternative to the current NP-HPLC method described in the European Pharmacopoeia (Timolol Maleate Monograph). The newly developed pSFC method achieved a resolution of 2.0 within 5 min, representing a 3-fold reduction in run-time and an 11-fold reduction in solvent consumption relative to the NP-HPLC method.

Chapter 3 details the development of an improved HPLC application using the most up-to-date stationary phase technology available. This chapter focuses on the use of superficially porous particles or so called “*coreshell*” stationary phase technology which has seen resurgence in recent years particularly in HPLC applications due performance improvements over more traditional fully porous HPLC stationary phases. A new stability indicating reversed phase HPLC (RP-HPLC) method was developed and validated under current ICH guidance for the determination of prednisolone acetate (PAC) and impurities in an ophthalmic suspension. The developed method is presented as an alternative to a modified version of the current RP-HPLC method described in the USP monograph for the assay of PAC in an ophthalmic suspension and is capable of identifying and quantifying PAC and eight selected PAC impurities and degradation products in an ophthalmic suspension. Using an Agilent Poroshell column with step gradient elution, all peaks of interest are eluted in

33 min with resolution of 1.5 between the critical pairs. This method represents optimal HPLC performance for the selected separation and was used as yardstick for comparison purposes between the HPLC and SFC applications.

Chapter 4 focuses on demonstrating the potential of SFC to complement HPLC in the QC laboratory by developing and validating an orthogonal achiral separation for the same PAC sample described in Chapter 3. To be deemed viable, the new pSFC method had to be capable of meeting the ICH requirements for a stability indicating method for trace impurity analysis of the PAC sample, whilst providing an equivalent if not better separation to the RP-HPLC method described in Chapter 3. The validation strategy employed was more statistically based compared to the more traditional method characterisation based strategies employed for the validation of methods in Chapters 2 and 3. The statistical approach selected for the method validation was the total error approach with accuracy profiles for two regression models, based on  $\beta$ -expectation tolerance intervals. The accuracy profiles demonstrate that the new pSFC method is indeed fit for purpose and is capable of meeting the QC requirements for each compound of interest and can be presented as a viable alternative to the previously developed RP-HPLC method.

## **2.0 Chapter 2: Determination of (R)-timolol in (S)-timolol maleate active pharmaceutical ingredient: Validation of a new pSFC method with an established NP-HPLC method.**

### **2.1 Introduction**

The chromatographic separation of enantiomers presents significant challenges in analytical chemistry. Since amino acids and carbohydrates contain chiral centres, chirality is a fundamental characteristic of all living organisms. All essential physiological processes display enantioselectivity, where one enantiomer interacts more strongly with a certain target site than the other due to differences in its spatial configuration [72]. The term eutomer is given to the isomer which binds more strongly to the target site and generates the therapeutic response while the isomer which binds less strongly is called the distomer. The distomer can display no activity, less activity, an antagonistic activity, another activity through interaction with other target sites, or even toxic effects [72,73]. While it is well known that substantial pharmacological differences may exist between enantiomeric pharmaceuticals, it was not until after the thalidomide disaster in the 1960s that research activity increased in the field of chirality. Today the United States Food and Drug Administration (USFDA) requires enantiomeric studies to be performed on all new racemic drugs as described below [74] as do the European and Japanese regulatory authorities. These guidelines include the development of enantioselective identification and quantification methods for each active pharmaceutical ingredient with chiral properties. In addition pharmacokinetic and toxicological assays should be executed using both pure enantiomers and with the racemate. Furthermore, there is accumulating evidence demonstrating the medicinal advantage of using pure enantiomers over racemates as active drug substances [75]. As a result, numerous methods have recently been adopted to replace existing racemates with single enantiomeric drugs [76].

#### **2.1.1 *Properties of Timolol Maleate***

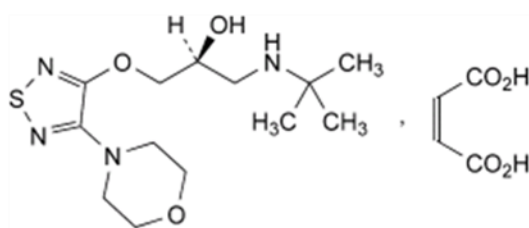
Beta adrenergic receptor blocking agents, commonly called  $\beta$ -blockers [77,78] are a group of drugs used to treat high blood pressure, heart failure and myocardial ischemia diseases [79-81]. Many  $\beta$ -blockers are available in the United States and European markets [78,82] since they were first launched in 1960s [83]. However, only a few of this class of drugs are sold as single enantiomers [84]. Most  $\beta$ -blockers depend on S-enantiomers for the disease therapies [85] as generally speaking, the S-enantiomers are more potent than the distomers [86].

Timolol maleate (s)-(-)-1-(tert.-butylamino)-3-[(4-morpholino-1,2,5-thiadiazol-3-yl)oxy]-2-propanol maleate (shown below in Figure 2.1) belongs to the thiadiazole class of compounds and is a non-selective  $\beta$ -adrenergic blocker which is used as a single enantiomer (S-timolol) for the treatment of hypertension, arrhythmias, angina pectoris, and for the secondary prevention of myocardial infarctions [87-92]. It is also used for the topical treatment of increasing intraocular pressure in patients with chronic open angle glaucoma and aphakia [93-97]. Like all  $\beta$ -adrenoceptor antagonists, timolol is contraindicated in patients with asthma and its inadvertent administration as eye drops to such patients continues to have severe and even fatal consequences [98]. Richards and Tattersfield [99] reported that the R-timolol enantiomer was considerably less potent as a  $\beta$ -adrenoceptor antagonist in animals than the clinically used S-timolol enantiomer, but only slightly less potent in reducing intraocular pressure [100]. The R-timolol enantiomer was reported to be 49 times less potent than S-timolol on  $\beta$ -adrenoceptor in animals and thirteen times less potent in constricting the airways of normal subjects, yet it is only four times less potent in reducing intraocular pressure in man [100]. These findings suggested that R-timolol might be a safer alternative for the treatment of glaucoma with less systemic side-effects than the S-enantiomer when applied as eye drops (in concentrations ranging between 0.25 and 4.0% (w/v)), as it has a smaller broncho-constricting effect [100]. However, despite this, the S-enantiomer is still the choice of drug substance used in the manufacture of timolol-containing products for the treatment of glaucoma.

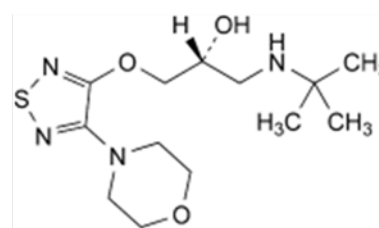
Timolol maleate was first synthesized in the Merck-Frosst laboratories in Montreal, Canada. Timolol maleate is soluble in water, methanol (MeOH) and ethanol. The  $pK_a$  of timolol base obtained by potentiometric titration in water at 25 °C is approximately 9.2 [92] and the native pH of a saturated aqueous solution of timolol maleate is approximately 4.0 [92]. The first non-patent literature reference to timolol maleate appeared in 1972 [94,101].

### **2.1.2 Analysis of Timolol Maleate by HPLC**

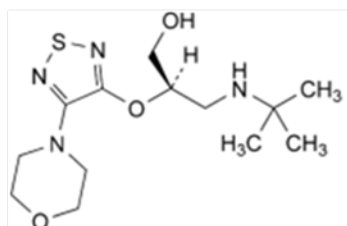
A 2008 review by Wang *et al.* discusses recent developments in enantio-separations of adrenergic pharmaceuticals [102]. Specifically, enantio-separation of timolol maleate has been previously reported using capillary electrophoresis (CE) and NP-HPLC.



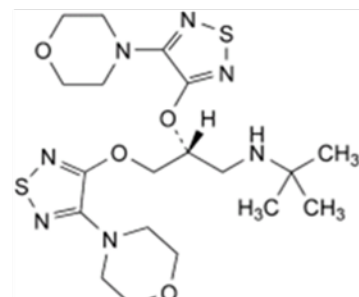
**S-timolol Maleate**



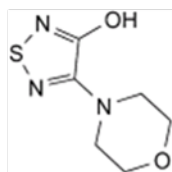
**R-timolol (Imp A)**



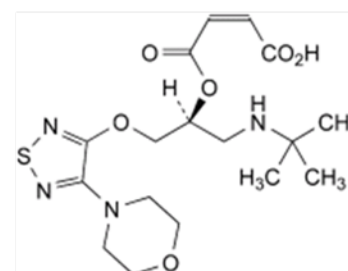
**Imp B**



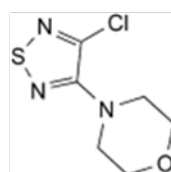
**Imp C**



**Imp D**



**Imp E**



**Imp F**

**Figure 2.1:** Molecular structure of *S*-timolol maleate, *R*-timolol (Impurity A) and European Pharmacopeia specified impurities B, C, D, E and F. Reproduced from [103].

NP-HPLC for the quantitation of *R*-timolol in *S*-timolol maleate was first reported in 1990 by Enein *et al.* [104] using a Chiralcel OD analytical column comprising cellulose tris-3,5 dimethylphenylcarbamate coated on 10  $\mu\text{m}$  silica gel (see Figure 2.2) and a mobile phase of hexane/isopropanol/diethylamine (95:5:0.4). In this study, the effects of 2-propanol, various aliphatic alcohols and diethylamine (DEA) concentrations in the mobile phase along with column temperature on the retention and enantioselectivity of the timolol enantiomers

were investigated. It was noted that the enantiomers failed to elute without an alcohol present in the mobile phase with branched-chain alcohols (particularly 2-propanol) exhibiting the best resolution ( $R_s$ ). Retention factor ( $k$ ), selectivity and  $R_s$  all decreased with increasing 2-propanol concentration, with the best  $R_s$  being obtained with 5% (v/v) 2-propanol.

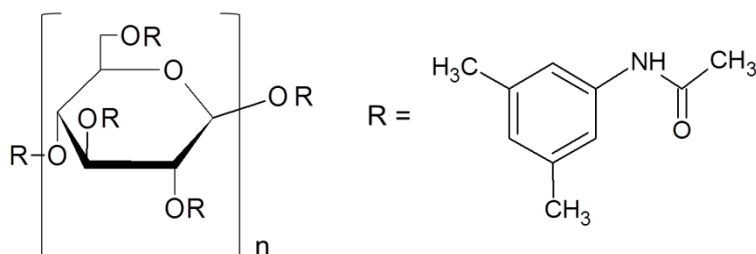


**Figure 2.2:** Molecular structure of the Chiracel OD chiral stationary phase (CSP). Reproduced from [103].

The effect of DEA concentration ranging from 0.0% to 1.0% (v/v) was also investigated. It was noted that no separation was obtained in the absence of DEA. The 1.0% (v/v) concentration gave the best enantioresolution of 4.32. However, in order to prevent the detrimental effect of the basic mobile phase on the stationary phase due to saponification, as ester groups were present in the packing material, only 0.4% (v/v) DEA was used, resulting in an  $R$  of 4.0 [104]. It was found that the Chiracel OD column was sensitive to small changes in column temperature. The  $R_s$  increased about 1.6-fold when the temperature was decreased from 30 °C to 5 °C. This increase in  $R_s$  with decreasing temperature supports the existence of both a simultaneous and stepwise binding chiral recognition mechanism on the CSP as proposed by Wainer *et al.* [105] in which the chiral recognition mechanism for the enantiomeric aromatic alcohols were studied. The proposed mechanism involves: (1) the formation of diastereomeric solute-CSP complexes through a hydrogen bonding interaction between the solute's alcoholic hydrogen and an ester carbonyl on the CSP; (2) the stabilisation of this complex through the insertion of the aromatic portion of the solute into a chiral cavity (or ravine) of the CSP; and (3) chiral discrimination between enantiomeric solutes due to difference in their steric fit in the chiral cavity. Therefore, an increase in temperature resulted in a corresponding increase in the conformational mobility of the solute, which destabilised the solute-CSP complex and reduced the stereoselectivity. The final optimised conditions were obtained when using the solvent system hexane: 2-propanol (95:5) contains 0.4% (v/v) DEA at 5 °C as illustrated in Figure 2.3 [104].

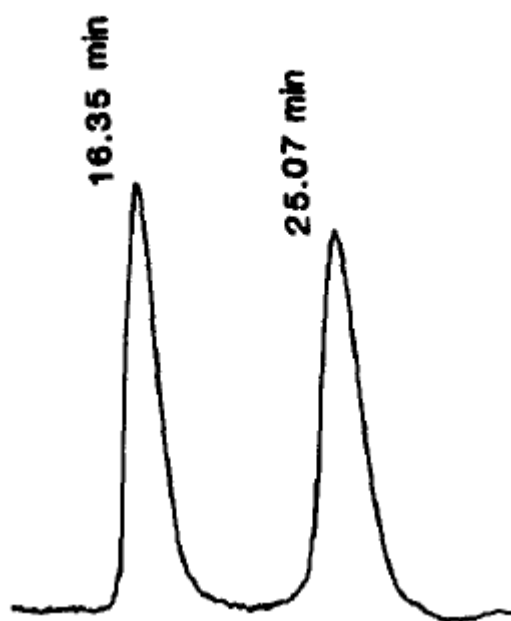


**Figure 2.3:** HPLC separation of timolol maleate enantiomers. Column: Chiralcel OD (250 mm x 4.6 mm I.D.); mobile phase, hexane-2-propanol-DEA (95:5:0.4); flow-rate, 0.7 mL.min<sup>-1</sup> ; chart-speed, 0.5 cm/mm; temperature, 5 °C; pressure, 250 p.s.i.; sample amount, 10 nmol; detector: UV (224 nm); sensitivity, 0.01 a.u.f.s. Reproduced from [104].

In 1994, Lacroix *et al.* [106] developed and validated NP-HPLC and proton nuclear magnetic resonance (<sup>1</sup>H-NMR) methods for the quantitation of the R-enantiomer in S-timolol maleate. The NP-HPLC method was based on the method previously developed by Enein *et al.* [104] which had been optimised for the separation of the R- and S-enantiomers. However, no data were provided in the Enein method on the selectivity of the method in the presence of other potential timolol impurities or on the limit of quantitation (LOQ) for the R-enantiomer in S-timolol maleate raw material. Therefore, Lacroix *et al.* set out to optimise the method on the newly available 5 µm particle size column (Chiralcel OD-H) which potentially offered higher efficiencies and the possibility that the Enein method could be modified and validated for the quantitation of the R-enantiomer in S-timolol maleate drug substance. Detection at 297 nm was used instead of 224 nm because this corresponds to a maximum in UV absorbance for the drug in MeOH. Also, several of the related compounds do not absorb at 297 nm, which minimised interference from these compounds. The composition of the mobile phase was changed to optimise the separation of the two enantiomers and other closely eluting compounds, particularly for (S)-1-[1,1-dimethylethyl]

amino]-2-[[4-(4-morpholinyl)-1,2,5-thiadiazol-3-yl]oxy]-3-propanol, a structural isomer of timolol. The final optimised conditions were; mobile phase of 0.2% (v/v) DEA and 4% (v/v) isopropanol in hexane ( $1 \text{ mL}\cdot\text{min}^{-1}$ ) for 15 min and UV detection at 297 nm on a Chiracel OD-H (cellulose tris-3,5-dimethylphenylcarbamate) column ( $5 \mu\text{m}$ ). Under the conditions described in this method, typical values for retention factors were  $k_1 = 1.64$  and  $k_2 = 2.80$ , for the R- and S-enantiomers, respectively; the separation factor ( $\alpha$ ) was 1.70 and  $R_s$ , 4.81 [106].

The effect of temperature on the separation was studied and it was found that an increase in temperature from ambient to  $40 \text{ }^\circ\text{C}$  caused a decrease in the retention times of the R- and S-enantiomers and also the structural isomer. Generally the  $R_s$  between the R- and S-enantiomers decreased while the  $R_s$  between R- and the structural isomer was only slightly affected.  $R_s$  between the R- and S-enantiomers of timolol increased when the proportion of isopropanol in the mobile phase was reduced from 5% to 1% (v/v). However, the  $R_s$  between R-timolol and the isomer decreased over the same range and these latter compounds were unresolved when the proportion of isopropanol was 1% (v/v) [106]. The relative standard deviation (RSD) of peak area responses for six replicate injections of a solution of R-timolol maleate at the 0.05% mass/mass (m/m) level was 17.8%. The LOQ for this method was 0.05% (m/m) R-timolol maleate [106].

In 2003, Marini *et al.* [107] developed a NP-HPLC method on a cellulose tris(3,5-dimethylphenylcarbamate) ( $5 \mu\text{m}$ ) CSP and a mixture of hexane, 2-propanol, and DEA as mobile phase for the simultaneous determination of R-timolol and other potential related substances in S-timolol maleate. The method was based on the NP-HPLC method described in the monograph of timolol maleate presented in the European Pharmacopeia (EP) [108]. An experimental design was elaborated in order to test the effects of three different selected factors, namely column temperature, the concentrations of 2-propanol and DEA. The three factors were studied simultaneously, with the effects being evaluated statistically to determine the optimum LC conditions. The developed LC method was then compared to the EP method [108] and was applied to the determination of R-timolol and other related substances in several samples of S-timolol maleate from different sources.

The EP method [108] used mobile phase consisting of hexane/isopropanol/DEA (95.8:4.0:0.2) (v/v/v). For system suitability purposes, a  $R_s$  of 4.0 between the enantiomers was specified. The optimised method developed by Marini *et al.* [107-110] permitted the separation of both enantiomers in the presence of other potential S-timolol impurities;

isotimolol, a degradation product, dimer maleate and dimorpholinothiadiazole (DMTDZ) which are potential synthesis impurities. The separation was achieved within 20 min by modifying the mobile phase to hexane/isopropanol/DEA (96.5:3.5:0.1) (v/v/v) and the column temperature (previously unspecified in the EP monograph) to 23 °C. Figure 2.4 illustrates representative chromatograms comparing the EP and optimised methods [107]. For the EP method,  $R_s$  was 1.3 between the critical peak pair (R-timolol and isotimolol) whereas with Marini's optimised method  $R_s$  was 1.7. Therefore, the developed LC method was proposed to be used for the simultaneous determination of S-timolol enantiomeric purity and for the determination of related substances in the revised version of the monograph of S-timolol maleate. However, this method was not adopted into later versions of the EP monograph and separate methods for the determination of enantiomeric purity and related substances still exist in the monograph of S-timolol maleate [103].

### **2.1.3 Analysis of Timolol Maleate by Capillary Electrophoresis (CE)**

In the case of electrophoretic separations, as a result of the higher separation efficiency of CE compared to conventional HPLC, it is theoretically possible to improve  $R_s$  and shorten the analysis times with CE compared to LC. However, one of the drawbacks is that the limit of detection (LOD) is often higher for CE than for LC due to the lower loading capacity of CE and the use of on-column detection. This high detection limit can result in issues for impurity analysis when using CE [111]. In 2004, Servais *et al.* investigated the use of non-aqueous capillary electrophoresis (NACE) with heptakis (2,3-di-O-methyl-6-O-sulfo)- $\beta$ -cyclodextrin (HDMS-b-CD) as chiral selector in combination with potassium camphorsulfonate [112]. The best timolol enantio-separation was observed with 30 mM HDMS-b-CD and 30 mM potassium camphorsulfonate, all in MeOH containing 0.75 M formic acid which gave a  $R_s$  of 8.5 within 12.5 min as shown in Figure 2.5.

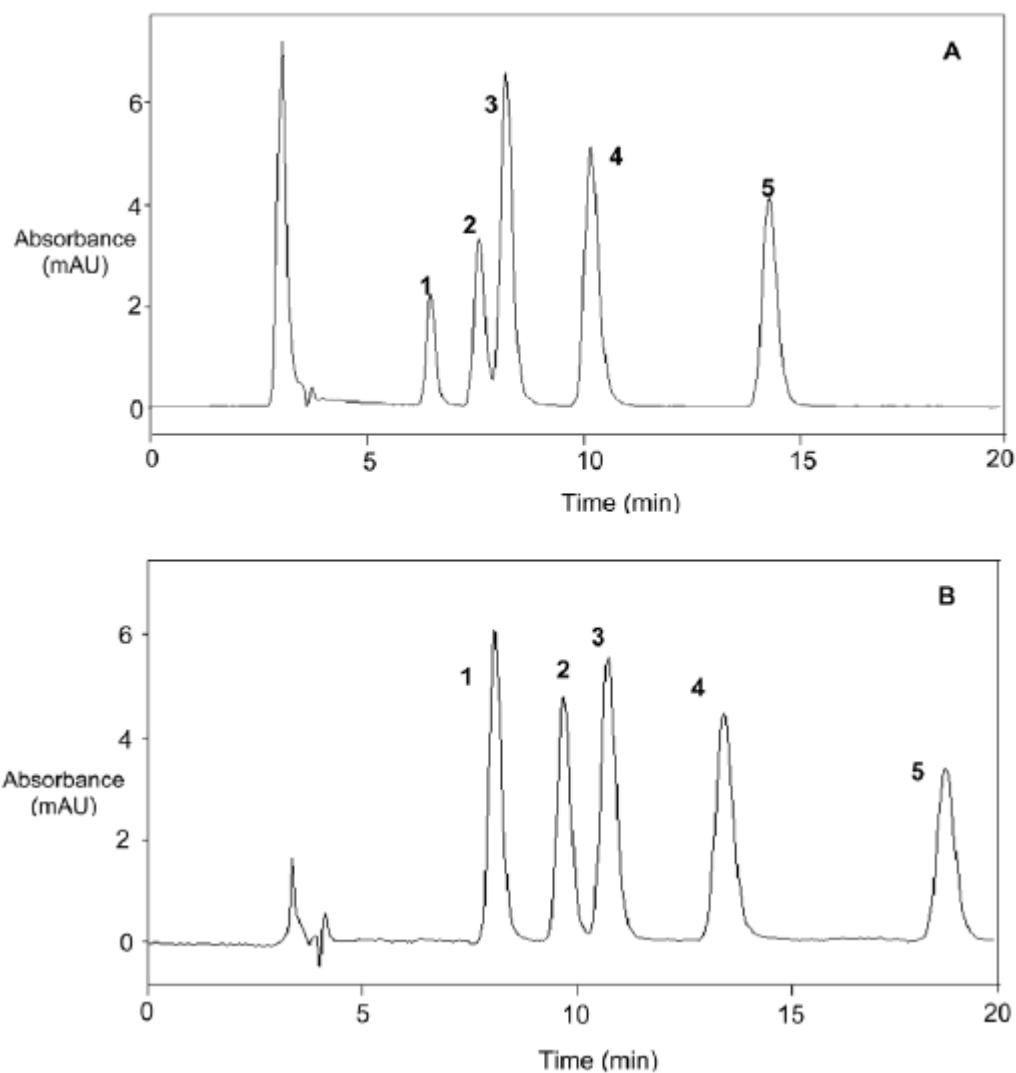


**Figure 2.4:** Typical chromatograms of a solution containing *S*-timolol, *R*-timolol, and other related substances. (a) Application of the LC conditions described in the EP monograph (DEA 0.2% and 2-propanol 4.0% (v/v)) 36. (b) Application of the optimal LC conditions ( $T$  23 °C, DEA 0.1% and 2-propanol 3.5% (v/v)). Peaks: 1: Dimer maleate. 2: *R*-timolol. 3: isotimolol. 4: *S*-timolol. 5: DMTDZ. Reproduced from [107].

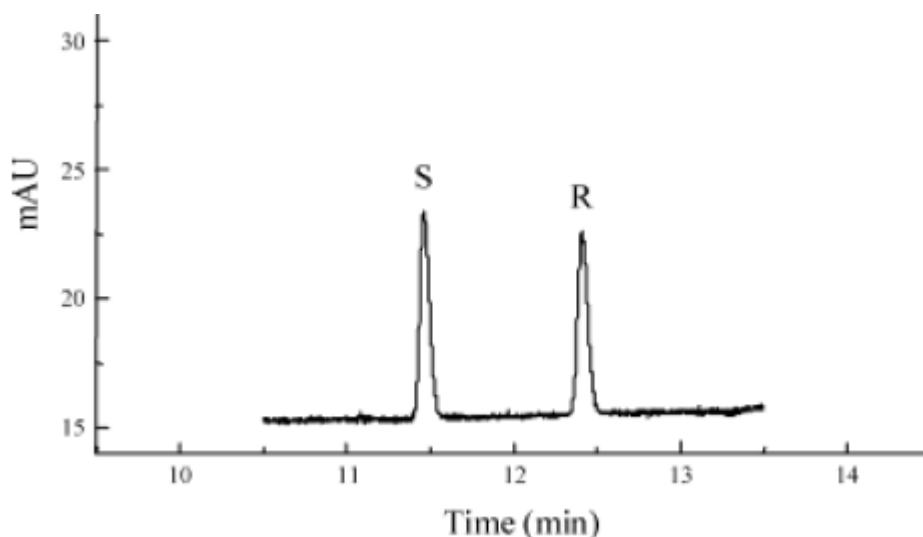


**Figure 2.5:** *Enantio-separation of a reconstituted racemic mixture of timolol maleate. Buffers: 30 mM HDMS-b-CD, 30 mM potassium camphorsulfonate and 0.75 M formic acid in MeOH. Capillary: 50  $\mu$ m, total length: 48.5 cm, effective length: 40 cm. Voltage: 25 kV. Injection: 50 mbar, 5 sec. Capillary temperature: 15  $^{\circ}$ C. Detection: UV @ 295 nm. Peak concentrations 50  $\mu$ g.mL $^{-1}$  in MeOH. Reproduced from [112].*

In 2006, Marini *et al.* investigated the use of NACE to determine the enantiomeric purity of timolol maleate [113]. The main goal of this work was to achieve adequate separation while maintaining a LOD of 0.1% for the R-timolol and other impurities investigated using the NACE method developed by Servais *et al.* [112]. Another goal of this study was to confirm the specificity of the LC method previously developed for the determination of timolol maleate enantiomeric purity [107-110] by using the NACE method as an orthogonal method to the NP-HPLC method. Once the equivalence of the two methods was demonstrated, the NACE method could be proposed as an alternative to the NP-HPLC method.

The final optimised method used for the study included the use of an internal standard for quantification to compensate for the injection variability due to the low volume of sample solutions introduced in the capillary and by the possible solvent evaporation from sample solutions [114]. Pyridoxine at a concentration of 5  $\mu$ g.mL $^{-1}$  was selected as internal standard with the best resolution results ( $R_s$  9.2) being obtained by using a S-timolol solution at a concentration of 2 mg.mL $^{-1}$  and by introducing this solution in the capillary under a pressure of 5 kPa during 8 sec. The applied voltage was 25 kV and UV detection was set at

295 nm for data acquisition. Figure 2.6 shows a typical electropherogram of an S-timolol maleate solution spiked with R-enantiomer (0.1%) and containing the internal standard [113].

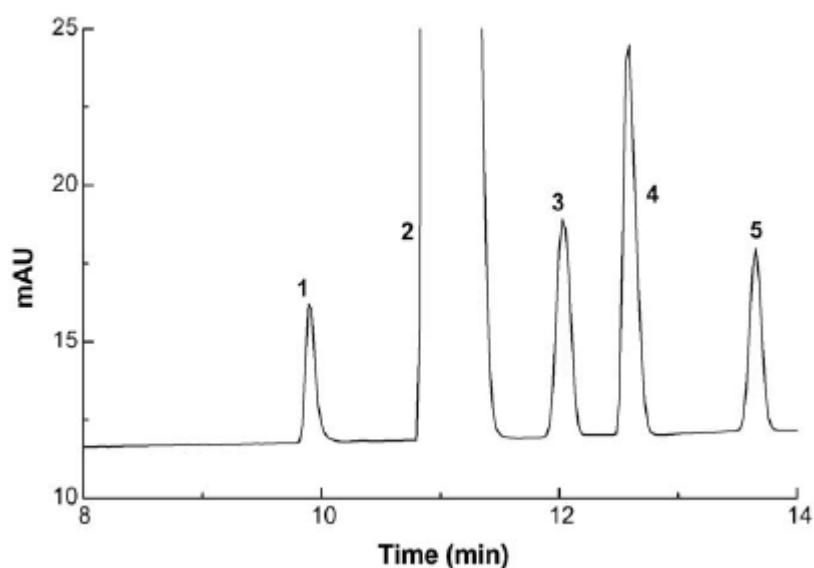


**Figure 2.6:** Typical electropherogram of a mixture solution containing the main timolol impurities and the pyridoxine used as internal standard. Chromatographic conditions; Column: uncoated fused silica capillaries having 50  $\mu\text{m}$  internal diameter and 48.5 cm length (40 cm to the detector). Applied voltage: 25 kV. Selected BGE-CD: 30mM potassium camphorSO<sub>3</sub><sup>-</sup> and 30mM HDMS- $\beta$ -CD in methanol acidified with 0.75M formic acid. Injection: made by pressure (50 mbar) for a period of 8 s (corresponding to 23.4 nL, i.e. 2.5% of the total volume of the capillary). Capillary temperature: 15 °C. Peaks and concentrations: (1) pyridoxine (10  $\text{g}\cdot\text{mL}^{-1}$ ), (2) S-timolol (2  $\text{mg}\cdot\text{mL}^{-1}$ ), (3) R-timolol (1.0% or 20  $\text{g}\cdot\text{mL}^{-1}$ ), (4) isotimolol (1.09% or 21.8  $\text{g}/\text{mL}$ ) and (5) dimer maleate (0.51% or 10.3  $\text{g}\cdot\text{mL}^{-1}$ ). Reproduced from [113].

A comparison was made between the NACE and NP-HPLC methods by analysing the same S-timolol samples with both methods. It was concluded that the two analytical methods were equivalent because the difference of the means observed were comprised within the 95% agreement limits [113].

In 2007 Hedeland *et al.* demonstrated the enantioresolution of timolol using 1S,4R-(+) ketopinic acid [(+)-KPA] as chiral selector in NACE [111]. The method was applied to determine the enantiomeric impurity R-timolol in the presence of S-timolol with a LOD requirement of 1% to satisfy the EP specification [115]. During method development, the

detection wavelength was set at 220 nm for all experiments. The background electrolyte (BGE) containing the chiral selector selector [100 mM (+)-KPA] and 40 mM KOH in MeOH:ethanol [(40:60), (v/v)] was selected for the enantiomeric purity determination of S-timolol. Under these conditions, the R-timolol impurity was observed to be the fastest migrating enantiomer, with the enantioresolution of  $R_s = 4.2$  obtained for a racemic mixture of 0.2 mM timolol. However, in the absence of a stacking technique, a maximum of 1 mM S-timolol could be injected (35 mbar over 5 sec). In an attempt to decrease the LOD of the method, the possibility of pre-concentration by Field amplified sample stacking (FASS) and transient Isotachopheresis (tITP) were evaluated. Through the use of FASS, the LOD was improved to 1% R-timolol.

However, it was observed that the use of tITP seemed to be a more efficient pre-concentration technique in this study as illustrated in Figure 2.7. The tITP conditions used in this study were based on the work by Shihabi [116]. The capillary was first flushed with the BGE containing the chiral selector. A plug of 100 mM NaAc in MeOH (the leading electrolyte) was injected by pressure (25 mbar over 1 second) after the chiral BGE and before the sample injection (S-timolol 2 mM, 35 mbar over 5 sec). Triethanolamine (200 mM in MeOH) was used as the anodic solution (i.e., the terminating electrolyte), and the chiral BGE was used as the cathodic solution [111]. By injection of a sample with high concentration, the LOD could be decreased from 2.5 to 0.2% for the R-enantiomer using tITP. A typical electropherogram at the LOD are shown in Figure 2.7(c). Furthermore, it was noted that the migration time decreased from 23 to 10.5 min in the tITP system. This decrease in migration time was due to the cathodic EOF ( $1.1 \times 10^{-5} \text{ cm}^2 \text{ V}^{-1} \text{ s}^{-1}$ ), caused by the tailing electrolyte. Only in the selector BGE, the EOF was anodic ( $-1.9 \times 10^{-5} \text{ cm}^2 \text{ V}^{-1} \text{ s}^{-1}$ ) [111].

#### **2.1.4 Chiral analysis by SFC**

To date, HPLC utilising polysaccharide CSPs remains the most widely used technique for enantioseparations in the pharmaceutical industry [116,117]. However, despite its popularity there are a number of disadvantages associated with this separation technique including; (1) relatively long analysis times, (2) limited sample throughput and (3) the high consumption of toxic and flammable solvents. Also, there can be issues in terms of up-scaling of the chiral separation method to a preparative level, especially with reversed-phase liquid chromatography [118]. Therefore, SFC is currently experiencing a renaissance (particularly within the pharmaceutical industry) as a valuable alternative chromatographic technique for

chiral separations due to its relative environmental benignity [119,120]. Evidence of this is seen from the increased publication of review papers relating to SFC applications [121-124].

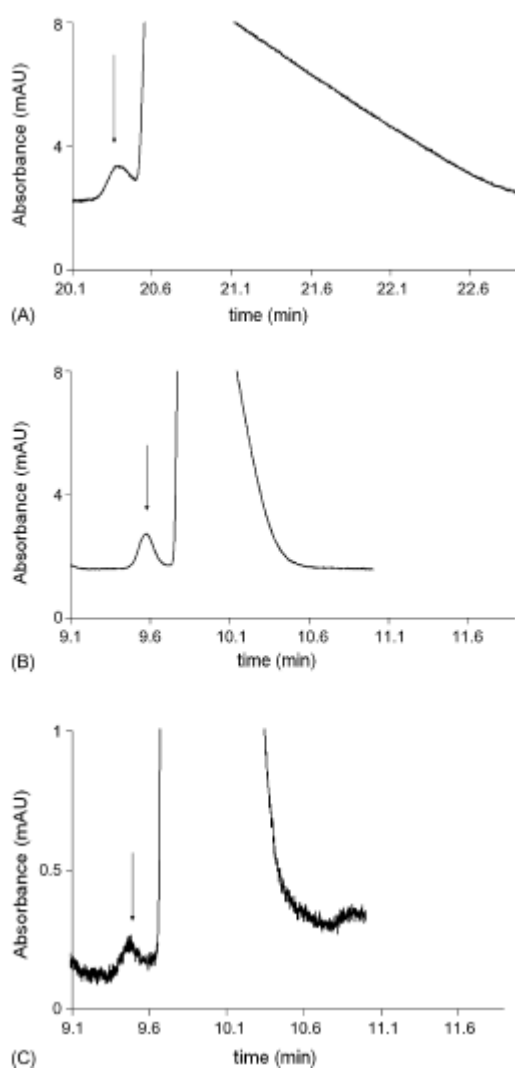


**Figure 2.7:** Peak sharpening of *S*-timolol. BGE: 100 mM (+)-KPA and 40 mM KOH in MeOH:EtOH (3:2, v/v). 30 kV, Ldet 23 cm Sample: 2 mM *S*-timolol and 0.05 mM *R*-timolol (2.4%) dissolved in MeOH. (a) Normal injection pressure injection at 35 mbar over 5 s, (b) transient ITP, leading electrolyte: 100 mM NaAc in MeOH (25 mbar over 1 s). Terminating electrolyte: 200 mM triethanolamine in MeOH (anodic vial). (c) Transient ITP at LOD (0.2% *R*-timolol). Conditions as in (B). The arrow in the electropherograms (a–c) points out the position of the *R*-timolol peak. Reproduced from [111].

There has also been an increase in the number of industrial users driven in part by the increased investment of major instrument manufacturers in the production of commercial

availability of SFC instrumentation which exhibits significantly improved performance characteristics relative to the instrumentation of the early 1990's [125,126] as noted in Chapter 1. Also, the potential benefits over conventional HPLC in terms of solvent cost reduction and waste removal are becoming ever more important to satisfy the need for more environmentally friendly modes of analysis. As a result, packed column SFC is becoming more widely used for chiral separations and has the potential to replace HPLC as a first choice technique for enantioseparations and purifications in drug discovery and development processes.

However, SFC has historically suffered from a serious lack of sensitivity and has rarely found a place in trace analysis or regulated environments [57,127]. One of the major obstacles is that (until recently) SFC instruments employing UV detection were less sensitive compared to HPLC-UV instruments making the detection of trace level impurities very challenging [128]. A recent review by De Klerk *et al.* reveals that SFC is becoming ever more popular for enantioseparation of pharmaceuticals [129]. Gyllenhaal *et al.* demonstrated the use of a Hypercarb packed column using L-(+)-tartaric acid as chiral selector to resolve enantiomers of selected  $\beta$ -blockers [130]. Medvedovici *et al.* used polysaccharide stationary phases to separate  $\beta$ -agonists [131]. Lui *et al.* used three macrocyclic glycopeptide chiral selectors and compared their performance in the separation of a range of  $\beta$ -blockers [132]. However, at the time our work was undertaken, to the best of our knowledge, no report has appeared in the literature describing the use of SFC for the enantioseparation of timolol maleate or indeed any active pharmaceutical ingredient used in ophthalmic medications.

During the last decades, a large number of CSPs have been developed to achieve chiral separation of a wide variety of racemic compounds and enantio-separations on CSPs has thus far been one of the most popular applications of SFC [129,133,134]. A wide range of CSPs have been used in SFC including Pirkle type, cyclodextrins and derivatized polysaccharide-based CSPs. The polysaccharide-based stationary phases, mainly the tris(3,5-dimethylphenylcarbamate) of amylose (Chiralpak AD) and cellulose (Chiralcel OD), have proven to be two of the most successful and widely applied CSPs due to the high number of compounds resolved in normal phase mode. Fortuitously, these polysaccharide-based stationary phases are also among the most successful in chiral SFC applications. The derivatized polysaccharide phase, Chiralcel OD-H, incorporates a cellulose carbamate derivative coated on silica gel as the chiral selector and has been used to separate R-timolol and S-timolol as described above.

Although fundamental studies of the chiral recognition mechanisms on polysaccharide CSPs have been reported, [135-137] a clear description of the chromatographic processes operating on these CSPs is still missing. However, a clear difference in enantioselectivity has been observed between SFC and LC modes with hydrogen bonding being found to play an important role in the differential binding of the enantiomers to the CSPs in SFC applications [134]. Consequently, method development in chiral SFC, as in chiral NP-HPLC, generally relies on a systematic screening of CSPs and mobile phases, in a preferential order or in parallel based on personal experience of the analyst. However, with shorter retention times compared to conventional NP-HPLC, method development with chiral SFC is faster without sacrificing efficiency [129]. The mobile phase components to be optimised are relatively limited, with only a few organic modifiers commonly used and investigations into the effect of pH generally omitted with CO<sub>2</sub>-based mobile phases. As with NP-HPLC, temperature can play a significant role in SFC method development particularly in chiral separations [138].

With this in mind, the aim of this study was to develop an alternative pSFC limit test assay for the determination of S-timolol maleate enantiomeric purity and compare it to the current EP NP-HPLC compendial method of analysis which uses a cellulose tris(3,5-dimethylphenylcarbamate) coated silica stationary phase [104,107,109,110] under normal phase conditions [103]. The developed method was compared with the existing normal phase method using standard analytical performance criteria.

## **2.2 Experimental**

### **2.2.1 Instrumentation and Software**

Both NP-HPLC and pSFC assays were carried out on a 4.6 mm x 250 mm Chiralcel OD-H column packed with 5 µm silica particles coated with cellulose tris(3,5-dimethylphenylcarbamate) from Daicel Limited Industries (Tokyo, Japan). The NP-HPLC assay was performed on a Waters Alliance 2695 HPLC system coupled with Waters 2487 Dual Wavelength Absorbance Detector (Waters, Milford, MA, USA). Chromatographic data was acquired and processed using Waters Empower<sup>TM</sup> 2 software. For the optimised NP-HPLC assay the mobile phase of hexane/2-propanol/DEA (960:40:2) was delivered at 1.0 mL.min<sup>-1</sup> at ambient column temperature [103]. Injection volume was 5 µL and detection was by UV at 297 nm with data acquisition at 5 Hz. The pSFC method development and validation was performed on an Agilent 1260 Infinity Analytical SFC system coupled with an

Aurora SFC Fusion A5 CO<sub>2</sub> delivery system equipped with a DAD detector (Agilent Technologies, Santa Clara, CA, USA). Chromatographic data was acquired and processed using Agilent Chemstation Rev B.04.03 software. For the optimised pSFC assay, the mobile phase of (93:7) CO<sub>2</sub>/0.1% (v/v) triethylamine (TEA) in MeOH was delivered isocratically at a flow rate of 4.0 mL.min<sup>-1</sup>. Column temperature was set to 40 °C with backpressure regulation set to 130 bar. An injection loop of 5 µL was over-filled with 15 µL of sample and peaks were detected at 297 nm with data acquisition at 20 Hz.

### 2.2.2 *Materials and Reagents*

Samples of S-timolol maleate and R-timolol base and impurities B, C, D and F were obtained from the EP Secretariat (Strasbourg, France). (**Note:** R-timolol is also known as Impurity A). *N*-hexane of LC grade was purchased from Romil (Waterbeach, Cambridge, UK). Methylene chloride, HPLC grade MeOH and 2-propanol was from Merck (Darmstadt, Germany), and reagent grade DEA and reagent grade TEA from Sigma Aldrich (Dublin, Ireland). Food grade CO<sub>2</sub> (99.9% v/v minimum) was purchased from BOC Ltd. (Dublin, Ireland).

### 2.2.3 *Solution preparation for Timolol NP-HPLC analysis*

**Note:** Solution preparation for the NP-HPLC assay and the SFC assay (below) is also detailed in Table 2.1 for the sake of clarity.

All standard solutions were prepared (and diluted as appropriate) in methylene chloride/2-propanol (10:30) using actinic glassware to protect from light. Two stock standards of S-timolol maleate and one stock standard of R-timolol were prepared based on timolol free base at 9.5 mM and 7.6 x 10<sup>-2</sup> mM respectively. Both S-timolol maleate stock standards were diluted to 9.5 x 10<sup>-2</sup> mM for recovery and method precision studies. A racemic mixture containing S-timolol maleate and R-timolol at a concentration of 4.7 x 10<sup>-2</sup> mM was prepared from stock standard dilutions and used as a control resolution mixture (CRM) to assess R<sub>s</sub> and to calculate a relative response factor (RRF) for R-timolol relative to S-timolol maleate. Finally, a solution of S-timolol maleate and R-timolol was prepared at 9.5 x 10<sup>-2</sup> mM and 9.5 x 10<sup>-4</sup> mM respectively (R-timolol concentration being equivalent to 1.0 % of the S-timolol maleate concentration). This solution was used to generate data for comparative purposes with the pSFC method.

#### **2.2.4 Solution preparation for Timolol pSFC analysis**

All standard solutions were prepared in 100% MeOH using actinic glassware. Four stock standards of S-timolol maleate and three stock standards of R-timolol were prepared based on timolol free base at 28 mM and  $2.3 \times 10^{-1}$  mM respectively. Two of the S-timolol maleate stock standards were diluted to  $2.8 \times 10^{-1}$  mM for recovery and method precision studies. Standards were prepared containing S-timolol maleate at  $2.8 \times 10^{-1}$  mM and R-timolol at  $5.7 \times 10^{-3}$  mM,  $2.8 \times 10^{-3}$  mM,  $1.4 \times 10^{-3}$  mM,  $2.8 \times 10^{-4}$  mM,  $1.4 \times 10^{-4}$  mM, equivalent to 2.0, 1.0, 0.5, 0.1 and 0.05 % of the S-timolol maleate concentration. These standards were used for validation of the SFC method. A solution containing S-timolol maleate and R-timolol at  $1.4 \times 10^{-1}$  mM was prepared as a CRM to assess  $R_s$  and to calculate an RRF for R-timolol maleate relative to S-timolol maleate.

#### **2.2.5 Solution preparation for evaluation of Timolol pSFC Specificity**

A solution was prepared containing all of the EP timolol specified impurities i.e. **B** ((2*RS*)-3-[(1,1-dimethylethyl)amino]-2-[[4-(morpholin-4-yl)-1,2,5-thiadiazol-3-yl]oxy]propan-1-ol), **C**((2*RS*)-*N*-(1,1-dimethylethyl)-2,3-bis[[4-(morpholin-4-yl)-1,2,5-thiadiazol-3-yl]oxy]propan-1-amine), **D**(4-(morpholin-4-yl)-1,2,5-thiadiazol-3-ol), **E** ((2*Z*)-4-[(1*S*)-1-[(1,1-dimethylethyl)amino]methyl]-2-[[4-(morpholin-4-yl)-1,2,5-thiadiazol-3-yl]oxy]ethoxy]-4-oxobut-2-enoic acid) and **F** (4-(4-chloro-1,2,5-thiadiazol-3-yl)morpholine) by dissolving 5 mg of the timolol for system suitability standard obtained from the EP Secretariat (Strasbourg, France) in 1 mL of MeOH. Impurity E was generated as described in the EP [103] by reacting timolol maleate (2 mg) with maleic acid (20 mg) in acetonitrile (10 mL). 1 mL of this solution was then evaporated under nitrogen before being dried at 105 °C for 1 hour. The reagent was then reconstituted with 1 mL of MeOH. 200 µL of the Impurity E solution was added to a vial of EP system suitability mix (containing impurity B, C, D and F) containing 800 µL of MeOH to generate an impurity mix solution containing all of the specified timolol impurities.

### **2.3 Results and discussion**

#### **2.3.1 Timolol pSFC Method Development**

All pSFC development work was carried out on same Chiralcel OD-H cellulose tris(3,5-dimethylphenylcarbamate) stationary phase as was used for the NP-HPLC assay [103,108]. This stationary phase was selected primarily so that a direct comparison could be made between the pSFC method described here, and the previously developed NP-HPLC assay.

Furthermore, a recent report by Khater *et al.* [139] reveals that the Chiralcel OD-H stationary phase still offers the most versatility when compared with four generic versions of the Chiralcel OD (CelluCoat, RegisCell, Lux Cellulose-1, Reprosil OM) and the immobilised version (ChiralPak IB). For these reasons, alternative CSPs were not used during method development.

A CRM was prepared containing the R-timolol and S-timolol at  $1.4 \times 10^{-1}$  mM which was used to assess the chromatography. The chromatography was assessed in the first instance by measuring  $R_s$  between the enantiomers but these initial screening studies using MeOH alone as the modifier resulted in very poor peak shape and correspondingly poor sensitivity as shown in Figure 2.8(a). In HPLC separations, poor peak shape due to tailing issues and in some cases, a lack of peak elution have been attributed to the presence of so called “active sites” on the surface of the stationary phase support [140]. For silica based columns, these active sites usually consist of different types of residual silanol groups (germinal, vicinal etc.) or metal ion contamination resulting from the stationary phase manufacturing process. The presence of these active sites can result in an unwanted competing secondary retention mechanism resulting in severe tailing. Additives are very polar substances that are added to the mobile phase in low concentrations and are expected to facilitate solute elution and improve peak shapes by covering up, adsorbing onto or even reacting with these so called active sites [140].

In pSFC, additives appear to have four major functions; (1) Coverage of so called “active sites”, (2) Altering the polarity of the stationary phase, (3) Altering the polarity of the mobile phase or (4) Suppression of ionization or ion pair formation by solutes. Although the functions of additives can be broadly defined, the exact role of additives in pSFC still remains unclear with further study required if a mechanistic understanding of their actions is to be achieved. Due to the lack of comprehensive understanding of all the secondary retention mechanisms that give rise to poor peak shape and tailing in pSFC, there are generally no set rules when it comes to choosing an additive for a given separation other than the additive being a stronger acid or stronger base than the sample components being separated as well as being compatible with the choice of detector. In general, acidic additives should be used for acidic solutes and basic additives for basic solutes [140]. The  $pK_a$  of timolol base has been reported as 9.2 (determined via potentiometric titration in water at 25 °C) [141] and so TEA was selected as the basic additive and added to the MeOH modifier at 0.1% (v/v). This concentration was selected based upon reports by Aboul-Enein *et al.* who selected 0.4% (v/v)

DEA in their NP-HPLC assay, observing that the absence of base on the mobile phase resulted in no separation, whereas higher levels (1% v/v) could result in damage to the silica support particle [104].

The effect of the additive was immediate, with peak shape and sensitivity being dramatically improved as shown in Figure 2.8(b). Elution order remained unaffected but  $R_s$  of 2.82 and peak asymmetries of 0.82 for both R-timolol and S-timolol was achieved by the inclusion of the additive to the mobile phase. Although other workers [109,110] and the EP monograph [103] have indicated the use of DEA as the basic additive in NP-HPLC assays, in the work presented herein, no further efforts were made to investigate the effect of alternative basic additives or the effect of TEA concentration, since adequate  $R_s$  was achieved for the purposes of a limit test.

**Table 2.1:** Solution preparation for NP-HPLC and pSFC analysis

<b>Solutions for NP-HPLC</b>				
<b>Diluent</b>	<b>Solution</b>	<b>Analyte</b>	<b>Concentration (mM)<sup>a</sup></b>	<b>% R-timolol w.r.t S-timolol</b>
Methylene chloride/2-propanol (10:30)	R-timolol Stock standard	R-timolol	$7.6 \times 10^{-2} \text{ mM}$	<i>n/a</i>
	S-timolol Stock standard	S-timolol	$9.5 \text{ mM}$	
	Recovery/method precision standards	S-timolol	$9.5 \times 10^{-2} \text{ mM}$	
	CRM mixture	R-timolol S-timolol	$4.7 \times 10^{-2} \text{ mM}$	
	S-timolol/R-timolol spiked standards	R-timolol S-timolol	$9.5 \times 10^{-4} \text{ mM}$	
<b>Solutions for pSFC</b>				
<b>Diluent</b>	<b>Solution</b>	<b>Analyte</b>	<b>Concentration (mM)<sup>a</sup></b>	<b>% R-timolol w.r.t S-timolol</b>
MeOH	R-timolol Stock standard	R-timolol	$2.3 \times 10^{-1} \text{ mM}$	<i>n/a</i>
	S-timolol Stock standard	S-timolol	$28 \text{ mM}$	
	Precision studies	S-timolol	$2.8 \times 10^{-1} \text{ mM}$	
	S-timolol/R-timolol spiked standards	R-timolol	$5.7 \times 10^{-3} \text{ mM}, 2.8 \times 10^{-3} \text{ mM}, 1.4 \times 10^{-3} \text{ mM},$ $2.8 \times 10^{-4} \text{ mM}, 1.4 \times 10^{-4} \text{ mM},$	2.0%, 1.0%, 0.5%, 0.1%, 0.05%
		S-timolol	$2.8 \times 10^{-1} \text{ mM}$	
	CRM mixture	R-timolol S-timolol	$1.4 \times 10^{-1} \text{ mM}$	50%

<sup>a</sup> Based on timolol free base M.W. 316.4 g

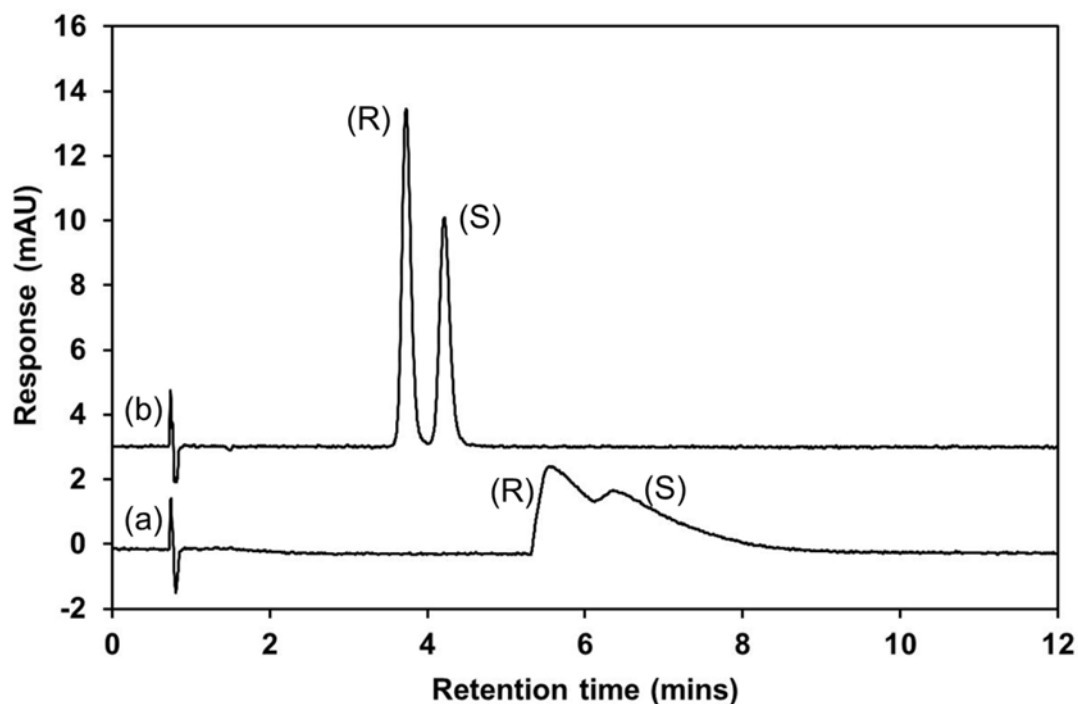


**Figure 2.8:** Separation of *R*-timolol and *S*-timolol via pSFC using a mobile phase without (a) and with (b) the presence of 0.1% (v/v) TEA of the MeOH modifier. Chromatographic conditions; Column: 4.6 mm x 250 mm Chiralcel OD-H, 5  $\mu$ m. Flow rate: 4.0 mL.min<sup>-1</sup>. Injection volume: 15  $\mu$ L. Column temperature: 40 °C. Back-pressure regulation: 130 bar. Detection: 297 nm. Mobile phase: (93:7) CO<sub>2</sub>/MeOH for chromatogram (a) and (93:7) CO<sub>2</sub>/0.1% (v/v) TEA in MeOH for chromatogram (b). Peak assignment and concentration: (R): *R*-timolol at  $1.4 \times 10^{-1}$  mM and (S): *S*-timolol at  $1.4 \times 10^{-1}$  mM.

The remainder of the development work involved performing optimisation experiments in which flow rate and mobile phase composition were adjusted to reduce runtimes for increased sample throughput, while maintaining USP  $R_s > 2$  and peak tailing  $< 1.5$  for both enantiomers in the CRM. Isocratic methods were favoured over gradient methods to eliminate the necessary system equilibration time after each run. A series of chromatograms were generated with varying amounts of modifier. The selected optimised conditions described above were used with modifier concentrations of 3, 5, 7, 9, 11, 15, and 20% (v/v) respectively. For this investigation, the CRM contained both *R*- and *S*-timolol at a concentration of  $1.4 \times 10^{-1}$  mM. A plot of  $k$  and  $R_s$  values versus % modifier concentration is shown in Figure 2.10 where the non-linear effect of modifier concentrations on the retention factors of *R*-timolol and *S*-timolol is demonstrated. As expected, retention decreased steadily as % MeOH increased with a corresponding decrease in resolution at higher modifier

contents. For example, 20% MeOH (containing 0.1% TEA) resulted in resolution of 0.7 whereas with 10% modifier the resolution was 1.5.

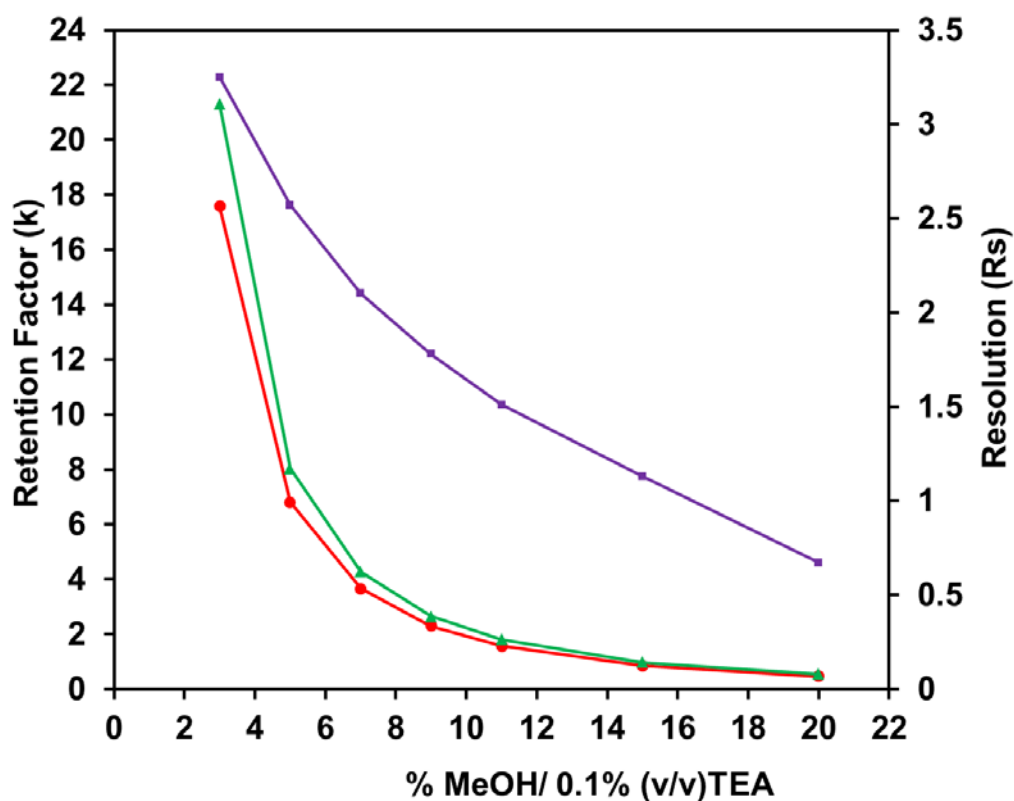


**Figure 2.9:** Plot of retention factor ( $k$ ) of *R*-timolol (red) and *S*-timolol (green) along with resolution ( $R_s$ ) between *R*-timolol and *S*-timolol (purple) versus % MeOH/0.1% (v/v) TEA concentration via pSFC. Chromatographic conditions as in Figure 2.8(b).

As a compromise between runtime and  $R_s$  a final mobile phase composition of (93:7)  $\text{CO}_2$ /0.1 % (v/v) TEA in MeOH at a flow rate of  $4.0 \text{ mL}\cdot\text{min}^{-1}$  was selected as optimum which resulted in a 5 min runtime and  $R_s$  of 2.01 between the enantiomers. Both enantiomers eluted within a retention time window of just 0.5 min as shown in Figure 2.10(a) with chromatographic efficiency of 18,064 N/m and 18,676 N/m observed *R*-timolol and *S*-timolol respectively for pSFC method; versus 18,464 and 18,342 for the EP method. The developed SFC method is therefore three times faster than the optimised normal phase separation described by Marini *et al.* [109,110] and the EP method reproduced in Figure 2.10(b) for comparative purposes. The EP method [103] also specifies a  $R_s$  of 4.0 between the enantiomers using this stationary phase and mobile phase system. While this large  $R_s$  requirement may seem excessive, based on Figure 2.4 it is evident that the  $R_s$  was

chosen to allow for detection of Impurity B (isotimilol), which is observed to elute between the R-timolol and S-timolol peaks under the method conditions specified in the EP. Furthermore, the optimised pSFC method is also over twice as fast as the CE method described by Hedeland *et al.* [111] and three times faster than the NACE methods described by Servais *et al.* [112] and Marini *et al.* [113] based upon the migration time of the second enantiomer. As such, this pSFC method represents an improvement over previously published enantio-separations of timolol maleate. (It should be noted that the injection cycle time was < 21 sec and therefore did not contribute significantly to overall runtimes). To help improve pSFC method the limit of detection, timolol concentrations were increased threefold compared to the NP-HPLC assay for the pSFC method validation.

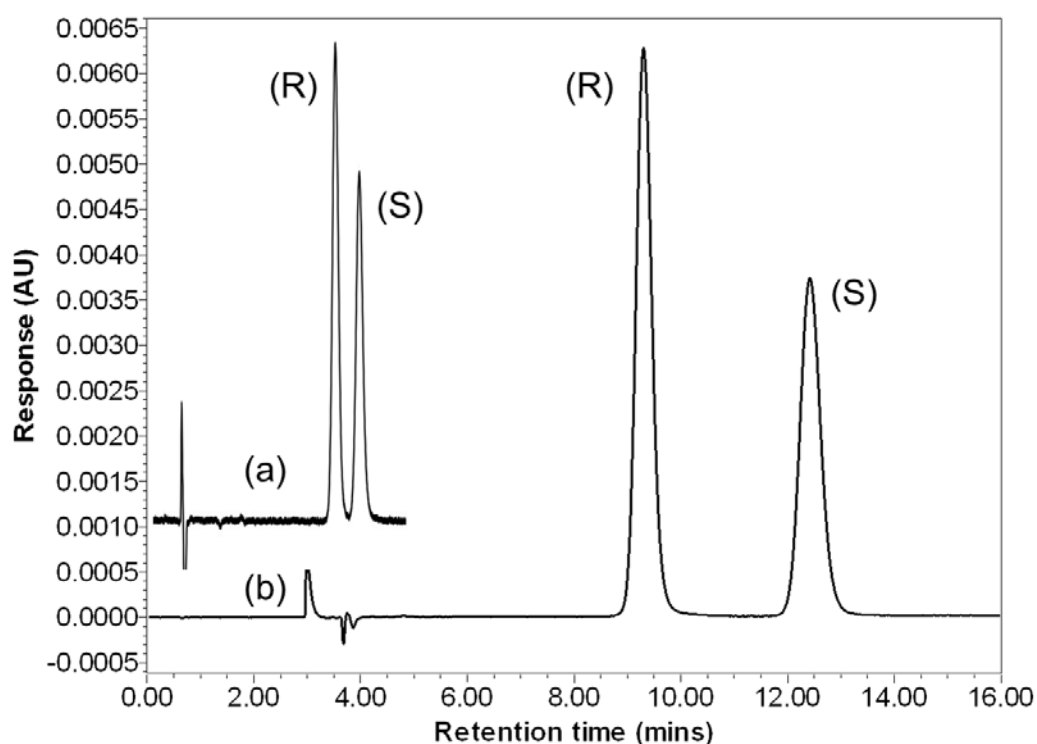


**Figure 2.10:** Comparison of optimised pSFC separation (a) and normal phase separation (b) of timolol enantiomers. Chromatographic conditions for (a) are as given in Figure 2.8(b). Chromatographic conditions for (b); Column: 4.6 mm x 250 mm Chiralcel OD-H, 5  $\mu$ m. Mobile phase: hexane/2-propanol/DEA (960:40:2). Flow rate: 1.0 mL.min<sup>-1</sup>. Injection volume: 5  $\mu$ L. Column temperature: Ambient. Detection: UV at 297 nm [103].

### **2.3.2 Timolol pSFC Method Validation**

The pSFC method was developed to offer an alternative to the existing NP-HPLC assay currently in use within industry (Allergan Pharmaceuticals) and reported by Marini *et al.* [109,110]. R-timolol is an unwanted impurity in S-timolol drug substance and in the pharmaceutical industry, the purity of an active pharmaceutical ingredient can be determined using either a limit test or a quantitative test. The NP-HPLC assay is described in the EP [103] as a limit test based upon a specification of not more than (NMT) 1.0% of R-timolol in the presence of S-timolol. The ICH requirements for the validation of a limit test are specificity and LOD [142]. Therefore, in the first instance, these two analytical performance criteria were initially evaluated to demonstrate the applicability of the developed SFC method as a limit test and the results are evaluated below. For a quantitative test relative to a “limit test”, additional analytical performance characteristics must be evaluated, namely: accuracy, precision, LOQ, linearity, range and robustness [142,143]. Therefore, further selected validation criteria were then studied to demonstrate the additional potential of this method as a quantitative test for R-timolol impurity in S-timolol and the results presented hereafter.

#### **2.3.2.1 Validation of Timolol pSFC Method as a Limit Test – Specificity and LOD**

The LOD is defined as the smallest quantity of the target substance (in this case, R-timolol) that can be detected relative to baseline noise, but not accurately quantified in the sample [142]. Baseline noise was compared with the peak height of a standard containing 0.5% R-timolol in the presence of S-timolol as seen in Figure 2.11 below. The magnitude of baseline noise was measured in a blank chromatogram over a distance equivalent to 5 times the peak width at half height of the R-timolol peak, centred around its expected retention time (noise window: 3.8 min). The LOD results are summarised in Table 2.2 and indicate that the LOD was found to be 0.5% for R-timolol in the presence of S-timolol maleate, satisfying the requirement for the limit test method [103] to be able to detect R-timolol at the 1.0% level of the S-timolol maleate peak.

The specificity of a method is defined as the ability to assess unequivocally the analyte in the presence of components which may be expected to be present [142]. The EP specifies five impurities shown in Figure 2.1 which can potentially be present in S-timolol drug substance; Impurity A (R-timolol), Impurity B (isotimolol), Impurity C, Impurity D, Impurity E and Impurity F [103]. A commercially available EP impurity system suitability mixture comprising S-timolol spiked with all known impurities was used to assess the

specificity of the method (Impurity E was added separately to this mixture). However, only Impurity A (R-timolol) and Impurity E could be individually identified by retention time. Nevertheless Figure 2.12 clearly indicates that all five impurity peaks are baseline separated from R- and S-timolol, demonstrating the specificity of the method for the determination of R-timolol in S-timolol drug substance.

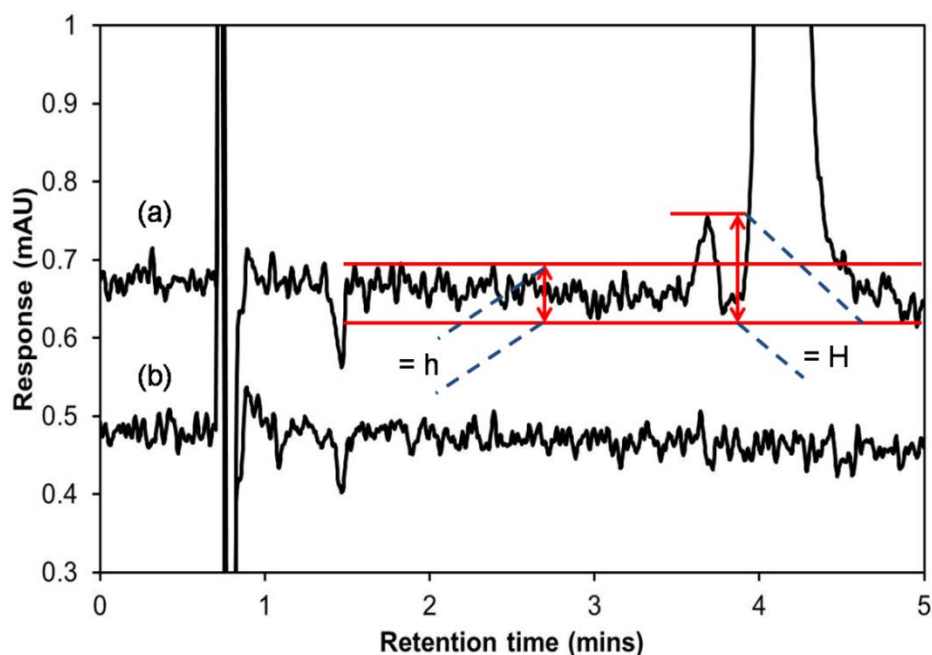


**Figure 2.11:** Chromatograms of (a), pSFC sample containing R-timolol at the LOD of 0.5% in the presence of S-timolol maleate demonstrating the USP signal-to-noise (SN) calculation  $2(H)/h$  [143]. (b), MeOH blank demonstrating specificity and the low baseline noise. Chromatographic conditions are as given in Figure 2.8(b).

### 2.3.2.2 Investigation of Timolol pSFC Method as a potential Quantitative Impurities

#### Assay

The additional analytical performance characteristics evaluated to demonstrate the potential of the method for quantitative analysis for R-timolol impurity in S-timolol were; precision, robustness and accuracy.

### 2.3.2.3 Timolol pSFC Precision studies: Repeatability and Intermediate Precision

The repeatability of the pSFC method was evaluated by preparing a standard containing R-timolol at 1.0% relative to S-timolol maleate concentration and injecting six times on Day #1. Intermediate precision was determined by preparing two separate fresh preparations

of the standard on Day #2 and injecting each six times. As shown in Table 2.2, the relative standard deviations (% RSD) values were  $\leq 2.7\%$  for both repeatability and intermediate precision. Retention time precision for R-timolol was  $\leq 0.1\%$  within day and between days.

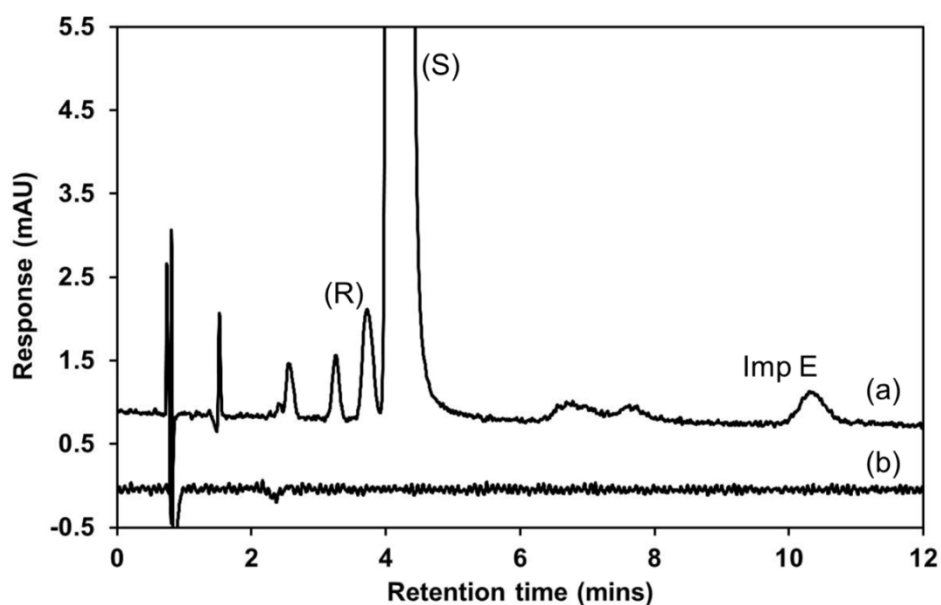


**Figure 2.12:** Chromatograms of (a) EP timolol for system suitability CRS spiked with Imp E demonstrating  $R_s$  of all specified impurities from R-timolol, (b) MeOH blank. Chromatographic conditions are as given in Figure 2.8(b).

#### 2.3.2.4 Timolol pSFC Robustness

The robustness of an analytical method is a measure of its ability to remain unaffected by small, but deliberate changes in method parameters and provides an indication of its reliability of the analytical method during normal usage. In this study, based both upon ICH Q2R1 recommendations [142], the experimental conditions that were altered were: flow rate ( $\pm 0.5 \text{ mL}\cdot\text{min}^{-1}$ ), column temperature ( $\pm 5 \text{ }^\circ\text{C}$ ) and column back-pressure ( $\pm 10 \text{ bar}$ ). The range of variance was selected to evaluate method robustness in the event that a different SFC instrument (with different performance characteristics) was used with the method. Firstly, for each selected experimental condition, three injections of the CRM mixture were made and standard chromatographic performance criteria were evaluated, namely: relative retention time (RRT); i.e. the ration of R-timolol retention time versus S-timolol retention time,  $R_s$ , selectivity and peak symmetry. When compared with the chromatogram obtained under optimised conditions (Figure 2.13), deviations in chromatographic performance were not significant as shown in Table 2.2 and in all cases,  $R_s$  was  $\geq 1.9$ . Specifically, RRT

changed by only 1%,  $R_s$  by 10%, selectivity by < 1% and peak symmetry by 3%. Furthermore, for each condition investigated, six injections of an R-timolol standard (at 1.0% with respect to S-timolol) were made and changes in repeatability, if any, were evaluated. Relative to the optimum chromatographic conditions, there was no significant effect upon repeatability as shown in Table 2.2, demonstrating that the method is capable of maintaining the desired performance regardless of the robustness challenges under investigation. The equivalency of chromatographic performance at each stress condition relative the optimum conditions was evaluated by calculating the ratio of the means, with equivalency of 1.0 reported in all cases (See Table 2.2).

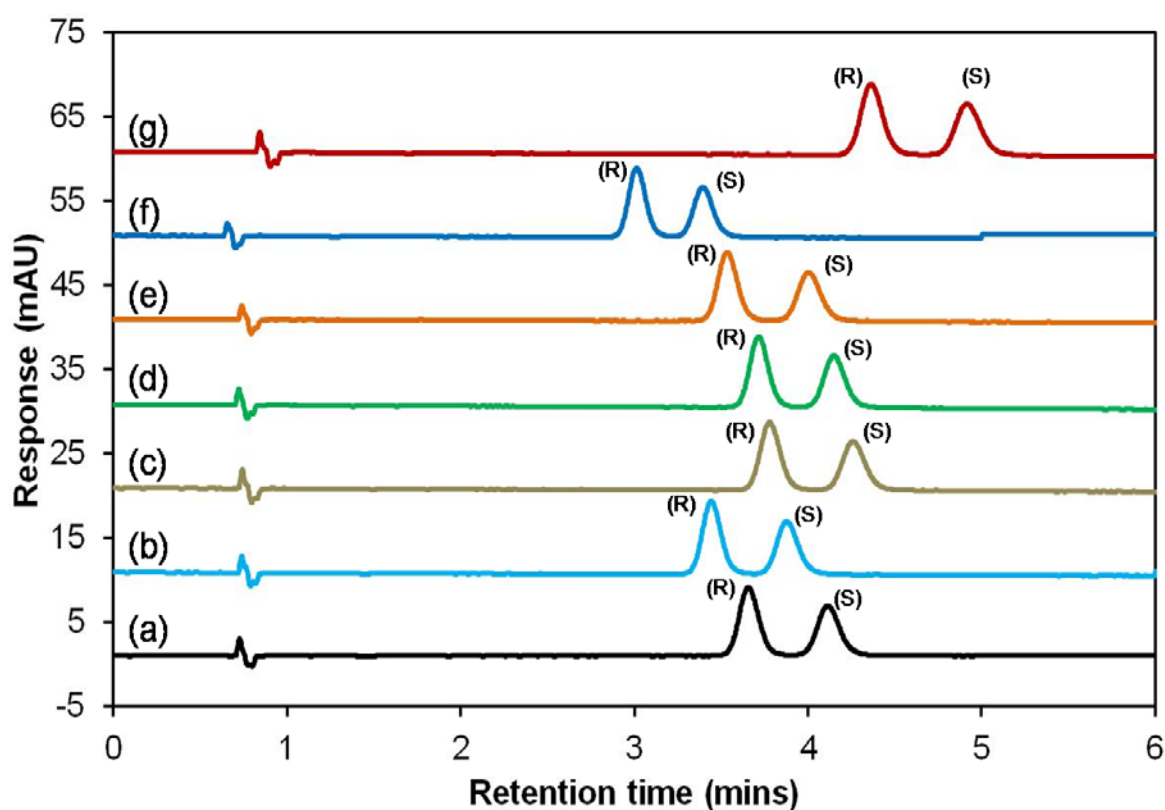


**Figure 2.13:** Typical chromatograms of the CRM containing R-timolol and S-timolol maleate at  $1.4 \times 10^{-1}$  mM. under robustness conditions (a), Optimal (b), 140 bar (c), 120 bar (d), 45 °C (e), 35 °C (f), 4.5 mL.min<sup>-1</sup> and (g), 3.5 mL.min<sup>-1</sup>. R-timolol peak elutes first. Chromatographic conditions are given in Figure 2.8(b).

### 2.3.2.5 Timolol pSFC Accuracy

To assess the accuracy of the 1.0% R-timolol sample solutions used in the validation studies for both the HPLC and pSFC methods, S-timolol was used as an external bracketing standard.

To eliminate differences in UV response between R-timolol and S-timolol, relative response factors (RRF) were generated by calculating the differences in peak area versus concentration for the CRM solution, since both enantiomers were present at the same concentration. The RRF values for both the HPLC and pSFC methods are shown in Table 2.2. Recovery values of 98% and 101% are reported for R-timolol in the NP-HPLC and pSFC methods respectively.

### **2.3.3 Analytical Performance Comparison: pSFC versus NP-HPLC**

The pSFC method offered comparable performance to the NP-HPLC method in terms of peak response, precision and detection limit (with increased sample concentration). A comparison of the pSFC and NP-HPLC methods is outlined in Table 2.3. For comparative purposes, Figure 2.14 illustrates chromatograms from both methods in which the benefits of pSFC over NP-HPLC in terms of analysis time and solvent consumption are obvious. To our knowledge Figure 2.14 represents the fastest enantiomeric separation of timolol enantiomers reported to date.

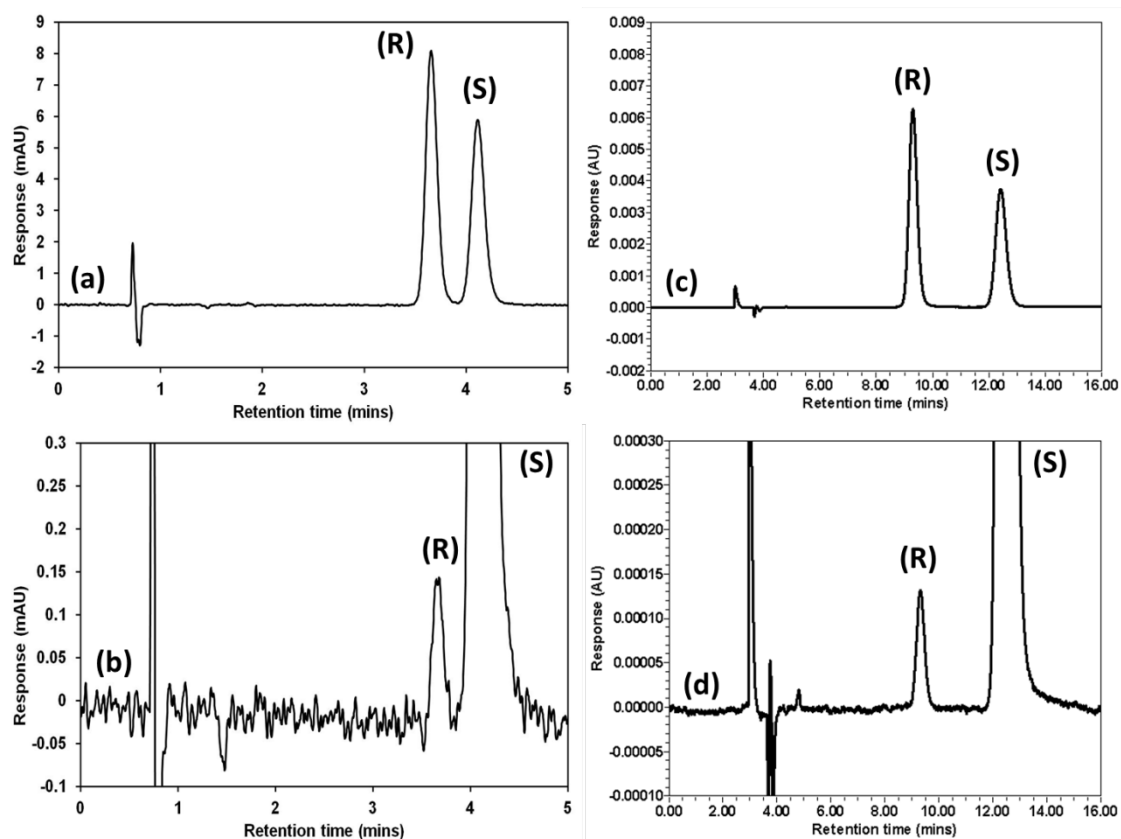


**Figure 2.14:** Typical chromatograms comparing pSFC (a,b) and NP-HPLC (c,d) for the analysis of R-timolol in the presence of S-timolol maleate. Chromatograms (a,c) are the CRM, and (b,d) are R-timolol at 1.0% with respect to S-timolol. Chromatographic conditions for (a,b) are as given in Figure 2.8(b). Chromatographic conditions for (c,d) are given in Figure 2.10.

**Table 2.2:** Analytical performance for determination of R-timolol impurity in S-timolol maleate

<b>Robustness</b>							
Condition	R-timolol RRT <sup>b</sup>	Rs <sup>b,c</sup>	Selectivity <sup>b</sup>	R-timolol peak symmetry <sup>b</sup>	S-timolol peak symmetry <sup>b</sup>	R-timolol % area <sup>d</sup>	Equivalency <sup>e</sup>
Optimum conditions <sup>a</sup>	0.89	2.0	1.12	0.89	0.86	1.05	1.0
Flow rate: 4.5 mL.min <sup>-1</sup>	0.89	1.9	1.13	0.90	0.86	1.03	1.0
Flow rate: 3.5 mL.min <sup>-1</sup>	0.89	2.2	1.13	0.86	0.85	1.05	1.0
Column temperature: 35 °C	0.88	2.0	1.13	0.90	0.83	1.07	1.0
Column temperature: 45 °C	0.90	2.0	1.12	0.92	0.86	1.05	1.0
Backpressure: 120 bar	0.89	2.1	1.13	0.88	0.85	1.08	1.0
Backpressure: 140 bar	0.89	2.0	1.13	0.90	0.84	1.08	1.0
<b>Repeatability and intermediate precision</b>							
	Standard 1		Standard 2		Standard 3		
	Day-1	Day-2	Day-1	Day-2	Day-1	Day-2	
R-timolol retention time % RSD	< 0.1%	< 0.1%	< 0.1%	< 0.1%	< 0.1%	< 0.1%	< 0.1%
R-timolol peak area % RSD	2.1%	1.8%	2.7%	2.0%	2.0%	2.7%	
<b>Limit of detection</b>							
	S/N	% area					
R-timolol	3.4	0.52					
<b>Accuracy</b>							
R-timolol	101%						

<sup>a</sup> Flow rate: 4.0 mL.min<sup>-1</sup>, Column temperature: 40 °C, backpressure regulation: 130 bar.

<sup>b</sup> n=3.

<sup>c</sup> R<sub>s</sub> calculated as  $R = 2(t_{r1} - t_{r2}) / (W_{B(1)} - W_{B(2)})$

<sup>d</sup> n=6

<sup>e</sup> Ratio of analytical performance criterion versus performance under optimum conditions

**Table 2.3:** Comparison between HPLC and pSFC analytical conditions and performance

Parameters	NP-HPLC	pSFC
Column	Chiracel OD-H <sup>®</sup> Cellulose tris (3,5-dimethylphenylcarbamate) 5 $\mu$ m, 250 x 4.6 mm i.d.	
Column temperature	Ambient	40 °C
Flow rate	1.0 mL.min <sup>-1</sup>	4.0 mL.min <sup>-1</sup>
Detection	297 nm 5Hz acquisition rate	297 nm 20Hz acquisition rate
Flow cell	10 mm path length, 10 $\mu$ L volume flow cell	10 mm path length, 13 $\mu$ L volume high pressure flow cell
Injection volume	5 $\mu$ L on a 100 $\mu$ L loop	15 $\mu$ L on a 5 $\mu$ L loop
Back pressure	-	130 bar
Analysis type	Isocratic	Isocratic
Run time	16 min	5 min
Mobile phase	Mixture of DEA, 2-propanol and hexane (2:40:960)	93 % supercritical fluid CO <sub>2</sub> , 7 % MeOH containing 0.1% (v/v) TEA
Sample diluent	Mixture of methylene chloride and 2-propanol a (10:30)	MeOH
R-timolol RRF CRM	0.80	0.83
R-timolol RRT CRM	0.75	0.89
R-timolol, S-timolol tailing factors	1.2, 1.3	1.1, 1.1
R-timolol, S-timolol plate count	18,064 N/m, 18,676 N/m	18,464 N/m, 18,342 N/m
Resolution CRM	4.8	2.0
S-timolol peak area repeatability <sup>a</sup>	0.4%	0.2%
R-timolol peak area repeatability <sup>b</sup>	2.5%	2.1%
% recovery of R-timolol	98% <sup>c</sup>	101% <sup>c</sup>
S-timolol working standard concentration	9.5 x 10 <sup>-2</sup> mM	1.4 x 10 <sup>-1</sup> mM
Analysis time per sample	16 min	5 min
Solvent usage per sample	16 mL	1.4 mL

<sup>a</sup> (n = 6)<sup>b</sup> 1.0% R-timolol in S-timolol, (n=6)<sup>c</sup> 1.0% R-timolol in S-timolol

## 2.4 Conclusion

A pSFC method has been described in which the R- and S-enantiomers of timolol have been separated on a Chiralcel OD-H stationary phase within 5 min, representing a 3-fold decrease in runtime and an 11-fold decrease in solvent consumption relative to the industry standard, EP method based upon NP-HPLC [103]. The reduction in runtime is due in part to the restrictive  $R_s$  requirement between the R- and S-enantiomers placed on the EP method to allow for the detection of Impurity B (isotimolol). Based on the chromatographic evidence observed in Figure 2.12, Impurity B (isotimolol) does not elute between the R- and S-enantiomers under the pSFC conditions, hence the runtime could be reduced as only baseline  $R_s$  between the R- and S-enantiomers was required. Also, due to the low viscosity and high diffusivity of the pSFC mobile phase, a 4-fold increase in flow rate was possible, thus reducing the runtime for the pSFC method. The method validation parameters required for a limit test for R-timolol in S-timolol (specificity and detection limit) were established for the pSFC method. In addition, the potential of this method to be used for quantitation of R-timolol impurity was investigated by evaluation of further analytical performance criteria (robustness, precision, accuracy). Clearly the developed pSFC assay demonstrates potential as a full quantitative assay, and represents the fastest separation of timolol enantiomers to date, relative to previously reported NP-HPLC or NACE-based methods. Future work will involve the use of shorter chiral columns packed with smaller particles (3  $\mu\text{m}$ ) in order to further decrease runtimes in chiral pSFC. Dissolution of the samples in a more non-polar solvent such as heptane or heptane/isopropanol mixtures compared with MeOH may also result in improved chromatographic efficiency.

### **3.0 Chapter 3: Development and Validation of a new stability indicating Reversed Phase liquid chromatographic method for the determination of Prednisolone acetate and impurities in an ophthalmic suspension.**

#### **3.1 Introduction**

It is a technical requirement of the International Conference on Harmonization (ICH) for registration of pharmaceuticals for human use [144] that impurities present in an active pharmaceutical ingredient (API) as well as the final drug product be quantified and/or identified. Impurities may be derived from the API and/or final drug product manufacturing process or may be generated over time due to poor stability of either the API or drug product. Many process-related impurities have similar chemical structures as the API or can often co-elute with components of the drug product sample matrix, such that method specificity is a key analytical performance criterion for any chromatographic method used for drug product release testing or stability indicating assays.

Prednisolone acetate (PAC) is a synthetic glucocorticoid steroid which is used as the API either alone or in combination with an additional API in several commercial ophthalmic suspensions used for the treatment of a wide range of inflammatory conditions of the eye. PAC is produced by the esterification of prednisolone and is defined as a pro-drug with modified pharmacokinetic properties compared to prednisolone [145,146]. The usefulness of pro-drugs in ophthalmic drug delivery has been comprehensively discussed in a number of reviews [147,148]. Acetate ester pro-drugs such as PAC have been designed to increase the lipophilicity and the corneal absorption of the parent steroid [149-152]. Enzymatic transformation of pro-drugs in ocular tissues is often utilised for releasing the active drug. In fact, PAC hydrolyses completely to prednisolone in vitro and in vivo, and the enzymatic conversion is assumed to occur in the cornea [153,154]. Although ester pro-drugs are usually more stable in vitro than in vivo, they may exhibit chemical instability in aqueous eye-drop formulations [155]. Since PAC is vulnerable to enzymatic and chemical hydrolysis [156] it is important to monitor the concentration of PAC and related substances over time in such suspensions. Figure 3.1 illustrates the molecular structure of PAC along with its eight known impurities (and potential degradants).

There have been numerous publications reporting on the chromatographic determination of either prednisolone or PAC in tissue culture media [156] and various

biological fluids [157-163] including aqueous humour [157], human serum [158], plasma [159], urine [159,161,162] and swine plasma [160,163].

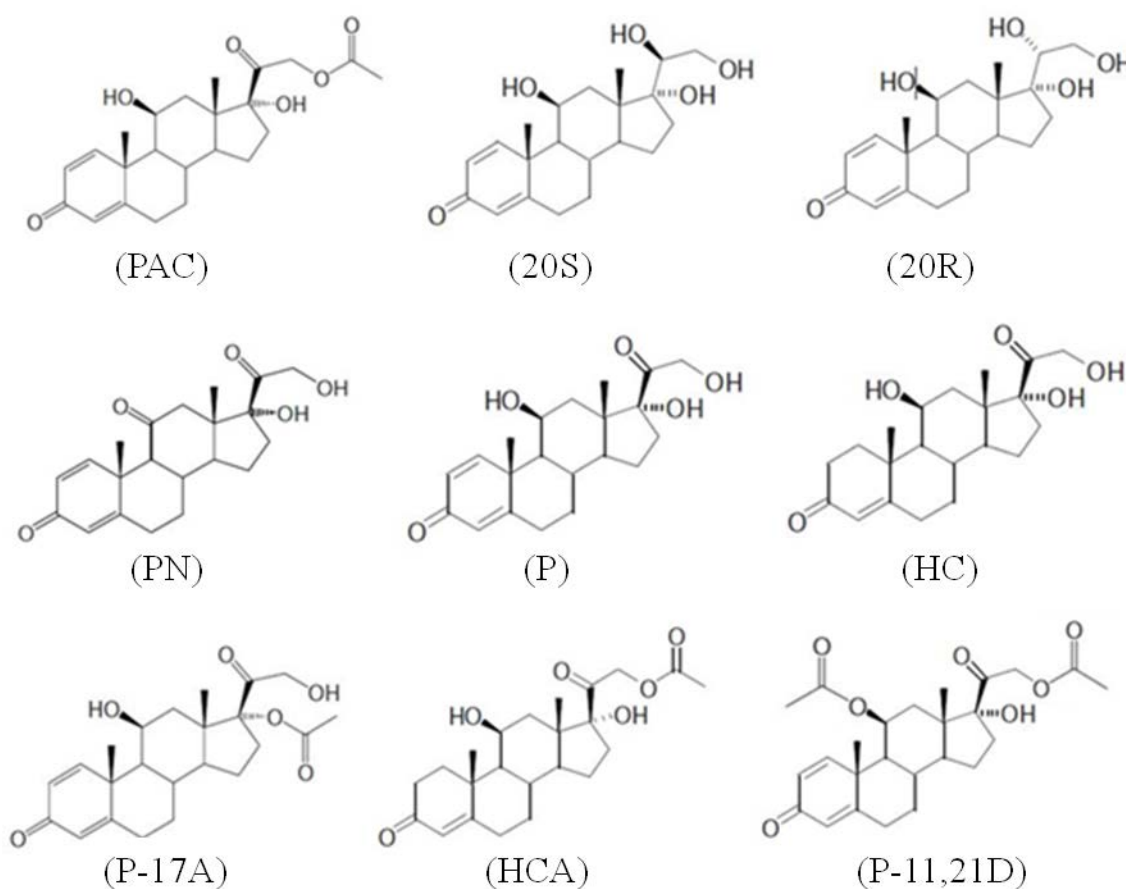


**Figure 3.1:** Molecular structure of Prednisolone Acetate (PAC) and impurities 20(S), 20(R), PN, P, HC, P-17A, HCA, P-11,21D reproduced from [173].

Fewer studies have been reported on the determination of PAC and related impurities (originating either from the manufacturing process or due to drug product/drug substance stability issues) in ophthalmic suspensions. Barot *et al.* reported on the determination of PAC and ofloxacin in eye drops using a spectrophotometric method, but the method did not permit quantitation of PAC impurities [164]. Musharraf *et al.* developed a stability indicating thin-layer chromatography method for PAC in the presence of its degraded products, generated by either acidic, alkaline or neutral hydrolysis, or oxidation and wet heating degradation [165]. The authors subsequently applied the method to “ophthalmic samples”. A number of micellar electrokinetic capillary chromatographic methods have been reported by Gallego *et al.* [166-168] for the determination of either prednisolone [166] or prednisolone acetate [167] in pharmaceutical products, but only reported one method [168] for the

simultaneous determination of both pharmaceuticals in the presence of other compounds (naphazoline, Zn-bacitracin, sulfacetamide and phenylephrine) in pharmaceutical products. The runtime was 8 min and limits of quantification were  $1.0 \text{ mg.L}^{-1}$  for all components, but again, the method was not applicable to the determination of PAC in the presence of all known impurities.

Reversed phase HPLC (RP-HPLC) assays have appeared in the literature [169-171] most notably the work of Razzaq *et al.* who developed and validated an isocratic separation of moxifloxacin and prednisolone on a BDS Hypersil C8 column using a methanol/phosphate buffer mobile phase [171]. The authors used the method as a stability indicating assay for both drug substances in selected pharmaceutical formulations which had been subjected to oxidative, thermal and other stress conditions. Nevertheless, impurities were neither identified nor quantified. The current USP monograph describes an isocratic RP-HPLC method for the assay of PAC in an ophthalmic suspension using a water/acetonitrile mobile phase (60:40) and a  $C_{18}$  (USP designation: L1) column [172]. While the method identifies the impurity prednisolone P, it is not quantitative for impurities. The European Pharmacopoeia describes a RP-HPLC method for the assay of PAC related substance in PAC drug substance [173]. The method is capable of identifying and quantifying PAC and three specified impurities; hydrocortisone acetate (HCA), P and prednisolone 11,21-diacetate (P-11,21D) which are quantified as a percentage of the PAC peak. However, despite an extensive review of the literature, no method has been reported for the quantitation of prednisolone acetate and all known impurities shown in Figure 3.1 in an ophthalmic suspension. With this in mind, we set out to develop and validate a stability indicating RP-HPLC method for the analysis of prednisolone acetate (PAC) and eight potential impurities in a drug product ophthalmic suspension. **Note:** P and prednisolone 17-acetate (P-17A) are degradants of PAC whereas HCA and P-11,21D are process impurities [173]. The European Pharmacopoeia specifies that hydrocortisone (HC), prednisone (PN), (20S)-hydroxyprednisolone (20(S)) and (20R)-hydroxyprednisolone (20(R)) are potential impurities of P; i.e. the main degradant of PAC. The ophthalmic suspension chosen for this work was proprietary formulation containing PAC at 1%. The developed method has potential as a stability indicating assay for PAC in ophthalmic suspension, capable of identifying and quantifying PAC impurities as well as potential P impurities. Method development, validation and preliminary accelerated stability studies is described herein.

## 3.2 Experimental

### 3.2.1 Instrumentation and Software

All assays were performed on a Waters Alliance 2695 HPLC system equipped with a Waters 2487 dual wavelength absorbance detector and a Waters 2996 photodiode array (PDA) detector (Waters, Milford, MA, USA). The detection wavelength was 254 nm with data acquisition at 5 Hz. The column for the modified version of the USP RP-HPLC method [174] was a Waters  $\mu$ Bondapak C<sub>18</sub> (10  $\mu$ m) 3.9 mm x 300 mm column (Waters, Milford, MA, USA). The injection volume was 30  $\mu$ L and the mobile phase of acetonitrile/water (40:60) was delivered at 2.0 mL.min<sup>-1</sup> at ambient column temperature. The gradient RP-HPLC method was developed and validated on an Agilent Poroshell 120 EC-C<sub>18</sub> 100 mm x 4.6 mm, 2.7  $\mu$ m column (Agilent Technologies, Santa Clara, CA, USA). Mobile phase A consisted of acetonitrile/water (10:90), while mobile phase B was acetonitrile, using a flow rate of 1.2 mL.min<sup>-1</sup>. The optimised gradient programme was as follows: 0.0-15.0 min (8.9% B), 15.0-15.1 min (8.9% to 16.7% B), 15.1-26.0 min (16.7% B), 26.0-26.1 min (16.7% to 33.4% B), 26.1-30.0 min (33.4% B) and 30.0-30.1 min (33.4% to 8.9% B). The column temperature was 60 °C and the injection volume was 10  $\mu$ L. Chromatographic data were acquired and processed using Waters Empower<sup>TM</sup> 2 software. Regression analysis for PAC and impurities was carried out using SigmaPlot version 9.0 software and Microsoft Excel 2010.

### 3.2.2 Materials and Reagents

Prednisolone acetate (PAC) was obtained from Sanofi Aventis (Paris, France). Prednisolone-11,21 diacetate (P-11,21D) was obtained from Steraloids Inc. (Newport, RI, USA). Hydrocortisone (HC) and hydrocortisone acetate (HCA) were obtained from US Pharmacopoeia (USP) (Rockville, Maryland, USA). Prednisolone 17-acetate (P-17A), (20S)-hydroxyprednisolone (20S), (20R)-hydroxyprednisolone (20R) and prednisone (PN) were obtained from LGC Standards (Teddington, Middlesex, UK). Prednisolone (P) was from Sigma Aldrich (St Louis, Missouri, USA). Reagent grade sodium acetate, glacial acetic acid (100%), HPLC grade acetonitrile (ACN) and methanol (MeOH) were purchased from Merck (Darmstadt, Germany). Deionised water was produced from a Millipore Milli-Q Plus Purifier system (Molsheim, France).

### 3.2.3 *Solution preparation for PAC RP-HPLC analysis*

All solutions were prepared in low actinic glassware to protect from light. (**Note:** Solutions described in this work belong to one of two subclasses. “Working standards” were used for quantitative purposes as external calibrators and did not contain matrix components. “Working samples” are simulated samples, containing PAC at 100% label strength plus spiked matrix components at label strength and spiked impurities at appropriate spike levels). Stock standard solutions of PAC and individual impurities were prepared in MeOH as described in Table 3.1. External PAC standard curves for quantification of both impurity levels and PAC in working samples involved the use of Calibration Set #1 or Calibration Set #2 respectively, prepared as shown in Table 3.1 using 0.1 M sodium acetate pH 4.0/MeOH (50:50) as diluent. For the preparation of working samples, an additional matrix spiking solution containing the matrix components of the ophthalmic suspension was prepared in deionised water. In this work, the exact formulation of the matrix is proprietary but included compounds which act as preservatives, ophthalmic lubricants (“artificial tears”), antipyretics, vasoconstrictors and mydriatics. All other solutions described hereafter (except the above external PAC standards for quantification) were spiked at 1:50 with the stock matrix spiking solution to ensure that matrix components were present at label strength after dilution. For PAC accuracy and linearity studies, a series of working samples were prepared (n=5) containing PAC at 40% to 160% (w/w) of product LS after dilution (including a 1:50 matrix solution spike). Method detection limits were determined using serial dilutions of a 0.1 mg.L<sup>-1</sup> mixed PAC/impurities standard. For impurity accuracy and linearity studies, impurity solutions were prepared at 5 concentrations ranging from 0.1 mg.L<sup>-1</sup> to 4.0 mg.L<sup>-1</sup>, equivalent to 0.05% to 2.0% of PAC working standard concentration. Each solution also contained a fixed concentration of PAC at 0.2 mg.mL<sup>-1</sup>. For precision, specificity and robustness studies a 0.2 mg.mL<sup>-1</sup> PAC working standard was spiked with each. For the comparison study between both HPLC methods, a 0.2 mg.mL<sup>-1</sup> PAC working standard was prepared in the appropriate diluent as well as a separate impurity standard mixture containing each impurity at a concentration of 2.0 mg.L<sup>-1</sup> equivalent to 1.0% of PAC concentration after dilution. (**Note:** For the sake of clarity, solution preparation is also detailed in Table 3.1).

**Table 3.1: Solution preparation for validation of RP-HPLC method**

Diluent	Solution	Analyte	Concentration	% w.r.t PAC Label Strength
MeOH	PAC stock standard	PAC	2.0 mg.mL <sup>-1</sup>	n/a
	Impurity stock standards	Individual impurities	0.20 mg.mL <sup>-1</sup>	n/a
MeOH/100 mM sodium acetate buffer pH 4.0 (50:50)	Solution A Precision/specificity/robustness spiked sample	PAC	0.20 mg.mL <sup>-1</sup>	100.0%
		Impurities	1.2 mg.L <sup>-1</sup>	0.60%
MeOH/100 mM sodium acetate buffer pH 4.0 (50:50) plus stock matrix spiking solution at 1:50	External PAC working standard (Calibration Set #1)	PAC	0.1 mg.L <sup>-1</sup> , 0.2 mg.L <sup>-1</sup> , 1.0 mg.L <sup>-1</sup> , 2.0 mg.L <sup>-1</sup> , 4.0 mg.L <sup>-1</sup>	0.05%, 0.10%, 0.50%, 1.0%, 2.0%
	External PAC working standard (Calibration Set #2)	PAC	80.0 mg.L <sup>-1</sup> , 0.16 mg.mL <sup>-1</sup> , 0.20 mg.mL <sup>-1</sup> , 0.24 mg.mL <sup>-1</sup> , 0.32 mg.mL <sup>-1</sup>	40.0%, 80.0%, 100.0%, 120.0%, 160.0%
	LOD/LOQ studies.	PAC/Impurities	0.1 mg.L <sup>-1</sup>	0.05%
	PAC accuracy/linearity studies	PAC	0.1 mg.L <sup>-1</sup> , 0.2 mg.L <sup>-1</sup> , 1.0 mg.L <sup>-1</sup> , 2.0 mg.L <sup>-1</sup> , 4.0 mg.L <sup>-1</sup>	0.05%, 0.10%, 0.50%, 1.0%, 2.0%
	PAC accuracy/linearity studies	PAC	80.0 mg.L <sup>-1</sup> , 0.16 mg.mL <sup>-1</sup> , 0.20 mg.mL <sup>-1</sup> , 0.24 mg.mL <sup>-1</sup> , 0.32 mg.mL <sup>-1</sup>	40.0%, 80.0%, 100.0%, 120.0%, 160.0%
	Impurity accuracy/linearity studies	PAC <sup>a</sup> (Impurities)	0.20 mg.mL <sup>-1</sup> (0.1 mg.L <sup>-1</sup> , 0.2 mg.L <sup>-1</sup> , 1.0 mg.L <sup>-1</sup> , 2.0 mg.L <sup>-1</sup> , 4.0 mg.L <sup>-1</sup> )	100.0% (0.05%, 0.10%, 0.50%, 1.0%, 2.0%)
MeOH/40 mM phosphate buffer pH 3.4 (70:30)	Method comparison sample	PAC	0.20 mg.mL <sup>-1</sup>	100.0%
	Method comparison impurity solution	Impurities	2.0 mg.L <sup>-1</sup>	1.00%

<sup>a</sup> PAC omitted from P and HCA impurity accuracy/linearity studies due presence of these impurities in PAC standard material

### 3.3 Results and discussion

#### 3.3.1 PAC RP-HPLC Method Development

A method capable of the identification and quantitation of PAC and selected process impurities/degradants in ophthalmic suspensions is essential in ensuring that the method is suitable for drug product release testing and routine drug product stability studies. As a starting point, the initial phase of the development work therefore focused on the USP monograph method for the analysis of PAC in ophthalmic suspensions [174] with certain modifications made to improve method performance. Specifically, a diluent of 40 mM phosphate buffer pH 3.4/MeOH (30:70) was used instead of 50% ACN. MeOH was selected due to its protic nature to improve working sample stability by minimizing base catalyzed hydrolysis of PAC to P. The working standard and working sample concentrations were increased from 0.1 mg.mL<sup>-1</sup> to 0.2 mg.mL<sup>-1</sup> and the injection volume increased from 10 µL to 30 µL in order to improve limits of detection and method accuracy. It should be noted that the USP monograph method is capable of identifying (but not quantifying) the impurity P in ophthalmic suspensions where PAC is the main active pharmaceutical ingredient (API). A mixture of PAC and impurities (PN, P, 20(S), 20(R), HC, P-17A, HCA, P-11,21D) each at 2.0 mg.L<sup>-1</sup> or 1% (w/w) of PAC label strength was injected and as illustrated in Figure 3.2(a), several co-elutions were evident with the given chromatographic conditions, namely: 20(S)/20(R), PN/P/HC and PAC/HCA. Furthermore, a 1:50 dilution of solution PAC sample was prepared and assayed to determine if there was any additional co-elution with matrix components; a significant matrix peak at ~ 2.2 min had the same retention time as the co-eluting 20(S) and 20(R) peaks as illustrated in Figure 3.2(b). Clearly, the modified USP method was incapable of quantifying all remaining seven known PAC-related impurities (besides P) in ophthalmic solutions.

An opportunity therefore presented itself to significantly improve the utility of the method by adopting more modern column technologies (a C<sub>18</sub> core-shell stationary phase), to improve the efficiency of the chromatographic separation. To exploit the benefits of core-shell column technology, a 100 mm x 4.6 mm Agilent Poroshell 120 EC-C<sub>18</sub> 2.7 µm column was selected which, in contrast with the 10 µm fully porous support particle exhibited by the Waters µBondapak stationary phase, comprises a 2.7-µm superficially porous particle with a 1.7-µm solid core and a 0.5-µm porous shell. Core-shell (or “superficially porous”)

particles have high loading capacities because 75% of the volume of these particles is porous [175].

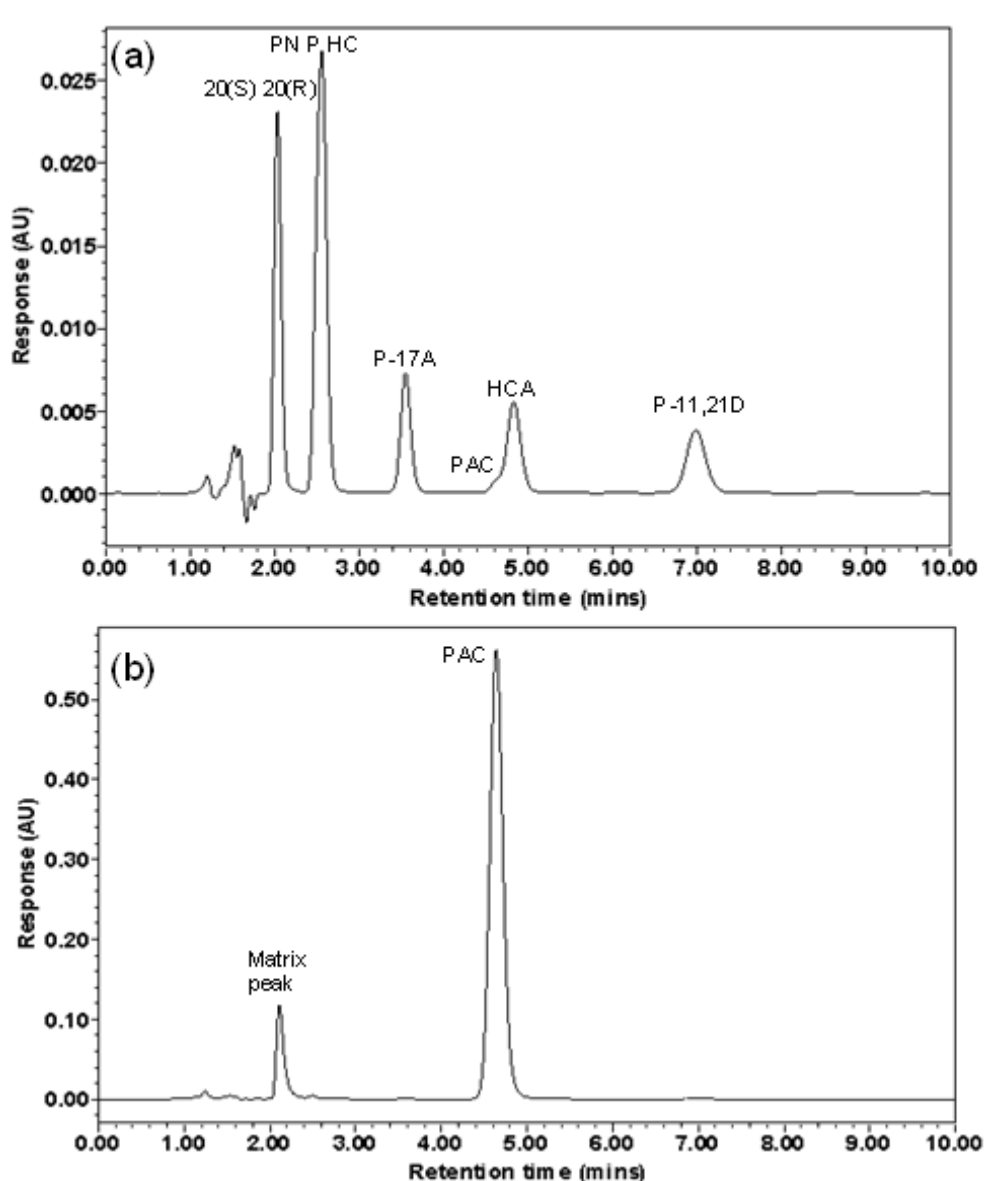


**Figure 3.2:** (a): Separation of eight selected PAC impurities at  $2.0 \text{ mg.L}^{-1}$  or 1% (w/w) of PAC LS. (b): chromatogram of  $0.20 \text{ mg.mL}^{-1}$  PAC sample. Chromatographic conditions: Column: Waters  $\mu$ Bondapak C18 ( $10 \mu\text{m}$ )  $3.9 \text{ mm} \times 300 \text{ mm}$ . Mobile phase: acetonitrile/water (40:60). Injection volume:  $30 \mu\text{L}$ . Column temperature: ambient. Detection:  $254 \text{ nm}$ .

Most importantly,  $4.6 \text{ mm}$  i.d. columns packed with these particles provide efficiencies equivalent to those of columns packed with  $1.7\text{-}\mu\text{m}$  fully porous particles, with the additional advantage of operating at back pressures that are 2-3 times lower [176,177].

Therefore, these particles make it possible to achieve ultra-high performance liquid chromatography (UPLC)-like performance when the HPLC connecting tubing is modified to minimise extra-column volumes and the detector flow-cell volume is reduced appropriately [178]. The pore size of the two particle types was broadly similar at 125 Å and 120 Å for the  $\mu$ Bondapak and Poroshell materials respectively but as expected, both stationary phases exhibit very different surface areas of 330 m<sup>2</sup>.g<sup>-1</sup> and 130 m<sup>2</sup>.g<sup>-1</sup> respectively. The decrease in surface area for the Poroshell phase can be expected to be offset by the increased efficiency due to improved packing quality (spherical rather than irregular particle shape), reduced particle size and reduced diffusion path lengths.

The Agilent Poroshell stationary phase also fulfils the USP requirement for an L1 stationary phase (octadecyl saline (ODS or C<sub>18</sub>) chemically bounded to porous silica or ceramic particles – 1.5 to 10  $\mu$ m in diameter) but offers significantly different C<sub>18</sub> selectivity relative to the Waters  $\mu$ Bondapak phase. Although the carbon load for both stationary phases was 10%, nevertheless the column comparison function (Fs) value describing the similarity (or difference) in selectivity between both stationary phases was 13.4, based on the Hydrophobic Subtraction Model first described by Snyder *et al.* [179]. Initial method development was performed using the same working standard/sample concentrations as the modified USP method described above, but using a diluent of 100 mM sodium acetate pH 4.0/MeOH (50:50). A mobile phase flow rate of 1.2 mL.min<sup>-1</sup> was used along with an injection volume of 10  $\mu$ L and a detection wavelength of 254 nm. However, a number of different gradient programs and column temperatures were used during method optimisation (with a water/acetonitrile mobile phase) as illustrated in Table 3.2. The goal was to separate all critical peak pairs with a resolution of at least 1.5. Figure 3.3 provides representative chromatograms of the development conditions outlined in Table 3.2. The elution order was confirmed by running individual standard injections of PAC [179] and the selected impurities under the optimised conditions.

The polarity of the selected analytes (log P values) varied widely from 0.26  $\pm$  0.51 for 20(S) to 3.04  $\pm$  0.60 for P11,21D [180]. Therefore, the final developed gradient (Test 11 from Table 3.2) incorporated an initial isocratic hold to resolve early eluting peaks followed by a two-step gradient in order to resolve mid-gradient peaks and elute the strongly retained analytes within a reasonable timeframe. Column temperature was observed to be critical for the separation of PN, P and HC. It was not possible to separate PN and P under any gradient conditions below 40 °C and it was not until the column temperature was increased to 60 °C

that the required resolution of  $\geq 1.5$  between critical pairs was obtained. Once the conditions were optimised, mobile phase A was pre-mixed (water/acetonitrile 90/10, v/v) to prevent bacterial growth in mobile phase A. The final optimised chromatogram is shown below in Figure 3.4.

### **3.3.2 PAC RP-HPLC Method Validation**

The following validation elements were assessed for PAC and selected impurities: accuracy, linearity, precision, limit of detection (LOD), limit of quantitation (LOQ), specificity and robustness. For quantitative purposes, two separate PAC external calibration curves were generated; at low levels for impurities (Calibration Set #1) and higher levels for PAC (Calibration Set #2).

#### **3.3.2.1 PAC RP-HPLC Accuracy/Linearity studies**

Both external PAC calibration regression lines (Calibration Set #1 and #2) yielded  $r^2$  values  $> 0.999$ , but the y-intercepts were larger than the standard error of the intercept, demonstrating a need for multi-point calibration to be used for quantitative purposes, both for impurities and for PAC in working samples. Impurity accuracy was determined in the presence of PAC at  $0.2 \text{ mg.mL}^{-1}$  in each sample to verify that chromatographic resolution between the impurities and the main PAC peak could be maintained across all examined impurity concentration levels. Conversely, impurity accuracy studies for P and P-11,21D were conducted in the absence of PAC since the PAC standard material contained detectable levels of these two impurities. The Response factor (RF) for each impurity was calculated using the ratio of the slopes (impurity slope/PAC slope). Although RF values were  $0.8 < \text{RF} < 1.2$  for all impurities and could therefore be excluded from calculations, nevertheless % recovery values were improved when RF values were accounted for. Corrected % recovery values ranged from 80% to 100% for most impurities (except for PN and P11,21D which exhibited lower recovery values at lower impurity concentrations) as shown in Table 3.3. Recovery of PAC in working samples was determined at each concentration level by using the equation of the line (Calibration Set #2) to calculate the actual concentration at each level and expressing this result as a percentage of the theoretical concentration, with values ranging from 99.6% to 100.4 % (Table 3.3).

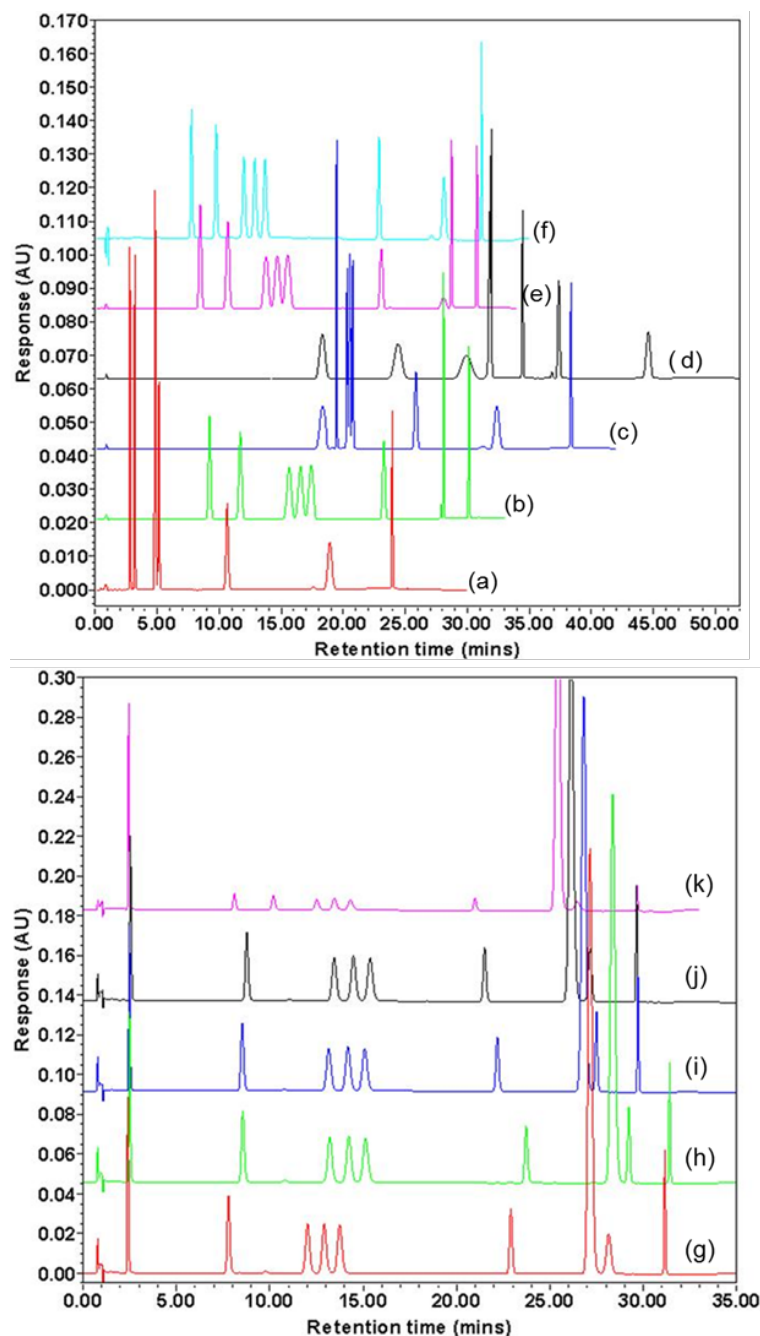


**Figure 3.3:** Representative chromatograms of development injections under development conditions outlined in Table 3.2 below Test 1 (a), Test 2 (b), Test 3 (c), Test 4 (d), Test 5 (e), Test 6 (f), Test 7 (g), Test 8 (h), Test 10 (i) and Test 11 (j). Top: Chromatograms of PAC impurity mix. Test 1 to Test 6 impurity mix contained PAC impurities at  $20.0 \text{ mg.L}^{-1}$  or  $10.0\%$  (w/w) of PAC after dilution. Bottom: Chromatograms of PAC samples spiked with impurities. Test 7 to Test 10 contained PAC sample spiked with impurities at  $20.0 \text{ mg.L}^{-1}$  or  $10.0\%$  (w/w) of PAC after dilution. Test 11 contained PAC sample spiked with impurities at  $4.0 \text{ mg.L}^{-1}$  or  $2.0\%$  (w/w) of PAC after dilution.

**Table 3.2: RP-HPLC PAC method optimisation**

Test	Flow rate mL.min <sup>-1</sup>	Run time	Column temperature (°C)	Mobile Phase Components	Gradient composition			R <sub>s</sub>	R <sub>s</sub>
					Time	% A	% B	PN/P	P/HC
Test 1	1.2	30 min	40	A = 25% ACN B = 100% ACN	0.0	100.0	0.0	-	1.70
					20.0	100.0	0.0		
					20.1	80.0	20.0		
					26.0	80.0	20.0		
					26.1	100.0	0.0		
					30.0	100.0	0.0		
Test 2	1.2	34 min	50	A = 100% H <sub>2</sub> O B = 100% ACN	0.0	82.0	18.0	1.36	1.27
					16.0	82.0	18.0		
					16.1	75.0	25.0		
					26.0	75.0	25.0		
					26.1	60.0	40.0		
					31.0	60.0	40.0		
					31.1	82.0	18.0		
					34.0	82.0	18.0		
Test 3	1.2	42 min	55	A = 100% H <sub>2</sub> O B = 100% ACN	0.0	85.0	15.0	1.13	1.23
					17.0	85.0	15.0		
					17.1	75.0	25.0		
					35.0	75.0	25.0		
					35.1	60.0	40.0		
					40.0	60.0	40.0		
					40.1	85.0	15.0		
					42.0	85.0	15.0		
Test 4	1.2	52 min	55	A = 100% H <sub>2</sub> O B = 100% ACN	0.0	85.0	15.0	2.15	-
					30.0	85.0	15.0		
					30.1	70.0	30.0		
					45.0	70.0	30.0		
					45.1	60.0	40.0		
					50.0	60.0	40.0		
					50.1	85.0	15.0		
					52.0	85.0	15.0		
Test 5	1.2	34 min	60	A = 100% H <sub>2</sub> O B = 100% ACN	0.0	82.0	18.0	1.28	1.15
					17.0	82.0	18.0		
					17.1	75.0	25.0		
					27.0	75.0	25.0		
					27.1	60.0	40.0		
					32.0	60.0	40.0		
					32.1	82.0	18.0		
					34.0	82.0	18.0		

**Table 3.2:** RP-HPLC PAC method optimisation (contd.)

Test	Flow rate mL.min <sup>-1</sup>	Run time	Column temperature (°C)	Mobile Phase Components	Gradient composition			R <sub>s</sub> PN/P	R <sub>s</sub> P/HC
					Time	% A	% B		
Test 6	1.2	35 min	60	A = 100% H <sub>2</sub> O B = 100% ACN	0.0	82.0	18.0	2.08	1.83
					18.0	82.0	18.0		
					18.1	75.0	25.0		
					27.0	75.0	25.0		
					28.0	60.0	40.0		
					32.0	60.0	40.0		
					32.1	82.0	18.0		
					35.0	82.0	18.0		
Test 7	1.2	35 min	60	A = 100% H <sub>2</sub> O B = 100% ACN	0.0	82.0	18.0	2.08	1.83
					18.0	82.0	18.0		
					18.1	75.0	25.0		
					27.0	75.0	25.0		
					28.0	60.0	40.0		
					32.0	60.0	40.0		
					32.1	82.0	18.0		
					35.0	82.0	18.0		
Test 8	1.2	35 min	60	A = 10% ACN B = 100% ACN	0.0	91.1	8.9	2.14	1.78
					18.0	91.1	8.9		
					18.1	83.3	16.7		
					27.0	83.3	16.7		
					28.0	66.6	33.3		
					32.0	66.6	33.3		
					32.1	91.1	8.9		
					35.0	91.1	8.9		
Test 9	1.2	32 min	60	A = 10% ACN B = 100% ACN	0.0	91.1	8.9	2.15	1.78
					16.0	91.1	8.9		
					16.1	83.3	16.7		
					25.0	83.3	16.7		
					26.5	66.6	33.3		
					30.0	66.6	33.3		
					31.0	91.1	8.9		
					32	91.1	8.9		

**Table 3.2:** RP-HPLC PAC method optimisation (contd.)

Test	Flow rate mL.min <sup>-1</sup>	Run time	Column temperature (°C)	Mobile Phase Components	Gradient composition			R <sub>s</sub>	R <sub>s</sub>
					Time	% A	% B	PN/P	P/HC
Test 10	1.2	32 min	60	A = 10% ACN B = 100% ACN	0.0	91.1	8.9	2.18	1.78
					15.0	91.1	8.9		
					15.1	83.3	16.7		
					25.0	83.3	16.7		
					26.5	66.6	33.3		
					30.0	66.6	33.3		
					30.1	91.1	8.9		
					32.0	91.1	8.9		
Test 11	1.2	34 min	60	A = 10% ACN B = 100% ACN	0.0	91.1	8.9	2.22	1.89
					15.0	91.1	8.9		
					15.1	83.3	16.7		
					26.0	83.3	16.7		
					26.1	66.6	33.3		
					30.0	66.6	33.3		
					30.1	91.1	8.9		
					34.0	91.1	8.9		

### 3.3.2.2 PAC RP-HPLC Precision

“Solution A” was used for precision studies because impurities were spiked at 0.6% w.r.t PAC; this level being close to the median of the impurity linearity range (0.05% to 2.0%). Repeatability was assessed by making six replicate injections of the same preparation of “Solution A” on Day-1, and the % RSD for concentration of PAC was 0.1% while for the impurities the % RSD ranged from 0.1% to 0.5%. Intermediate precision was then assessed by assaying the same solution preparation on a different day (Day-2) using a different HPLC system, column and mobile phase. The % RSD for concentration was calculated on Day-2 along with equivalency (calculated as the ratio of the means (R/M) based on concentration mean results for PAC and each impurity from Day-1). The Day-2 % RSD for PAC concentration was 0.5% while for the impurities the % RSD ranged from 0.5% to 1.6% (n=6). The equivalency result for PAC and all impurities was 1.0. Retention time precision for all analytes across both days was < 0.1 % RSD. Repeatability and intermediate precision for PAC and impurities are summarised in Table 3.3.

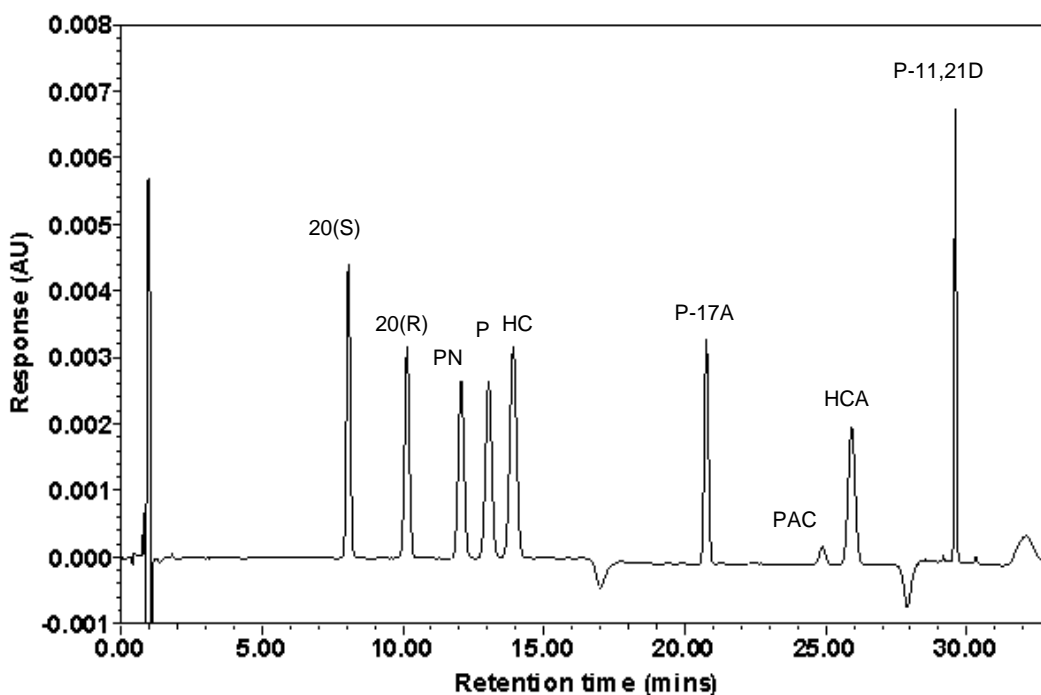


**Figure 3.4:** Chromatogram of PAC impurity standard mixture containing the eight selected PAC impurities prepared at  $2.0 \text{ mg.L}^{-1}$  or 1% (w/w) of PAC LS. Chromatographic conditions: Column: 100 mm x 4.6 mm Agilent Poroshell 120 EC-C<sub>18</sub>, 2.7  $\mu\text{m}$ . Mobile phase A: acetonitrile/water (10:90). Mobile phase B: acetonitrile. Gradient: 0.0-15.0 min (8.9% B), 15.0-15.1 min (8.9% to 16.7% B), 15.1-26.0 min (16.7% B), 26.0-26.1 min (16.7% to 33.4% B), 26.1-30.0 min (33.4% B) and 30.0-30.1 min (33.4% to 8.9% B). Flow rate:  $1.2 \text{ mL.min}^{-1}$ . Injection volume: 10  $\mu\text{L}$ . Column temperature: 60 °C. Detection: 254 nm.

### 3.3.2.3 PAC RP-HPLC Specificity and Solution Stability

Specificity of the HPLC method was assessed by assaying “Solution A” using PDA detection. All peaks in the chromatogram were separated with a resolution of  $\geq 1.5$  and were found to be spectrally pure across the bandwidth using PDA detection (See Figure 3.5). A placebo blank containing all sample matrix components was also assayed and showed that there were no interfering peaks with a signal-to-noise (S/N) ratio greater than 10:1 at the retention time of PAC or any of the impurities being investigated. In fact, the only significant sample matrix component was a peak at approximately 2.5 min in the chromatogram. The result demonstrated that there were no interfering peaks at the retention time of the PAC or any of the impurity peaks under investigation as a result of the sample matrix.

The developed method was used to examine solution stability prior to full method validation studies. Working standard and working sample solutions were stored in both amber and clear glassware at ambient temperature, and tested immediately and after 5 days.

In clear glassware, the PAC peak area decreased by 6.8% and 9.5% in standard and sample solutions respectively whereas in amber glassware, the change was  $\leq 0.6\%$ . Regardless of glassware type, there was notable changes in sample impurity profiles over five days (for example; +37% for P, +86% for P-17A, +289% for HCA and -10% for P11, 21D). Interestingly the peak area of the main sample matrix peak (2.5 min, Figure 3.5(a)) only changed by 0.6% over the test period. Working standard and sample solutions were therefore prepared in amber glassware immediately before analysis. A forced degradation study was also performed by adjusting the pH of a working sample solution (containing matrix components) to 9.4 with 5N NaOH and storing at 45 °C for 48 hours. The PAC concentration (1.1% w/v) decreased by 26%, and P (0.3% w/w) increased by 3,300 %, P-17A (0.03% w/w) increased by 66%, HCA (0.6% w/w) decreased by 24% and P-11,21D (0.3% w/w) decreased by 32%. This preliminary study and the aforementioned PDA spectral analysis is indicative of the potential utility of this method as a stability assay.

#### ***3.3.2.4 PAC RP-HPLC Method Detection Limits and Acceptance Criteria***

The LOD and LOQ were determined using the signal-to-noise approach in which baseline noise was compared with the peak height. The magnitude of baseline noise was measured in a blank chromatogram over a distance equivalent to 5 times the peak width at half height of the peak, centred around its expected retention time. The LOQ/LOQ standard solution was diluted until a S/N ratio of approximately 3:1 and 10:1 was reached for LOD and LOQ respectively for each analyte (n=3). The LOQ's of PAC and all eight impurities were below the 0.1% reporting threshold required for trace impurity analysis outlined in ICH Q3B(R2) [144]. The % recovery at the LOQ ranged from 92.5% for 20(R) to 114.9% for HC/P-17A as shown in Table 3.3. The acceptance limit for the main API (PAC) is  $\pm 10\%$  of the label claim whereas current European Pharmacopoeia [173] impurity specifications for P and HCA are not more than 1.0% and not more than 0.5% for P-11,21D. The limit for total impurities is 2.0%. The remaining impurities are classified [173] as “unspecified”, with a limit of not more than 0.1%. Limits will be established for these impurities after detailed long-term stability studies, which will be the subject of future work.

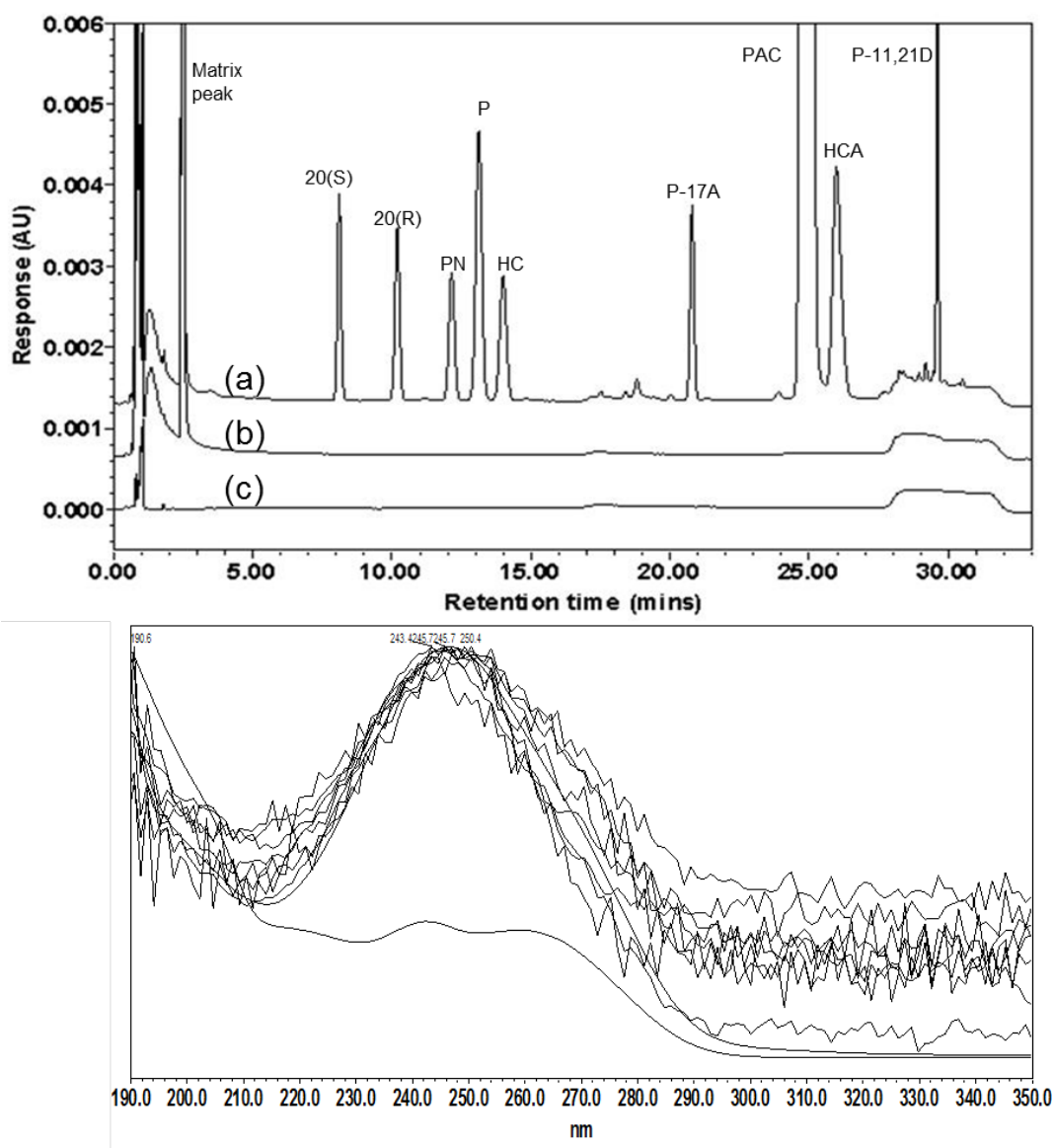


**Figure 3.5:** Top: (a) Chromatogram of  $0.20 \text{ mg.mL}^{-1}$  PAC spiked with eight selected PAC impurities at  $1.2 \text{ mg.L}^{-1}$  prepared in placebo blank diluent. (b) Chromatogram of placebo blank solution. (c) Chromatogram of MeOH/buffer diluent. Chromatographic conditions as in Figure 3.4. Bottom: UV spectral overlays of matrix peak, PAC and all eight impurity peaks generated by photodiode array detection as part of the specificity study.

### 3.3.2.5 PAC RP-HPLC Robustness

To assess the robustness of the new HPLC method, “Solution A” was assayed under deliberately altered chromatographic conditions. Column temperatures of  $60 \text{ }^{\circ}\text{C}$  (nominal),  $58 \text{ }^{\circ}\text{C}$  and  $62 \text{ }^{\circ}\text{C}$  and flow rates of  $1.1 \text{ mL.min}^{-1}$ ,  $1.2 \text{ mL.min}^{-1}$  (nominal) and  $1.3 \text{ mL.min}^{-1}$  were assessed. Furthermore, mobile phase A was adjusted to 9% ACN, 10% ACN (nominal)

and 11% ACN. The results obtained were assessed for system suitability to ensure that the separation requirements were maintained under the altered conditions and robustness was assessed by examination of equivalency (calculated as the ratio of the means,  $n=6$ ). For all column temperature tests, the resolution between the critical pairs PN/P, P/HC and PAC/HCA remained  $\geq 2.0$ . For the flow rate test at  $1.3 \text{ mL}\cdot\text{min}^{-1}$  and the mobile phase A composition test (9% ACN), resolution fell to 1.6 (although still baseline resolved) for the P/HC peak pair. The largest shift in relative retention times (RRT) equivalent to 12.5% was for 20(S) and 20(R), presumably since these eluted relatively early on the initial isocratic region of the gradient. The equivalency for PAC was 1.0 for all test conditions, but ranged from 1.0 to 1.1 for the impurities as shown in Table 3.3. Figure 3.6 shows overlaid chromatograms of “Solution A” at the selected column temperatures.

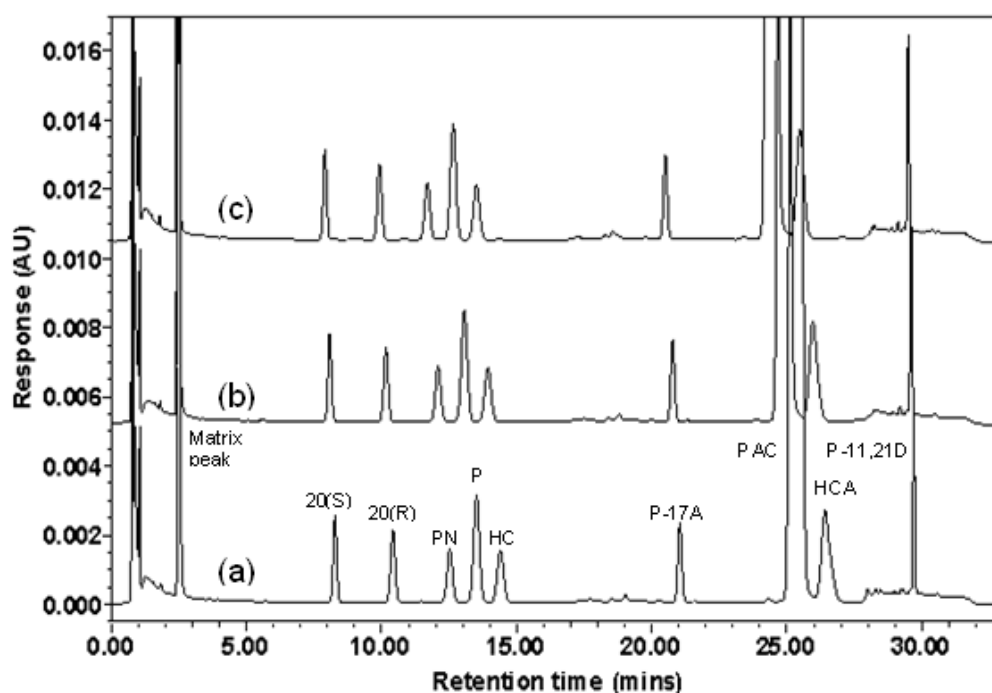


**Figure 3.6:** Overlaid chromatograms of  $0.20 \text{ mg}\cdot\text{mL}^{-1}$  PAC spiked with eight selected PAC impurities at  $1.2 \text{ mg}\cdot\text{L}^{-1}$  prepared in placebo blank diluent ran at (a)  $58 \text{ }^\circ\text{C}$ , (b)  $60 \text{ }^\circ\text{C}$  and (c)  $62 \text{ }^\circ\text{C}$ . All other chromatographic conditions are as described in Figure 3.4.

**Table 3.3:** Analytical performance for determination of PAC and selected impurities in a spiked ophthalmic suspension

<b>Accuracy</b>	PAC	20(S)	20(R)	PN	P	HC	P-17A	HCA	P-11,21D									
0.05%	96.3 ± 16.0	79.6 ± 2.2	80.2 ± 1.8	74.6 ± 6.3	87.3 ± 13.1	86.0 ± 12.3	65.5 ± 6.1	80.6 ± 5.4	64.7 ± 5.3									
0.10%	106.7 ± 8.4	86.9 ± 5.1	99.3 ± 3.9	86.2 ± 5.8	95.9 ± 6.2	84.0 ± 3.1	79.9 ± 1.2	89.1 ± 10.1	78.8 ± 1.1									
0.50%	99.7 ± 2.4	99.2 ± 1.2	99.2 ± 1.4	97.6 ± 1.4	98.6 ± 0.6	98.5 ± 1.1	96.7 ± 0.6	98.7 ± 4.2	91.7 ± 0.9									
1.00%	99.3 ± 2.4	98.8 ± 0.2	99.0 ± 0.3	98.9 ± 0.5	99.4 ± 1.3	98.2 ± 1.5	97.6 ± 1.0	97.8 ± 0.5	100.1 ± 1.1									
2.00%	100.2 ± 0.2	99.5 ± 0.2	99.8 ± 0.5	99.3 ± 0.5	99.7 ± 0.4	99.5 ± 0.8	99.1 ± 0.7	99.6 ± 0.7	98.6 ± 0.2									
40.00%	100.2 ± 0.4	---	---	---	---	---	---	---	---									
80.00%	100.2 ± 0.5	---	---	---	---	---	---	---	---									
100.00%	99.6 ± 0.4	---	---	---	---	---	---	---	---									
120.00%	100.4 ± 0.2	---	---	---	---	---	---	---	---									
160.00%	100.0 ± 0.4	---	---	---	---	---	---	---	---									
RF <sup>a</sup>	n/a	1.12	1.13	1.09	1.09	1.19	0.95	0.99	0.87									
<b>Linearity</b> <i>r</i> <sup>2</sup> ( <i>n</i> =5)	> 0.999	> 0.999	> 0.999	> 0.999	> 0.999	> 0.999	> 0.999	> 0.999	> 0.999									
<b>Precision</b> (% RSD)	Day-1	Day-2	Day-1	Day-2	Day-1	Day-2	Day-1	Day-2	Day-1	Day-2	Day-1	Day-2	Day-1	Day-2	Day-1	Day-2	Day-1	Day-2
<i>Retention time</i>	<0.1	<0.1	<0.1	<0.1	<0.1	<0.1	<0.1	<0.1	<0.1	<0.1	<0.1	<0.1	<0.1	<0.1	<0.1	<0.1	<0.1	<0.1
<i>Concentration</i>	0.1	0.5	0.3	0.9	0.3	1.6	0.3	2.2	0.1	2.2	0.4	1.3	0.5	0.6	0.3	0.5	0.1	0.5
<i>Equivalency</i> <sup>b</sup>	1.0	1.0	1.0	1.0	1.0	1.0	1.0	1.0	1.0	1.0	1.0	1.0	1.0	1.0	1.0	1.0	1.0	1.0

**Table 3.3:** Analytical performance for determination of PAC and selected impurities in a spiked ophthalmic suspension (contd.)

<b>Detection limits<sup>c</sup></b>	PAC	20(S)	20(R)	PN	P	HC	P-17A	HCA	P-11,21D
<i>LOD % (w/w)</i>	0.004	0.002	0.003	0.004	0.004	0.004	0.003	0.005	0.002
<i>LOQ % (w/w)</i>	0.015	0.007	0.010	0.014	0.014	0.013	0.010	0.018	0.008
<i>% Recovery (at LOQ)</i>	112.9	106.2	92.5	101.7	98.0	114.9	114.9	105.7	112.2
<b>Robustness<sup>d</sup></b>	PAC	20(S)	20(R)	PN	P	HC	P-17A	HCA	P-11,21D
Temperature: 60 °C <i>RRT(Resolution)</i>	1.00(2.1 <sup>e</sup> )	0.32	0.40	0.48(2.4 <sup>f</sup> )	0.52(2.0 <sup>e</sup> )	0.56	0.83	1.04	1.18
Temperature: 58 °C <i>RRT(Resolution)</i>	1.00(2.1 <sup>e</sup> )	0.33	0.41	0.49(2.4 <sup>f</sup> )	0.53(2.0 <sup>e</sup> )	0.57	0.83	1.04	1.17
<i>Equivalency<sup>h</sup></i>	1.0	1.0	1.0	1.0	1.0	1.0	1.0	1.0	1.0
Temperature: 62 °C <i>RRT(Resolution)</i>	1.00(2.3 <sup>e</sup> )	0.33	0.41	0.48(2.5 <sup>f</sup> )	0.52(2.1 <sup>e</sup> )	0.55	0.84	1.04	1.21
<i>Equivalency<sup>h</sup></i>	1.0	1.0	1.0	1.0	1.0	1.0	1.0	1.0	1.0
Flow: 1.1 mL.min <sup>-1</sup> <i>RRT(Resolution)</i>	1.00(2.4 <sup>e</sup> )	0.33	0.41	0.50(2.4 <sup>f</sup> )	0.53(2.0 <sup>e</sup> )	0.57	0.83	1.04	1.18
<i>Equivalency<sup>h</sup></i>	1.0	1.0	1.0	1.0	1.0	1.0	1.0	1.0	1.0
Flow: 1.3 mL.min <sup>-1</sup> <i>RRT(Resolution)</i>	1.00(1.9 <sup>e</sup> )	0.31	0.39	0.46(2.0 <sup>f</sup> )	0.50(1.6 <sup>e</sup> )	0.53	0.84	1.04	1.24
<i>Equivalency<sup>h</sup></i>	1.0	1.0	1.0	1.0	1.1	1.0	1.0	1.0	1.0
Mobile Phase A: 9% <i>RRT(Resolution)</i>	1.00(2.0 <sup>e</sup> )	0.35	0.45	0.53(2.1 <sup>f</sup> )	0.58(1.6 <sup>e</sup> )	0.61	0.83	1.04	1.13
<i>Equivalency<sup>h</sup></i>	1.0	1.0	1.0	1.0	1.1	1.0	1.0	0.9	1.0
Mobile Phase A: 11% <i>RRT(Resolution)</i>	1.00(2.0 <sup>e</sup> )	0.28	0.35	0.43(1.9 <sup>f</sup> )	0.47(1.7 <sup>e</sup> )	0.50	0.85	1.04	1.29
<i>Equivalency<sup>h</sup></i>	1.0	1.0	1.0	1.0	1.1	1.0	1.0	1.0	1.0

- <sup>a</sup> Calculated on ratio of the slopes (IMP slope/PAC slope) over 0.05% to 2.00%
- <sup>b</sup> Ratio of analyte concentration Day 2 versus analyte concentration Day 1
- <sup>c</sup> n=3.
- <sup>d</sup> n=6.
- <sup>e</sup> Rs calculated as  $Rs = 1.18(t_{r2}-t_{r1})/(W_1 h/2 - W_2 h/2)$  for critical pair PAC/HCA
- <sup>f</sup> Rs calculated as  $Rs = 1.18(t_{r2}-t_{r1})/(W_1 h/2 - W_2 h/2)$  for critical pair PN/P
- <sup>g</sup> Rs calculated as  $Rs = 1.18(t_{r2}-t_{r1})/(W_1 h/2 - W_2 h/2)$  for critical pair P/HC
- <sup>h</sup> Ratio of analyte concentration versus analyte concentration under optimum (nominal) conditions

**Table 3.4:** Comparison between HPLC analytical conditions and performance

Parameters	Modified USP HPLC method	New gradient HPLC method
Column	Waters $\mu$ Bondapak C <sub>18</sub> 3.9 mm x 300 mm, 10 $\mu$ m particle size	Agilent Poroshell <sup>®</sup> 120 EC-C <sub>18</sub> 100 mm x 4.6 mm, 2.7 $\mu$ m particle size
Column temperature	Ambient	60 °C
Flow rate	2.0 mL.min <sup>-1</sup>	1.2 mL.min <sup>-1</sup>
Detection	254 nm 5Hz acquisition rate	254 nm 5Hz acquisition rate
Injection volume	30 $\mu$ L	10 $\mu$ L
Analysis type	Isocratic	Gradient
Mobile phase	ACN/Water (40:60)	A: ACN/Water (10:90) B: ACN
Analysis time per sample (min)	10 min	33 min
Solvent usage per sample (ml)	8.0	9.2
Sample diluent	MeOH/40 mM phosphate buffer pH 3.4 (70:30)	MeOH/100 mM sodium acetate buffer pH 4.0 (50:50)

### 3.4 Conclusion

A method has been described in which PAC and all eight known impurities have been separated on an Agilent Poroshell 120 EC-C<sub>18</sub> column within 33 min and applied to the analysis of an ophthalmic suspension. In contrast with the modified USP method, the core-shell method was also capable of separation and quantitation of all eight selected impurities, necessitating only a moderate increase in solvent consumption (due to the gradient programme) from 8 mL to 9.2 mL per injection. Table 3.4 provides a direct comparison of analytical conditions between the modified USP method and the newly developed gradient method.

#### **4.0 Chapter 4: Development of an orthogonal method for the determination of Prednisolone acetate and impurities in an ophthalmic suspension using supercritical fluid chromatography: Validation based on the Total Error Approach with Accuracy Profiles.**

##### **4.1 Introduction**

With the global drive for faster more environmentally friendly separation techniques, the aim of this chapter was to demonstrate the potential of pSFC as a viable alternative, or complementary technique to the established technique of HPLC, in the highly regulated world of the Quality Control (QC) laboratory. To achieve this aim, any new pSFC method has to be shown to be able to provide equivalent, if not exceed the analytical performance of the established HPLC method for a given application. For this body of work, it was decided to attempt to develop and validate a pSFC method as an alternative to the RP-HPLC method for the determination of PAC and its related impurities in an ophthalmic suspension described in Chapter 3 above. For a pSFC method of this type to be accepted into the QC laboratory, it has to be capable of meeting the requirements for the quantitation of trace level impurities and be accompanied by a detailed validation report that proves that the method is indeed fit for its intended purpose.

##### **4.1.1 Analysis of Steroids by SFC**

A review of the literature revealed that a number of steroid based applications using SFC have been reported. Baiocch *et al.* [181] attempted to develop a capillary supercritical chromatography (cSFC) method using pure CO<sub>2</sub> as the mobile phase for several steroidal substances including prednisolone (P) and prednisolone acetate (PAC). The goal was to optimise the separation and to study the underlying separation mechanism. The test compounds selected were separated on diverse stationary phases using supercritical CO<sub>2</sub> as the mobile phase along with flame-ionization (FID) and electron-capture detectors (ECD) to compare chromatographic results and to optimise resolution. However, some substances including PAC were found to have long retention times and were poorly detected (low sensitivity) using FID. The authors attributed such behaviour in part to the slight solubility of these compounds in supercritical CO<sub>2</sub> due to their polar nature. It was noted that an increase in the polarity of the compounds corresponded to a diminution of sensitivity that was particularly dramatic for PAC compared to P given that the only difference was the presence of the acetate group, which doesn't imply a great difference in polarity. Therefore, the authors employed more specific chromatographic conditions with a more sensitive detection

system (ECD), which exploited the presence of several keto and free hydroxy groups, in an attempt to improve the quality of the results. A chromatographic separation with ECD detection on an OV-1701 stationary phase was developed which provided shorter retention time, better peak shape and sensitivity for PAC. The reproducibility of qualitative and quantitative determinations was close to 1.0% for retention time with an RSD close to  $\pm 5.0\%$  for peak area. The detection limit ranged from 1.0 to 5.0 ppm.

Several publications of rapid separations of polyfunctional corticosteroids have been reported. Berry *et al.* [182] separated eight steroids in less than 6 min using 20% methoxyethanol in carbon dioxide with a (5  $\mu\text{m}$ ) 4.6 mm x 100 mm silica column. Lesellier *et al.* [183] separated eleven steroids, including hydrocortisone (HC), in less than 2 min using 6.1% methanol in  $\text{CO}_2$  and a (3  $\mu\text{m}$ ) 4.6 mm x 75 mm cyanopropyl column. Berger *et al.* [1] reported the separation of four hydroxysteroids in less than 10 sec using a 1.5  $\mu\text{m}$  pellicular diol packing in a 30 mm column. Yaku *et al.* [184] investigated the retention behaviour of synthetic corticosteroids in pSFC. The authors used seven polar synthetic corticosteroids, (including HC) which contained 1 to 4 hydroxyl groups as test compounds to systematically study the influence of stationary phase, modifiers, column pressure and temperature on pSFC retention and compare the retention mechanism to both normal and reversed-phase retention mechanisms respectively. Four stationary phases of varying polarity were screened using the test compounds under SFC operating conditions of; mean pressure 209 bar, flow-rate of  $\text{CO}_2$  3.0  $\text{mL}\cdot\text{min}^{-1}$ , flow-rate of methanol 0.4  $\text{mL}\cdot\text{min}^{-1}$  and column temperature of 40  $^\circ\text{C}$ . The four stationary phases included; Cosmosil 5  $\text{NH}_2$  modified with aminopropyl, Ultaron VX-SIL, Inertsil ODS-2 and Zorbax phenyl. All column dimensions were (5  $\mu\text{m}$ ) 4.6 mm x 150 mm. Under the above conditions, the authors concluded that the  $\text{NH}_2$  column exhibited the best selectivity and peak shape along with reasonable retention time compared to the other columns.

To assess the effect of modifiers, the authors selected several modifiers of varying polarity including; tetrahydrofuran (THF), 95% ethanol, 99.5% ethanol, 1-propanol, 2-propanol and methanol (MeOH). No peaks eluted from the  $\text{NH}_2$  stationary phase when pure  $\text{CO}_2$  was used as the mobile phase, which demonstrated the need for a modifier. Of the modifiers studied, MeOH was found to give the best resolution and peak shape. Based on previous studies carried out on the effect of column and mobile phase polarity on the separation of steroids, Berger *et al.* [185] had concluded that the role of the modifier was to decrease the intensity of the solute-silanol interactions. Further work by Blilie and Greibrokk

[186] suggested that the modifier functioned as a deactivating agent by direct interaction with residual silanols, and also to increase the eluting power of the mobile phase. Janssen *et al.* [187] confirmed that only a few % of modifier was necessary for the deactivation of residual silanol groups on the silica support and demonstrated that almost the same % of THF and MeOH was required to cover 95% of the surface of the stationary phase. However, based on their observations, Yaku *et al.* [184] concluded that in the case of the separation of synthetic corticosteroids, the effect of the modifier is to enhance the solvent strength of the mobile phase rather than the deactivation of active sites on the silica support. This was born out by the fact that when MeOH was replaced with THF, no peaks eluted from the NH<sub>2</sub> stationary phase. Also, the retention factor of the selected test compounds decreased 2 to 4-fold with a 1.8-fold increase in MeOH concentration. The optimum separation was achieved using 16.7% MeOH as the modifier, with all test compounds eluted within 5 min with a minimum resolution of 1.6 between peaks.

The authors also investigated the effect of system back pressure at constant temperature on the separation. Retention factor was shown to reduce by a factor of 2 with an increase in the range of 105 – 219 bar. Theoretical plate counts showed maximum values at 124 and 141 bar while maximum resolution was observed from 124 – 159 bar. Above 159 bar, both plate count and resolution decreased demonstrating that pressure is a significant parameter when it comes to optimising pSFC operating conditions. Upon investigating the effects of temperature, from 22 – 58 °C, at constant pressure, the authors noted that the retention of all solutes increased with increasing temperature, due to the decrease in mobile phase density. It was noted that the separation factor ( $\alpha$ ) between neighbouring peaks changed very little with increasing temperature. Based on previous work carried out by Berger [38], the authors estimated that the critical temperature for the binary mobile phase used in their separation was in the range of 40 to 50 °C. Both plate count and resolution reached their maximums at 39 – 49 °C which led the authors to conclude that the optimum separation was achieved around the critical temperature of the mobile phase used in the separation.

For the comparison of retention mechanisms, both the NP-HPLC and pSFC separations were run on the NH<sub>2</sub> column, while the RP-HPLC separation was run on an ODS column. The elution orders of the NP-HPLC and pSFC separations were the same (as expected) while for the RP-HPLC separation, the elution order was almost the reverse, demonstrating the orthogonal nature of SFC compared to RP-HPLC. For the NP-HPLC and

pSFC separations, the authors concluded that the elution order was mainly governed by the number of hydroxyl groups possessed by the solute; i.e. those with one hydroxyl group eluting first followed by those with two hydroxyl groups etc. The second factor governing elution order in the NP-HPLC and pSFC separations was the size of the solutes dipole moment. The authors estimated the dipole moments for four of the corticosteroids using the molecular orbital method and found correlation between retention and the size of the calculated dipole moment for solutes containing the same number of hydroxyl groups; i.e. those with larger dipole moments being retained longer on the column. All three separations were shown to be comparable in terms of efficiency and resolution. However, the pSFC method was 4 times faster than the NP-HPLC method and 1.5 times faster than the RP-HPLC method demonstrating the potential advantages for the application of pSFC as a rapid method for quality control and routine analysis.

Wang *et al.* [128] developed an orthogonal pSFC method to an RP-HPLC method for mometasone furonate impurity analysis. On review of the literature, the authors noted that there had been very few publications involving the application of SFC for impurity analysis [188,189]. They attributed this to the lower sensitivity of SFC compared to HPLC. The authors evaluated three polar stationary phases including; 2-ethylpyridine, cyano, and silica. The best separation was achieved on a (5  $\mu\text{m}$ ) 4.6 mm x 250 mm silica column with optimum operating conditions using a shallow gradient of 5 to 15% MeOH in CO<sub>2</sub> over 15 min delivered at a flow rate of 4.0 mL.min<sup>-1</sup>. Mometasone furonate linearity was established from 0.1% to 120.0% of the nominal concentration, yielding an  $r^2$  value > 0.999. Accuracy at the assay level ranged from 99.8% to 101.6% while at the impurity level it ranged from 88.3% to 104.7%. Precision % RSD results of 0.7% (n=6) were obtained at the assay level while the recovery precision % RSD of each impurity was in the range of 1.4 to 5.4%. The LOQ of the method was determined to be 0.05% (relative to the active) for the impurities. The developed pSFC method was compared to the established RP-HPLC method which was run on a (5  $\mu\text{m}$ ) 4.6 mm x 250 mm ODS column. Both methods gave comparable results for linearity, accuracy, precision (repeatability) and LOQ. However, the pSFC method provided baseline separation for all components with an analysis time less than one third of that required by the RP-HPLC method. This study demonstrated that if measures were taken to compensate for the lower inherent sensitivity of pSFC, it can be used as an alternative or complementary technique to HPLC for trace impurity analysis in the QC environment.

Lateef *et al.* [190] developed a pSFC method to replace the USP NP-HPLC method for the assay of P raw material. The developed method was run on an Agilent ZORBAX Rx-SIL (5  $\mu\text{m}$ ) 4.6 mm  $\times$  250 mm column with optimum operating conditions obtained with a mobile phase of (85:15)  $\text{CO}_2/\text{MeOH}$  delivered isocratically at a flow rate of 2.9  $\text{mL}\cdot\text{min}^{-1}$ . Column temperature was set to 40  $^\circ\text{C}$  with the back pressure regulator set to 150 bar. An injection loop of 5  $\mu\text{L}$  was over-filled with 15  $\mu\text{L}$  of sample and peaks were detected at 254 nm. The developed method was assessed for linearity, LOD, LOQ and robustness. The method was found to be linear over a range of 7 to 480  $\mu\text{g}\cdot\text{mL}^{-1}$  with an LOD and LOQ for PAC of 2  $\mu\text{g}\cdot\text{mL}^{-1}$  and 7  $\mu\text{g}\cdot\text{mL}^{-1}$  respectively. Robustness was assessed for flow rate ( $\pm 2\%$ ), column temperature ( $\pm 2.5\%$ ), injection volume ( $\pm 3\%$ ), absorption wavelength ( $\pm 1$  nm) and modifier concentration ( $\pm 1\%$ ). Of the conditions investigated, the method was found to be tolerant of changes to flow rate, column temperature and injection volume, while alterations to absorption wavelength and modifier concentration were not tolerated. The peak area repeatability % RSD for P at 100 ppm was 0.1% for ( $n = 4$ ), while for retention time % RSD was less than 0.2%, thus demonstrating the precision of the developed method. The developed method was then compared to the established NP-HPLC method for the assay of P in real samples. Both methods gave equivalent results for the sample tested with the pSFC method being approximately 4 times faster (5.5 min compared to 20 min) and approximately 17 times less expensive (per sample assayed) than the established NP-HPLC method.

#### **4.1.2 Method Validation using the Total Error Approach**

Figure 4.1 demonstrates that validation is one of the main steps in the life cycle of any analytical method; with the purpose of performing validation is to demonstrate that the analytical method is fit for its intended use. Given its importance, many official guidance documents have been published (ISO, GMP, FAD, ICH, etc.) which describe the criteria of validation to be tested depending on the type of analytical method being validated. However, despite the volume of such guidance documents, confusion can still remain as to whether or not the analytical method is indeed validated [191]. The main reason for this is that, although these guidance documents define validation criteria to be tested, they do not propose experimental approaches and are therefore most often limited to general concept [191]. To overcome this confusion, the commission of the Societe Francaise des Sciences et Techniques Pharmaceutiques (SFSTP) generated a report detailing the harmonization of approaches for the validation of quantitative analytical methods [192] in order to help the pharmaceutical industry to fully validate their analytical methods.

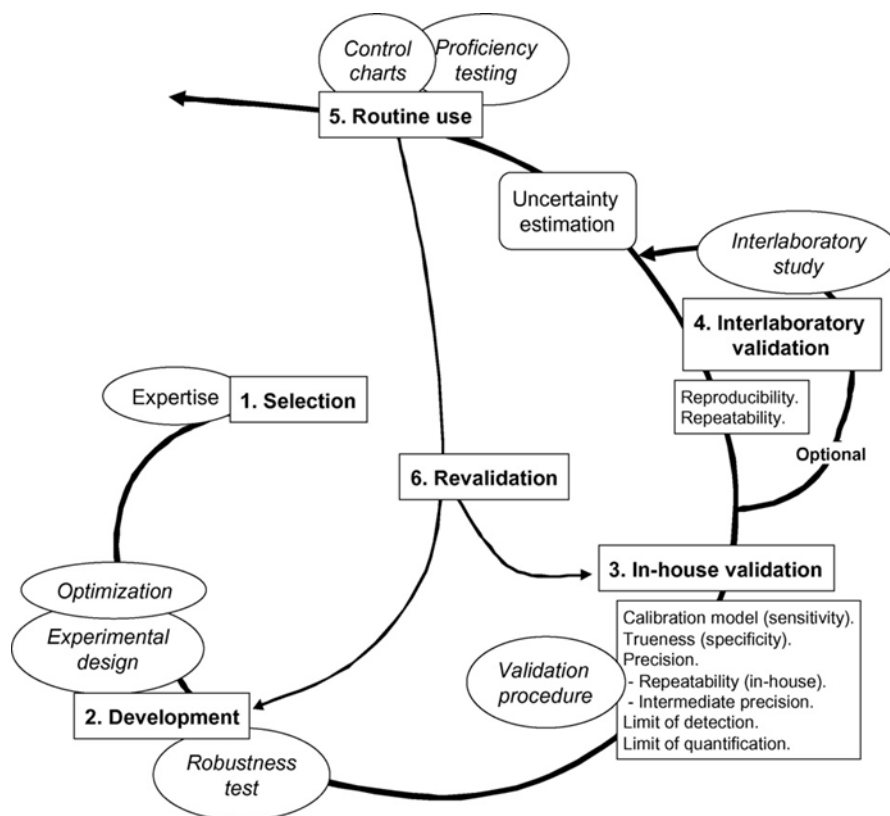


**Figure 4.1:** Lifecycle of an analytical method. Reproduced from [197].

The SFSTP report recommended a statistical based approach to validation of analytical methods based on two sided  $\beta$ -expectation tolerance intervals for total error. Using the total error approach, a predetermined number of experiments are carried out using the analytical method in order to generate estimations of method bias and method variance. These estimates are then used to compute tolerance interval which represents a region where, on average it is expected to find a defined proportion of the population of the results, i.e.  $\beta$  [193]. The calculated tolerance intervals are used to construct what is known as an “accuracy profile” which is a graphical representation, combining the calculated tolerance intervals, (based on the total error (method bias + standard deviation)), bias and the predefined method acceptance limits ( $\lambda$ ). An example of an accuracy profile is shown in Figure 4.2.

Using this validation approach, it is possible to unambiguously demonstrate the fitness-for-purpose of the new analytical method as stated in all regulatory documents [191]. To aid with the implementation of this novel validation strategy, Hubert *et al.* produced a series of papers detailing the rationale behind the approach [191], experimental design necessary to implement the approach [194], a practical worked example for reference [195]

and finally, illustrating the applicability of the validation approach by presenting real examples of its application to method validations over a wide range of method types [196]. Other authors have also produced publications on the implementation of the total error validation approach including M. Feinberg [197], A. Gustavo Gonzalez *et al.* [198] and D. Hoffman *et al.* [199].

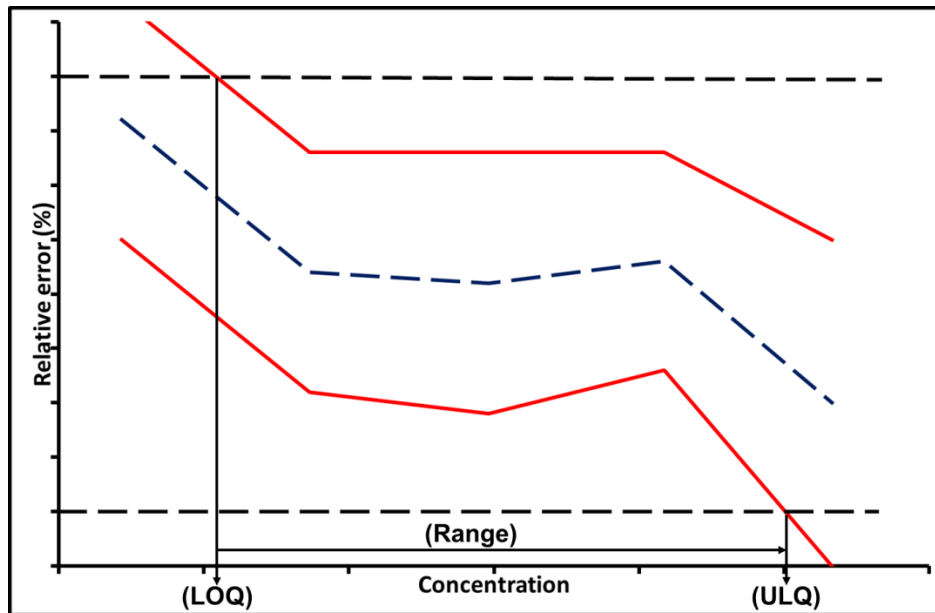


**Figure 4.2:** Example of an accuracy profile. The red lines represent the upper and lower relative tolerance intervals respectively, the dashed blue line represents the mean relative bias and the dashed black lines represent the acceptance limits of the method ( $\pm\lambda$ ). The intersection points of the tolerance intervals with the acceptance limits represent the calculated LOQ and ULQ.

The objective of any so called “good analytical method” is to be able to quantify as accurately as possible the unknown quantities present in samples tested in the laboratory; i.e. that the difference between the “measured value” ( $x$ ) and the “true value” ( $\mu_T$ ) (which will always remain unknown), is as low as possible, or at least lower than an acceptable limit [191]. This can be expressed in Equation 1 [191]:

$$-\lambda < x - \mu_T < \lambda \Leftrightarrow |x - \mu_T| < \lambda \quad \text{Eq. (1)}$$

Where  $\lambda$ , the acceptance limit which is set depending on the requirements or objective of the analytical method. Thus, two important concepts are introduced for this approach to method validation, namely (i) acceptance limits ( $\lambda$ ) for the performance of the method must be defined and (ii), the analyst must take responsibility in the decision of accepting the performance of the method with respect to its intended use [191].

Every analytical method used for quantitative analysis is subject to inherent errors [200]. Therefore, one of the guiding principles in statistical analysis is that no quantitative results are of any value unless they are accompanied by some measure of the errors inherent within them [200]. The types of inherent errors of most importance in a quantitative analytical method can be categorised as “*random errors*” and “*systematic errors*”. Random errors affect the precision or reproducibility of an experiment and are associated more with analyst input, but may also arise from instrumentation imprecision or environmental factors e.g. temperature fluctuations. Systematic errors, also called “*bias*”, affect the accuracy of the experiment and are associated more with the equipment used in the experiment. Random errors, known as the “*true variance*” ( $\sigma_M^2$ ) is measured by standard deviation whereas systematic errors ( $\mu_M$ ) is measured as “*true bias*” of the analytical method. As with the true value ( $\mu_T$ ), the actual value for both ( $\sigma_M^2$ ) and ( $\mu_M$ ) will always remain unknown for a given analytical method. However, estimations for ( $\sigma_M^2$ ) and ( $\mu_M$ ) can be made from the experiments carried out during the validation of the analytical method [191]. The reliability of these estimates depends on the adequacy of the measurements performed on samples of known concentration, experimental design and the number of replicates performed during the validation phase [191]. Once these estimates for ( $\sigma_M^2$ ) and ( $\mu_M$ ) have been obtained, they can be used to evaluate the ability of the analytical method to quantify with sufficient accuracy each of the unknown quantities the method will be subject to in its future application; i.e. to determine if the method is a “*good analytical method*” [201,202].

Deciding on what the acceptance limits ( $\lambda$ ) of the analytical method will be depends on its intended use, e.g. the analysis of bulk pharmaceutical compounds, dosage forms or bioanalysis. However, as all analytical methods have inherent errors, it is next to impossible to be able to state that every future result generated will lie within the selected acceptance limits ( $\lambda$ ). To overcome this dilemma, the analyst has to try to control the risk associated with the analytical method by starting with the assumption that only an acceptable maximum proportion of future measurements will fall outside the defined acceptance limits ( $\lambda$ ), e.g. 5%

of all future results will fall outside  $\lambda$ . Therefore, a method can be qualified as acceptable if it is very likely (i.e. with a guarantee) that the difference between every measurement ( $x$ ) and the true value ( $\mu_T$ ) is inside the predefined acceptance limits ( $\lambda$ ) [191]. Equation 2 describes this concept which lies at the heart of this validation approach [191]:

$$P(|x - \mu_T| < \lambda) \geq \beta \quad \text{Eq. (2)}$$

Where  $\beta$  is the proportion of measurements lying within the acceptance limits ( $\lambda$ ) fix a priori according to the objectives of the method. Therefore, the expected proportion of measurements ( $P$ ) expressed as a percentage, which fall outside the acceptance limits ( $\lambda$ ) represents the risk of the analytical method [191].

In this context, the purpose of method validation is, via a selectively designed set of experiments, to provide the analyst with good estimates of the standard deviation of the intermediate precision of the method ( $\hat{\sigma}_M$ ), along with estimates of method bias ( $\hat{\mu}_M$ ). These estimates will be more reliable if the experimental design and the number of experiments performed in method validation are appropriate [195,203,204]. Details of the experimental design required to achieve good estimates for both ( $\hat{\sigma}_M$ ) and ( $\hat{\mu}_M$ ); i.e. validation protocols, are outlined in Part II of the summary report produced by Hubert *et al.* [195]. In this report, it is emphasised that it is necessary to perform these validation studies in the same way that the analytical method will be run during routine use; i.e. that the samples used should be prepared in the same sample matrix as the samples tested in routine use. These estimates of both ( $\hat{\sigma}_M$ ) and ( $\hat{\mu}_M$ ) are then used to calculate the confidence interval that allows the evaluation of the proportion of the measurements that will lie inside the acceptance limit ( $\lambda$ ). The confidence interval used is the so-called “two-sided  $\beta$ -expectation tolerance interval” proposed by Mee [205], which defines an interval where the expected proportion of future results will fall in  $\beta$  [191] and obeys the following property;

$$E_{\hat{\mu}, \hat{\sigma}}\{P[|x_i - \mu_T| < \lambda] / \hat{\mu}_M, \hat{\sigma}_M\} \geq \beta \quad \text{Eq. (3)}$$

With ( $E$ ) meaning the “expected value” of the result and ( $x_i$ ) the overall mean result for series  $i$ .

Although the estimations of method bias ( $\hat{\mu}_M$ ) and method variance ( $\hat{\sigma}_M$ ) are essential elements to compute the evaluation of the expected proportion of measurements

within the acceptance limits (i.e. the calculated tolerance intervals), the decision of whether a method is indeed a “*good method*” is not based on these estimates [191]. Instead, the calculated tolerance intervals are used to construct what is known as an accuracy profile which is a graphical representation, combining the calculated tolerance intervals, (based on the total error (bias + standard deviation)), bias and acceptance limits ( $\lambda$ ). Therefore, the accuracy profile can be used as the decision making tool which not only brings together the objectives of the procedure with those of validation, but also allows the analyst to visually evaluate the capacity of the procedure to fulfil its objectives and to control the risk associated with its routine use [191,206].

The main steps involved in the generation of an accuracy profile are summarised as follows;

### ***Step 1: Design of Experiments***

The validation protocols must outline a sufficient but realistic number of experiments to ensure the data generated is of high enough quality to give good estimation of method bias ( $\hat{\mu}_M$ ) and method variance ( $\hat{\sigma}_M$ ). Two types of solutions must be prepared for use in the validation experiments namely (i) calibration standards (CSs) and (ii) validation standards (VSs). CSs are solutions containing reference standard material at a known concentration which are prepared in sample diluent without any sample matrix components being present. VSs which are solutions containing reference standard material at a known concentration which are prepared in sample diluent, which also includes all of the sample matrix components and are designed to mimic “*real samples*”. A typical validation experimental design involves replicate preparations of CSs and VSs, (at several concentrations over the selected concentration range) which are then analysed in series under the specified analytical conditions. Several such series are performed with fresh CSs and VSs being prepared (from common stocks) for each individual series. Typically, different series are prepared and run on different days. For ease of calculation, it is important that the study design is balanced, i.e. the repetition number is identical in every series for each concentration level [195].

### ***Step 2: Determination of the Response Function***

CSs are used to determine what is termed the “*response function*” of the method. The response function is the relationship between the response (signal or response of the apparatus)  $Y$  and the quantity (concentration)  $X$  [195]. This relationship is characterised by a function that must be strictly monotonic (i.e. strictly increasing or decreasing) over the

considered determination interval [195,207,208]. Two families emerge from this set: those which are linear in their parameters (i.e. if it is a linear combination of its parameters) and those which are non-linear. Most physico-chemical methods will use the straight line (through zero point or not) linear response function models [195].

### **Step 3: Response Function Fitting**

The suggested approach to fit the response function is to use the “*maximum likelihood method*” which consists in finding the parameters values that maximize the function representing the likelihood to observe the generated result [195]. For pharmaceutical based assays of dosage forms the main type of response function will be either linear (L) or linear through 0 (L<sub>0</sub>);

$$\text{Straight line: } Y = \alpha + \beta X \quad \text{Eq. (4)}$$

$$\text{Straight line through 0: } Y = \beta X \quad \text{Eq. (5)}$$

Where;

$Y$  is the dependent variable,  $X$  is the explanatory variable,  $\beta$  is the slope of the line and  $\alpha$  is the intercept of the line.

### **Step 4: Calculation of the Inverse Prediction**

Inverse predictions are the back-calculated concentrations generated from the response function model. These calculations are typically carried out on the VSs. It should be noted that what is really important is not the quality of the response function fit, but rather the quality of the inverse predictions (or back-calculated concentrations) generated by the response function model. Therefore, preference must be given to a model giving good results rather than a model presenting a good quality of fit [195]. Back-calculated concentrations generated using the two linear response functions described above are calculated as follows [195]:

$$\text{Straight line: } x_{ijk,calc} = \frac{y_{ijk} - \hat{\alpha}_i}{\hat{\beta}_i} \quad \text{Eq. (6)}$$

$$\text{Straight line through 0: } x_{ijk,calc} = \frac{y_{ijk}}{\hat{\beta}_i} \quad \text{Eq. (7)}$$

Where;

$x_{ijk,calc}$  is the  $k^{\text{th}}$  back-calculated concentration of the  $i$  series  $j$  level,  $\hat{\beta}_i$  is the  $i$  series slope of the regression line,  $y_{ijk}$  is the  $k^{\text{th}}$  response of the  $i$  series  $j$  level and  $\hat{\alpha}_i$  is the  $i$  series y-intercept.

**Step 5: Estimation of Precision (Repeatability and Intermediate Precision)**

The back-calculated concentrations generated from the VSs are used to estimate the precision of the analytical method. The first step in calculating the between-series ( $\sigma_{B,j}^2$ ) and the within-series ( $\sigma_{W,j}^2$ ) variances is to calculate the mean sum of squares for both within-series (MSE) and between-series (MSM) respectively. The following equations can be used to determine the MSE and MSM values for a given data set [195]:

$$\text{MSM}_j = \frac{1}{p-1} \sum_{i=1}^p n_{ij} (\bar{x}_{ij,calc} - \bar{x}_{j,calc})^2 \quad \text{Eq. (8)}$$

$$\text{MSE}_j = \frac{1}{\sum_{i=1}^p n_{ij} - p} \sum_{i=1}^p \sum_{k=1}^{n_{ij}} (\bar{x}_{ijk,calc} - \bar{x}_{ij,calc})^2 \quad \text{Eq. (9)}$$

Where;

$\bar{x}_{ij,calc}$  is the  $k^{\text{th}}$  back-calculated concentration of the  $i$  series  $j$  level,  $\bar{x}_{j,calc}$  is the mean back-calculated concentration of the  $j$  level,  $n$  is the number of replicates and  $p$  is the number of series run [195]. Once no experimental data is missed; i.e. the same number of replicates for the same concentration levels were performed for each series run, the above calculations can be carried out by performing single factor analysis of variance (ANOVA) using statistical software to automatically generate the MSM and MSE results [209]. Once the MSM and MSE values have been determined for a given data set, the variance components ( $\sigma_{B,j}^2$ ) and ( $\sigma_{W,j}^2$ ) are estimated as follows for each concentration level [195]:

If  $MSM_j > MSE_j$ , then;

$$\sigma_{W,j}^2 = MSE_j \quad \text{Eq. (10)}$$

$$\sigma_{B,j}^2 = \frac{MSM_j - MSE_j}{n} \quad \text{Eq. (11)}$$

Where  $n$  equals the repetition number in each series.

If  $MSM_j < MSE_j$ , then;

$$\sigma_{W,j}^2 = \frac{1}{pn - 1} \sum_{i=1}^p \sum_{k=1}^k (x_{ijk,calc} - \bar{x}_{j,calc})^2 \quad \text{Eq. (12)}$$

$$\sigma_{B,j}^2 = 0 \quad \text{Eq. (13)}$$

The within-series variance ( $\sigma_{W,j}^2$ ) provides the repeatability variance estimate, while the sum of the within-series ( $\sigma_{W,j}^2$ ) and between-series ( $\sigma_{B,j}^2$ ) variance provides an estimation of the intermediate precision variance as follows [195]:

$$\text{repeatability: } \sigma_{Re,j}^2 = \sigma_{W,j}^2 \quad \text{Eq. (14)}$$

$$\text{intermediate precision: } \sigma_{Ip,j}^2 = \sigma_{W,j}^2 + \sigma_{B,j}^2 \quad \text{Eq. (15)}$$

### ***Step 6: Estimation of Trueness (bias)***

The back-calculated concentrations generated from the VSs are also used to estimate the trueness of the analytical method. The trueness (or bias) of an analytical method expresses the closeness of agreement between the average trial result and the acceptance reference value, also known as the conventional true value [195,210,211]. The bias at each concentration level ( $j$ ), is obtained by calculating the difference between the introduced concentrations (arithmetic) mean ( $\bar{x}_j$ ) and the calculated concentration mean ( $\hat{\mu}_j$ ) [195]. The bias can be expressed in absolute, relative or in recovery terms as follows:

$$\text{absolute bias}_j = \hat{\mu}_j - \bar{x}_{.j}. \quad \text{Eq. (16)}$$

$$\text{relative bias}_j(\%) = 100 \times \frac{\hat{\mu}_j - \bar{x}_{.j}}{\bar{x}_{.j}}. \quad \text{Eq. (17)}$$

$$\text{recovery}_j(\%) = 100 \times \frac{\hat{\mu}_j}{\bar{x}_{.j}}. \quad \text{Eq. (18)}$$

### **Step 7: Tolerance Interval Calculation**

The role of the tolerance interval is to provide a guarantee or representation of what results will be produced by the analytical method during routine analysis [195]. The  $\beta$ -expectation tolerance interval as proposed by Mee [205] uses the estimations of trueness and precision parameters  $\mu_j$  (the mean of the back-calculated concentrations at  $j$ -concentration level),  $\sigma_{B,j}^2$  and  $\sigma_{W,j}^2$  at each concentration level of the VS to calculate the expected proportion of results located within the acceptance limits ( $\pm\lambda$ ) [195]. In relative terms, the following equation is used to calculate the lower and upper  $\beta$ -expectation tolerance intervals [195]:

$$L_j = \text{bias}_j(\%) - Q_t \left( v; \frac{1+\beta}{2} \right) \sqrt{1 + \frac{1}{pnB_j^2}} CV_{IP,j} \quad \text{Eq. (19)}$$

$$U_j = \text{bias}_j(\%) + Q_t \left( v; \frac{1+\beta}{2} \right) \sqrt{1 + \frac{1}{pnB_j^2}} CV_{IP,j} \quad \text{Eq. (20)}$$

Where;

$$CV_{IP,j} = 100 \times \frac{\sigma_{IP,j}}{\bar{x}_{.j}} \quad \text{Eq. (21)}$$

$$R_j = \frac{\hat{\sigma}_{B,j}^2}{\hat{\sigma}_{W,j}^2} \quad \text{Eq. (22)}$$

$$B_j = \sqrt{\frac{R_j + 1}{nR_j + 1}} \quad \text{Eq. (23)}$$

$$v = \frac{(R_j + 1)^2}{(R_j + 1/n)^2 / (p - 1) + (1 - (1/n)) / pn} \quad \text{Eq. (24)}$$

$$Q_t \left( v; \frac{1 + \beta}{2} \right) = \text{the } \beta \text{ quantile of the Student t distribution with } v \text{ degrees of freedom} \quad \text{Eq. (25)}$$

Two terms are contained in the tolerance interval: (i) trueness and (ii) up to a factor, the intermediate precision coefficient variation. Therefore, the tolerance interval may be considered as an expression of the results accuracy. However, the tolerance interval incorporates an additional dimension; i.e. the chance or risk of future results, conditional to past results (i.e. the results generated during the method validation), to fall within (or outside) the acceptance limits. Therefore, the method can be considered accurate, at  $\beta$  chance level, for the concentration level in question, if the tolerance interval is included within the acceptance limits ( $\pm\lambda$ ) defined a priori, according to the method objectives [195].

#### ***Step 8: Construction of the Accuracy Profile and decision making***

The accuracy profile is a 2D-graphical representation of the calculated results, with the x-axis comprised of the concentration levels and the y-axis comprised of the tolerance interval limits and accuracy expressed as either concentration or percent. The accuracy profile contains four main elements namely; (i) the upper and lower tolerance limits (which are achieved by joining on one hand the lower limits between themselves, and, on the other hand, the upper limits between themselves), (ii) the individual bias results, (iii) the mean bias (which are achieved by joining the mean bias results at each concentration level) and (iv) the acceptance limits ( $\pm\lambda$ ). Figure 4.2 represents an example accuracy profile (calculated in relative terms) for analytical results observed during method validation. From the accuracy profile a number of key validation elements can be determined which can be used to support the claim that the analytical method is indeed validated and fit for its intended use. The first of these is to demonstrate that the correct response function has been selected in order to achieve the objectives of the analytical method which are defined a priori. In Figure 4.2 it can be seen that the tolerance intervals (red lines) exceed the method acceptance limits (dashed black

lines) at the extremes. In this case the analytical method is deemed not validated over the selected concentration range. However, it should be noted that this could change if an alternative response function was selected to back-calculate the concentration results. The alternative accuracy profile based on results generated using a different response function may well result in the tolerance intervals being included within the acceptance limits. Thus, it is recommended that at least more than one response function is examined when using the total error validation approach [195].

Figure 4.2 also demonstrates that the accuracy profile can be used to determine the LOQ and upper limits of quantitation (ULQ) of the analytical method. By definition, the LOQ and ULQ estimates must have a sufficient degree of accuracy and precision. Therefore, as both these elements (accuracy and precision) are used in the construction of the accuracy profile, the intersections between the tolerance interval and the acceptance limits by definition, represents the LOQ and ULQ for the analytical method. Between these two limits lies the dosing range for the analytical method. If no intersections take place between the tolerance intervals and the acceptance limits, then the LOQ and the ULQ will default to the extreme concentration values investigated during the validation experiments [195].

In summary, at the end of the validation process, the only decision that has to be made is whether or not the analytical method is valid. The accuracy profile generated from the total error approach can be used to answer this question. With the accuracy profile, the analytical interpretation is easy and all the useful required statistics, such as trueness, precision, quantitation limits, risk, linearity are integrated. In addition, the accuracy profile makes possible a visual representation of the future performance of the analytical method [195]. For example, in the case where an accuracy profile was generated with  $\beta$  set at 95% and the method acceptance limits at  $\pm 20\%$ , if the tolerance intervals did not exceed the acceptance limits for any concentration level in the selected range, then it can be said that for all future results generated using the analytical method, 95 times out of 100 the result generated will be within  $\pm 20\%$  of the true value. Or alternatively, in terms of defining the risk associated with the analytical method, there is a 5% risk that all future results will be greater than  $\pm 20\%$  from the true value. Being able to provide such information allows the analyst to be able to meet one of the guiding principles in statistical analysis; i.e. being able to provide quantitative results of value, accompanied by a measure of the errors inherent within them. In the interests of clarity, a detailed worked example for the calculation of the

relative  $\beta$ -expectation tolerance intervals is provided in Appendix A. **Note:** a t-distribution table is provided in Appendix B to facilitate the reader with future calculations.

A critical analysis of several analytical method validation strategies in the framework of the fit-for-purpose concept was carried out by A. Bouabidi *et al.* [193]. The authors compared the validation of two quantitative HPLC analytical methods using the classical descriptive, difference and equivalence approaches along with the total error approach based on accuracy profiles. By employing Monte Carlo Simulations to data generated using the various validation methodologies, the authors demonstrated that the only validation approach that gave enough guarantees of the valid method providing results with a high probability of being inside the acceptance limits or specifications, was the total error with accuracy profiles methodology [193]. The authors also made reference to the fact that the more traditional validation methodologies look at method performance in terms of bias and precision rather than at the repeatability of the results. This is a contradiction in terms as the objective of method validation is to provide evidence that the analytical method is capable of providing accurate or acceptable results when used routinely in the QC laboratory.

However, this can be achieved with the total error approach based on accuracy profiles as it provides a measure of credibility for the results that will be generated using the analytical method in the future [193]. Therefore, the total error approach based on accuracy profiles methodology allows the analyst to control the risk of accepting an unsuitable method while simultaneously providing a guarantee that all future results generated using the method will be included within the predefined acceptance limits set a priori [193]. In addition, the accuracy profile also makes possible a visual representation of the future performance of the analytical method [195]. Therefore, the accuracy profile can be used to answer this question of whether or not the analytical method is valid. With the accuracy profile, the analytical interpretation is easy in which all the useful required statistics, such as trueness, precision, quantitation limits, risk, linearity are integrated.

Part IV in the series by Hubert *et al.* [196] presents a number of applications of the total error approach to method validation in various fields including: drugs control, impurities quantification by HPLC in raw materials, biological analysis and food analysis. The purpose of this publication was to demonstrate the potential universalism of the total error approach for whatever analytical method was being validated. The authors also made reference to examples where the total error validation approach was applied to LC methods with UV or

fluorescence detection [110,212-219], CE methods [113,220] and a gas chromatography (GC) method [221]. While a detailed discussion of each of the applications listed above is beyond the scope of this present work, it was noted that all applications only considered the analysis of a single peak with only two applications; one HPLC [110] and one CE [113] (summarised in Section 2.1.2 and Section 2.1.3 above) employing the total error validation approach for impurity level analysis.

In a recent review of the analytical lifecycle of SFC methods performed by Andri *et al.* [222], the authors highlighted important scientific outputs in the field of analytical SFC and also included discussions on the topic of SFC method validation. Their review of the literature revealed that there were only a limited number of papers dealing with SFC method validation, with most SFC applications being essentially qualitative or preparative and only a few being quantitative [222]. They also noted that of the reported validated SFC methods, only Dispas *et al.* had employed the total error approach to SFC method validation [223].

In their work Dispas *et al.* stated that previous SFC publications had failed to fully assess the quantitative performance of SFC and therefore set about to publish the first work on the evaluation of the quantitative performances of SFC from method development to validation [223]. Their work consisted of evaluating the quantitative performances of an ultra-performance SFC (UPSFC) method compared to a UPLC to demonstrate that, based on the method performance, the UPSFC method could be a viable alternative to the UPLC method. Both the UPSFC and UPLC methods were developed using a Quality by Design (QbD) approach to ensure robust methods were generated. The methods were subsequently validated using the total error approach with accuracy profiles, prior to their use in a QC laboratory for the manufactured medicines control. The selected application was a screening method for the identification and quantitation of several antibiotics including; phenoxymethylpenicillin (penicillin V), doxycycline, levofloxacin, metronidazole, amoxicilline, trimethoprim and clindamycin to aid in the fight against poor quality counterfeit medicines. The European Medicines Agency (E.M.A.) defined specifications of  $\pm 5\%$  for the assay of active substance(s) were employed for the dosing range studied; i.e. at five concentration levels ranging from 50 to 150% of the target concentration. Amoxicilline was selected for the method validation tests as a worst-case test, as it was the most polar compound of the test compounds investigated and hence had very low solubility in the organic solvent. For the validation of the UPSFC method, the CSs and VSs were prepared at 7.5 times the concentration compared to the UPLC method due to the lower sensitivity of

UPSFC–UV than UPLC–UV, which the authors attributed to the difference of solvating power between supercritical fluids and liquids.

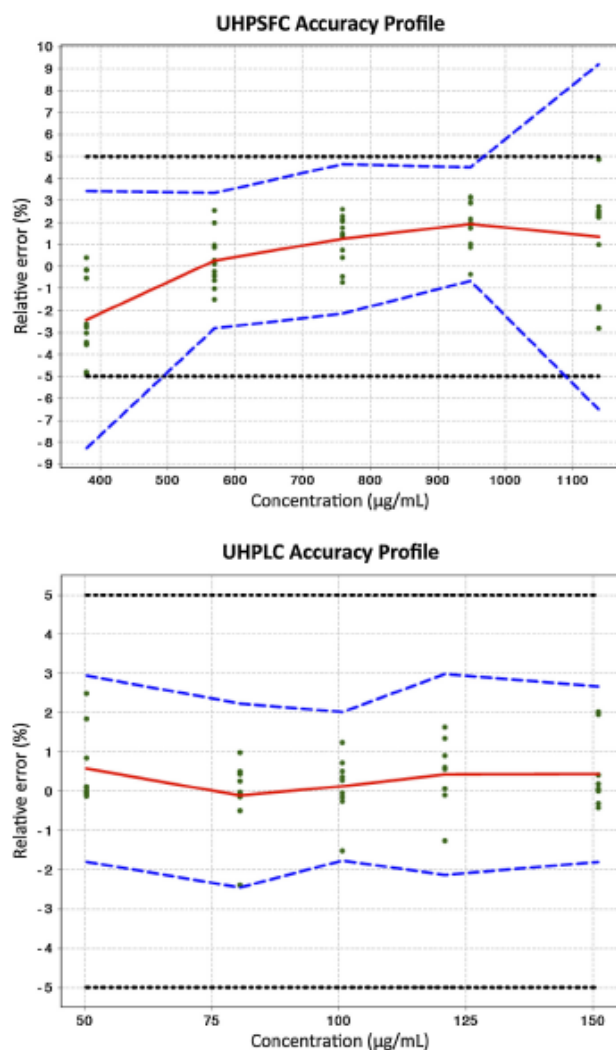
In terms of the precision criterion, it was observed that while the UPLC method showed lower RSD values ( $< 1\%$  for repeatability and intermediate precision) across the entire concentration range studied, the UPSFC method RSD values are close to 1 (highest value: 1.22% for level 2); over the three median concentration levels which correspond to 80– 120% of the targeted concentration. However, these UPSFC precision results meet the E.M.A. and ICH requirements and therefore, despite the lower precision than the UPLC method, the UPSFC method was acceptable to meet the precision specifications for pharmaceutical finish product.

Figure 4.3 illustrates the accuracy profiles generated for both the UPSFC and UPLC methods. As illustrated, the UPSFC method upper and lower 95%  $\beta$ -expectation tolerance limits (%) exceeded the acceptance limits set at  $\pm 5\%$  for the extremities of the concentration range investigated. Therefore, the UPSFC method was only able to provide accurate results over the concentration range corresponding from 65.8 to 129.1% of the target concentration, whereas the UPLC method was considered valid over the complete concentration range tested (i.e. from 50 to 150% of the target concentration). However, despite this, the UPSFC method was valid at least in the 80–120% of the target concentration interval with acceptance limits set at  $\pm 5\%$ , which demonstrated its suitability for the quality control of manufactured medicines [223].

Finally, the authors applied both the UPSFC and UPLC methods to test real samples ( $n=3$ ). The results obtained were similar for both methods with;  $105.9 \pm 1.6\%$  (mean  $\pm$  RSD) obtained for the UPSFC method and  $106.6 \pm 1.9\%$  (mean  $\pm$  RSD) for UPLC method. Thus, the authors concluded that compared to the well-established UPLC technique, UPSFC showed real promise in the field of QC quantitative analysis. Their study was the first demonstration of a successful total error approach validation of UPSFC method, thus opening the door of pharmaceutical industry QC lab [223]. Their work also demonstrated the application of UPSFC outside the academia research context and provided QC laboratories of the pharmaceutical industry with a new eco-friendly tool for the quantitative analysis [223].

Therefore, despite an extensive review of the literature, to the best of our knowledge no SFC method has been reported for the quantitation of PAC and its related impurities (shown in Figure 3.1) in an ophthalmic suspension. We were also unable to find any

application of the total error validation approach for SFC methods designed for trace impurity analysis. With this in mind, we set out to develop a stability-indicating SFC method with orthogonal selectivity to the RP-HPLC method described in Chapter 3, for the analysis of PAC and eight related impurities in a drug product ophthalmic suspension, and to validate the developed method using the total error approach described above.



**Figure 4.3:** Accuracy profile obtained for the validation of the quantification amoxicilline in pharmaceutical formulation by considering linear regression as model for the calibration curve. The acceptance limits have been fixed at  $\pm 5\%$ . The plain red line represents the relative bias, the dashed blue lines are the 95%  $\beta$ -expectation tolerance limits and the dotted black lines are the acceptance limits. Top: UPSFC method; bottom: UPLC method. Reproduced from [223].

## 4.2 Experimental

### 4.2.1 Instrumentation and Software

The Thar SFC Method Station Analytical System (Thar SFC /Waters), Pittsburgh, PA) was equipped with a Fluid Delivery Module (CO<sub>2</sub> pump and solvent pump), Analytical-2-Prep column oven capable of holding ten analytical columns up to 250 mm in length, Alias autosampler, automated back pressure regulator and a Waters 2998 photodiode array (PDA) detector (Waters, Milford, MA, USA). Injection loops of 10  $\mu$ L and 100  $\mu$ L were used during initial method development. The maximum flow rate, pressure and column temperature were 10 mL.min<sup>-1</sup>, 400 bar and 90 °C respectively. The instrument control data collection was conducted using Waters Empower<sup>TM</sup> 2 software.

The Agilent 1260 Infinity Analytical SFC system was equipped with a PDA detector and coupled to an Aurora SFC Fusion A5 CO<sub>2</sub> delivery system (Agilent Technologies, Santa Clara, CA, USA). A 5  $\mu$ L injection loop was fitted which operated in the full loop mode with needle overfill and methanol was used as the solvent wash. The column oven was capable of holding two analytical columns up to 250 mm in length. The maximum flow rate, pressure and column temperature of the instrument are 5 mL.min<sup>-1</sup>, 600 bar and 70 °C respectively. Peaks were integrated at a wavelength of 254 nm using Agilent Chemstation software Rev B.04.03.

The Waters Acquity UPC<sup>2</sup> system (Waters, Milford, MA, USA) was equipped with a PDA detector. A 10  $\mu$ L loop was fitted which operated in the partial loop mode with needle overfill, with methanol used as the wash solvent. The column oven was capable of holding two analytical columns up to 150 mm in length. The maximum flow rate and pressure of the instrument are 4 mL.min<sup>-1</sup> and 413 bar respectively, while the column oven is compatible with temperatures of up to 90 °C. Peaks were integrated at a wavelength of 254 nm using Waters Empower<sup>TM</sup> 3 software.

Columns used included: Phenomenex Luna Silica, Phenomenex Luna CN, Phenomenex Luna NH<sub>2</sub>, Phenomenex Luna HILIC (Phenomenex, Madrid Avenue, Torrance, CA, USA) and Waters Viridis SFC 2-Ethylpyridine (Waters, Milford, MA, USA) all with dimensions of 100 Å (5  $\mu$ m) 4.6 mm x 250 mm. Also, Waters Torus DEA and Torus PIC 130 Å (1.7  $\mu$ m) 3.0 mm x 100 mm columns were used.

#### **4.2.2 Materials and Reagents**

Materials and reagents were as described in Chapter 3 Section 3.2.2 with the following exception; CO<sub>2</sub> was food grade purchased from BOC Ltd. (Dublin, Ireland). The final drug product Samples of the PAC 1.0% (w/v) ophthalmic suspension were obtained from Allergan Pharmaceuticals Ltd. (Westport, Ireland).

#### **4.2.3 Solution preparation for PAC pSFC analysis**

**Note:** All solutions were prepared in low actinic glassware to protect from light.

##### **4.2.3.1 pSFC PAC Matrix Placebo solution preparation**

For the preparation of the validation standards (VS) and impurity validation standards (IVS) described below, an additional matrix spiking solution containing the matrix components of the ophthalmic suspension was prepared as described in Chapter 3 Section 3.2.3 All VS and IVS described hereafter were spiked (3:50) with the stock matrix spiking solution to ensure that matrix components were present at label strength after dilution.

##### **4.2.3.2 pSFC PAC Column Screening Study Standard Preparation**

For the initial column screening study, a stock standard solution of PAC was prepared in MeOH at a concentration of 2 g.L<sup>-1</sup>. Impurity stock standards of P-11,21D, HCA, P-17A, HC, P, 20(R) and 20(S) were prepared in MeOH at a concentration of 40 mg.L<sup>-1</sup>. From the stock solutions, a working solution was prepared in MeOH containing PAC at 200 mg.L<sup>-1</sup> and impurities at 4 mg.L<sup>-1</sup>; i.e. at approximately 2% of the PAC concentration.

##### **4.2.3.3 pSFC PAC Calibration and Validation Standard Preparations**

For the PAC calibration standards (CS) preparation, a stock solution was prepared at approximately 6 mg.mL<sup>-1</sup> in MeOH. The solution was then diluted with MeOH in order to obtain final concentrations of 480, 540, 600, 660 and 720 mg.L<sup>-1</sup>, equivalent to approximately 80%, 90%, 100%, 110% and 120% of nominal PAC concentration. For the PAC VS preparation, the same stock solution used for the PAC CS was diluted with MeOH across the same concentration range as above, but spiked with matrix solution as described in Section 3.2.3. The VS were independently prepared for each series to mimic as much as possible its corresponding PAC formulation in routine analysis. The validation experiments were conducted by means of running four sequences (with freshly prepared CS and VS) over

four separate days on the same UPSFC system. Triplicate injections of each concentration level were made for both the CS and VS.

#### ***4.2.3.4 pSFC PAC Impurity Calibration and Validation Standard Preparations***

For the impurity level calibration standards (ICS) preparation, the same stock solution used for the PAC CS was used. For each of the eight selected impurities, stock solutions were prepared at 0.2 mg.mL<sup>-1</sup> in MeOH. A PAC and impurity ICS was then prepared by diluting with MeOH in order to obtain final concentrations for PAC and impurities of 0.30, 0.60, 3.00, 6.00 and 12.00 mg.L<sup>-1</sup>, equivalent to approximately 0.05%, 0.10%, 0.50%, 1.00% and 2.00% of nominal PAC concentration. For the impurity level IVS preparation, the same stock solutions of PAC and the eight selected impurities used for the ICS were diluted with MeOH across the same concentration range as above, but spiked with matrix solution as described in Section 2.3.1 The IVS were independently prepared for each series to mimic as much as possible its corresponding PAC formulation in routine analysis.

**Note:** Due to a limited supply of impurity reference standard material, the impurity level validation experiments were conducted by means of running four series (two ICS and two IVS) over four separate days on the same UPSFC system. Triplicate injections of each concentration level were made for both the ICS and IVS. Response function and back-calculated amounts were obtained from all four series and used in the various calculations required to employ the total error validation approach.

#### ***4.2.3.5 pSFC PAC Real Sample Preparation***

For the preparation of real samples, the PAC-containing formulation was diluted 3 mL into a 50 mL amber volumetric flask with MeOH to give a nominal PAC concentration of 600 mg.L<sup>-1</sup>.

### **4.3 Results and discussion**

#### ***4.3.1 PAC pSFC Method Development***

The main objective of this work was to develop and validate a pSFC method, which could provide orthogonal selectivity along with comparable quantitative performance to that of the established RP-HPLC method, for the analysis of PAC and its eight selected impurities in an ophthalmic suspension. Initial method development was carried out on a Thar method station and consisted of performing a column screening study to select the most appropriate

stationary phase for the separation. Four traditional NP-HPLC polar stationary phases were selected, namely; Phenomenex Luna silica gel (Si), cyanopropyl-bonded silica (CN), propanediol-bonded silica (Diol) and aminopropyl-bonded silica (NH<sub>2</sub>) columns along with the Waters Viridis SFC 2-Ethylpyridine (2-EP) column which was developed more specifically for pSFC applications. All column dimensions were (5 μm) 4.6 mm x 250 mm. For the initial screening, neat MeOH which is considered to be the first choice for the elution of polar compounds in pSFC was used as the modifier [16]. Initial screening was carried out using the standard solutions described in Section 4.2.3.2 employing a shallow gradient of 14 to 18% modifier over 8.5 min with a 1 min equilibration. The chromatographic conditions employed in the initial screening study are detailed in Figure 4.4 along with representative chromatograms. Table 4.2 summarises separation performance in terms of retention time window, peak asymmetry at 10% and resolution at half height (0.5). The normalised resolution product (NRP) which is a measure of how evenly spaced the peaks are in a chromatogram was calculated as described by K.L. Ng *et al.* [224].

As shown in Figure 4.4 (a), on the Si column, only six peaks (of a total of eight peaks including PAC) were visible in the chromatogram. Although the  $R_s$  values at half height of the visible peaks were acceptable; i.e. > 1.5, the fact that only six peaks were observed indicates that there were some co-elutions occurring. Also, peak asymmetry of the PAC peak was poor (< 0.8). On the CN column Figure 4.4 (b), all peaks eluted very early in the chromatogram indicating less retention compared to the Si column. Once again, only six of the eight expected peaks were observed which also indicates that there were some co-elutions occurring.  $R_s$  values for three of the visible peak pairs were less than the required value of 1.5 and the peak asymmetry for peak 2 was poor (< 0.8).

**Table 4.1:** Solution preparation for validation of UPSFC method

Diluent	Solution	Analyte	Concentration	% w.r.t PAC Label Strength
MeOH	PAC stock standard	PAC	6.0 mg.mL <sup>-1</sup>	n/a
	Impurity stock standards	Individual impurities	0.20 mg.mL <sup>-1</sup>	n/a
MeOH	PAC CS	PAC	480 mg.L <sup>-1</sup> , 540 mg.L <sup>-1</sup> , 600 mg.L <sup>-1</sup> , 660 mg.L <sup>-1</sup> , 720 mg.L <sup>-1</sup>	80.0%, 90.0%, 100.0%, 110.0%, 120.0%
MeOH plus stock matrix spiking solution at 3:50	PAC VS	PAC	480 mg.L <sup>-1</sup> , 540 mg.L <sup>-1</sup> , 600 mg.L <sup>-1</sup> , 660 mg.L <sup>-1</sup> , 720 mg.L <sup>-1</sup>	80.0%, 90.0%, 100.0%, 110.0%, 120.0%
MeOH	PAC ICS	PAC	480 mg.L <sup>-1</sup> , 540 mg.L <sup>-1</sup> , 600 mg.L <sup>-1</sup> , 660 mg.L <sup>-1</sup> , 720 mg.L <sup>-1</sup>	80.0%, 90.0%, 100.0%, 110.0%, 120.0%
		Impurities	0.3 mg.L <sup>-1</sup> , 0.6 mg.L <sup>-1</sup> , 3.0 mg.L <sup>-1</sup> , 6.0 mg.L <sup>-1</sup> , 12.0 mg.L <sup>-1</sup>	0.05%, 0.10%, 0.50%, 1.0%, 2.0%
MeOH plus stock matrix spiking solution at 3:50	PAC IVS	PAC	480 mg.L <sup>-1</sup> , 540 mg.L <sup>-1</sup> , 600 mg.L <sup>-1</sup> , 660 mg.L <sup>-1</sup> , 720 mg.L <sup>-1</sup>	80.0%, 90.0%, 100.0%, 110.0%, 120.0%
		Impurities	0.3 mg.L <sup>-1</sup> , 0.6 mg.L <sup>-1</sup> , 3.0 mg.L <sup>-1</sup> , 6.0 mg.L <sup>-1</sup> , 12.0 mg.L <sup>-1</sup>	0.05%, 0.10%, 0.50%, 1.0%, 2.0%
MeOH	Method comparison sample	PAC	0.60 mg.mL <sup>-1</sup>	100.0%
	Method comparison impurity solution	Impurities	3.6 mg.L <sup>-1</sup>	0.6%

<sup>a</sup> PAC omitted from P and HCA impurity accuracy/linearity studies due presence of these impurities in PAC standard material

A similar situation was noted on the Diol column Figure 4.4 (c). Only six peaks of the eight expected peaks were observed which also indicates that there were some co-elutions occurring. Of the visible peaks,  $R_s$  values for peaks 5 and 6 was less than the required value of 1.5 and the peak asymmetry for peaks 2 and 5 were poor ( $< 0.8$ ). On the  $\text{NH}_2$  column Figure 4.4 (d), only five peaks of the eight expected peaks were noted in the initial injection. However, with replicate injections additional peaks were observed at the beginning of the chromatogram which indicated that not all peaks were eluting from the column under the given conditions.  $R_s$  values for the visible peak pairs were far greater than the required value of 1.5 and the peak asymmetry for the visible peaks were good (0.8-1.2). This observation; i.e. good peak asymmetry and resolution between the peaks that were observed, suggested that the  $\text{NH}_2$  column provided the greatest retention for the selected analytes. Finally, on the 2-EP column Figure 4.4 (e), only six peaks of the eight expected peaks were observed which also indicates that there were some co-elutions occurring.  $R_s$  values for two of the peak pairs were less than the required value of 1.5 and the peak asymmetry for peaks 2 and 5 were poor ( $< 0.8$ ).

The results of the screening study demonstrated that maximum retention was obtained on the  $\text{NH}_2$  column while minimum retention was obtained on the CN column. Although most columns gave promising results in terms of peak asymmetry (demonstrating that an additive wasn't necessary component of the mobile phase composition), given the co-elution and poor resolution observed under the given conditions for the Si, CN, Diol and 2-EP columns, it was decided to investigate optimising this gradient further on the  $\text{NH}_2$  column in order to obtain the desired separation.

As not all peaks in the mix were eluted from the  $\text{NH}_2$  column under the original gradient conditions, it was decided to increase the flow rate to  $4.0 \text{ mL}\cdot\text{min}^{-1}$  and the gradient from 15 to 23% modifier over 7 min with a 1 min equilibration step. To determine the elution order of the impurity peaks, the individual impurity stock standards were run under the new conditions. Figure 4.5 shows that all eight peaks were baseline resolved with good peak asymmetry, (at 10% ranging from 0.91 for HCA to 1.19 for P-11,21D), in less than eight min under the altered gradient conditions. The NRP under the selected conditions was calculated as 0.41. The elution order was found to be in agreement with that observed by Yaku *et al.* [184] for corticosteroids containing 1 to 4 hydroxyl groups using an  $\text{NH}_2$  stationary phase in that the analytes were eluted in order of increasing number of hydroxyl groups.

**Table 4.2:** Summary of column screening results from the Thar Method Station

Column	Si	CN	Diol	NH <sub>2</sub>	2-EP
<b>Parameter</b>					
<b>Peaks observed</b>	6	6	6	5	6
<b>RT Window</b>	5.17	1.16	5.23	6.05	4.07
<b>Rs @ 0.5/(Asym @ 10%)</b>					
<b>Peak 1</b>	N/A/(0.81)	N/A/(0.85)	N/A/(0.86)	N/A/(0.90)	N/A/(0.90)
<b>Peak 2</b>	2.7/(0.85)	1.4/(0.67)	4.9/(0.74)	7.7/(1.03)	3.9/(0.51)
<b>PAC</b>	1.5/(0.77)	1.2/(1.02)	1.6/(1.07)	2.8/(1.00)	1.3/(0.94)
<b>Peak 4</b>	2.7/(0.87)	3.3/(0.85)	8.3/(0.97)	4.4/(0.94)	7.0/(0.95)
<b>Peak 5</b>	3.4/(0.87)	1.2/(0.91)	10.7/(0.62)	11.9/(1.18)	6.1/(0.74)
<b>Peak 6</b>	12.9/(0.98)	1.2/(1.03)	1.0/(1.17)	N/D/(N/D)	1.2/(1.16)
<b>NRP</b>	0	0	0	N/A <sup>1</sup>	0

<sup>1</sup> = Not all peaks eluted at the selected runtime

Upon the completion of the initial column screening study and selection of the NH<sub>2</sub> stationary phase, it was decided to further optimise the separation on an Agilent 1260 Infinity Analytical SFC system coupled with an Aurora SFC Fusion A5 CO<sub>2</sub> delivery system. The system was selected to provide greater sensitivity than the Thar system which was required for the analysis of PAC potential impurities at trace levels in the final product. As the column dimensions remained the same, it was envisioned that the transfer onto the Agilent system would be straight forward. However, system differences coupled with the fact that an additional impurity, prednisone (PN), (which had been omitted from the original screening study due to the unavailability of reference standard material at the time the study was undertaken) was included in the mix meant that the method parameters had to be re-optimised on the Agilent system. As the method was to be used for real samples, a placebo solution containing the matrix components of the ophthalmic suspension was prepared in deionised water and included during the method optimisation to ensure method specificity. The initial method requirements were set to be the same as for the previously developed RP-HPLC assay described in Chapter 3 above. All peaks had to be baseline resolved with  $R_s > 1.5$  and a detection limit of 0.05% of the nominal PAC concentration for the selected impurities. The final optimised pSFC method conditions on the Agilent system are described in Figure 4.6 which demonstrates all peaks being separated in less than 11 min. Due to the addition of the PN impurity, stock standards of PAC and each impurity were run on the final optimised conditions to determine the elution order. No selectivity changes for the PAC impurities were noted between the Thar and Agilent systems with the PN peak eluting between PAC and P-17A. However, on the Agilent system, the newly optimised conditions did result in a

selectivity change for the matrix peak. Using the newly optimised conditions, the matrix peak was seen to elute at the beginning of the chromatogram, prior to any peaks of interest, thus demonstrating the specificity of the method (See Figure 4.6). The cause of this selectivity change was not investigated at the time as it had no negative impact on the separation. However, given the differences in the operating conditions between the two systems; i.e. the higher column temperature on the Agilent system; a possible cause may be that the matrix peak was more susceptible to temperature changes than the other peaks in the separation. The retention time window for the Agilent separation was approximately 7 min, while peak symmetry ranged from 0.87 for the PN peak to 1.21 for the PAC peak. The NRP for the separation was 0.34.

While the above method conditions satisfied the separation goal for the new method, (i.e. all peaks were baseline resolved) it was noted that the sensitivity was much lower on the pSFC method compared to that of the RP-HPLC method. Therefore, the criterion of being able to detect impurities at 0.05% of the nominal PAC concentration was not achievable with the proposed nominal PAC concentration of 200 mg.L<sup>-1</sup>. To compensate for this lack of sensitivity, the nominal concentration of working solutions was increased three fold compared to that of the RP-HPLC method, giving a PAC nominal working concentration of 600 mg.L<sup>-1</sup>. This increase in concentration allowed for impurity peaks to be detected at the 0.10% level relative to the PAC main peak. Although a sensitivity level of 0.05% was not met for the pSFC method, the 0.10% value was deemed acceptable based on the fact that for the selected ophthalmic suspension used in this work, the maximum recommended daily dose equates to approximately 624 µL (based on in-house drop size studies). This in turn equates to 6.2 µg (based on a label claim of 1%). Therefore, according to Attachment 1 of ICH Q3B(R2) [144], the reporting threshold for degradation products of PAC in the selected ophthalmic suspension was 0.1%, with an identification threshold and the quantification threshold of 1.0%.

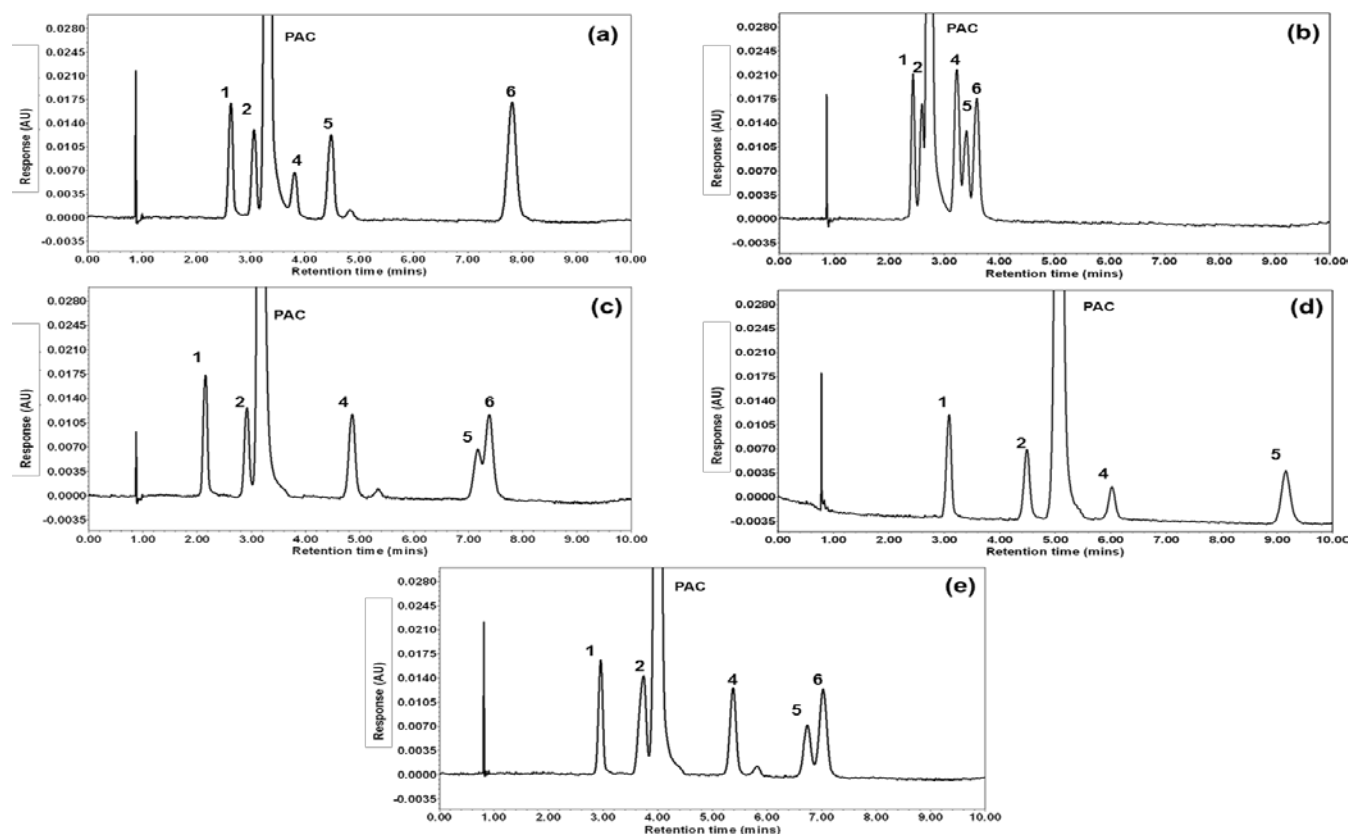


**Figure 4.4:** Representative chromatograms of development injections conducted on the Thar method station using Si (a), CN (b), Diol (c),  $\text{NH}_2$  (d) and 2-EP (e) stationary phases. Sample contained PAC at  $200 \text{ mg.L}^{-1}$  and impurities at  $4 \text{ mg.L}^{-1}$ , i.e. at approximately 2% of the PAC concentration. Chromatograms (a) to (e) expanded view to show baseline detail. Chromatographic conditions; Columns: ( $5 \mu\text{m}$ )  $4.6 \text{ mm} \times 250 \text{ mm}$ . Flow rate:  $3.5 \text{ mL.min}^{-1}$ . Injection volume:  $10 \mu\text{L}$ . Column temperature:  $40 \text{ }^\circ\text{C}$ . Back-pressure regulation: 120 bar. Detection: 254 nm. Mobile phase: 14 to 18% MeOH over 8.5 min with a 1 min equilibration step. Note: individual injections of impurities were not made for peak assignment purposes.

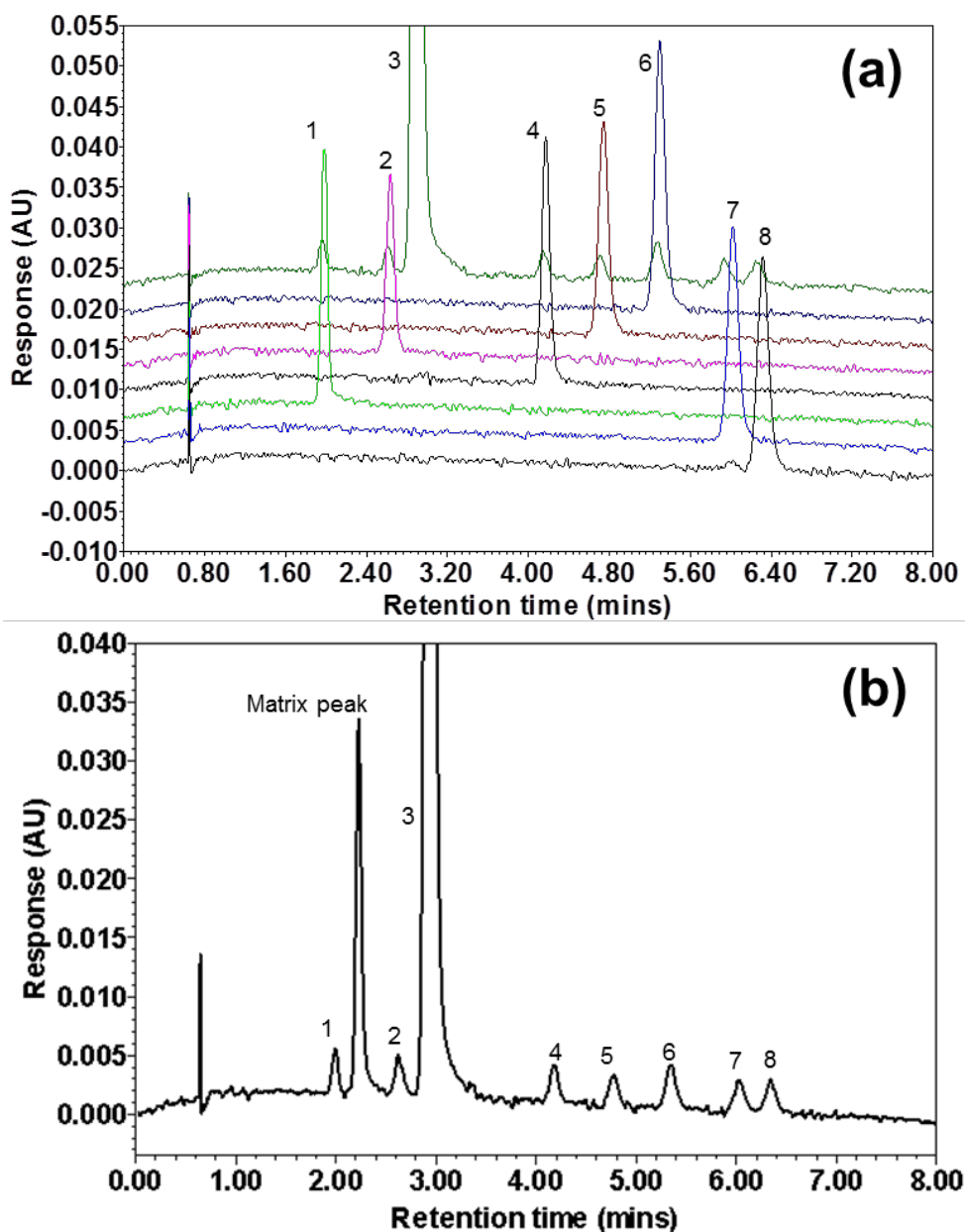


**Figure 4.5:** (a) Overlaid chromatograms of PAC standard at  $200 \text{ mg.L}^{-1}$  and impurity stock standards at  $40 \text{ mg.L}^{-1}$  conducted on the Thar method station using the  $\text{NH}_2$  stationary phase to determine the elution order sequence of the separation. (b) Chromatogram of PAC sample at  $200 \text{ mg.L}^{-1}$  spiked with impurities at  $4 \text{ mg.L}^{-1}$ . Chromatographic conditions; as per Figure 4.3 with the following exceptions; Flow rate:  $4.0 \text{ mL.min}^{-1}$ . Mobile phase: 15 to 23% MeOH over 7 min with a 1 min equilibration step. Peak elution order; P-11,21D (1), HCA (2), PAC (3), P-17A (4), HC (5), P (6), 20(R) (7) and 20(S) (8).

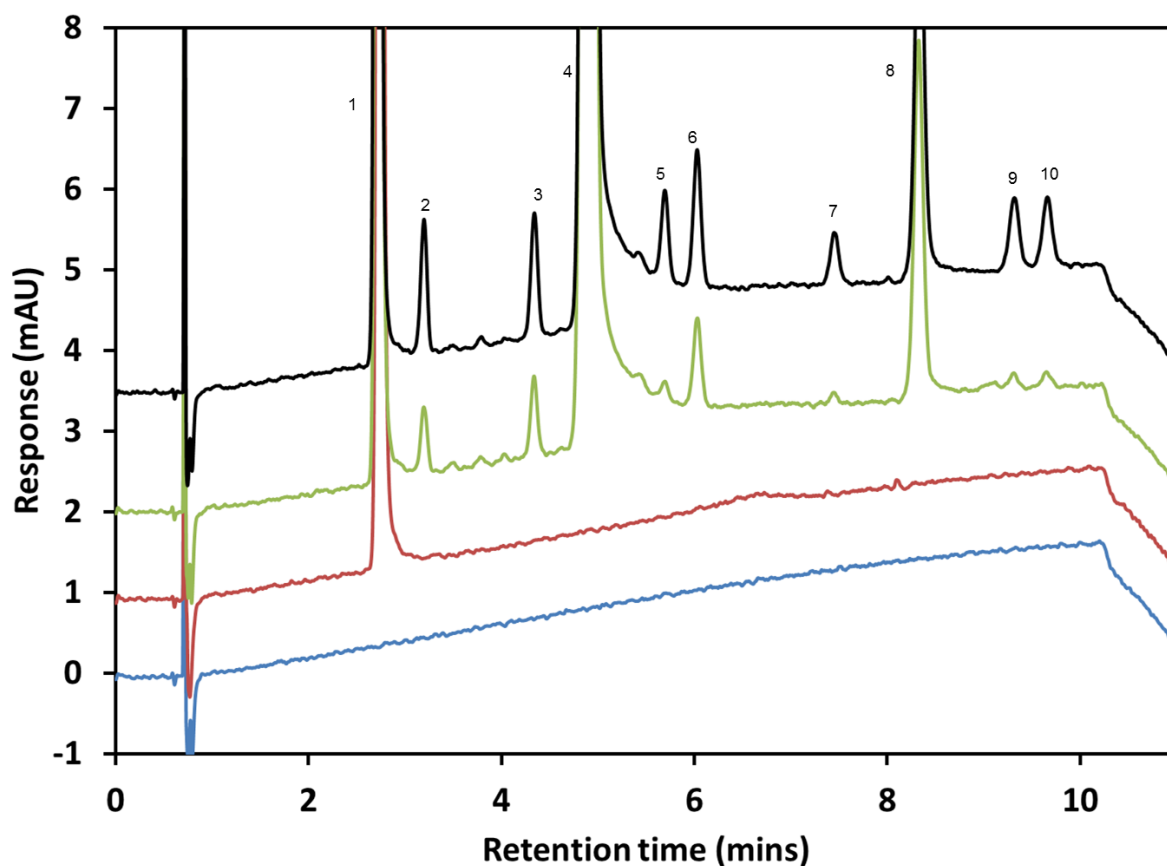


**Figure 4.6:** Overlaid chromatograms (expanded view to show baseline detail) of spiked sample containing PAC at  $600 \text{ mg.L}^{-1}$  and impurities  $3 \text{ mg.L}^{-1}$  (0.50%) (black), spiked sample containing PAC at  $600 \text{ mg.L}^{-1}$  and impurities  $0.6 \text{ mg.L}^{-1}$  (0.10%) (green), placebo blank containing sample matrix components at 100% of nominal working concentration (red) and a MeOH blank injection (blue) conducted on the Agilent Aurora system using the  $\text{NH}_2$  stationary phase. Peak elution order; matrix peak (1), P-11,21D (2), HCA (3), PAC (4), PN (5), P-17A (6), HC (7), P (8), 20(R) (9) and 20(S) (10). Chromatographic conditions; Column: ( $5 \mu\text{m}$ )  $4.6 \text{ mm} \times 250 \text{ mm}$ . Flow rate:  $4.0 \text{ mL.min}^{-1}$ . Injection volume:  $15 \mu\text{L}$ . Column temperature:  $50 \text{ }^\circ\text{C}$ . Back-pressure regulation: 120 bar. Detection: 254 nm. Mobile phase: 10 to 20% MeOH over 9.5 min with a 1 min equilibration step.

### 4.3.2 Method Transfer onto an Ultra Performance SFC (UPSFC) system

It had been intended to complete the validation of the developed pSFC method on the Agilent system. However, when an opportunity arose to work on a Waters Ultra Performance SFC (UPSFC) system, which was provided on loan from Waters, it was decided to attempt a method transfer onto the Waters UPSFC system and complete the method validation on the Waters UPSFC system. However, the maximum column length which the Waters UPSFC system could accommodate was 150 mm. Therefore, a geometric method transfer onto a shorter column was necessary in order to use the Waters UPSFC system for method validation. In order to maintain the same separation when scaling a gradient separation from one column to another, one must ensure that the overall chemistry of the systems remains the same. To achieve this, the same brand and series of column packing should be selected along with the same mobile phase and column temperature as for the original method [225]. It is also important to maintain the column plate number (N) which is based on the ratio of column length (L) to particle size ( $d_p$ ) (i.e.  $N = L/d_p$ ). The plate number of the original column was 50000, (i.e.  $250/0.005$ ). Therefore, in order to maintain the same plate number on the 150 mm column, a 3  $\mu\text{m}$  particle size was required (i.e.  $150/0.003 = 50000$ ). Fortunately, Phenomenex produced such a column; i.e. (3  $\mu\text{m}$ ) 3.0 mm x 150 mm  $\text{NH}_2$  column. Hence, this column was selected for the method transfer onto the Waters UPSFC system.

Performing a geometric transfer of a gradient method onto a shorter column not only requires that the correct particle size be selected in order to maintain column plate number, but also that injection volume, flow rate and gradient time be scaled accordingly to maintain the same gradient retention factor ( $k^*$ ) as in the original method conditions. The calculated geometric transfer gradient conditions were set on the Waters UPSFC system. To maintain the original separation, the column temperature was set to 50 °C and the back pressure regulator was set to 120 bar. A standard solution containing PAC at 600  $\text{mg}\cdot\text{L}^{-1}$  and the eight selected impurities at 12  $\text{mg}\cdot\text{L}^{-1}$  (equivalent to 2% of PAC nominal concentration) was prepared in MeOH and run on the Waters UPSFC system under the above conditions. The resulting chromatogram is shown in Figure 4.7.

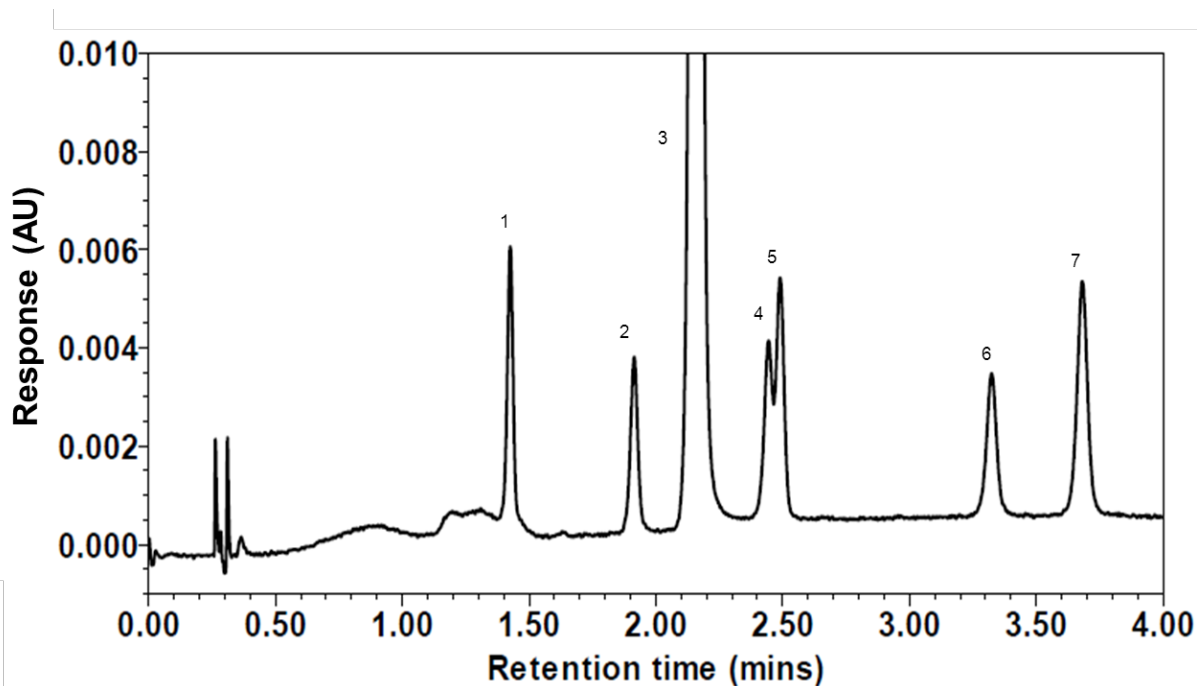


**Figure 4.7:** Expanded chromatogram of spiked sample containing PAC at  $600 \text{ mg.L}^{-1}$  and impurities  $12 \text{ mg.L}^{-1}$  conducted on the Waters UPC2 system under the geometric transfer conditions. Chromatographic conditions; Column: NH2 ( $3 \mu\text{m}$ )  $3.0 \text{ mm} \times 150 \text{ mm}$ . Flow rate:  $2.84 \text{ mL.min}^{-1}$ . Injection volume:  $1.27 \mu\text{L}$ . Column temperature:  $50 \text{ }^\circ\text{C}$ . Back-pressure regulation:  $120 \text{ bar}$ . Detection:  $254 \text{ nm}$ . Mobile phase:  $10$  to  $20 \%$  MeOH over  $3.41 \text{ min}$  with a  $0.5 \text{ min}$  equilibration step. Peak elution order; P-11,21D (1), HCA (2), PAC (3), PN (4), P-17A (5), HC (6) and P (7).

As shown in Figure 4.7 only seven peaks (of a total of nine peaks including PAC) were observed under the geometric transfer conditions. Also, peaks 4 and 5 were not totally resolved ( $R_s = 0.3$ ). This result was surprising given the fact the Waters UPSFC system has a smaller reported dwell volume,  $440 \mu\text{L}$  [226] versus  $700 \mu\text{L}$  [16] for the Agilent system. Therefore, it would be expected that under similar operating conditions, all peaks would elute slightly earlier on the Waters UPSFC system given that no compensation was made in the gradient table for the slight dwell volume differences between the two systems. Also, efficiency loss due to the influence of extra-column band broadening (arising from instrumental contributions) could also be ruled out given that the extra-column band broadening ( $\sigma_{\text{ext}}^2$ ) for both systems has been experimentally characterised and found to be identical for both systems i.e.  $85 \mu\text{L}^2$  [227].

As the overall chemistry of the system had not changed and given that the differences in the observed chromatography could not be explained by differences in system dwell or extra column volumes, it was decided to investigate the effects of system pressure and column temperature in an attempt to fine tune the separation rather than alter the composition of the binary fluid. It has been reported that when performing a gradient of MeOH in CO<sub>2</sub>, increasing the system back pressure at constant temperature can result in a decrease in peak retention time for early eluting peaks, provided that the concentration of the modifier is relatively low [228]. The reason for this is that the compressibility of the binary mobile phase remains relatively high once the modifier concentration is low. Therefore, increasing the system back pressure induces higher mobile phase density and thus leads to lower retention factors. As the percentage of modifier increases, the compressibility of the binary fluid decreases and thus variations in pressure have little or no effect on retention [228]. Therefore, to increase the eluting strength of the mobile phase it was decided to increase the back pressure from 120 bar to 200 bar while maintaining all other method parameters previously calculated for the geometric transfer. The resulting chromatogram is shown in Figure 4.8 and demonstrates that the increase in pressure did increase the eluting strength of the mobile phase with all 9 peaks being visible. However, resolution values between peaks 4 and 5 ( $R_s = 1.1$ ) along with peaks 8 and 9 ( $R_s = 0.6$ ) were less than the required 1.5. Also, peaks 8 and 9 did not fully elute within the gradient time.

It was decided to further increase the back pressure to 220 bar to see if any further gains in terms of reduced retention time and increased resolution could be achieved. The resulting chromatogram is shown in Figure 4.9 and demonstrates that although a slight reduction in peak retention times were noted for most peaks compared to that observed in Figure 4.8, with the maximum retention time decrease noted for peak 1 of 3.2%. There was a slight improvement in resolution between the critical pair, peaks 4 and 5 ( $R_s = 1.2$ ) however, for critical pair, peaks 8 and 9, the resolution deteriorated ( $R_s = 0.2$ ). This indicated that there would be little to no improvement to be gained by increasing the back pressure further.

In an attempt to fine tune the previous attempt, it was decided to reduce the column temperature from 50 °C to 45 °C while maintaining the pressure at 220 bar. Unlike for HPLC separations, a reduction in column temperature at constant pressure in SFC separations has the effect of increasing the eluting strength of the mobile phase due to an increase in mobile phase density.

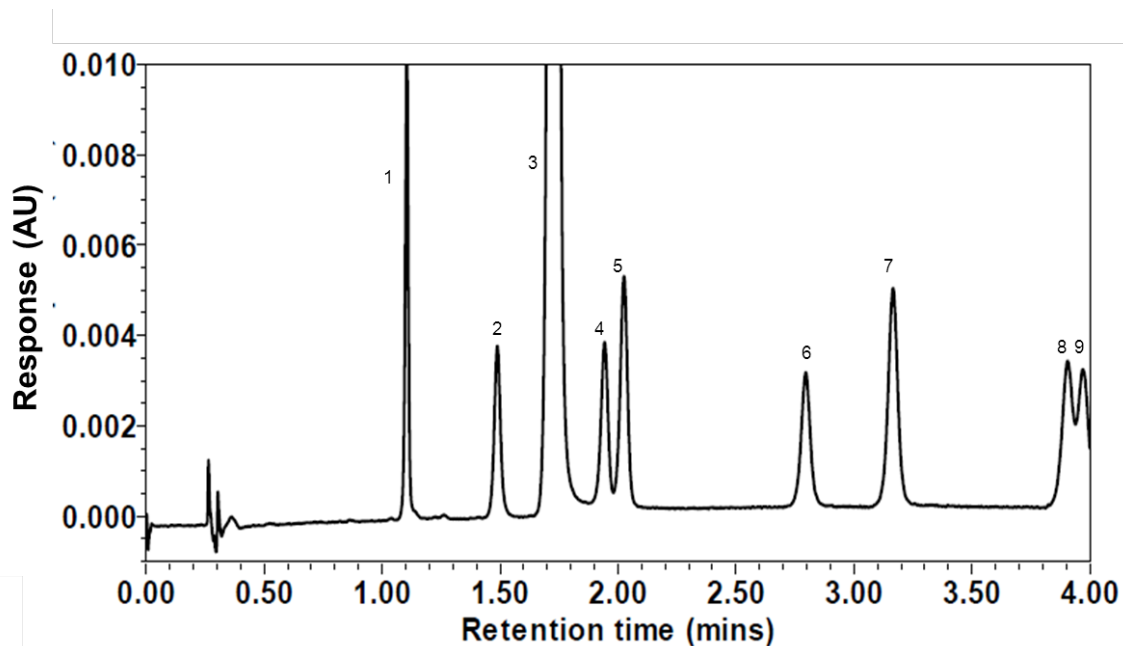


**Figure 4.8:** Expanded chromatogram of spiked sample under the geometric transfer conditions described in Figure 4.7 with the following exceptions; Back-pressure regulation: 200 bar. Peak elution order; P-11,21D (1), HCA (2), PAC (3), PN (4), P-17A (5), HC (6), P (7), 20(R) (8) and 20(S) (9).

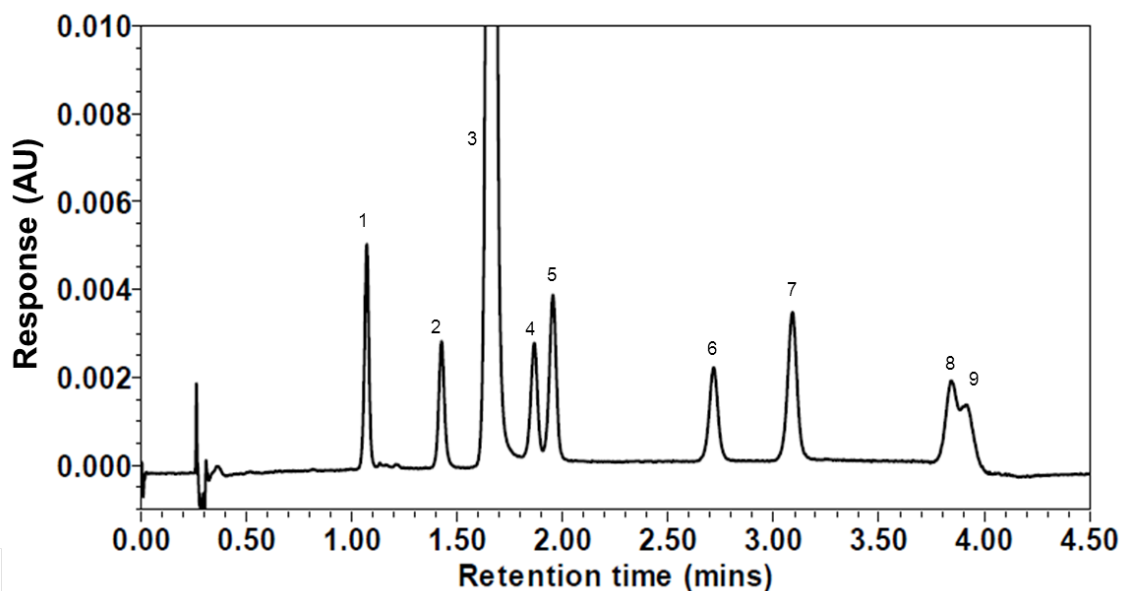


**Figure 4.9:** Expanded chromatogram of spiked sample under the geometric transfer conditions described in Figure 4.7 with the following exceptions; Back-pressure regulation: 220 bar. Peak elution order; as per Figure 4.8.

The resulting chromatogram is shown in Figure 4.10 and demonstrates that although a slight reduction in peak retention times were noted for most peaks compared to that observed in Figure 4.9, with the maximum retention time decrease noted for peak 1 of 5.6%. There was a slight deterioration in resolution between critical pairs, peaks 4 and 5 ( $R_s = 0.9$ ) and peaks 8 and 9 ( $R_s = 0.0$ ).

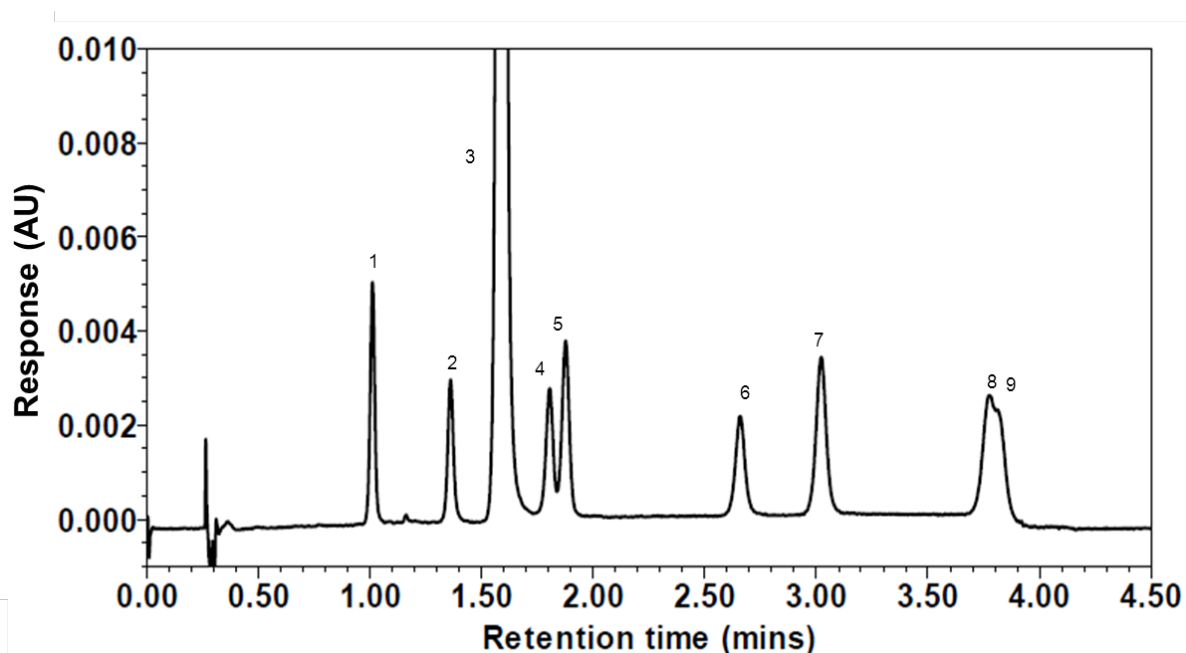


**Figure 4.10:** Expanded chromatogram of spiked sample under the geometric transfer conditions described in Figure 4.7 with the following exceptions; Column temperature: 45 °C. Back-pressure regulation: 220 bar. Peak elution order; as per Figure 4.8.

In a final attempt to improve resolution, the column temperature was changed from 45 °C to 55 °C while maintaining the back pressure at 220 bar. It was envisioned that the increase in column temperature would reduce the eluting strength of the mobile phase slightly and therefore may improve the resolution between the critical pairs. As the eluting strength of the mobile was being reduced, it was also decided to extend the gradient time by 0.73 min to allow all peaks to elute from the column. The resulting chromatogram is shown in Figure 4.11 and demonstrates that although a slight increase in peak retention times were noted for most peaks compared to that observed in Figure 4.10, with the maximum retention time increase noted for peak 9 of 14%. There was a slight improvement in resolution between critical pairs, peaks 4 and 5 ( $RS = 1.3$ ) and for peaks 8 and 9 ( $Rs = 0.5$ ).

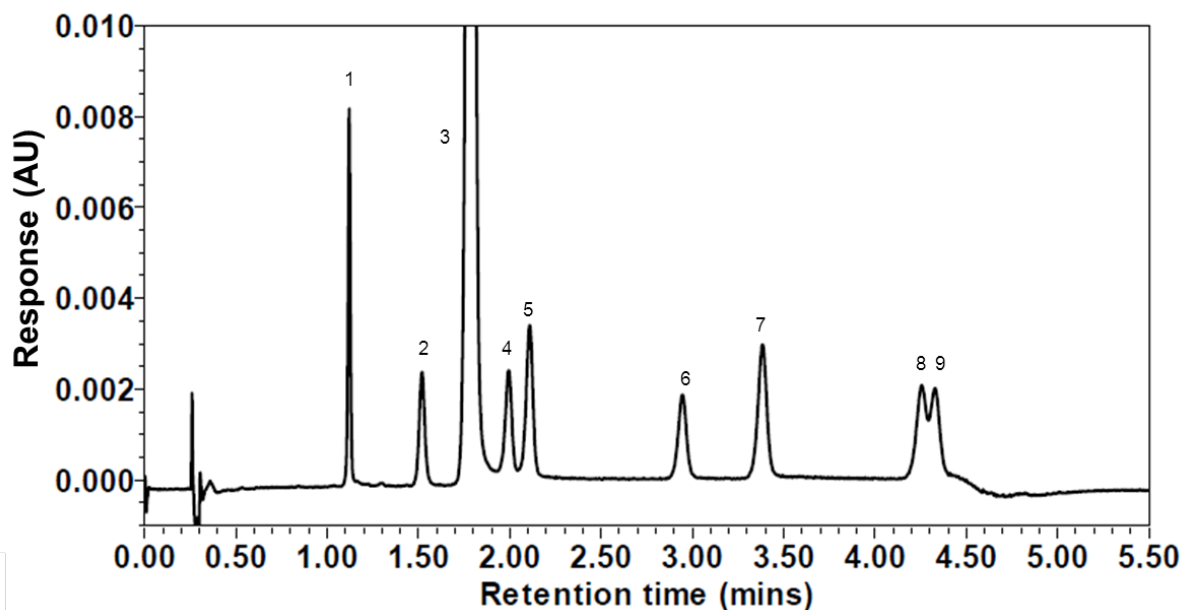


**Figure 4.11:** Expanded chromatogram of spiked sample under the geometric transfer conditions described in Figure 4.7 with the following exceptions; Column temperature: 55 °C. Back-pressure regulation: 220 bar. Mobile phase: 10 to 20 % MeOH over 4.14 min with a 1.0 min equilibration step. Peak elution order; as per Figure 4.8.

It has been recognised that in SFC, the most important factor in controlling separations is the composition of the binary mixture, with back pressure and column temperature being used more to fine tune the separation [36,37]. Therefore, at this point it was decided to abandon the calculated geometric transfer conditions and recommence solvent strength screening studies on the Waters UPSFC system in an attempt to obtain the desired separation on the (3  $\mu$ m) 150 mm x 3.0 mm NH<sub>2</sub> column. Several screening attempts were made in which shallow gradients over extended times were employed. However, despite these efforts, the required separation could not be achieved. The best separation was obtained under conditions outlined in Figure 4.12 with all peaks eluted within 9 min. However, the resolution between peaks 4 and 5 ( $R_s = 1.1$ ) and peaks 8 and 9 ( $R_s 1.0$ ) was still inadequate (i.e. < 1.5). Therefore, it was then decided to forgo any further method transfer/development attempts on the (3  $\mu$ m) 150 mm x 3.0 mm NH<sub>2</sub> column and seek an alternative column in order to generate the desired separation.

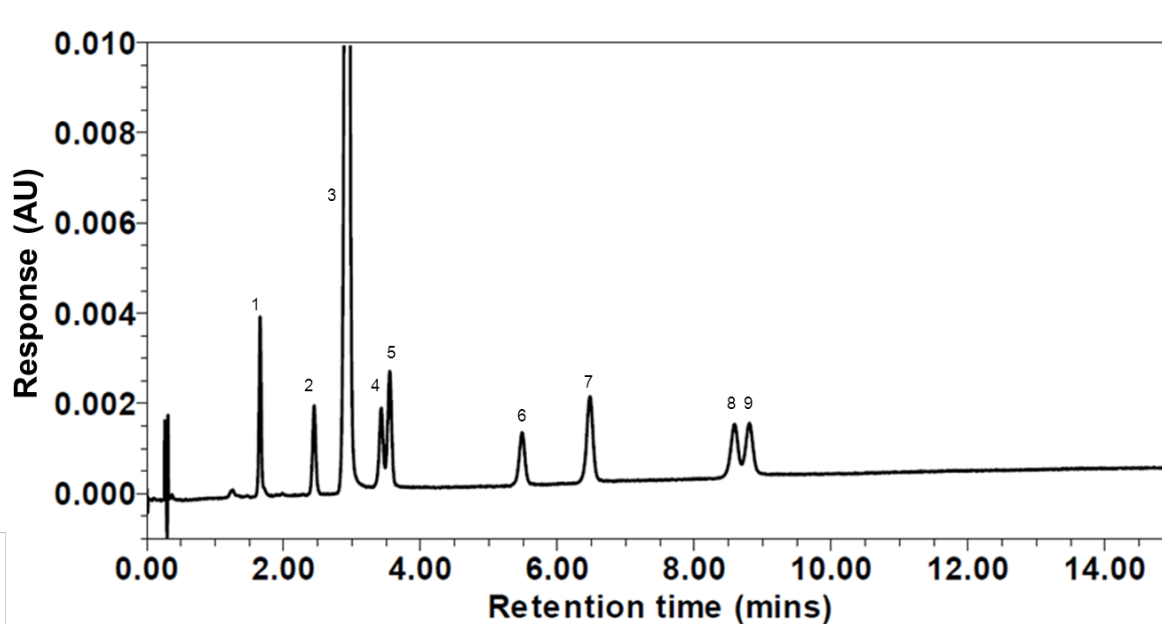


**Figure 4.12:** Expanded chromatogram of spiked sample under conditions described in Figure 4.7 with the following exceptions Mobile phase: 10 to 20 % MeOH over 15 min with a 5 min hold followed by a 2 min equilibration step. Peak elution order; as per Figure 4.8.

#### 4.3.3 PAC Method Development on UPSFC system

One way of improving resolution is to use a more efficient column; i.e. a column with a higher plate number (N). Increasing plate number can be achieved by either increasing column length for a given particle size, or by reducing the particle size for a given column length. However, the smallest particle size commercially available in the Phenomenex Luna NH<sub>2</sub> column range was the 3  $\mu$ m particle, which meant that it was the most efficient column that could have been employed given the restraints imposed by the size of the Waters UPSFC column oven; i.e. 150 mm.

In an attempt to maintain the good peak shape and selectivity observed on the Phenomenex NH<sub>2</sub> stationary phase, it was decided to try to obtain a stationary phase of similar chemistry (i.e. amino-based) but with a smaller particle size. At the time this work was being conducted, Waters had just launched their Acquity UPC<sup>2</sup> Torus sub-2  $\mu$ m range of columns for achiral separations on the Waters UPSFC system. This range of columns included two amino-based stationary phases; namely Torus 2-PIC (2-picolylamine) and Torus DEA (diethylamine). According to the manufacturer, the Torus 2-PIC Columns were designed for general use and are the first choice for a wide range of applications with acidic and basic

compounds. The Torus 2-PIC phase demonstrates enhanced performance compared to conventional 2-EP, displaying improved peak shape, added retention, and novel selectivity [229]. In addition, these columns provide extra flexibility to method development as they can be used with or without additives, while still maintaining exceptional peak shape for a wide range of compounds. The Torus DEA Columns are designed to be orthogonal to the Torus 2-PIC phase. These columns provide a complementary selectivity to the 2-PIC phase and are designed to provide superior peak shape for very strong bases, with or without additives [229]. The column dimensions selected were (1.7  $\mu\text{m}$ ) 100 mm x 3.0 mm which according to Novakova *et al.* [16], (for sub-2  $\mu\text{m}$  particles) represents the best compromise to minimise column efficiency loss, solvent consumption and allow flow rate flexibility for UPSFC separations on the Waters UPSFC system. It was also envisioned that the increased plate number for these columns, (i.e.  $100/0.0017 = 58823$ ) would help improve the resolution issue noted on the Phenomenex column.

A similar screening approach to that described previously was applied with both the PIC and DEA columns in which a spiked sample containing PAC at  $600 \text{ mg.L}^{-1}$  and the eight selected impurities at  $12 \text{ mg.L}^{-1}$  (equivalent to 2% of PAC nominal concentration) was used. Figure 4.13 details the first screening conditions on the DEA column. As a spiked PAC sample was used in this initial study and therefore it was expected to see 10 peaks in total due to the addition of the sample matrix peak. Figure 4.13 shows the results of the first screening study on the DEA column. Only 9 of the expected 10 peaks were eluted in less than 4 min. Also, the resolution results obtained for critical pair, peak 8 and 9 ( $R_s = 1.0$ ) did not meet the required value of  $> 1.5$ . As shown in Figure 4.13, by injecting stock impurity solutions, the missing peak was identified as P-17A, which was co-eluting with the PAC peak under the selected conditions.

From this initial starting point, several additional screening runs were made in which the gradient range, gradient time and flow rate were all altered in an effort to achieve the desired separation. Eventually, the desired separation was achieved on the DEA column under conditions of described in Figure 4.14. The resolution between critical pairs, peaks 4 and 5 ( $R_s = 1.8$ ) and peaks 9 and 10 ( $R_s = 1.8$ ) met the desired resolution of  $\geq 1.5$ . The elution order was confirmed by running a placebo blank solution, PAC standard solution at  $600 \text{ mg.L}^{-1}$  and impurity stock solutions at  $200 \text{ mg.L}^{-1}$ . In comparison the Phenomenex  $\text{NH}_2$  column, a selectivity difference was noted on the DEA column involving the P-17A which eluted before the PAC peak on the DEA column (See Figure 4.6 and Figure 4.14).

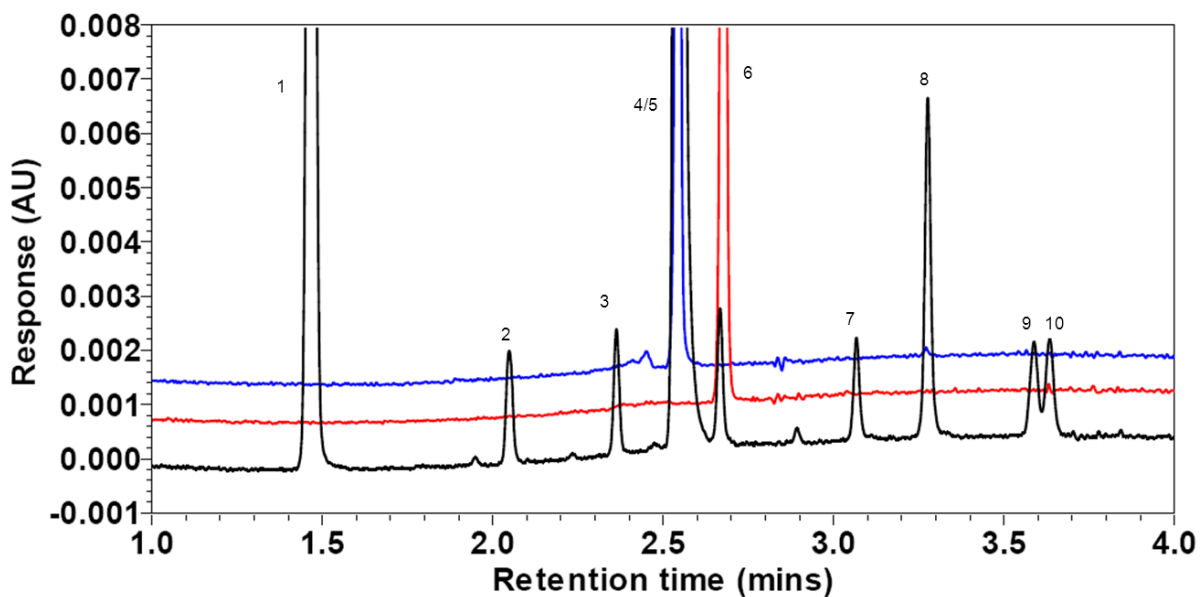


**Figure 4.13:** Expanded overlaid chromatograms of spiked sample containing PAC at  $600 \text{ mg.L}^{-1}$  and impurities  $6 \text{ mg.L}^{-1}$  (black), P-17A impurity stock at  $200 \text{ mg.L}^{-1}$  (blue) and PN impurity stock at  $200 \text{ mg.L}^{-1}$  (red) conducted on the Waters UPC<sup>2</sup> system under initial screening conditions. Chromatographic conditions; Column: DEA ( $1.7 \mu\text{m}$ )  $3.0 \text{ mm} \times 100 \text{ mm}$ . Flow rate:  $2.0 \text{ mL.min}^{-1}$ . Injection volume:  $1.0 \mu\text{L}$ . Column temperature:  $50 \text{ }^\circ\text{C}$ . Back-pressure regulation: 138 bar. Detection: 254 nm. Mobile phase: 2 to 30 % MeOH over 5 min with a followed by a 1 min equilibration step. Peak elution order; matrix peak (1), P-11,21D (2), HCA (3), PAC/P-17A (4/5), PN (6), HC (7), P (8), 20(R) (9) and 20(S) (10).

As HCA, P-17A, PAC and PN all contain the same number of hydroxyl groups along with estimated LogP values of 1.41 for PN and 2.30 for HCA, P-17A and PAC; the selectivity change noted on the DEA column versus the  $\text{NH}_2$  column may be as a result of differences in the steric interactions of the solutes with the different stationary phases. In fact, steric effects have been reported to appear more dramatic in SFC than in LC [230].

For the sake of completion, it was decided to screen the PIC column to see if any additional improvements could be made in terms of resolution or reduction of analysis time over the DEA column. It was also envisioned that if successful, the PIC column could be offered as an alternative to the DEA column or vice versa for the proposed application. Based on the initial screening conditions employed with the DEA column, it was decided to reduce the gradient for the PIC column screening. Therefore, the first screening attempt on the PIC

column employed conditions described in Figure 4.15 which shows that only 9 of the expected 10 peaks eluted in less than 9 min.

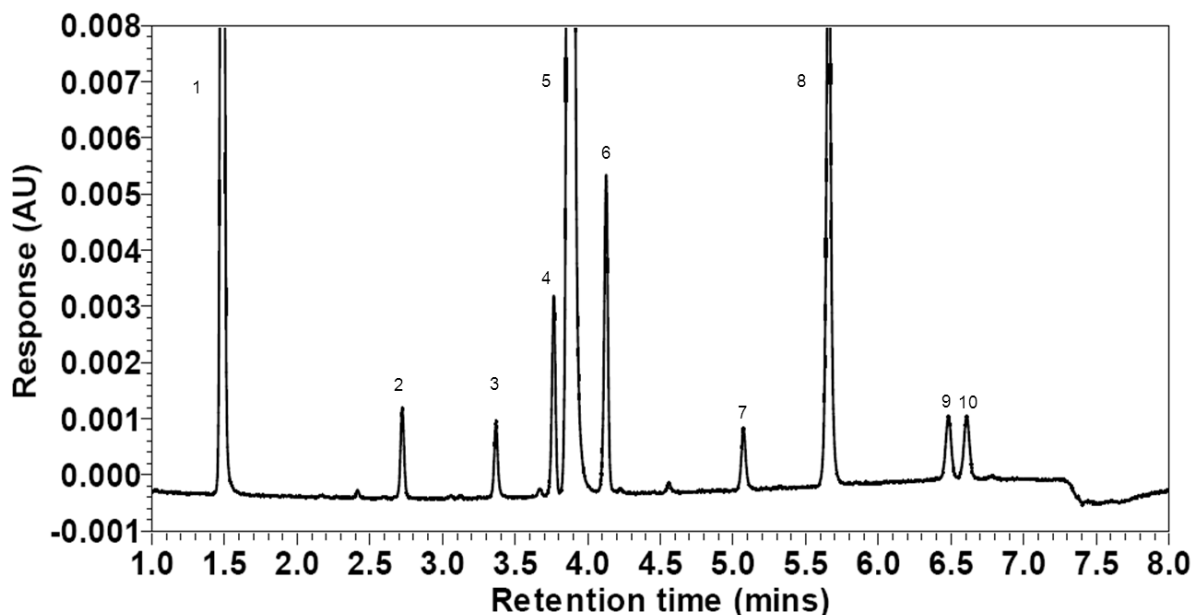


**Figure 4.14:** Chromatogram of spiked sample containing PAC at  $600 \text{ mg.L}^{-1}$  and impurities  $6 \text{ mg.L}^{-1}$ . Chromatographic conditions; Column: DEA ( $1.7 \mu\text{m}$ )  $3.0 \text{ mm} \times 100 \text{ mm}$ . Flow rate:  $2.5 \text{ mL.min}^{-1}$ . Injection volume:  $1.0 \mu\text{L}$ . Column temperature:  $50 \text{ }^\circ\text{C}$ . Back-pressure regulation: 138 bar. Detection: 254 nm. Mobile phase: 2 to 13.6 % MeOH over 6.2 min with a 1.8 min equilibration step. Peak elution order; matrix peak (1), P-11,21D (2), HCA (3), P-17A (4), PAC (5), PN (6), HC (7), P (8), 20(R) (9) and 20(S) (10).

However, the resolution results obtained for critical pair, peak 9 and 10 was  $\geq 1.5$  ( $R_s = 2.5$ ), indicating that the PIC column may be a suitable candidate for the separation. In an attempt to identify the missing peak, both the P-17A and PN stock impurity standards were run under the same conditions. As shown in Figure 4.15 the missing peak was identified as PN, which was co-eluting with the PAC peak. However, despite several attempts to modify the gradient conditions, we were unable to resolve the PAC and PN peaks on the PIC column. Therefore, the DEA column was selected as the alternative column to the  $\text{NH}_2$  column and was used in the validation of the new UPSFC method.

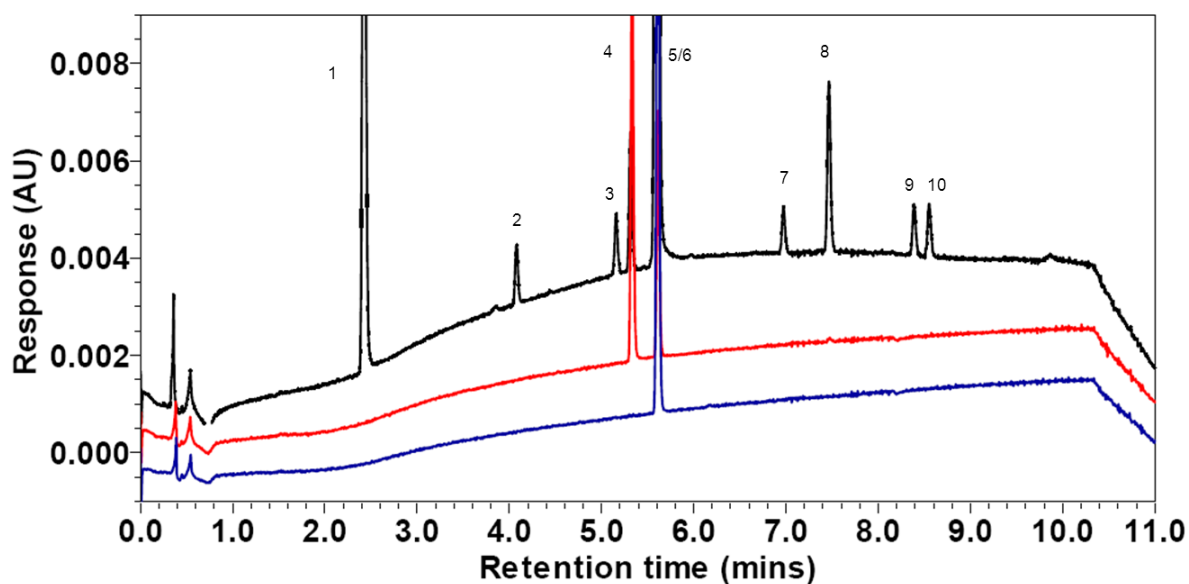


**Figure 4.15:** Expanded overlaid chromatograms of spiked sample containing PAC at  $600 \text{ mg.L}^{-1}$  and impurities  $6 \text{ mg.L}^{-1}$  (black), P-17A impurity stock at  $200 \text{ mg.L}^{-1}$  (red) and PN impurity stock at  $200 \text{ mg.L}^{-1}$  (blue). Chromatographic conditions; Column: PIC ( $1.7 \mu\text{m}$ )  $3.0 \text{ mm} \times 100 \text{ mm}$ . Flow rate:  $2.0 \text{ mL.min}^{-1}$ . Chromatographic conditions as per Figure 4.14 except for: Mobile phase: 2 to 20 % MeOH over 10 min with a followed by a 1 min equilibration step. Peak elution order; matrix peak (1), P-11,21D (2), HCA (3), P-17A (4), PAC/PN (5/6), HC (7), P (8), 20(R) (9) and 20(S) (10).

#### 4.3.4 PAC UPSFC Robustness

To assess the robustness of the new UPSFC method, a sample solution containing PAC at  $600 \text{ mg.L}^{-1}$  and the eight selected impurities spiked at  $6 \text{ mg.L}^{-1}$  (equivalent to 1% of PAC nominal concentration) was assayed under deliberately altered chromatographic conditions. As there was no requirement to control mobile phase pH for the new UPSFC method, the three parameters selected for investigation were column temperature, system back pressure and flow rate. Modifier composition or gradient times were not assessed as part of the formal robustness challenges as it was noted during method development that slight alterations to either parameter could have a detrimental effect on the separation in terms of maintaining the desired resolution of  $> 1.5$  between critical pairs. Each parameter was assessed individually; i.e. alterations were made to the parameter under investigation whilst all other parameters were maintained at nominal values. The results obtained for replicate injections ( $n=2$ ) of the sample solution were then assessed for system suitability to ensure that the separation requirements (resolution  $\geq 1.5$ ) were maintained under the altered conditions.

Column temperature was assessed at 40 °C, 45 °C, 50 °C (nominal), 55 °C and 60 °C. Back pressure was assessed at 110 bar, 120 bar, 138 bar (nominal), 150 bar and 160 bar. Flow rate was assessed at 2.3 mL.min<sup>-1</sup>, 2.4 mL.min<sup>-1</sup>, 2.5 mL.min<sup>-1</sup> (nominal), 2.6 mL.min<sup>-1</sup> and 2.7 mL.min<sup>-1</sup>. Plots of retention time and resolution (for critical pairs PAC/P-17A and 20(R)/20(S)) versus the selected parameter are shown in Figure 4.16 to Figure 4.18. The slopes of the lines generated for each peak under the various robustness challenges are also included in the plots. Significant differences (> 10%) between the peak slopes under a given condition can be an indication that the condition is likely to have a significant influence on the separation in terms of selectivity and elution order.

Figure 4.16 demonstrates that for column temperature the retention time of all peaks increased with increasing temperature, with a maximum increase of 26.8% exhibited for the P-11,21D peak. This correlates with the fact that increasing column temperature results in a decrease in mobile phase density and hence the eluting strength of the mobile phase. While no elution order change was noted for any of the temperatures investigated, it can be seen that for the temperatures studied < 50 °C, resolution fell below 1.5 between the 20(R)/20(S) critical pair. This observation coupled with the fact that the difference between the 20(R)/20(S) slopes is approximately 9.1%, confirms that temperature has a significant influence in the separation of these two peaks. Also, it should be noted that the slope of the matrix peak was significantly different (62% on average) from the slopes of the other peaks in the separation. This indicates that temperature has a significant influence over the elution of the matrix peak relative to the other peaks. This observation may be the reason for the elution order change noted for the matrix peak and P-11,21D in Section 4.3.1 above when the method was run on the Agilent system and the column temperature was increased by 10 °C.

Figure 4.17 demonstrates that for back pressure the retention time of all peaks decreased with increasing pressure, with a maximum decrease of 13.6% exhibited for the matrix peak. This correlates with the fact that increasing back pressure results in an increase in mobile phase density and hence the eluting strength of the mobile phase and explains why the analytes eluted faster from the column. Interestingly, while no elution order change was noted for any of the pressures investigated, resolution was seen to increase sharply between P17 and PAC above 138 bar, which correlates with the difference between the slopes of these two peaks being 16.7%. It was also interesting to note that between the pressure of 110 bar to 120 bar, and 138 bar to 150 bar, baseline resolution is lost between the 20(R)/20(S) critical pair even though there was no difference noted in the slopes of these two peaks.

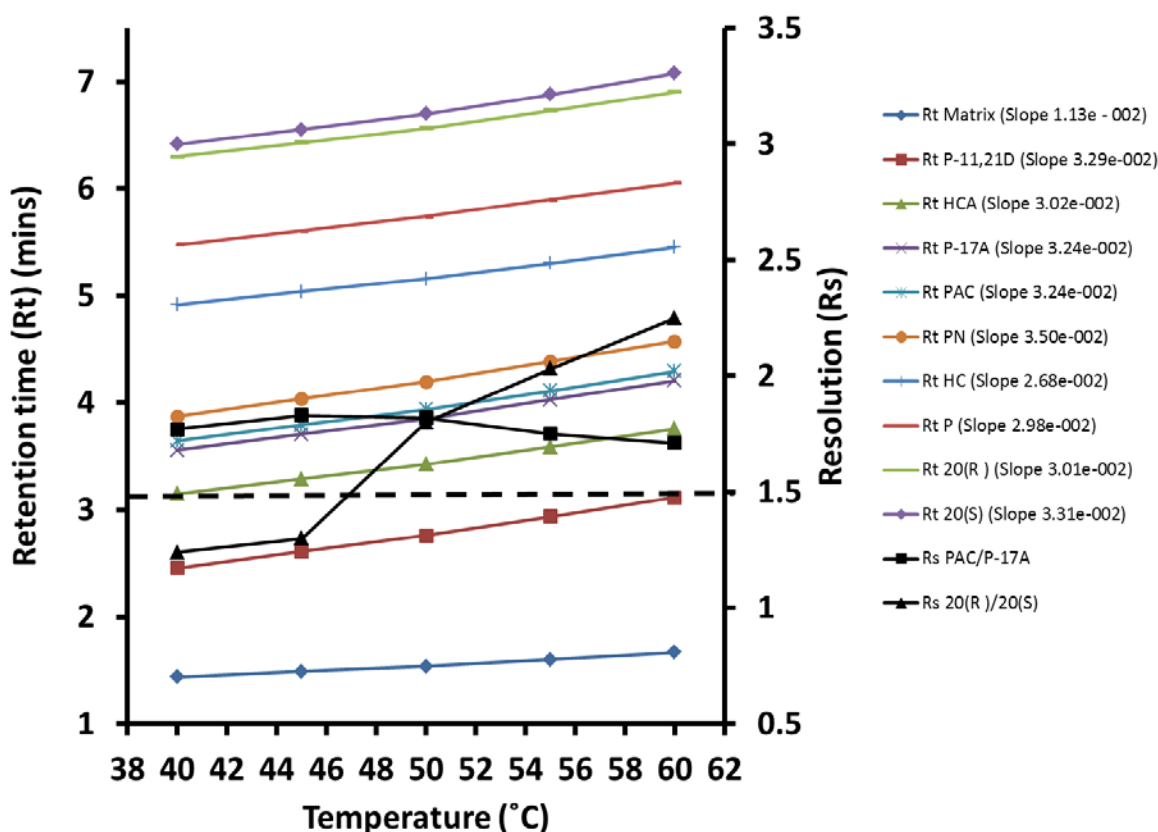


**Figure 4.16:** Plot of retention time (*Rt*) and resolution (*Rs*) versus column temperature. Chromatographic conditions as per Figure 4.14 with temperatures of 40, 45, 50, 55 and 60 °C. Dashed line indicates the minimum resolution requirements between critical peak pairs.

Figure 4.18 demonstrates that for flow rate, the retention time of all peaks decreased with increasing flow rate, with a maximum decrease of 18.7% exhibited for the matrix peak. This correlates with the fact that by increasing the flow rate, the analytes eluted faster from the column. While no elution order change was noted for any of the flow rates investigated, it can be seen that at flow rates below 2.5 mL.min<sup>-1</sup>, baseline resolution is lost between the P17/PAC critical pair even though the difference between the slopes of these two peaks was only 4.5%.

Based on the results of this robustness study, it was concluded that to maintain the system suitability requirement of maintaining resolution > 1.5 between critical pairs; the separation was able to withstand a 10% increase in column temperature from nominal, a 10% decrease in system back pressure from nominal and an 8% increase in flow rate from nominal. However, the separation cannot withstand a 10% decrease in column temperature

from nominal, a 10% increase in system back pressure from nominal or an 8% decrease in flow rate from nominal.

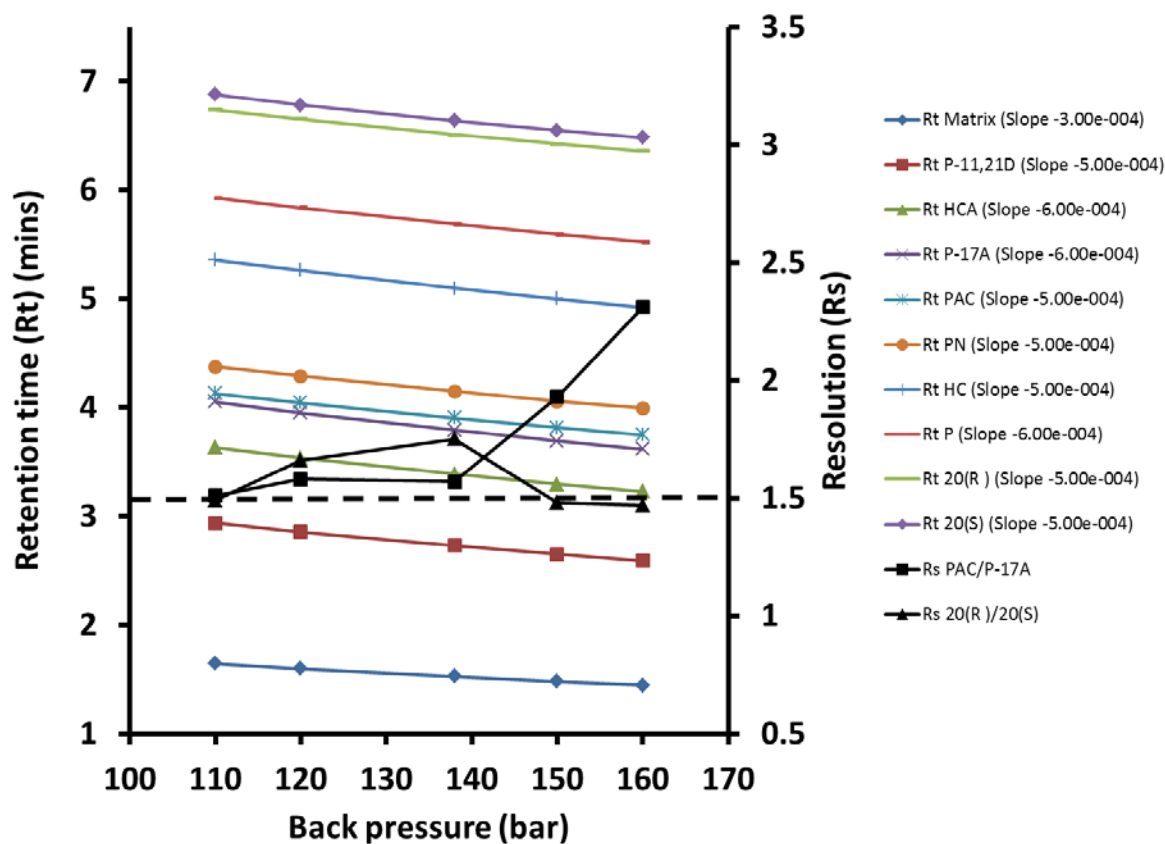


**Figure 4.17:** Plot of retention time (*Rt*) and resolution (*Rs*) versus back pressure (bar). Chromatographic conditions as per Figure 4.14 with back pressures of 110, 120, 138, 150 and 160 bar. Dashed line indicates the minimum resolution requirements between critical peak pairs.

While there may be some argument for increasing the flow rate to  $2.6 \text{ mL}\cdot\text{min}^{-1}$  (In order to increase resolution of P-17A and PAC at  $2.5 \text{ mL}\cdot\text{min}^{-1}$  from  $R_s = 1.6$  to  $R_s = 1.8$  at  $2.6 \text{ mL}\cdot\text{min}^{-1}$ , it was decided to stay with  $2.5 \text{ mL}\cdot\text{min}^{-1}$  to ensure that the overall system pressure was maintained below the 400 bar limit of the Waters UPSFC system. Based on Figure 1.6 which describes the relationship between the calculated critical temperature, pressure and concentration of organic modifier, it can be stated that for operating conditions of the new UPSFC method, conditions transition from supercritical to subcritical over the course of the gradient; i.e. from the point in the gradient where the % MeOH exceeds approximately 5%. However, despite this transition there was no adverse effect observed on

the chromatographic performance of the UPSFC method indicating that strict supercritical conditions were not necessary to obtain a satisfactory separation.

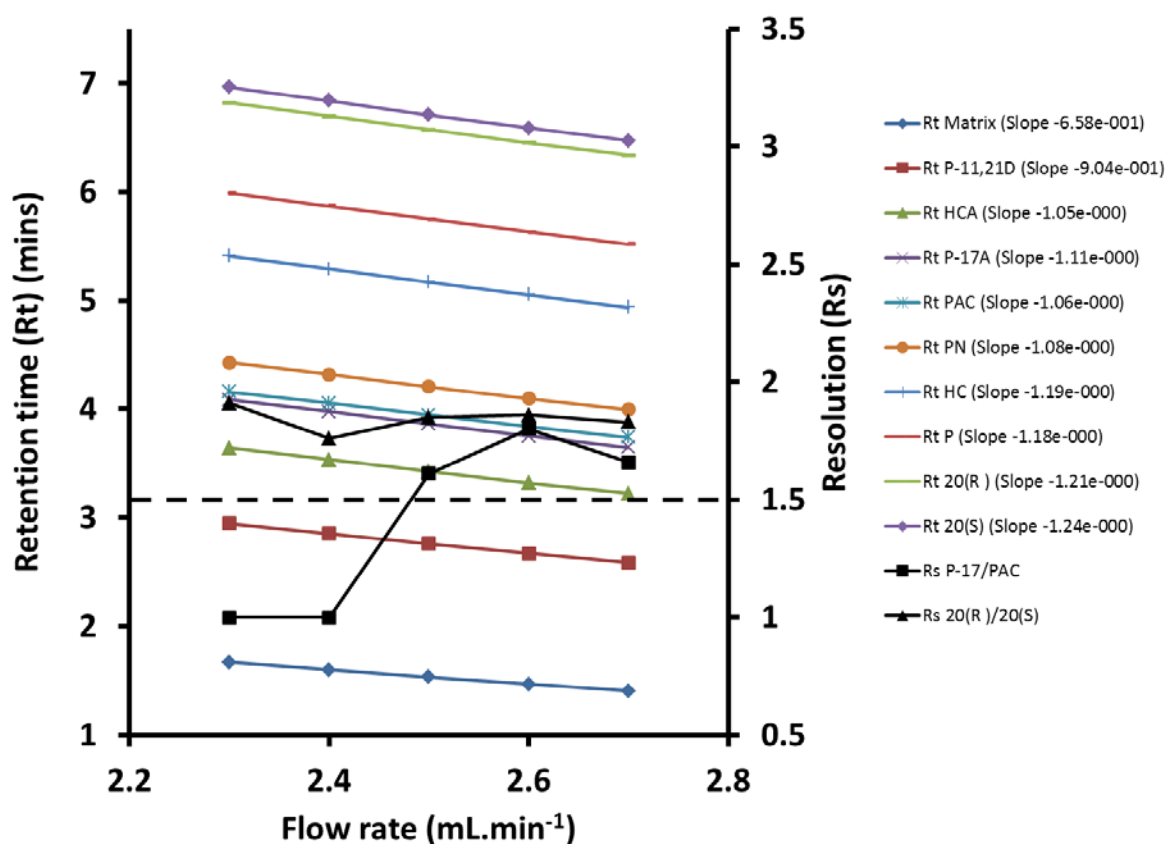


**Figure 4.18:** Plot of retention time ( $R_t$ ) and resolution ( $R_s$ ) versus flow rate ( $\text{mL}\cdot\text{min}^{-1}$ ). Chromatographic conditions as per Figure 4.14 with flow rates of 2.3, 2.4, 2.5, 2.6 and 2.7  $\text{mL}\cdot\text{min}^{-1}$ . Dashed line indicates the minimum resolution requirements between critical peak pairs.

#### 4.3.5 PAC UPSFC Method Validation

The validation of the new UPSFC method was carried out for PAC and the eight selected impurities using the total error approach to generate accuracy profiles based on  $\beta$ -expectation tolerance intervals. As stated in Section 4.1.2 above, the  $\beta$ -expectation tolerance interval defines an interval where it is expected that a defined proportion (i.e.  $\beta$ ) of future results will fall. For PAC at the assay concentration, the  $\beta$ -expectation tolerance limits was set at 95% with the acceptance limits set at  $\pm 10\%$  which was in agreement with the product specifications of the selected ophthalmic suspension. For PAC and selected impurities at the impurity concentration, the  $\beta$ -expectation tolerance limits was set at 90% with the acceptance

limits set at  $\pm 20\%$ , due to the greater degree of variance expected for trace level analysis. The developed UPSFC method was validated for PAC and impurities to ICH recommendations using the total error approach for trueness and precision, accuracy, limit of detection (LOD), limit of quantitation (LOQ) and linearity. Method specificity/stability indication along with solution stability was also assessed as per ICH Q2R1 guidance [142].

#### **4.3.5.1 PAC UPSFC Specificity/Stability Indication and Solution Stability**

Method specificity was demonstrated by the analysis of a placebo blank solution containing only the pharmaceutical excipients, a MeOH blank solution and a sample solution spiked with each of the selected impurities at a concentration of  $3.6 \text{ mg.L}^{-1}$  (equivalent to 0.6% of nominal PAC concentration) using PDA detection. All peaks in the spiked sample chromatogram were separated with a resolution of  $\geq 1.5$  and found to be spectrally pure across the bandwidth using PDA detection. Figure 4.19 shows overlaid chromatograms of the MeOH blank, placebo blank, a PAC sample spiked with impurities equivalent to 0.1% of PCA concentration and a PAC standard. Figure 4.19 demonstrates that there were no interfering peaks with a signal-to-noise (S/N) ratio greater than 10:1 at the retention time of PAC or any of the impurities being investigated in the placebo blank or MeOH blank injections. In fact, the only significant sample matrix component was a peak at approximately 1.3 min in the placebo blank chromatogram. Therefore, the new UPSFC method can be considered specific for PAC and the eight selected impurities.

A forced degradation study was also performed on a PAC sample solution as described in Section 3.3.2.3 to promote the base hydrolysis of PAC. The stressed PAC sample was then analysed using the UPSFC method along with an un-stressed sample as a control to determine the amount of PAC degradation. Under the stress conditions, the PAC concentration decreased by 11.5%. In terms of impurities, the P concentration increased by 2,066%, P-17A decreased by 100%, HCA decreased by 13%, P-11,21D decreased by 32%, PN decreased by 18%, HC increased by 19% and 20(S) increased by 293%. 20(R) was not detected in either the control or stressed sample preparations. This preliminary study and the aforementioned PDA spectral analysis are indicative of the potential utility of this UPSFC method as a stability assay for routine stability monitoring.

The developed UPSFC method was used to examine solution stability prior to full method validation studies. PAC working standards and working sample solutions were prepared and stored in amber glassware at ambient laboratory temperature. The working

standards were prepared at two concentration levels, namely 100% and 1% of nominal to accommodate for both assay and trace impurity analysis using PAC as the reference standard. The prepared standards and sample solutions were tested immediately and again after 6 and 7 days respectively using the developed UPSFC method.

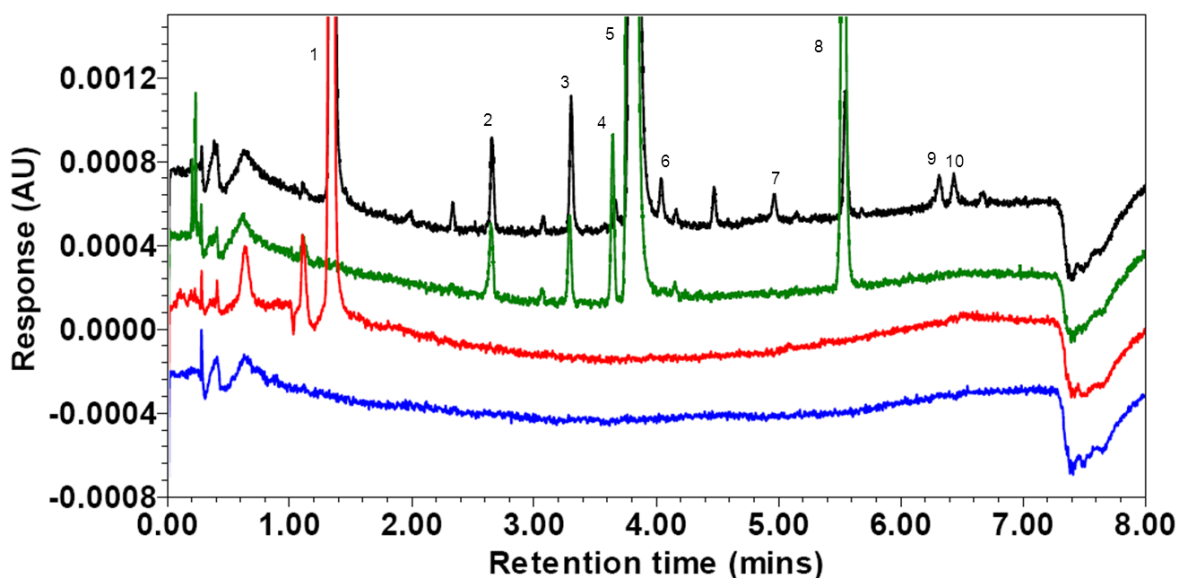


**Figure 4.19:** Overlaid chromatograms of MeOH blank (blue), placebo blank (red), PAC standard at  $600 \text{ mg.L}^{-1}$  (green) and spiked sample containing PAC at  $600 \text{ mg.L}^{-1}$  and impurities  $0.6 \text{ mg.L}^{-1}$  (black) expanded view to show detail. Chromatographic conditions and peak elution order as per Figure 4.14.

For standard stability, the 1% standard showed a decrease in PAC peak area of 0.44% whereas the 100% standard showed a decrease of 0.06% after 6 days storage. For the sample stability, the PAC peak area showed a decrease of 1.72% after 7 days storage. However, there was a notable change in the sample impurity profile after 7 days (for example; +628% for P, +1229% for P-17A, -0.54% for HCA, -9.14% for P11,21D, +211.54% for PN, +12.16% for HC and, +7.37% for 20(S)). Therefore, it was concluded that working standards at 1% and 100% of nominal could be prepared in amber glass and stored at ambient room temperature for up to 6 days. However, working sample solutions were prepared in amber glassware immediately before performing routine analysis.

#### **4.3.5.2 PAC UPSFC Trueness and Precision**

The trueness and precision of the UPSFC method were estimated from the back-calculated amounts of the VS and IVS preparations (See Table 4.1). The back-calculated amounts were calculated from the CS and ICS using both L and L<sub>o</sub> response functions. Impurity response factors (RFs) were calculated for each of the selected impurities using the ratio of the slopes versus PAC (i.e. impurity slope/PAC slope) for both the L and L<sub>o</sub> response functions (See Table C.1 and Table C.2). Some RF values were found to be outside 0.8 < RF < 1.2 range, which according to the current European Pharmacopoeia [231] meant they were required to be included in quantitative calculations when PAC was used as the external reference standard. However, as was the case for the RP-HPLC method described in Chapter 3, it was noted that the % recovery values for all impurities improved when RF values were included in the quantitative calculation; i.e. even for those whose RFs were within the 0.8 < RF < 1.2 range. Therefore, it was decided to include RFs for all impurity quantitative calculations.

Trueness was expressed in term of relative bias (%) whereas the precision was determined by computing the relative standard deviation (RSD (%)) for repeatability and between-series intermediate precision at each concentration level of VS and IVS respectively. The relative bias (%) and RSD (%) results for PAC and the eight selected impurities based on both response functions studied are presented in Table C.3 to Table C.22 of Appendix C and graphically in Figure 4.20. For PAC at nominal concentration, the relative bias (%) and RSD (%) for repeatability and between-series intermediate precision were all equivalent when either the L or L<sub>o</sub> model was selected as the response function (See Table C.3 and Table C.4). However, at the impurity concentration levels, there was significant improvement in the relative bias (%), particularly at the lowest concentration levels, when the L<sub>o</sub> model was selected as the response function (See Table C.5 and Table C.6). This trend was repeated for all selected impurities as shown in Table C.7 to Table C.22 and graphically in Figure 4.20.

#### **4.3.5.3 PAC UPSFC Accuracy**

The accuracy profile, which takes into account the total error (i.e. systematic and random errors) can be used as a decision tool in deciding whether or not a method can be considered accurate over a given concentration range. For PAC at assay concentration level, the upper and lower 95%  $\beta$ -expectation tolerance limits (%) did not exceed the acceptance limits set a priori at  $\pm 10\%$  for the concentration range investigated, when either the L or L<sub>o</sub> response functions were used (See Figure D.1). Consequently, the UPSFC method was able to provide

accurate results for PAC from 80 to 120% of the target assay concentration when either the L or L<sub>o</sub> response function were used to calculate results. Recovery values (%) ranged from 99.81 to 100.18% for the L response function and from 98.70 to 100.25% for the L<sub>o</sub> response function (See Table C.3 and Table C.4).

#### 4.3.5.4 PAC UPSFC Impurity Accuracy and LOQ/LOD limits

For PAC and the selected impurities at the impurity concentration level, the acceptance limits were set a priori at  $\pm 20\%$  for the upper and lower 90%  $\beta$ -expectation tolerance limits (%). As stated previously in Section 4.1.2, the intersections between the tolerance interval and the acceptance limits by definition represents the LOQ and ULQ of the analyte under the analytical method conditions. Conventionally, a conservative method of LOD determination consists of calculation of the LOD as approximately three times less than the LOQ. Table 4.3 summarises the LOQ results for PAC and the selected impurities based on the accuracy profiles generated using the L and L<sub>o</sub> response functions as illustrated in Figures D.2 to D.10. Table 4.3 also summarises the estimated LOD concentrations based on the observed LOQ values (i.e.  $LOD = LOQ/3$ ) along with the % recovery ranges for PAC and the selected impurities as detailed in Tables C.5 to C.22 for both the L and L<sub>o</sub> response functions. However, based on the signal-to-noise approach (peak height versus baseline noise), it was decided to conservatively set the LOD for both the L and L<sub>o</sub> response functions at 0.05% for PAC and the selected impurities as illustrated in Figure 4.21 due to the level of detector noise associated with SFC.

**Table 4.3:** Impurity level accuracy and LOQ/LOD limits based on accuracy profiles

Response function	LOQ <sup>a</sup>		Estimated LOD <sup>a</sup>		Recovery range (%)	
	L	L <sub>o</sub>	L	L <sub>o</sub>	L	L <sub>o</sub>
PAC	0.17	0.05	0.057	0.017	97.8 - 116.9	96.2 - 100.6
P-11,21D	0.43	0.15	0.143	0.050	100.5 - 125.6	100.5 - 104.3
HCA	0.62	0.20	0.207	0.067	100.9 - 136.5	99.9 - 105.6
P-17A	0.45	0.05	0.150	0.017	99.5 - 122.5	99.8 - 103.5
PN	0.28	0.10	0.093	0.033	100.6 - 119.3	100.1 - 105.2
HC	0.52	0.08	0.173	0.026	99.5 - 118.7	99.1 - 101.1
P	0.43	0.20	0.143	0.067	100.5 - 118.0	99.7 - 102.8
20(R)	0.37	0.05	0.123	0.017	100.1 - 113.9	99.5 - 101.1
20(S)	0.37	0.22	0.123	0.073	100.2 - 116.3	99.4 - 103.5

<sup>a</sup> = % w.r.t PAC Label Claim

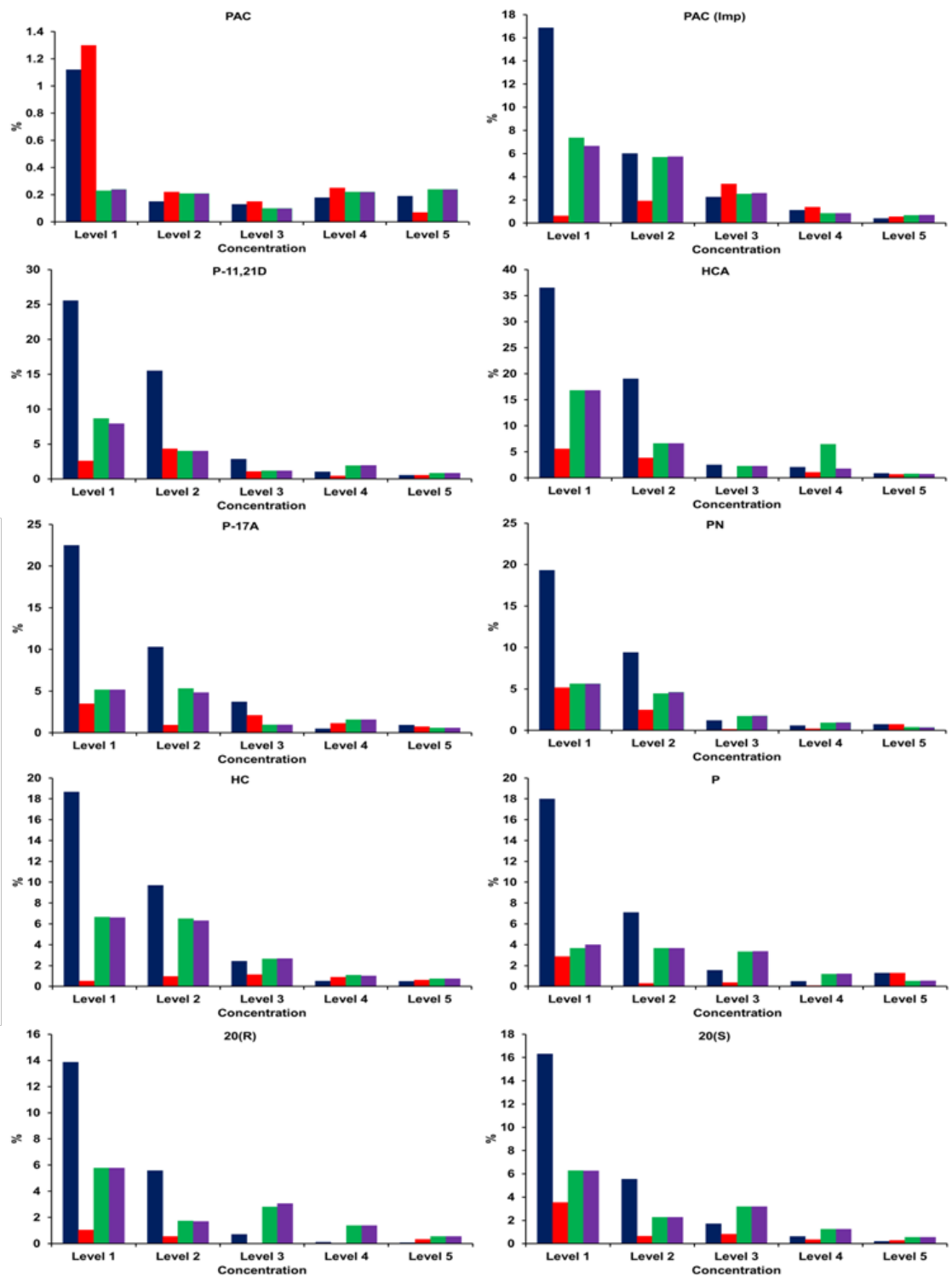


**Figure 4.20:** Plots of relative bias (%) and repeatability RSD (%) for PAC and impurity results generated using the L and Lo response functions over the selected concentration ranges. Blue = relative bias (%) for the L response function; red = relative bias (%) for the Lo response function; green = repeatability RSD (%) for the L response function and purple = repeatability RSD (%) for the Lo response function.

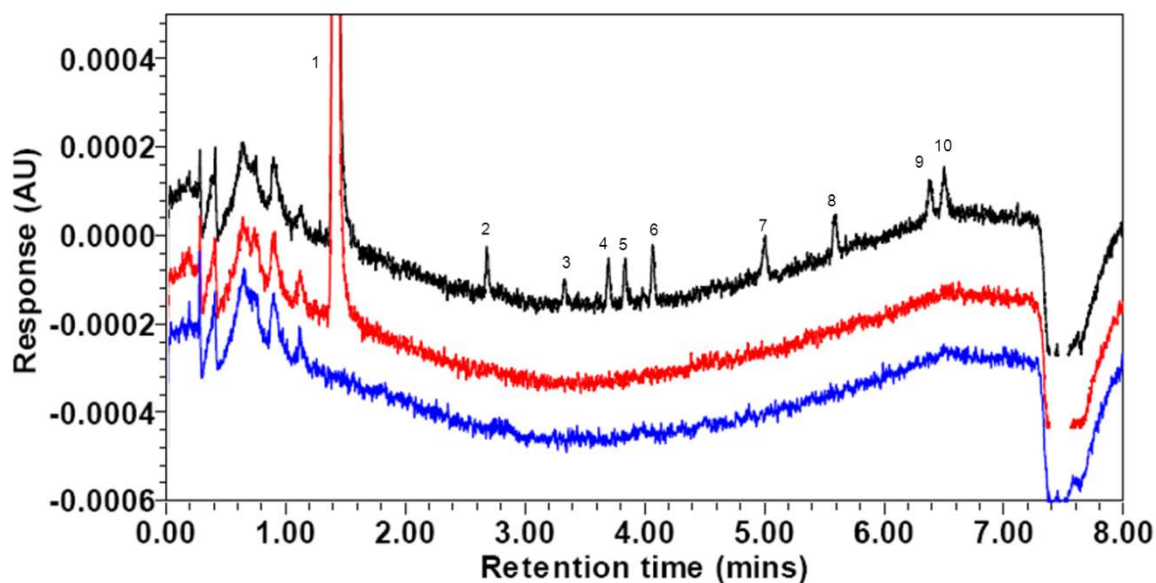


**Figure 4.21:** *Overlaid chromatograms of MeOH blank (blue), placebo blank (red) and spiked placebo containing PAC and impurities at  $0.3 \text{ mg}\cdot\text{L}^{-1}$  (black). Expanded view to show detail. Chromatographic conditions and peak elution order as per Figure 4.14.*

#### 4.3.5.5 PAC UPSFC Linearity

The linearity of an analytical method can be defined as its ability within a given range to obtain results (not signals) that are directly proportional to the concentrations (quantities) of the analyte in the sample [192]. For PAC at the assay level, each series included five concentration levels ranging from 80 to 120% of the nominal assay value. For PAC and each of the selected impurities at impurity level, each series included five concentration levels ranging from 0.05 to 2.0% of the nominal assay value. For all series, a single regression line was fitted based on the calculated concentrations versus the introduced concentrations for both the L and  $L_o$  response functions. From the regression analysis, the correlation coefficient ( $r^2$ ), slope and y-intercept were calculated.

The results for PAC at the assay level are presented in Table C.3 and Table C.4 for the L and  $L_o$  response functions respectively. For both response functions the  $r^2$  values were  $> 0.99$  with slopes of 1.02. The results for PAC and each of the selected impurities at impurity level are presented in Table C.5 to Table C.22 for the L and  $L_o$  response functions. For both response functions the  $r^2$  values were  $> 0.99$  with slopes of 1.0. The results demonstrates good linearity for the new UPSFC method for PAC at assay and impurity level,

along with each of the selected impurities at impurity level, whether the L and L<sub>o</sub> response function was used to back-calculate the sample results.

#### ***4.3.6 Selection of Appropriate Response Function for PAC UPSFC Quantitative Analysis***

Having calculated the two sided  $\beta$ -expectation tolerance intervals of the validation samples and subsequent generation of accuracy profiles for PAC and selected impurities, all that remained was to select the most appropriate response function; i.e. either L or L<sub>o</sub>, for use with the new UPSFC method during routine quantitative analysis. As stated previously, when it comes to selecting the most appropriate response function preference must be given to a model giving good results rather than a model presenting a good quality of fit [195]. Therefore, it is important to keep in mind the requirements of the method when it comes to making this decision. For the new UPSFC method, one of the main goals was to develop a method that could provide comparable or sufficient sensitivity to that of the RP-HPLC method for the trace analysis of the select impurities in an ophthalmic suspension. Therefore, when comparing the two selected response functions, preference was given to the model that could provide the lower LOQ values for PAC and selected impurities.

On review of Tables C.3 to Table C.22 (Appendix C) along with the accuracy profiles in Figure D.1 to Figure D.10 (Appendix D) it is clear that the response function that best satisfied the main goal of the method was the L<sub>o</sub> response function. Estimated LOQ values were significantly lower for the L<sub>o</sub> model ( $\leq 0.22\%$ ) compared to those of the linear model ( $\leq 0.62\%$ ) for the selected impurities. This enabled the new UPSFC method to meet the identification threshold and quantification threshold of 1.0% for degradation products of PAC as per Attachment 1 of ICH Q3B(R2) [144] which were defined a priori for the ophthalmic suspension in question. Also, the L<sub>o</sub> model provided equivalent linearity to that of the L model whilst recovery (%), repeatability % RSD and intermediate precision % RSD were all equivalent if not better, (particularly at the lowest concentrations) for the L<sub>o</sub> model. Thus, there was no impact on the quality of fit by selecting the L<sub>o</sub> model. Finally, as shown in Table C.1, based on the regression analysis of PAC at assay and impurity level for all the ICS series, and all bar series 4 of the CS, the y- intercept was less than the standard error of the y-intercept, which gives strong support for the use of a single point calibration curve during routine analysis [232]. Therefore, the proposed PAC standard concentration levels for

such single point calibration curves during routine quantitative analysis were 100% and 1% for assay and impurity level calculations respectively.

#### **4.3.7 Analytical Performance Comparison; UPSFC versus RP-HPLC**

The other goal of this method development was to provide orthogonal selectivity to that of the previously developed RP-HPLC method described in Chapter 3. Figure 4.22 demonstrates the dramatically different elution order of the new UPSFC method compared to the RP-HPLC method. This can be attributed to the normal phase-like retention mechanism of SFC. The orthogonality of two chromatographic separations was also quantitatively described by calculating the coefficient of determination ( $r^2$ ) of relative retention times from both methods. In order to provide a direct comparison between the two methods, the matrix peak was selected as the reference peak when calculating the relative retention times as it was the first peak to elute in both separations. As shown in Figure 4.23, the  $r^2$  is only about 0.06, which indicates a significant selectivity difference between two separation methods [128]. Having such an orthogonal UPSFC method also aids in confirming the selectivity of the original RP-HPLC method for the separation of PAC and the selected impurities [233].

In terms of analytical performance, the UPSFC method represents a 4 fold decrease in analysis time compared to the RP-HPLC method. There was also a significant 6.5 fold reduction in solvent consumption per injection with the UPSFC method, which demonstrated the potential of the UPSFC method for higher sample throughput and reduced solvent purchase/disposal costs if implemented into routine analysis. Both methods demonstrated good linearity for PAC and selected impurity peaks ( $r^2 > 0.99$ ) over a wide sample concentration range. Both methods were fully validated to meet current ICH requirements for specificity, trueness and precision, accuracy, LOD, LOQ, linearity and robustness. The accuracy results were comparable between the two methods at both assay and impurity levels. However, as expected the UPSFC method was found to be less sensitive than the RP-HPLC method. Even when measures such as increased sample concentration and the use of reference wavelength compensation function were employed, the LOQs of all peaks were higher in the UPSFC method ( $< 0.22\%$  for  $L_o$  response function) than for the RP-HPLC method ( $< 0.05\%$ ). However, despite the higher LOQs of the UPSFC method compared to the RP-HPLC method, they were sufficient to meet the identification threshold and quantification threshold of 1.0% for degradation products of PAC as per Attachment 1 of ICH Q3B(R2) [144] for the ophthalmic suspension in question. The UPSFC also meets the current European

Pharmacopoeia [234] impurity specifications for P and HCA are not more than 1.0% and not more than 0.5% for P-11,21D thus demonstrating the potential for the method to be used in routine stability studies. A comparison of the UPSFC and RP-HPLC analytical conditions and performance is outlined in Table 4.4.

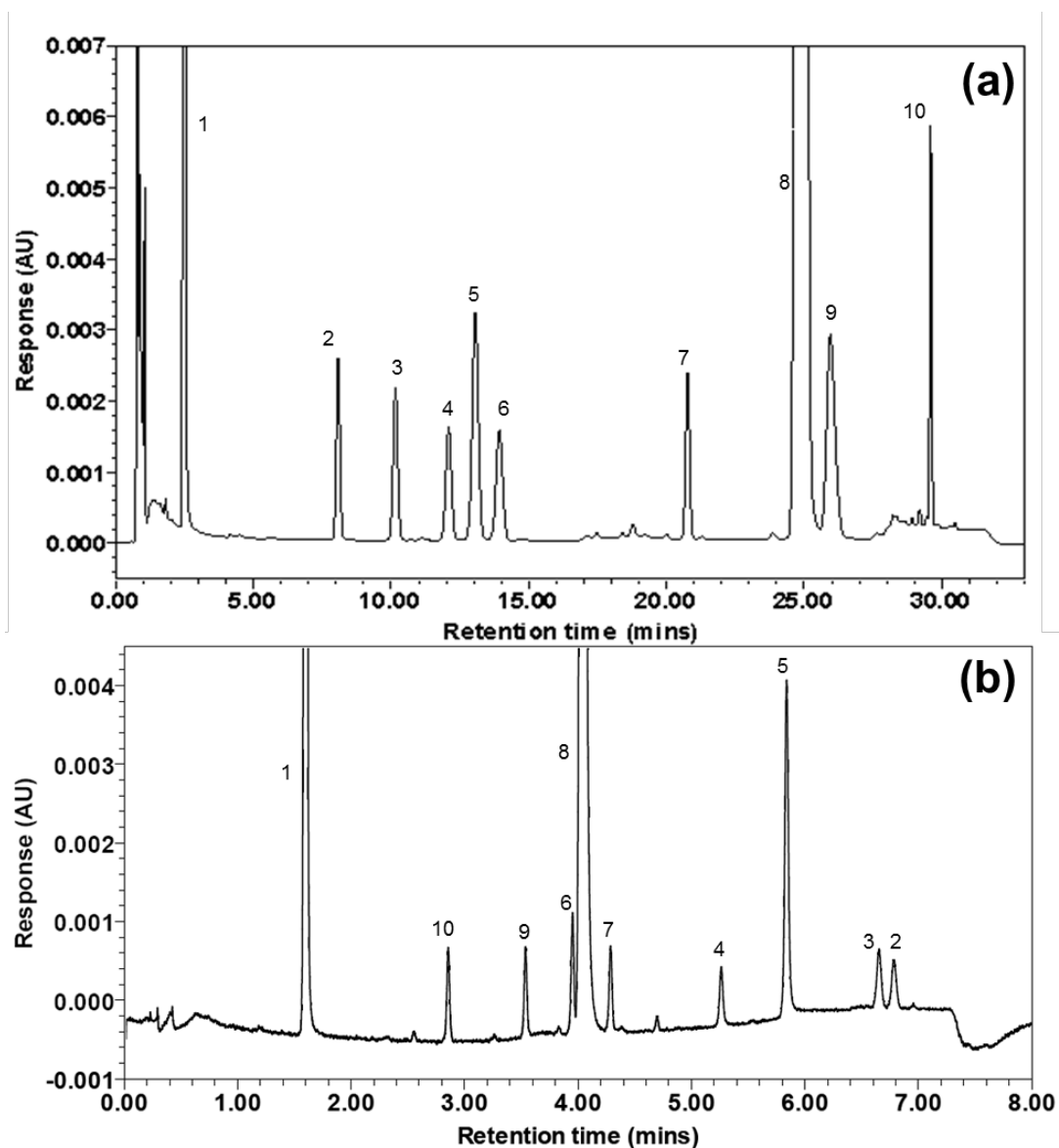


**Figure 4.22:** (a) Chromatogram of spiked sample containing PAC at  $200 \text{ mg.L}^{-1}$  and impurities  $1.2 \text{ mg.L}^{-1}$  under RP-HPLC conditions. Chromatographic conditions as per Figure 3.4. (b) Chromatogram of spiked sample containing PAC at  $600 \text{ mg.L}^{-1}$  and impurities  $3.6 \text{ mg.L}^{-1}$  under UPSFC conditions. Chromatographic conditions as per Figure 4.14. Peak elution order; matrix peak (1), 20(S) (2), 20(R) (3), PN (4), P (5), HC (6), P-17A (7), PAC (8), HCA (9) and P-11,21D (10).

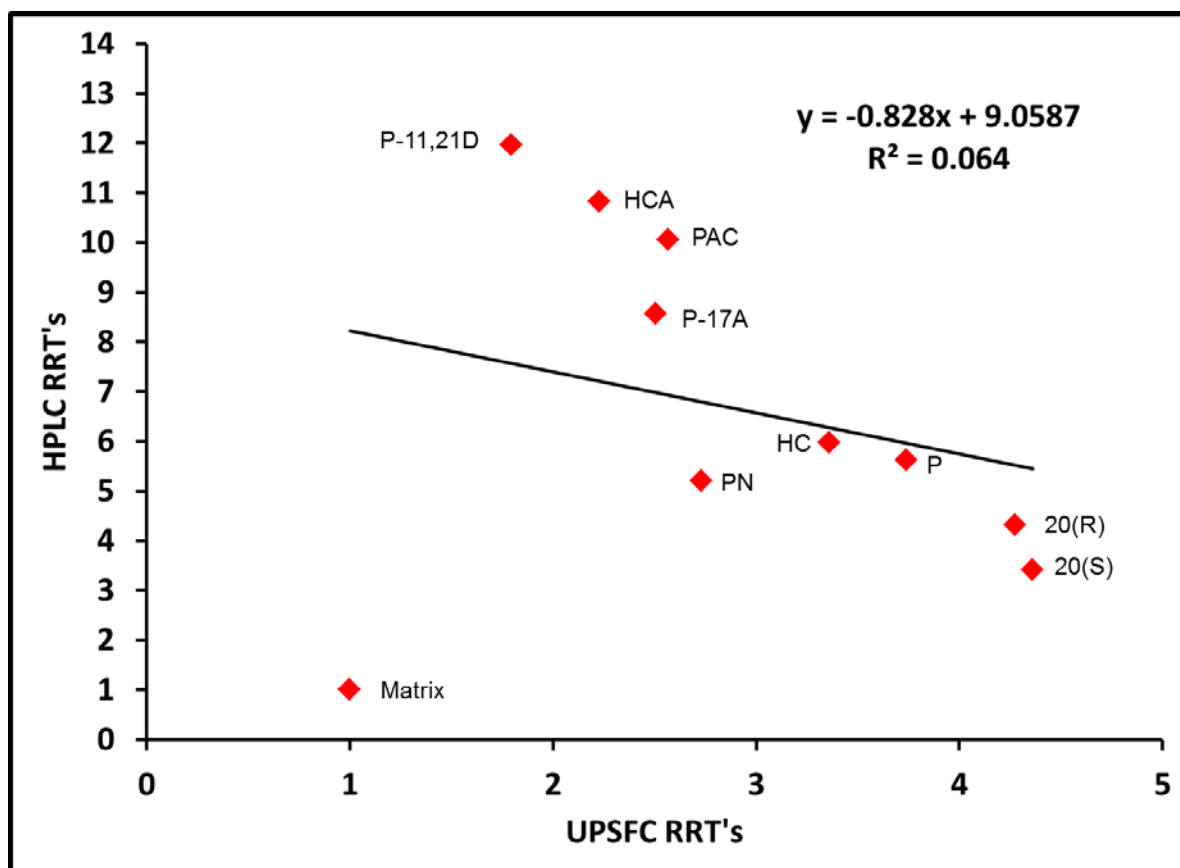


**Figure 4.23:** Comparison of relative retention times (vs matrix peak) in UPSFC method and in RP-HPLC method.

**Table 4.4:** Comparison between RP-HPLC and UPSFC analytical conditions and performance

Parameters	HPLC method	UPSFC method
Column	Agilent Poroshell 120 EC-C18 (2.7 $\mu\text{m}$ )100mm $\times$ 4.6mm	Waters Torus DEA (1.7 $\mu\text{m}$ )100mm $\times$ 4.6mm
Column temperature	60 $^{\circ}\text{C}$	50 $^{\circ}\text{C}$
Flow rate	1.2 mL.min $^{-1}$	2.5 mL.min $^{-1}$
Detection	254 nm 5Hz acquisition rate	254 nm 20Hz acquisition rate
Flow cell	10 mm path length, 10 $\mu\text{L}$ volume flow cell	10 mm path length, 13 $\mu\text{L}$ volume high pressure flow cell
Injection volume	10 $\mu\text{L}$	1 $\mu\text{L}$
Back pressure	-	138 bar
Analysis type	Gradient	Gradient
Run time	33 min	8 min
Mobile phase	A: Mixture of acetonitrile and water (10:90) B: Acetonitrile	A: CO $_2$ B: MeOH
Solvent usage	9.1 mL per injection	1.4 mL per injection
Sample diluent	Mixture MeOH/100 mM sodium acetate buffer pH 4.0 (50:50)	MeOH

#### 4.4 Conclusion

The new UPSFC method was shown to be a truly orthogonal chromatographic method to that of the established RP-HPLC method for the analysis of PAC and its selected impurities in an ophthalmic suspension. The new UPSFC method also operates with higher separation efficiency, providing faster analyses time and with less consumption of organic solvent compared to the RP-HPLC method. The use of the total error validation approach and generation of accuracy profiles not only meets all the ICH requirements for method validation, but also demonstrated the repeatability of the method (often an issue for SFC separations in the past) and provided a degree of confidence in the selection of the best response function (i.e.  $L_o$ ) for use during routine quantitative analysis. The new UPSFC method was found to be capable of meeting the impurity identification and quantitation thresholds defined by both the ICH Q3B(R2) and current EP for the selected PAC impurities. Therefore, based on the total error validation approach, the new UPSFC method can be considered validated for the determination of PAC and selected impurities in an ophthalmic suspension.

## 5.0 Conclusions and future work

The aim of this research project was to demonstrate the potential of SFC to be used as a viable alternative or complementary technique to HPLC in the highly regulated world of the Pharma QC laboratory. To do this, the historical weaknesses of poor reproducibility and low sensitivity associated with SFC had to be overcome, to allow the application of SFC for routine trace level analysis on selected pharmaceutical ingredients/products.

This aim had been achieved by the development and validation of both chiral and achiral SFC applications described in Chapters 2 and 4 above. The chiral application described in Chapter 2 was shown to be capable of providing an alternative to the EP method based upon NP-HPLC for determining the enantiomeric purity of timolol maleate raw material. The achiral application described in Chapter 4 was also shown to be an acceptable alternative to the established RP-HPLC method for the trace impurity analysis of PAC in an aqueous ophthalmic suspension. Both SFC methods demonstrated significant improvements in terms of reduced analysis times and solvent consumption compared to their LC counterparts.

The success of these applications was due in no small part to the availability of holistically designed SFC instrumentation and stationary phases. This renewed focus by instrument manufacturers such as Agilent and Waters have resulted many of the historically challenges of poor reproducibility and low sensitivity becoming less of an issue for SFC applications.

From an environmental perspective, initiatives such as the Registration, Evaluation, Authorisation and Restriction of Chemicals (REACH) directive [235] are continuing to focus on reducing the use of environmentally harmful chemicals. In this context, by adopting the principals of green chemistry, SFC offers an attractive alternative to the established LC techniques (particularly NP-HPLC) in helping QC laboratories achieve these goals.

From a regulatory perspective, industry guidance such as the new FDA guidance entitled "*Analytical Procedures and Methods Validation for Drugs and Biologics*" [236] are now placing greater focus on employing appropriate statistical methods when; developing new test methods, evaluating existing test methods, evaluating measurement system performance and interpreting or treating of analytical data like determining equivalence of two test methods. This guidance also suggests that to fully understand the effect of changes in

method parameters on an analytical procedure, a systematic approach for a method robustness study (e.g., a design of experiments with method parameters) should be used. This approach involves an initial risk assessment and follow with multivariate experiments. Such approaches allow the analyst to understand factorial parameter effects on method performance.

The FDA guidance states that to fully understand the effect of changes in method parameters on an analytical procedure, one should adopt a systematic approach for a method robustness study (e.g., a design of experiments with method parameters). One should begin with an initial risk assessment and follow with multivariate experiments. Such approaches allow one to understand factorial parameter effects on method performance. Evaluation of a method's performance may include analyses of samples obtained from various stages of the manufacturing process from in-process to the finished product. Knowledge gained during these studies on the sources of method variation can help you assess the method performance. The guidance also states that statistical analysis of validation data can be used to evaluate validation characteristics against predetermined acceptance criteria and that all statistical procedures and parameters used in the analysis of the data should be based on sound principles and appropriate for the intended evaluation. In this context, the work carried out by the likes of Dispas *et al.* [223], where DOE principals were employed at the method development stage, along with the use of the total error approach for method validation stage (also employed in Chapter 4), demonstrate the ability of SFC to satisfy this new regulatory guidance.

Therefore, in the context of both the updated environmental and regulatory guidance, the work presented in Chapters 2 and 4 above demonstrate the now real potential for SFC to move beyond the realm of academic research or chiral preparative applications. Thus, with the continuous improvements being made in the design of SFC instrumentation, along with the ever expanding range of published SFC analytical applications; SFC is finally showing real potential in offering the QC analyst an alternative/complementary technique to that of the established techniques (i.e. LC, GC and CE) in the QC laboratory.

## 6.0 References

- [1] T.A. Berger, Packed Column SFC, The Royal Society of Chemistry Chromatography Monograph Series, R.M. Smith ed., Cambridge, UK, 1995.
- [2] [http://chemwiki.ucdavis.edu/Core/Physical\\_Chemistry/Physical\\_Properties\\_of\\_Matter/States\\_of\\_Matter/Phase\\_Transitions/Phase\\_Diagrams](http://chemwiki.ucdavis.edu/Core/Physical_Chemistry/Physical_Properties_of_Matter/States_of_Matter/Phase_Transitions/Phase_Diagrams).
- [3] T.A. Berger, Chromatography: Supercritical Fluid, Historical Development, in: I.D. Wilson, C. Pool (Eds.), Handbook of Methods and Instrumentation in Separation Science Vol. 1, Academic Press, 2009, pp: 653.
- [4] <http://www1.chem.leeds.ac.uk//People/CMR/criticalpics.html>
- [5] <http://www.enen.co.kr/index2.html>
- [6] “What is a supercritical fluid”, Budapest University of Technology and Economics, 2013.
- [7] L.T. Taylor, J. Supercritical Fluids, 47, (2009) 566.
- [8] M. Saito, J. Biosci and Bioeng, 115, 6 (2013) 590.
- [9] E. Lesellier, C. West, J. Chromatogr. A1382 (2015) 2.
- [10] E. Klesper, A.H. Corwin, D.A. Turner, J. Org. Chem. 27 (1962) 700.
- [11] J.C. Giddings, M.N. Myers, L.M. McLarne, R.A. Keller, Sci. 162 (1968) 67.
- [12] J.F. Deye, T.A. Berger, A.G. Anderson, Anan. Chem. 62 (1990) 615.
- [13] T.A. Berger, Chemical basis for the instrumentation used in packed column supercritical fluid chromatography, in: K. Anton, C. Berger, Supercritical Fluid Chromatography with Packed Columns, Marcel Dekker Inc., New York, Basel, Hong Kong, 1998, pp. 19.
- [14] G.O. Cantrell, R.W. Stringham, J.A. Blackwell, J.D. Weckwerth, P.W. Carr, Anal. Chem. 68 (1996) 3645.
- [15] J.A. Blackwell, R.W. Stringham, J.D. Weckwerth, Anal. Chem. 69 (1997) 409.
- [16] L. Nováková, A. Grand-Guillaume Perrenoud, I. Francois, C. West, E. Lesellier, D. Guillarme, Anal. Chim. Acta 824 (2014) 18.
- [17] T.A. Berger, J.F. Deye, J. Chromatogr. A 547 (1991) 377.
- [18] Y. Okamoto, M. Kawashima, K. Hatada, K, J. Am. Chem. Soc. 106 (1984) 5357.
- [19] Y. Okamoto, M. Kawashima, K. Hatada, K, J. Chromatogr. 363 (1986) 173.
- [20] K. W. Phinney, Anal. Bioanal. Chem. 382 (2005) 639.
- [21] D. Mangelings, Y. V. Heyden, J. Sep. Sci. 31 (2008) 1252.
- [22] A.M.V. Schou-Pedersen, J. Østergaard, M. Johansson, S. Dubant, R.B. Fred-eriksen, S.H. Hansen, J. Pharm. Biomed. Anal. 88 (2014) 256.
- [23] A.J. Alexander, L. Zhang, T.F. Hooker, F.P. Tomasella, J. Pharm. Biomed. Anal. 78–79 (2013) 243.

- [24] E. Lesellier, K. Gaudin, P. Chaminade, A. Tchaplá, A. Baillet, *J. Chromatogr. A* 1016 (2003) 111.
- [25] V. Goss, A. Cazenave-Gassiot, A. Pringle, A. Postle, *Curr. Anal. Chem.* 10 (2014) 121.
- [26] D. Tognarelli, A. Tsukamoto, J. Caldwell, W. Caldwell, *Bioana.* 2 (2010) 5.
- [27] J. Zheng, J.D. Pinkston, P.H. Zoutendam, L.T. Taylor, *Anal. Chem.* 78 (2006) 1535.
- [28] M. Ishibashi, T. Ando, M. Sakai, A. Matsubara, T. Uchikata, E. Fukusaki, *J. Chromatogr. A* 1266 (2012)143.
- [29] X. Yang, B. Ma, X. Zheng, C. Lin, *Anal. Methods* 6 (2014) 4769.
- [30] D. Johnston, M. Ashraf-Khorassani, L.T. Taylor, *Chromatographia* 57 (2003) 533.
- [31] J.P. Kithinji, K.D. Bartle, M.W. Raynor, A.A. Clifford, *Analyst* 115 (1990) 125.
- [32] S. Bijttebier, E. D'Hondt, B. Noten, N. Hermans, S. Apers, V. Exarchou, *Food Chem.* 165 (2014) 371.
- [33] T.A. Berger, B.K. Berger, *Chromatographia* 76 (2013) 393.
- [34] V. Abrahamsson, I. Rodriguez-Meizoso, C. Turner, *J. Chromatogr. A* 1250 (2012) 63.
- [35] C. Desmorteux, M. Rothaupt, C. West, E. Lesellier, *J. Chromatogr. A* 1216 (2009) 7088.
- [36] T.A. Berger, *J. Chromatogr. A* 785 (1997) 3.
- [37] T.A. Berger, *Anal. Chem.* 62 (1990) 1181.
- [38] T.A. Berger, *J. of H. Res. Chromatogr.* 14 (1991) 312.
- [39] J.N. Fairchild, J.F. Hill, P.C. Iraneta, *LC-GC N. Am.* 31 (2013) 326.
- [40] V. Abrahamsson, M. Sandahl, *J. Chromatogr. A* 1306 (2013) 80.
- [41] S. Fekete, I. Kohler, S. Rudaz, J.L. Veuthey, *J. Pharm. Biomed. Anal.* 87 (2014) 105.
- [42] E. Lesellier, *J. Chromatogr. A* 1216 (2009) 1881.
- [43] E. Lesellier, *J. Sep. Sci.* 31 (2008) 1238.
- [44] H.S.H. Yip, M. Ashraf-Khorassani, L.T. Taylor, *Chromatographia* 65 (2007) 655.
- [45] A. Cazenve-Gassiot, R. Boughtflower, J. Caldwell, R. Coxhead, L. Hitzel, S. Lane, P. Oakley, C. Holyoak, F. Pullen, G.J. Langley, *J. Chromatogr. A* 1189 (2008) 254.
- [46] A.J. Alexander, T.F. Hooker, F.P. Tomasella, *J. Pharm. Biomed. Anal.* 70 (2012) 77.
- [47] J. Lundgreen, J. Salomonsson, O. Gyllenhaal, E. Johansson, *J. Chromatogr. A* 1154 (2007) 360.
- [48] C. West, E. Lesellier, *J. Chromatogr. A* 1110 (2006) 181.
- [49] C. West, E. Lesellier, A. Tchaplá, *J. Chromatogr. A* 1048 (2004) 99.
- [50] C. West, E. Lesellier, *J. Chromatogr. A* 1087 (2005) 64.
- [51] C. West, E. Lesellier, *J. Chromatogr. A* 1110 (2006) 200.

- [52] C. West, S. Khater, E. Lesellier, J. Chromatogr. A 1250 (2012) 182.
- [53] C. West, E. Lesellier, J. Chromatogr. A 1110 (2006) 191.
- [54] C. West, E. Lesellier, J. Chromatogr. A 1169 (2007) 205.
- [55] C. West, E. Lesellier, J. Chromatogr. A 1115 (2006) 233.
- [56] T.A. Berger, Chromatography: Supercritical Fluid, Instrumentation, in: I.D. Wilson, C. Pool (Eds.), Handbook of Methods and Instrumentation in Separation Science Vol. 1, Academic Press, 2009, pp: 659.
- [57] T.A. Berger, B.K. Berger, J. Chromatogr. A 1218 (2011) 2320.
- [58] Y. Hirata, Y. Kawaguchi, Y. Funada, J. Chromatogr. Sci. 34 (1996) 58.
- [59] Y. Sun, B.Y. Shekunov, P. York, Chem. Eng. Commun. 190 (2003) 1.
- [60] J.E. France, K.J. Voorhees, J. High Resolut. Chromatogr. 11 (1988) 692.
- [61] A. Pereira, F. David, G. Vanhoenacker, C. Brunelli, P. Sandra, LC–GC N. Am. 29 (2011).
- [62] A. Grand-Guillaume Perrenoud, J.L. Veuthey, D. Guillarme, J. Chromatogr. A 1266 (2012) 158.
- [63] T. Fornstedt, R. E. Majors, LC-GC E. 28 (2015).
- [64] A. Tarafder, K. Kaczmarek, D. P. Poe, G. Guiochon, J. Chromatogr. A 1258 (2012) 124.
- [65] K. Kaczmarek, D. P. Poe, G. Guiochon, J. Chromatogr. A 1218 (2011) 6531.
- [66] M. Enmark, P. Forssen, J. Samuelsson, T. Fornstedt, J. Chromatogr. A 1312 (2013) 124.
- [67] F. Kamarei, F. Gritti, G. Guiochon, J. Chromatogr. A 1306 (2013) 89.
- [68] M. Enmark, J. Samuelsson, E. Forss, P. Forssen, T. Fornstedt, J. Chromatogr. A 1354 (2014) 129.
- [69] R. Majors, D. Raynie, LC-GC E. 24 (2011).
- [70] P.T. Anastas and J.C. Warner, Green Chemistry: Theory and practice, Oxford University Press, New York, 1988.
- [71] P. Sandra, A. Pereira, M. Dunkle, C. Brunell, F. David, LC-GC E. 23 (2010).
- [72] W.A. Bonner, Chirality 12 (2000) 114.
- [73] N.M. Maier, P. Franco, W. Lindner, J. Chromatogr. A 906 (2001) 3.
- [74] Food & Drug Administration. FDA's policy statement for the development of new stereoisomeric drugs. 57 Fed. (1992) Reg. 22249.
- [75] B.S. Sekhon, J. Mod. Med. Chem., 1 (2013) 10.
- [76] J. Agustian, A.H. Kamaruddin, S. Bhatia, Process Biochem. 45 (10) (2010) 1587.
- [77] W.H. Frishman, Circulation 107 (2003) 117.
- [78] M.J. Reiter, Prog. Cardiovasc. Dis. 47 (2004) 11.
- [79] J. Agustian, A.H. Kamaruddin, S. Bhatia, Process Biochem. 45 (2010) 1587.

- [80] H.L. Kennedy, *Am. J. Med.* 110 (2001) 2.
- [81] R. Mehvar, D. R. Brocks, *J. Pharm. Pharm. Sci.* 4 (2001) 185.
- [82] W.H. Frisman, *Circulation* 107 (2003) 117.
- [83] Bryan, J. *Pharmacogen J.* 279 (2007) 538.
- [84] D.J. Cordato, L.E. Mather, G.K. Herkes, *J. Clin. Neurosci.* 10 (2003) 649.
- [85] J.A. Nathanson, *J. Pharmac. Exp. Ther.* 245 (1998) 94.
- [86] T. Walle, J.G. Web, E.E. Bagwel, U.K. Wale, H.B. Daniel, T.E. Gaffney, *Biochem. Pharmac.* 37 (1998) 115.
- [87] A.B. Rofman, F.K. Stanley. A.G.Munir, B. Thiyagarajan, F.J. Nancarrow, B.W. Abrams, *Hypertension*, 2 (1980) 643.
- [88] A.J. Franciosa, D.E. Freis, J. Conway, *Circulation* 48 (1973) 118.
- [89] H.W. Frishman, D.C. Furberg, T.W. Friedewald, *N. Engl. J. Med.* 310 (1984) 830.
- [90] The International Collaborative Study Group. *N. Engl. J. Med.* 310 (1984) 9.
- [91] The Norwegian Multicenter Study Group. *N. Engl. J. Med.* 304 (1981) 801.
- [92] D.J. Mazzo, A.E. Loper, *Timolol Maleate in: K. Florey (Eds.), Analytical Profiles of Drug Substances, Vol. 16, Academic Press, 1987 pp. 641.*
- [93] T.J. Zimmerman, *Invest. Ophth. Vis. Sci.* 16 (1977) 687.
- [94] K. Dickstein, R. Hapnes, T. Aarsland, *Am. J. Ophth.* 132 (2001) 626.
- [95] W.H. Frishman, *N. Engl. J. Med.* 306 (1982) 1456.
- [96] R.C. Heel, R.N. Brogden, T.M. Speight, G.S. Avery, *Drugs* 17 (1979) 38.
- [97] W.P. Boger, *Drugs* 18 (1979) 25.
- [98] F.T. Fraunfelder, A.F. Barker, *N. Engl. J. Med.* 311 (1984) 1441.
- [99] R. Richards, A. Tattersfield, *Br. J. Clin. Pharmacol.* 20 (1985) 459.
- [100] R. Richards, A. Tattersfield, *Br. J. Clin. Pharmacol.* 24 (1987) 485.
- [101] B.K. Wasson, W.K. Gibson, R.S. Stuart, H.W.R. Williams, C.H. Yates, *J. Med. Chem.* 15 (1972) 651.
- [102] Z. Wang, J. Ouyang, W.R.G. Baeyens, *J. Chromatogr. B* 862 (2008) 1.
- [103] *Eur. Pharmacop.(Version 7.5): Timolol Maleate monograph.*
- [104] H.Y. Aboul-Enein, M.R. Islam, *J. Chromatogr. A* 511 (1990) 109.
- [105] I.W. Wainer, R.M. Stiffin, T. Shibata, *J. Chromatogr. A* 411 (1987) 139.
- [106] P.M. Lacroix, B.A. Dawson, R.W. Sears, D.B. Black, *Chirality* 6 (1994) 484.
- [107] R.D. Marini, P. Chiap, B. Boulanger, W. Dewe, P. Hubert, J. Crommen, *J. Sep. Sci.* 26 (2003) 809.
- [108] *Eur. Pharmacop. 4th Edition, Addendum 2002, Council of Europe, Strasbourg.*

- [109] R.D. Marini, B. Boulanger, Y. Vander Heyden, P. Chiap, J. Crommen, P. Hubert, *Anal. Chim. Acta* 531 (2005) 131.
- [110] R.D. Marini, P. Chiap, B. Boulanger, S. Rudaz, E. Rozet, J. Crommen, Ph. Hubert, *Talant.* 68 (2006) 1166.
- [111] Y. Hedeland, J. Lehtinen, C. Pettersson, *J. Chromatogr. A* 1141 (2007) 287.
- [112] A.C. Servais, M. Fillet, P. Chiap, W. Dewé, P. Hubert, J. Crommen, *Electrophoresis* 25 (2004) 2701.
- [113] R.D. Marini, A-C. Servais, E. Roze, P. Chiap, B. Boulanger, S. Rudaz, J. Crommen, Ph. Hubert, M. Fillet, *J. Chromatogr. A* 1120 (2006) 102.
- [114] K.D. Altria, LC–GC E. September 2002.
- [115] Eur. Pharmacop. European Directorate for the Quality of Medicines, Nordlingen, 2005.
- [116] Z.K. Shihabi, *Electrophoresis* 23 (2002) 1628.
- [117] T.J. Ward, K.D. Ward, *Ana. Chem.* 82 (2010) 4712.
- [118] K. De Klerck, D. Mangelings, D. Clicq, F. De Boever, Y. Vander Heyden, *J. Chromatogr. A* 1234 (2012) 72.
- [119] L. Miller, M. Potter, *J. Chromatogr. B* 875 (2008) 230.
- [120] W.R. Leonard, D.W. Henderson, R.A. Miller, G.A. Spencer, O.S. Sudah, M. Biba, C.J. Welch, *Chirality* 19 (2007) 693.
- [121] L.T. Taylor, *J. Super. Flu.* 47 (2009) 566.
- [122] W. Ren-Qi, O. Teng-Teng, N. Siu-Choon, T. Weihua, *Trends in Analytical Chemistry* 37 (2012) 83.
- [123] B. Chankvetadze, *J. Chromatogr. A* 1269 (2012) 26.
- [124] L.T. Taylor, *Anal. Chem.* 82 (2010) 4925.
- [125] K. De Klerck, D. Mangelings, Y. Vander Heyden, LC-GC E. Supp: May (2013) 24.
- [126] R.L. Stevenson, *Am. Lab.* 45 (2013) 36.
- [127] R. Helmy, M. Biba, J. Zang, B. Mao, K. Fogelman, V. Vlacho, P. Hosek, C.J. Welch, *Chirality* 19 (2007) 787.
- [128] Z. Wang, H. Zhang, O. Liu, B. Donovan, *J. Chromatogr. A* 1218 (2011) 2311.
- [129] K. De Klerck, D. Mangelings, Y. Vander Heyden, *J. Pharm. Biomed. Anal.* 69 (2012) 77.
- [130] O. Gyllenhaal, A. Karlsson, *J. Biomed. Biophys. Methods* 54 (2002) 169.
- [131] A. Medvedovici, P. Sandra, L. Toribio, F. David, *J. Chromatogr. A* 785 (1997) 159.
- [132] Y. Liu, A. Berthod, C.R. Mitchell, T.L. Xiao, B. Zhang, D.W. Armstrong, *J. Chromatogr. A* 978 (2002) 185.
- [133] K.L. Williams, L.C. Sander, *J. Chromatogr. A* 785 (1997) 149.
- [134] H. Nelander, S. Andersson, K. Öhlén, *J. Chromatogr. A* 1218 (2011) 9397.

- [135] C. Roussel, B. Bonnet, A. Piederriere, C. Suteu, *Chirality* 13 (2001) 56.
- [136] R.B. Kasat, N.H.L. Wang, E.I. Franses, *J. Chromatogr. A* 1190 (2008) 110.
- [137] S. Ma, S. Shen, H. Lee, M. Eriksson, X. Zeng, J. Xu, K. Fandrick, N. Yee, C. Senanayake, N. Grinberg, *J. Chromatogr. A* 1216 (2009) 3784.
- [138] R.W. Stringham, J.A. Blackwell, *Anal. Chem.* 68 (1996) 2179.
- [139] S. Khater, Y. Zhang, C. West, *J. Chromatogr. A* 1303 (2013) 83.
- [140] M. Ventura, B. Murphy, W. Goetzinger, *J. Chromatogr. A* 1220 (2012) 147.
- [141] K. Kontturi, L. Murtomaki, *J. Pharm. Sci-US.* 81 (1992) 970.
- [142] ICH [Validation of Analytical Procedures: Methodology (Q2R1)], International Conference on Harmonization, November 1996.
- [143] United States Pharmacop. No. 31-NF- 26, (2008), ch. 621.
- [144] International Conference on Harmonisation of Technical Requirements for Registration of Pharmaceuticals for Human Use: Impurities in New Drug Products Q3B(R2), (2006).
- [145] H. Derendorf, H. Mollmann, A. Griiner, D. Haack and G. Gyselby, *Clin. Pharmacol. Ther.* 39 (1986) 313.
- [146] H. Derendorf, E Rohdewald, G. Hochhaus and H. Mollmann, *J. Pharm. Biomed. Anal.* 4 (1986) 197.
- [147] V.H.L. Lee, V.H.K. Li, *Adv. Drug. Deliv. Rev.* 3 (1989) 1.
- [148] V.H.L. Lee, H. Bundgaard, Improved ocular drug delivery with prodrugs. In: K.B. Sloan (Ed.), *Drugs and the Pharmaceutical Sciences*, Vol. 53: Prodrugs, Topical and Ocular Drug Delivery, Marcel Dekker, Inc., New York, (1992) pp. 221.
- [149] R.D. Schoenwald, R.L. Ward, *J. Pharm. Sci.* 67 (1978) 787.
- [150] A. Kupferman, A.R. Berrospi, H.M. Leipowitz. *Arch. Ophthalmol.* 100 (1982) 640.
- [151] H.M. Leibowitz, A.R. Berrospi, A. Kupferman, G.V. Restropo, V. Galvis, J.A. Alvarez, *Am. J. Ophthalmol.* 83 (1977) 402.
- [152] A. Kupferman, M.V. Pratt, K. Suckewer, H.M. Leibowitz, *Arch. Ophthalmol.* 91 (1974) 373.
- [153] D. Musson, A. Bidgood, O. Olejnik, *Pharm. Res. (Suppl.)* 6 (1989) 1.
- [154] D. Musson, A. Bidgood, O. Olejnik, *J. Ocul. Pharmacol.* 7 (1991) 175.
- [155] T. Jarvinen, K. Jarvinen, *Advanced Drug Delivery Reviews*, 19 (1996) 203.
- [156] G.R. Cannell, R.H. Mortimer, D.J. Maguire, R.S. Addison, *J. Chromatogr.* 563 (1991) 341.
- [157] D.G. Musson, A.M. Bidgood, O. Olejnik, *J. Chromatogr.* 565 (1991) 89.
- [158] S.A. Doppenschmitt, B. Scheidel, F. Harrison, J.P. Surmann, *J. Chromatogr. B* 674 (1995) 237.
- [159] N. Shibata, T. Hayakawa, K. Takada, N. Hoshino, T. Minouchi, A. Yamaji, *J. Chromatogr. B* 706 (1998) 191.

- [160] A.S. Carlin, V.K. Prasad, *J. Chromatogr.* 425 (1988) 162.
- [161] A. Santos-Montes, R. Izquierdo-Hornillos, *J. Chromatogr. B* 724 (1999) 53.
- [162] V. Garg, W.J. Jusko, *J. Chromatogr.* 567 (1991) 3947.
- [163] V.K. Prasad, B. HO, C. Haneke, *J. Chromatogr.* 378 (1986) 305.
- [164] H.N. Barot, J.B. Dave, C.N. Patel, *IJPSR*, Vol. 3(6) (2012) 1817.
- [165] S.G. Musharraf, U. Fatima, R. Sultana, *Chem. Centr. J.* 6 (2012) 7.
- [166] J.M.L. Gallego, J. Perez Arroyo, *J. Sep. Sci.* 26 (2003) 947.
- [167] J.M. Lemus Gallego, J. Perez Arroyo, *J. Pharm. Biomed. Ana.* 31 (2003) 873.
- [168] J.M. Lemus Gallego, J. Perez Arroyo, *J. Chromatogr. B* 784 (2003) 39.
- [169] M.L. Rocci Jr., W.J. Jusko, *J. Chromatogr.* 224 (1981) 221.
- [170] A. Shalaby, M. Shahjahan, *J. Liq. Chromatogr.* 14 (1991) 1267.
- [171] S. N. Razzaq, *Chem. Centr. J.* 6 (2012) 94.
- [172] United States Pharmacop.No. 36-NF1, prednisolone acetate in ophthalmic suspension monograph, (2014).
- [173] Eur. Pharmacop.8th edition, prednisolone acetate monograph, (2014).
- [174] United States Pharmacop. No. 36-NF1, prednisolone acetate in ophthalmic suspension monograph, (2014).
- [175] J. Kirkland, T. Langlois, J. DeStefano, *Am. Lab.* 39 (2007) 18.
- [176] F. Gritti, G. Guiochon, *LC-GC N. Am.* 7(30) (July 2012) 586.
- [177] F. Gritti, A. Cavazzini, N. Marchetti, G. Guiochon, *J. Chromatogr. A* 1157 (2007) 289.
- [178] F. Gritti, C. Sanchez, T. Farkas, G. Guiochon, *J. Chromatogr. A* 1217 (2010) 3000.
- [179] N.S. Wilson, M.D. Nelson, J.W. Dolan, L.R. Snyder, R.G. Wolcott, P.W. Carr, *J. Chromatogr. A* 961 (2002) 171.
- [180] ACD ChemSketch, Version 12.01 ([www.acdlabs.com](http://www.acdlabs.com)).
- [181] C. Baiocchi, D. Giacosa, M.A. Roggero, E. Marengo *J. Chromatogr Sci*, 34, (1996) 399.
- [182] A.J. Berry, D.E. Games, J.A. Perkins, *J. Chromatogr.* 363 (1986) 147.
- [183] E. Lesellier, A. Tchaplal, C. Marty, A. Lebert, *J. Chromatogr.* 633 (1993) 9.
- [184] Koji Yaku, Keiichi Aoe, Noriyuki Nishimura, Tadashi Sato, Fujio Morishita, *J. Chromatogr. A*, 773 (1997) 277.
- [185] T.A. Berger, J.F. Deye, *J. Chromatogr. Sci.* 29 (1991) 280.
- [186] A.L. Blilie, T. Greibrokk, *Anal. Chem.* 57 (1985) 2239.
- [187] J.G.M. Janssen, P.J. Schoenmakers, C.A. Cramers, *J. High Resolut. Chromatogr.* 12 (1989) 645.
- [188] N.K. Jagota, J.B. Nair, R. Frazer, M. Klee, M.Z. Wang, *J. Chromatogr. A* 721 (1996) 315.

- [189] J.L. Bernal, M.J. del Nozal, H. Velasco, L. Toribio, J. Liq. Chromatogr. Related Technol. 19 (1996) 1579.
- [190] S. Salman Lateef, Vinayak AK . [www.agilent.com/chem](http://www.agilent.com/chem) © Agilent Technologies, Inc., 2012 Published in the USA, May 1, 2012 5991-0277EN.
- [191] Ph. Hubert, J.J. Nguyen-Huu, B. Boulanger, E. Chapuzet, P. Chiap, N. Cohen, P.A. Compagnon, W. Dewé, M. Feinberg, M. Lallier, M. Laurentie, N. Mercier, G. Muzard, C. Nivet, L. Valat, J. Pharm. Biomed. Anal. 36 (2004) 579.
- [192] Ph. Hubert, J.J. Nguyen-Huu, B. Boulanger, E. Chapuzet, P. Chiap, N. Cohen, P.A. Compagnon, W. Dewé, M. Feinberg, M. Lallier, M. Laurentie, N. Mercier, G. Muzard, C. Nivet, L. Valat, S.T.P. Pharma Pratiques 13 (3) (2003) 101.
- [193] A. Bouabidi, E. Rozet, M. Fillet, E. Ziemons, E. Chapuzet, B. Mertens, R. Klinkenberg, A. Ceccato, M. Talbi, B. Streel, A. Bouklouze, B. Boulanger, Ph. Hubert, J. Chromatogr. A 1217 (2010) 3180.
- [194] Ph. Hubert, J.J. Nguyen-Huu, B. Boulanger, E. Chapuzet, P. Chiap, N. Cohen, P.A. Compagnon, W. Dewé, M. Feinberg, M. Lallier, M. Laurentie, N. Mercier, G. Muzard, C. Nivet, L. Valat, E. Rozet, J. Pharm. Biomed. Anal. 45 (2007) 70.
- [195] Ph. Hubert, J.-J. Nguyen-Huu, B. Boulanger, E. Chapuzet, N. Cohen, P.-A. Compagnon, W. Dewé, M. Feinberg, M. Laurentie, N. Mercier, G. Muzard, L. Valat, E. Rozet, J. Pharm. Biomed. Anal. 45 (2007) 82.
- [196] Ph. Hubert, J.-J. Nguyen-Huu, B. Boulanger, E. Chapuzet, N. Cohen, P.-A. Compagnon, W. Dewé, M. Feinberg, M. Laurentie, N. Mercier, G. Muzard, L. Valat, E. Rozet, J. Pharm. Biomed. Anal. 48 (2008) 760.
- [197] M. Feinberg, J. Chromatogr. A 1158 (2007) 174.
- [198] A. Gustavo Gonzalez, M. Angeles Herrador, Tren. Anal. Chem. 26 (3) (2007) 227.
- [199] D. Hoffman, R. Kringle, Pharma. Res. 24 (6) (2007) 1157.
- [200] J. C. Miller, J. N. Miller, statistics for analytical chemistry, 3rd edition, chapter 1 (1993).
- [201] B. Boulanger, Ph. Hubert, P. Chiap, W. Dewé, Objectives of pre-study validation and decision rules, AAPS APQ Open forum, Washington, 2000.
- [202] B. Boulanger, Ph. Hubert, P. Chiap, W. Dewé, J. Crommen, Statistical analysis of the validation results, in: GMP, 2000.
- [203] J. Ermer, J. Pharm. Biomed. Anal. 24 (2001) 755.
- [204] J. Ermer, H.J. Ploss, J. Pharm. Biomed. Anal. 37 (2005) 859.
- [205] R.W. Mee, Technometrics 26 (1984) 251.
- [206] Food and Drug Administration, Process Analytical Technology (PAT) Initiative, 2002, <http://www.fda.gov/cder/OPS/PAT.html>.
- [207] B. Boulanger, W. Dewé, P. Chiap, J. Crommen, P.H. Hubert, J. Pharm. Biomed. Anal. 32 (2003) 753.

- [208] SANCO – Commission of the European Communities, Off. J. Eur. Commun. L221 (2002) 8.
- [209] I. Bouchaib, S.I Mohamed, E.H.E. Mestafa, A. Sanae, S. Taoufiq. *Int J Pharm Pharm Sci*, 6, 11 (2014), 413.
- [210] ISO 5725, Accuracy (trueness and precision) of measurement methods and results—Parts 1–4, Part 6, ISO, Geneva, Switzerland, 1994.
- [211] S. Huet, E. Jolivet, A. Messean, *La regression non lineaire*, Editions INRA, Paris, 1992.
- [212] M.A. Bimazubute, E. Rozet, I. Dizier, P. Gustin, Ph. Hubert, J. Crommen, P. Chiap, *J. Chromatogr. A* 1189 (2008) 456.
- [213] O. Rbeida, B. Christiaens, Ph. Hubert, D. Lubda, K.-S. Boos, J. Crommen, P. Chiap, *J. Pharm. Biomed. Anal.* 36 (2005) 947.
- [214] S. Henry de Hassonville, P. Chiap, J.F. Liégeois B. Evrard, L. Delattre, J. Crommen, G. Piel, Ph. Hubert, *J. Pharm. Biomed. Anal.* 36 (2004) 133.
- [215] B. Christiaens, P. Chiap, O. Rbeida, D. Cello, J. Crommen, Ph. Hubert, *J. Chromatogr. B* 795 (2003) 73.
- [216] O. Rbeida, B. Christiaens, P. Chiap, Ph. Hubert, D. Lubda, K.-S. Boos, J. Crommen, *J. Pharm. Biomed. Anal.* 32 (2003) 829.
- [217] O. Rbeida, P. Chiap, D. Lubda, K.-S. Boos, J. Crommen, Ph. Hubert, *J. Pharm. Biomed. Anal.* 36 (2005) 961.
- [218] P. Chiap, M. Piette, B. Evrard, F. Frankenne, B. Christiaens, G. Piel, D. Cataldo, J.-M. Foidart, L. Delattre, J. Crommen, Ph. Hubert, *J. Chromatogr. B* 817 (2005) 109.
- [219] E. Rozet, C. Hubert, A. Ceccato, W. Dewe, E. Ziemons, F. Moonen, K. Michail, R. Wintersteiger, B. Streel, B. Boulanger, Ph. Hubert, *J. Chromatogr. A* 1158 (2007) 126.
- [220] A.-C. Servais, M. Fille, R. Mol, G. W. Somsen, P. Chiap, G. J. de Jong, J. Crommen, *J. Pharm. Biomed. Anal.* 40 (2006) 752.
- [221] P. Jacobs, W. Dew, A. Flament, M. Gibella, A. Ceccato, *J. Pharm. Biomed. Anal.* 40 (2006) 294.
- [222] B. Andri, A. Dispas, R.D. Marini, P. Hubert, *Americ. J. Anal. Chem.* 7 (2016) 75.
- [223] A. Dispas, P. Lebruna, E. Ziemonsa, R. Marini, E. Rozeta, Ph. Hubert, *J. Chromatogr. A* 1353 (2014) 78.
- [224] K. L. Ng, B. Paull, P. R. Haddad, Ka. Tanaka *J. Chromatogr. A* 850 (1999) 17.
- [225] J.W. Dolan, *LCGC Europe* 27(1) (2014) 138.
- [226] A. Grand-Guillaume Perrenoud, J.L. Veuthey, D. Guillarme, *J. Chromatogr. A* 1266 (2012) 158.
- [227] A. Grand-Guillaume Perrenoud, C. Hamman, M. Goel, J.L. Veuthey, D. Guillarme, S. Fekete, *J. Chromatogr. A* 1314 (2013) 288.
- [228] C. Brunelli, Y. Zhao, M.-H. Brown, P. Sandra, *J. Chromatogr. A* 1185 (2008) 1299.

- [229] [http://www.waters.com/waters/en\\_IE/ACQUITY-UPC2-Trefoil-and-Torus-Columns](http://www.waters.com/waters/en_IE/ACQUITY-UPC2-Trefoil-and-Torus-Columns).
- [230] T.A. Berger, W.H. Wilson, J. Chromatogr. Sci. 31 (1993) 127.
- [231] European Pharmacopoeia 8th edition, Chromatographic separation techniques, 2015.
- [232] L. R. Snyder, J. J. Kirkland, J. W. Dolan, Introduction to modern liquid chromatography 3rd edition, (2010) Ch. 11, 511.
- [233] J. Pellett, P. Lukulay, Y. Mao, W. Bowen, R. Reed, M. Ma, R.C. Munger, J.W. Dolan, L. Wisley, K. Medwid, N.P. Toltl, C.C. Chan, M. Skibic, K. Biswas, K.A. Wells, L.R. Snyder, J. Chromatogr. A. 1101 (2006) 122.
- [234] European Pharmacopoeia 8th edition, prednisolone acetate monograph, 2015.
- [235] Regulation (EC) No 1907/2006 of the European Parliament and of the Council of 18 December 2006 concerning the Registration, Evaluation, Authorisation and Restriction of Chemicals (REACH), establishing a European Chemicals Agency.
- [236] Analytical Procedures and Methods Validation for Drugs and Biologics Guidance for Industry, FDA. 27 July 2015.  
<http://www.fda.gov/downloads/drugs/guidancecomplianceregulatoryinformation/guidances/ucm386366.pdf>

## Appendix A

### Worked example for calculation of relative $\beta$ -expectation tolerance intervals

The following is a worked example of the calculation of the relative  $\beta$ -expectation tolerance intervals ( $\beta$  set to 95%) for the data set outlined in Table A.1. The results in Table A.1 were back-calculated from VS with an introduced concentration of 477.92 mg.L<sup>-1</sup>, using a simple L function generated using CS ranging from 477.92 mg.L<sup>-1</sup> to 716.88 mg.L<sup>-1</sup>.

**Table A.1:** Back-calculated VS results obtained with a simple linear response function.

	<b>Series 1</b>	<b>Series 2</b>	<b>Series 3</b>	<b>Series 4</b>
<b>Conc. (mg.L<sup>-1</sup>)</b>	468.01	471.67	477.80	467.88
	470.48	470.86	478.78	468.87
	469.11	471.21	475.83	469.99

#### Step 1:

Using Eq. (8) and Eq. (9), calculate the MSM and MSE for the data presented in Table A.1 as follows;

$$MSM_j = \frac{1}{p-1} \sum_{i=1}^p n_{ij} (\bar{x}_{ij,calc} - \bar{x}_{j,calc})^2 \quad \text{Eq. (8)}$$

$$MSM_j = \frac{1}{4-1} \sum_{i=1}^4 3 (47.52) = 47.52$$

$$MSE_j = \frac{1}{\sum_{i=1}^p n_{ij} - p} \sum_{i=1}^p \sum_{k=1}^{n_{ij}} (\bar{x}_{ijk,calc} - \bar{x}_{ij,calc})^2 \quad \text{Eq. (9)}$$

$$MSE_j = \frac{1}{\sum_{i=1}^{p^4} 12 - 4} \sum_{i=1}^4 \sum_{k=1}^{12} (10.16) = 1.27$$

#### Step 2:

Use the calculated MSM and MSE results to determine within-series variance ( $\sigma_{W,j}^2$ ) and the between-series variance ( $\sigma_{B,j}^2$ ). In this example,  $MSM > MSE$ , therefore use Eq. (10) and Eq. (11);

$$\sigma_{W,j}^2 = MSE_j \quad \text{Eq. (10)}$$

$$\sigma_{W,j}^2 = 1.27$$

$$\sigma_{B,j}^2 = \frac{MSM_j - MSE_j}{n} \quad \text{Eq. (11)}$$

$$\sigma_{B,j}^2 = \frac{47.52 - 1.27}{3} = 15.42$$

**Step 3:**

Calculate the repeatability ( $\sigma_{Re,j}^2$ ) and intermediate precision ( $\sigma_{Ip,j}^2$ ) from the calculated within-series variance ( $\sigma_{W,j}^2$ ) and the between-series variance ( $\sigma_{B,j}^2$ ) using Eq. (14) and Eq. (15);

$$\text{repeatability: } \sigma_{Re,j}^2 = \sigma_{W,j}^2 \quad \text{Eq. (14)}$$

$$\text{repeatability: } \sigma_{Re,j}^2 = 1.27$$

$$\text{intermediate precision: } \sigma_{Ip,j}^2 = \sigma_{W,j}^2 + \sigma_{B,j}^2 \quad \text{Eq. (15)}$$

$$\text{intermediate precision: } \sigma_{Ip,j}^2 = 1.27 + 15.42 = 16.69$$

It should be noted here that the intermediate precision result is calculated as  $\sigma_{Ip,j}^2$ . Therefore the actual intermediate precision result is the square root of calculated result, i.e.

$$\sigma_{Ip,j} = \sqrt{16.69} = 4.085 \quad \text{Eq. (26)}$$

**Step 4:**

Calculate the intermediate precision result using Eq. (21);

$$CV_{IP,j} = 100 \times \frac{\sigma_{IP,j}}{\bar{x}_j} \quad \text{Eq. (21)}$$

$$CV_{IP,j} = 100 \times \frac{4.085}{477.92 \text{ mg. L}^{-1}} = 0.855$$

**Step 5:**

Calculate the relative bias using Eq. (17);

$$\text{relative bias}_j(\%) = 100 \times \frac{\hat{\mu}_j - \bar{x}_j}{\bar{x}_j} \quad \text{Eq. (17)}$$

$$\text{relative bias}_j(\%) = 100 \times \frac{471.71 - 477.92}{477.92} = -1.30$$

**Step 6:**

At this point, most of the elements necessary to calculate the relative  $\beta$ -tolerance intervals have been generated. However, before completing the calculation of the relative  $\beta$ -tolerance intervals, calculate  $R_j$ ,  $B_j$  and  $\nu$  using Eq. (22), Eq. (23) and Eq. (24) respectively;

$$R_j = \frac{\hat{\sigma}_{B,j}^2}{\hat{\sigma}_{W,j}^2} \quad \text{Eq. (22)}$$

$$R_j = \frac{15.42}{1.27} = 12.14$$

$$B_j = \sqrt{\frac{R_j + 1}{nR_j + 1}} \quad \text{Eq. (23)}$$

$$B_j = \sqrt{\frac{12.14 + 1}{(3)(12.14) + 1}} = 0.59$$

$$\nu = \frac{(R_j + 1)^2}{(R_j + 1/n)^2 / (p - 1) + (1 - (1/n)) / pn} \quad \text{Eq. (24)}$$

$$\nu = \frac{(12.14 + 1)^2}{(12.14 + 1/3)^2 / (4 - 1) + (1 - (1/3)) / (4)(3)} = 3.33 \cong 3$$

**Step 7:**

From Eq.(25), use the t-distribution table (See Attachment B) to obtain  $Q_t \left( \nu; \frac{1+\beta}{2} \right)$ , the  $\beta$  quantile with  $\nu$  degrees of freedom. In this example,  $\beta = 95\%$  confidence interval. Therefore, the value at 95% with 3 degrees is 3.182.

**Step 8:**

Calculate the lower and upper relative  $\beta$ -tolerance interval using Eq. (19) and Eq. (20) respectively;

$$L_j = bias_j (\%) - Q_t \left( v; \frac{1 + \beta}{2} \right) \sqrt{1 + \frac{1}{pnB_j^2} CV_{IP,j}} \quad \text{Eq. (19)}$$

$$L_j = -1.30 - \left( (3.182) \sqrt{1 + \frac{1}{((4)(3))(0.59)^2} 0.855} \right) = -4.33$$

$$U_j = bias_j (\%) + Q_t \left( v; \frac{1 + \beta}{2} \right) \sqrt{1 + \frac{1}{pnB_j^2} CV_{IP,j}} \quad \text{Eq. (20)}$$

$$U_j = -1.30 + \left( (3.182) \sqrt{1 + \frac{1}{((4)(3))(0.59)^2} 0.855} \right) = 1.73$$

## Appendix B

### T-Distribution table [B1]

Table entry for  $p$  and  $C$  is the critical value  $t^*$  with probability  $p$  lying to its right and probability  $C$  lying between  $-t^*$  and  $t^*$ .

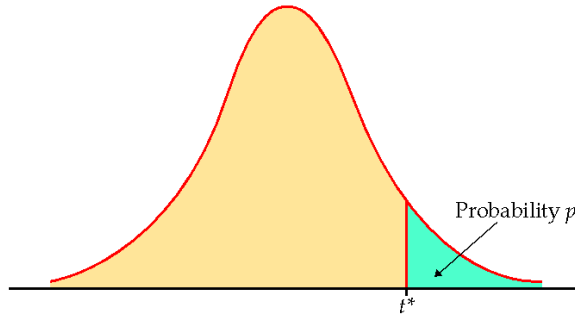


TABLE D												
t distribution critical values												
df	Upper-tail probability $p$											
	.25	.20	.15	.10	.05	.025	.02	.01	.005	.0025	.001	.0005
1	1.000	1.376	1.963	3.078	6.314	12.71	15.89	31.82	63.66	127.3	318.3	636.6
2	0.816	1.061	1.386	1.886	2.920	4.303	4.849	6.965	9.925	14.09	22.33	31.60
3	0.765	0.978	1.250	1.638	2.353	3.182	3.482	4.541	5.841	7.453	10.21	12.92
4	0.741	0.941	1.190	1.533	2.132	2.776	2.999	3.747	4.604	5.598	7.173	8.610
5	0.727	0.920	1.156	1.476	2.015	2.571	2.757	3.365	4.032	4.773	5.893	6.869
6	0.718	0.906	1.134	1.440	1.943	2.447	2.612	3.143	3.707	4.317	5.208	5.959
7	0.711	0.896	1.119	1.415	1.895	2.365	2.517	2.998	3.499	4.029	4.785	5.408
8	0.706	0.889	1.108	1.397	1.860	2.306	2.449	2.896	3.355	3.833	4.501	5.041
9	0.703	0.883	1.100	1.383	1.833	2.262	2.398	2.821	3.250	3.690	4.297	4.781
10	0.700	0.879	1.093	1.372	1.812	2.228	2.359	2.764	3.169	3.581	4.144	4.587
11	0.697	0.876	1.088	1.363	1.796	2.201	2.328	2.718	3.106	3.497	4.025	4.437
12	0.695	0.873	1.083	1.356	1.782	2.179	2.303	2.681	3.055	3.428	3.930	4.318
13	0.694	0.870	1.079	1.350	1.771	2.160	2.282	2.650	3.012	3.372	3.852	4.221
14	0.692	0.868	1.076	1.345	1.761	2.145	2.264	2.624	2.977	3.326	3.787	4.140
15	0.691	0.866	1.074	1.341	1.753	2.131	2.249	2.602	2.947	3.286	3.733	4.073
16	0.690	0.865	1.071	1.337	1.746	2.120	2.235	2.583	2.921	3.252	3.686	4.015
17	0.689	0.863	1.069	1.333	1.740	2.110	2.224	2.567	2.898	3.222	3.646	3.965
18	0.688	0.862	1.067	1.330	1.734	2.101	2.214	2.552	2.878	3.197	3.611	3.922
19	0.688	0.861	1.066	1.328	1.729	2.093	2.205	2.539	2.861	3.174	3.579	3.883
20	0.687	0.860	1.064	1.325	1.725	2.086	2.197	2.528	2.845	3.153	3.552	3.850
21	0.686	0.859	1.063	1.323	1.721	2.080	2.189	2.518	2.831	3.135	3.527	3.819
22	0.686	0.858	1.061	1.321	1.717	2.074	2.183	2.508	2.819	3.119	3.505	3.792
23	0.685	0.858	1.060	1.319	1.714	2.069	2.177	2.500	2.807	3.104	3.485	3.768
24	0.685	0.857	1.059	1.318	1.711	2.064	2.172	2.492	2.797	3.091	3.467	3.745
25	0.684	0.856	1.058	1.316	1.708	2.060	2.167	2.485	2.787	3.078	3.450	3.725
26	0.684	0.856	1.058	1.315	1.706	2.056	2.162	2.479	2.779	3.067	3.435	3.707
27	0.684	0.855	1.057	1.314	1.703	2.052	2.158	2.473	2.771	3.057	3.421	3.690
28	0.683	0.855	1.056	1.313	1.701	2.048	2.154	2.467	2.763	3.047	3.408	3.674
29	0.683	0.854	1.055	1.311	1.699	2.045	2.150	2.462	2.756	3.038	3.396	3.659
30	0.683	0.854	1.055	1.310	1.697	2.042	2.147	2.457	2.750	3.030	3.385	3.646
40	0.681	0.851	1.050	1.303	1.684	2.021	2.123	2.423	2.704	2.971	3.307	3.551
50	0.679	0.849	1.047	1.299	1.676	2.009	2.109	2.403	2.678	2.937	3.261	3.496
60	0.679	0.848	1.045	1.296	1.671	2.000	2.099	2.390	2.660	2.915	3.232	3.460
80	0.678	0.846	1.043	1.292	1.664	1.990	2.088	2.374	2.639	2.887	3.195	3.416
100	0.677	0.845	1.042	1.290	1.660	1.984	2.081	2.364	2.626	2.871	3.174	3.390
1000	0.675	0.842	1.037	1.282	1.646	1.962	2.056	2.330	2.581	2.813	3.098	3.300
$z^*$	0.674	0.841	1.036	1.282	1.645	1.960	2.054	2.326	2.576	2.807	3.091	3.291
	50%	60%	70%	80%	90%	95%	96%	98%	99%	99.5%	99.8%	99.9%
	Confidence level $C$											

[B1] [bcs.whfreeman.com/ips6e/content/cat\\_050/ips6e\\_table-d.pdf](https://bcs.whfreeman.com/ips6e/content/cat_050/ips6e_table-d.pdf)

**Appendix C**  
**UPSFC method validation data tables**

**Table C.1:** Response functions calculated using a simple linear regression model (L)

Series 1				Series 2				Series 3				Series4			
<b>PAC (CS)</b> <small>(m = 5; n = 3)</small>															
Slope	y-int	SE y-int	r <sup>2</sup>	Slope	y-int	SE y-int	r <sup>2</sup>	Slope	y-int	SE y-int	r <sup>2</sup>	Slope	y-int	SE y-int	r <sup>2</sup>
502.50	-4180.87	3908.31	0.998	502.13	227.13	1977.54	0.999	519.62	-16088.1	3515.04	0.998	489.39	10595.67	3059.94	0.999
<b>PAC (ICS)</b> <small>(m = 5; n = 3)</small>															
Slope	y-int	SE y-int	r <sup>2</sup>	Slope	y-int	SE y-int	r <sup>2</sup>	Slope	y-int	SE y-int	r <sup>2</sup>	Slope	y-int	SE y-int	r <sup>2</sup>
516.15	-52.23	25.67	0.999	511.43	-39.76	23.25	0.999	487.39	-11.56	11.80	0.999	486.80	0.70	6.92	0.999
<b>P-11,21D (ICS)</b> <small>(m = 5; n = 3)</small>															
Slope	y-int	SE y-int	r <sup>2</sup>	Slope	y-int	SE y-int	r <sup>2</sup>	Slope	y-int	SE y-int	r <sup>2</sup>	Slope	y-int	SE y-int	r <sup>2</sup>
350.27	-0.33	9.26	0.999	347.91	-4.25	9.80	0.999	354.14	14.66	15.67	0.999	354.78	11.53	8.29	0.999
<b>HCA (ICS)</b> <small>(m = 5; n = 3)</small>															
Slope	y-int	SE y-int	r <sup>2</sup>	Slope	y-int	SE y-int	r <sup>2</sup>	Slope	y-int	SE y-int	r <sup>2</sup>	Slope	y-int	SE y-int	r <sup>2</sup>
262.15	13.33	7.00	0.999	259.67	2.00	7.45	0.999	268.67	-4.20	14.62	0.999	279.42	-0.32	7.37	0.999
<b>P-17A (ICS)</b> <small>(m = 5; n = 3)</small>															
Slope	y-int	SE y-int	r <sup>2</sup>	Slope	y-int	SE y-int	r <sup>2</sup>	Slope	y-int	SE y-int	r <sup>2</sup>	Slope	y-int	SE y-int	r <sup>2</sup>
426.64	-14.08	30.36	0.998	425.56	7.10	12.83	0.999	440.79	-6.64	4.90	0.999	434.20	14.18	9.87	0.999
<b>PN (ICS)</b> <small>(m = 5; n = 3)</small>															
Slope	y-int	SE y-int	r <sup>2</sup>	Slope	y-int	SE y-int	r <sup>2</sup>	Slope	y-int	SE y-int	r <sup>2</sup>	Slope	y-int	SE y-int	r <sup>2</sup>
528.65	-36.17	32.33	0.998	523.82	-8.64	18.53	0.999	553.03	30.69	39.51	0.998	548.72	17.55	7.50	0.999
<b>HC (ICS)</b> <small>(m = 5; n = 3)</small>															
Slope	y-int	SE y-int	r <sup>2</sup>	Slope	y-int	SE y-int	r <sup>2</sup>	Slope	y-int	SE y-int	r <sup>2</sup>	Slope	y-int	SE y-int	r <sup>2</sup>
395.01	2.31	11.63	0.999	396.96	-7.90	17.51	0.999	417.58	-13.99	15.14	0.999	411.85	7.82	8.90	0.999
<b>P (ICS)</b> <small>(m = 5; n = 3)</small>															
Slope	y-int	SE y-int	r <sup>2</sup>	Slope	y-int	SE y-int	r <sup>2</sup>	Slope	y-int	SE y-int	r <sup>2</sup>	Slope	y-int	SE y-int	r <sup>2</sup>
553.85	-17.86	28.95	0.999	560.26	-15.71	18.87	0.999	577.00	-32.00	19.48	0.999	566.62	25.73	13.47	0.999
<b>20(R) (ICS)</b> <small>(m = 5; n = 3)</small>															
Slope	y-int	SE y-int	r <sup>2</sup>	Slope	y-int	SE y-int	r <sup>2</sup>	Slope	y-int	SE y-int	r <sup>2</sup>	Slope	y-int	SE y-int	r <sup>2</sup>
650.90	-19.45	24.04	0.999	634.24	22.27	15.07	0.999	678.73	-21.32	24.02	0.999	673.74	1.01	18.08	0.999
<b>20(S) (ICS)</b> <small>(m = 5; n = 3)</small>															
Slope	y-int	SE y-int	r <sup>2</sup>	Slope	y-int	SE y-int	r <sup>2</sup>	Slope	y-int	SE y-int	r <sup>2</sup>	Slope	y-int	SE y-int	r <sup>2</sup>
673.66	-0.23	11.52	0.999	667.17	10.86	15.06	0.999	698.59	-26.26	25.59	0.999	680.70	32.41	13.03	0.999
<b>Mean response factor (RF) Vs PAC (ICS)</b> <small>(m = 5; n = 3; p = 4)</small>															
<b>P-11,21D</b>		<b>HCA</b>		<b>P-17A</b>		<b>PN</b>		<b>HC</b>		<b>P</b>		<b>20(R)</b>		<b>20(S)</b>	
0.71		0.54		0.86		1.08		0.81		1.12		1.32		1.36	

m, number of concentration levels; n, number of replicates per concentration levels per series and p, number of series of experiments.

**Table C.2:** Response functions calculated using a linear through zero regression model ( $L_0$ )

Series 1		Series 2		Series 3		Series4	
<b>PAC (CS)</b> (m = 5; n = 3)							
<b>Slope</b>	<b>r<sup>2</sup></b>	<b>Slope</b>	<b>r<sup>2</sup></b>	<b>Slope</b>	<b>r<sup>2</sup></b>	<b>Slope</b>	<b>r<sup>2</sup></b>
495.64	0.999	502.50	0.999	493.22	0.999	506.78	0.999
<b>PAC (ICS)</b> (m = 5; n = 3)							
<b>Slope</b>	<b>r<sup>2</sup></b>	<b>Slope</b>	<b>r<sup>2</sup></b>	<b>Slope</b>	<b>r<sup>2</sup></b>	<b>Slope</b>	<b>r<sup>2</sup></b>
510.10	0.999	506.82	0.999	486.06	0.999	486.88	0.999
<b>P-11,21D (ICS)</b> (m = 5; n = 3)							
<b>Slope</b>	<b>r<sup>2</sup></b>	<b>Slope</b>	<b>r<sup>2</sup></b>	<b>Slope</b>	<b>r<sup>2</sup></b>	<b>Slope</b>	<b>r<sup>2</sup></b>
350.24	0.999	347.44	0.999	355.77	0.999	356.10	0.999
<b>HCA (ICS)</b> (m = 5; n = 3)							
<b>Slope</b>	<b>r<sup>2</sup></b>	<b>Slope</b>	<b>r<sup>2</sup></b>	<b>Slope</b>	<b>r<sup>2</sup></b>	<b>Slope</b>	<b>r<sup>2</sup></b>
263.65	0.999	259.90	0.999	268.21	0.999	279.39	0.999
<b>P-17A (ICS)</b> (m = 5; n = 3)							
<b>Slope</b>	<b>r<sup>2</sup></b>	<b>Slope</b>	<b>r<sup>2</sup></b>	<b>Slope</b>	<b>r<sup>2</sup></b>	<b>Slope</b>	<b>r<sup>2</sup></b>
425.08	0.999	426.35	0.999	440.10	0.999	435.79	0.999
<b>PN (ICS)</b> (m = 5; n = 3)							
<b>Slope</b>	<b>r<sup>2</sup></b>	<b>Slope</b>	<b>r<sup>2</sup></b>	<b>Slope</b>	<b>r<sup>2</sup></b>	<b>Slope</b>	<b>r<sup>2</sup></b>
524.93	0.999	522.93	0.999	556.20	0.998	550.53	0.999
<b>HC (ICS)</b> (m = 5; n = 3)							
<b>Slope</b>	<b>r<sup>2</sup></b>	<b>Slope</b>	<b>r<sup>2</sup></b>	<b>Slope</b>	<b>r<sup>2</sup></b>	<b>Slope</b>	<b>r<sup>2</sup></b>
395.25	0.999	396.17	0.999	416.18	0.999	412.64	0.999
<b>P (ICS)</b> (m = 5; n = 3)							
<b>Slope</b>	<b>r<sup>2</sup></b>	<b>Slope</b>	<b>r<sup>2</sup></b>	<b>Slope</b>	<b>r<sup>2</sup></b>	<b>Slope</b>	<b>r<sup>2</sup></b>
551.79	0.999	558.45	0.999	577.30	0.999	569.60	0.999
<b>20(R) (ICS)</b> (m = 5; n = 3)							
<b>Slope</b>	<b>r<sup>2</sup></b>	<b>Slope</b>	<b>r<sup>2</sup></b>	<b>Slope</b>	<b>r<sup>2</sup></b>	<b>Slope</b>	<b>r<sup>2</sup></b>
648.61	0.999	636.86	0.999	676.22	0.999	673.87	0.999
<b>20(S) (ICS)</b> (m = 5; n = 3)							
<b>Slope</b>	<b>r<sup>2</sup></b>	<b>Slope</b>	<b>r<sup>2</sup></b>	<b>Slope</b>	<b>r<sup>2</sup></b>	<b>Slope</b>	<b>r<sup>2</sup></b>
673.63	0.999	668.48	0.999	695.43	0.999	684.60	0.999
<b>Mean response factor (RF) Vs PAC (ICS)</b> (m = 5; n = 3; p = 4)							
<b>P-11,21D</b>	<b>HCA</b>	<b>P-17A</b>	<b>PN</b>	<b>HC</b>	<b>P</b>	<b>20(R)</b>	<b>20(S)</b>
0.71	0.54	0.87	1.08	0.82	1.13	1.33	1.37

m, number of concentration levels; n, number of replicates per concentration levels per series and p, number of series of experiments.

**Table C.3:** Validation results for PAC using the L response function to back-calculate VS amounts

<b>Validation criteria</b> (n = 3; p = 4)	<b>Level 1</b>	<b>Level 2</b>	<b>Level 3</b>	<b>Level 4</b>	<b>Level 5</b>
<b>Level (%)</b>	80	90	100	110	120
<b>Mean introduced concentration (mg.L<sup>-1</sup>)</b>	477.92	537.66	597.40	657.14	716.88
<b>Mean predicted concentration (mg.L<sup>-1</sup>)</b>	472.59	536.88	598.17	658.32	715.55
<b>Relative bias (%)</b>	-1.12	-0.15	0.13	0.18	-0.19
<b>Recovery (%)</b>	98.88	99.85	100.13	100.18	99.81
<b>Repeatability standard deviation</b>	1.106	1.128	0.586	1.429	1.744
<b>Intermediate precision standard deviation</b>	8.484	7.459	7.785	6.370	4.939
<b>Repeatability RSD (%)</b>	0.23	0.21	0.10	0.22	0.24
<b>Intermediate precision RSD (%)</b>	1.78	1.39	1.30	0.97	0.69
<b>Relative tolerance interval at 95% (%)</b>	6.31	4.93	4.63	3.44	2.12
<b>Lower relative <math>\beta</math> tolerance limit (%)</b>	-7.42	-5.07	-4.51	-3.26	-2.31
<b>Upper relative <math>\beta</math> tolerance limit (%)</b>	5.19	4.78	4.76	3.62	1.93
<b>Linearity</b> (m = 5; n = 3; p = 4)					
<b>Slope</b>	1.0167				
<b>y-intercept</b>	-11.055				
<b>r<sup>2</sup></b>	0.994				

m, number of concentration levels; n, number of replicates per concentration levels per series and p, number of series of experiments.

**Table C.4:** Validation results for PAC using the  $L_0$  response function to back-calculate VS amounts

<b>Validation criteria</b> ( $n = 3; p = 4$ )	<b>Level 1</b>	<b>Level 2</b>	<b>Level 3</b>	<b>Level 4</b>	<b>Level 5</b>
<b>Level (%)</b>	80	90	100	110	120
<b>Mean introduced concentration (mg.L<sup>-1</sup>)</b>	477.92	537.66	597.40	657.14	716.88
<b>Mean predicted concentration (mg.L<sup>-1</sup>)</b>	471.71	536.49	598.27	658.80	716.39
<b>Relative bias (%)</b>	-1.30	-0.22	0.15	0.25	-0.07
<b>Recovery (%)</b>	98.70	99.78	100.15	100.25	99.93
<b>Repeatability standard deviation</b>	1.127	1.139	0.579	1.451	1.712
<b>Intermediate precision standard deviation</b>	4.085	5.091	7.522	7.566	6.005
<b>Repeatability RSD (%)</b>	0.24	0.21	0.10	0.22	0.24
<b>Intermediate precision RSD (%)</b>	0.85	0.95	1.26	1.15	0.84
<b>Relative tolerance interval at 95% (%)</b>	3.03	3.36	4.48	4.09	2.96
<b>Lower relative <math>\beta</math> tolerance limit (%)</b>	-4.33	-3.58	-4.33	-3.83	-3.03
<b>Upper relative <math>\beta</math> tolerance limit (%)</b>	1.73	3.14	4.62	4.34	2.90
<b>Linearity</b> ( $m = 5; n = 3; p = 4$ )					
<b>Slope</b>	1.0239				
<b>y-intercept</b>	-15.353				
<b>r<sup>2</sup></b>	0.996				

m, number of concentration levels; n, number of replicates per concentration levels per series and p, number of series of experiments.

**Table C.5:** Validation results for PAC at impurity level using the L response function to back-calculate IVS amounts

<b>Validation criteria</b> (n = 3; p = 4)	<b>Level 1</b>	<b>Level 2</b>	<b>Level 3</b>	<b>Level 4</b>	<b>Level 5</b>
<b>Level (%)</b>	0.05	0.10	0.50	1.00	2.00
<b>Mean introduced concentration (mg.L<sup>-1</sup>)</b>	0.2989	0.5978	2.989	5.978	11.956
<b>Mean predicted concentration (mg.L<sup>-1</sup>)</b>	0.3493	0.6337	2.922	5.912	12.002
<b>Relative bias (%)</b>	16.86	6.00	-2.25	-1.10	0.39
<b>Recovery (%)</b>	116.86	106.01	97.76	99.90	100.38
<b>Repeatability standard deviation</b>	0.022	0.034	0.075	0.050	0.080
<b>Intermediate precision standard deviation</b>	0.054	0.043	0.075	0.123	0.089
<b>Repeatability RSD (%)</b>	7.36	5.69	2.51	0.84	0.67
<b>Intermediate precision RSD (%)</b>	18.11	7.45	2.51	2.06	0.77
<b>Relative tolerance interval at 95% (%)</b>	55.57	18.85	5.76	5.08	1.84
<b>Lower relative <math>\beta</math> tolerance limit (%)</b>	-38.71	-12.85	-8.01	-6.18	-1.45
<b>Upper relative <math>\beta</math> tolerance limit (%)</b>	72.43	24.85	3.51	3.99	2.23
<b>LOD (%)</b>	0.05 <sup>a</sup>				
<b>LOQ (%)</b>	0.17 <sup>b</sup>				
<b>Linearity</b> (m = 5; n = 3; p = 4)					
<b>Slope</b>	1.00000				
<b>y-intercept</b>	2.0 x 10 <sup>-12</sup>				
<b>r<sup>2</sup></b>	0.999				

m, number of concentration levels; n, number of replicates per concentration levels per series and p, number of series of experiments.

<sup>a</sup> = Based on signal-to-noise.

<sup>b</sup> = Estimated from accuracy profile.

**Table C.6:** Validation results for PAC at impurity level using the  $L_0$  response function to back-calculate IVS amounts

<b>Validation criteria</b> (n = 3; p = 4)	<b>Level 1</b>	<b>Level 2</b>	<b>Level 3</b>	<b>Level 4</b>	<b>Level 5</b>
<b>Level (%)</b>	0.05	0.10	0.50	1.00	2.00
<b>Mean introduced concentration (mg.L<sup>-1</sup>)</b>	0.2989	0.5978	2.989	5.978	11.956
<b>Mean predicted concentration (mg.L<sup>-1</sup>)</b>	0.3008	0.5867	2.888	5.896	12.023
<b>Relative bias (%)</b>	0.62	-1.91	-3.38	-1.37	0.56
<b>Recovery (%)</b>	100.64	98.14	96.62	98.62	100.56
<b>Repeatability standard deviation</b>	0.020	0.034	0.077	0.050	0.081
<b>Intermediate precision standard deviation</b>	0.020	0.038	0.091	0.138	0.104
<b>Repeatability RSD (%)</b>	6.66	5.75	2.58	0.84	0.68
<b>Intermediate precision RSD (%)</b>	6.66	6.37	3.06	2.31	0.87
<b>Relative tolerance interval at 95% (%)</b>	15.26	15.20	7.50	7.09	2.19
<b>Lower relative <math>\beta</math> tolerance limit (%)</b>	-14.64	-17.11	-10.87	-8.47	-1.64
<b>Upper relative <math>\beta</math> tolerance limit (%)</b>	15.89	13.30	4.12	5.72	2.75
<b>LOD (%)</b>	0.05 <sup>a</sup>				
<b>LOQ (%)</b>	0.05 <sup>b</sup>				
<b>Linearity</b> (m = 5; n = 3; p = 4)					
<b>Slope</b>	1.0059				
<b>y-intercept</b>	0.0508				
<b>r<sup>2</sup></b>	0.999				

m, number of concentration levels; n, number of replicates per concentration levels per series and p, number of series of experiments.

<sup>a</sup> = Based on signal-to-noise.

<sup>b</sup> = Estimated from accuracy profile.

**Table C.7:** Validation results for P-11,21D at impurity level using the L response function to back-calculate IVS amounts

<b>Validation criteria</b> (n = 3; p = 4)	<b>Level 1</b>	<b>Level 2</b>	<b>Level 3</b>	<b>Level 4</b>	<b>Level 5</b>
<b>Level (%)</b>	0.05	0.10	0.50	1.00	2.00
<b>Mean introduced concentration (mg.L<sup>-1</sup>)</b>	0.3119	0.6239	3.119	6.239	12.477
<b>Mean predicted concentration (mg.L<sup>-1</sup>)</b>	0.3916	0.7206	3.208	6.304	12.545
<b>Relative bias (%)</b>	25.55	15.51	2.84	1.05	0.54
<b>Recovery (%)</b>	125.55	115.50	102.85	101.04	100.54
<b>Repeatability standard deviation</b>	0.027	0.025	0.037	0.121	0.107
<b>Intermediate precision standard deviation</b>	0.069	0.062	0.100	0.121	0.128
<b>Repeatability RSD (%)</b>	8.66	4.01	1.19	1.94	0.86
<b>Intermediate precision RSD (%)</b>	22.03	9.97	3.19	1.94	1.03
<b>Relative tolerance interval at 95% (%)</b>	67.63	30.61	9.82	4.44	2.52
<b>Lower relative <math>\beta</math> tolerance limit (%)</b>	-42.09	-15.10	-6.99	-3.39	-1.98
<b>Upper relative <math>\beta</math> tolerance limit (%)</b>	93.18	46.12	12.66	5.49	3.07
<b>LOD (%)</b>	0.05 <sup>a</sup>				
<b>LOQ (%)</b>	0.43 <sup>b</sup>				
<b>Linearity</b> (m = 5; n = 3; p = 4)					
<b>Slope</b>	0.9980				
<b>y-intercept</b>	0.0886				
<b>r<sup>2</sup></b>	0.999				

m, number of concentration levels; n, number of replicates per concentration levels per series and p, number of series of experiments.

<sup>a</sup> = Based on signal-to-noise.

<sup>b</sup> = Estimated from accuracy profile.

**Table C.8:** Validation results for P-11,21D at impurity level using the  $L_0$  response function to back-calculate IVS amounts

<b>Validation criteria</b> (n = 3; p = 4)	<b>Level 1</b>	<b>Level 2</b>	<b>Level 3</b>	<b>Level 4</b>	<b>Level 5</b>
<b>Level (%)</b>	0.05	0.10	0.50	1.00	2.00
<b>Mean introduced concentration (mg.L<sup>-1</sup>)</b>	0.3119	0.6239	3.119	6.239	12.477
<b>Mean predicted concentration (mg.L<sup>-1</sup>)</b>	0.3200	0.6509	3.153	6.267	12.545
<b>Relative bias (%)</b>	2.60	4.34	1.07	0.45	0.54
<b>Recovery (%)</b>	102.60	104.33	101.09	100.45	100.55
<b>Repeatability standard deviation</b>	0.025	0.025	0.037	0.123	0.107
<b>Intermediate precision standard deviation</b>	0.05	0.040	0.070	0.132	0.128
<b>Repeatability RSD (%)</b>	7.95	4.01	1.19	1.97	0.86
<b>Intermediate precision RSD (%)</b>	7.95	6.42	2.25	2.11	1.02
<b>Relative tolerance interval at 95% (%)</b>	18.22	17.96	6.85	4.95	2.51
<b>Lower relative <math>\beta</math> tolerance limit (%)</b>	-15.62	-13.62	-5.78	-4.49	-1.97
<b>Upper relative <math>\beta</math> tolerance limit (%)</b>	20.82	22.29	7.92	5.40	3.06
<b>LOD (%)</b>	0.05 <sup>a</sup>				
<b>LOQ (%)</b>	0.15 <sup>b</sup>				
<b>Linearity</b> (m = 5; n = 3; p = 4)					
<b>Slope</b>	1.0039				
<b>y-intercept</b>	0.0151				
<b>r<sup>2</sup></b>	0.999				

m, number of concentration levels; n, number of replicates per concentration levels per series and p, number of series of experiments.

<sup>a</sup> = Based on signal-to-noise.

<sup>b</sup> = Estimated from accuracy profile.

**Table C.9:** Validation results for HCA at impurity level using the L response function to back-calculate IVS amounts

<b>Validation criteria</b> (n = 3; p = 4)	<b>Level 1</b>	<b>Level 2</b>	<b>Level 3</b>	<b>Level 4</b>	<b>Level 5</b>
<b>Level (%)</b>	0.05	0.10	0.50	1.00	2.00
<b>Mean introduced concentration (mg.L<sup>-1</sup>)</b>	0.3096	0.6191	3.096	6.191	12.383
<b>Mean predicted concentration (mg.L<sup>-1</sup>)</b>	0.4226	0.7370	3.173	6.321	12.491
<b>Relative bias (%)</b>	36.52	19.03	2.50	2.09	0.87
<b>Recovery (%)</b>	136.50	119.04	102.49	102.10	100.87
<b>Repeatability standard deviation</b>	0.052	0.041	0.070	0.401	0.095
<b>Intermediate precision standard deviation</b>	0.134	0.107	0.194	0.407	0.108
<b>Repeatability RSD (%)</b>	16.80	6.62	2.26	6.48	0.77
<b>Intermediate precision RSD (%)</b>	43.44	17.30	6.28	6.57	0.87
<b>Relative tolerance interval at 95% (%)</b>	133.49	53.16	19.32	15.50	2.12
<b>Lower relative <math>\beta</math> tolerance limit (%)</b>	-96.97	-34.13	-16.82	-13.41	-1.25
<b>Upper relative <math>\beta</math> tolerance limit (%)</b>	170.01	72.19	21.81	17.59	3.00
<b>LOD (%)</b>	0.05 <sup>a</sup>				
<b>LOQ (%)</b>	0.62 <sup>b</sup>				
<b>Linearity</b> (m = 5; n = 3; p = 4)					
<b>Slope</b>	1.0002				
<b>y-intercept</b>	0.1083				
<b>r<sup>2</sup></b>	0.999				

m, number of concentration levels; n, number of replicates per concentration levels per series and p, number of series of experiments.

<sup>a</sup> = Based on signal-to-noise.

<sup>b</sup> = Estimated from accuracy profile.

**Table C.10:** Validation results for HCA at impurity level using the  $L_0$  response function to back-calculate IVS amounts

<b>Validation criteria</b> (n = 3; p = 4)	<b>Level 1</b>	<b>Level 2</b>	<b>Level 3</b>	<b>Level 4</b>	<b>Level 5</b>
<b>Level (%)</b>	0.05	0.10	0.50	1.00	2.00
<b>Mean introduced concentration (mg.L<sup>-1</sup>)</b>	0.3096	0.6191	3.096	6.191	12.383
<b>Mean predicted concentration (mg.L<sup>-1</sup>)</b>	0.3268	0.6429	3.093	6.259	12.466
<b>Relative bias (%)</b>	5.57	3.83	-0.07	1.10	0.67
<b>Recovery (%)</b>	105.56	103.84	99.90	101.10	100.67
<b>Repeatability standard deviation</b>	0.052	0.041	0.070	0.110	0.094
<b>Intermediate precision standard deviation</b>	0.056	0.048	0.146	0.133	0.094
<b>Repeatability RSD (%)</b>	16.80	6.62	2.26	1.78	0.76
<b>Intermediate precision RSD (%)</b>	18.21	7.80	4.71	2.16	0.76
<b>Relative tolerance interval at 95% (%)</b>	42.70	18.72	14.40	5.30	1.74
<b>Lower relative <math>\beta</math> tolerance limit (%)</b>	-37.13	-14.89	-14.45	-4.20	-1.07
<b>Upper relative <math>\beta</math> tolerance limit (%)</b>	48.27	22.56	14.32	6.40	2.41
<b>LOD (%)</b>	0.05 <sup>a</sup>				
<b>LOQ (%)</b>	0.20 <sup>b</sup>				
<b>Linearity</b> (m = 5; n = 3; p = 4)					
<b>Slope</b>	1.0061				
<b>y-intercept</b>	0.0105				
<b>r<sup>2</sup></b>	0.999				

m, number of concentration levels; n, number of replicates per concentration levels per series and p, number of series of experiments.

<sup>a</sup> = Based on signal-to-noise.

<sup>b</sup> = Estimated from accuracy profile.

**Table C.11:** Validation results for P-17A at impurity level using the L response function to back-calculate IVS amounts

<b>Validation criteria</b> (n = 3; p = 4)	<b>Level 1</b>	<b>Level 2</b>	<b>Level 3</b>	<b>Level 4</b>	<b>Level 5</b>
<b>Level (%)</b>	0.05	0.10	0.50	1.00	2.00
<b>Mean introduced concentration (mg.L<sup>-1</sup>)</b>	0.3109	0.6217	3.109	6.217	12.434
<b>Mean predicted concentration (mg.L<sup>-1</sup>)</b>	0.3808	0.6857	3.224	6.188	12.548
<b>Relative bias (%)</b>	22.49	10.29	3.71	-0.48	0.92
<b>Recovery (%)</b>	122.48	110.29	103.70	99.53	100.92
<b>Repeatability standard deviation</b>	0.016	0.033	0.030	0.097	0.071
<b>Intermediate precision standard deviation</b>	0.064	0.057	0.106	0.178	0.088
<b>Repeatability RSD (%)</b>	5.15	5.31	0.96	1.56	0.57
<b>Intermediate precision RSD (%)</b>	20.46	9.11	3.42	2.86	0.71
<b>Relative tolerance interval at 95% (%)</b>	72.50	25.58	12.09	6.99	1.75
<b>Lower relative <math>\beta</math> tolerance limit (%)</b>	-50.01	-15.29	-8.38	-7.46	-0.83
<b>Upper relative <math>\beta</math> tolerance limit (%)</b>	95.00	35.87	15.81	6.51	2.66
<b>LOD (%)</b>	0.05 <sup>a</sup>				
<b>LOQ (%)</b>	0.45 <sup>b</sup>				
<b>Linearity</b> (m = 5; n = 3; p = 4)					
<b>Slope</b>	1.0014				
<b>y-intercept</b>	0.0605				
<b>r<sup>2</sup></b>	0.999				

m, number of concentration levels; n, number of replicates per concentration levels per series and p, number of series of experiments.

<sup>a</sup> = Based on signal-to-noise.

<sup>b</sup> = Estimated from accuracy profile.

**Table C.12:** Validation results for P-17A at impurity level using the  $L_0$  response function to back-calculate IVS amounts

<b>Validation criteria</b> (n = 3; p = 4)	<b>Level 1</b>	<b>Level 2</b>	<b>Level 3</b>	<b>Level 4</b>	<b>Level 5</b>
<b>Level (%)</b>	0.05	0.10	0.50	1.00	2.00
<b>Mean introduced concentration (mg.L<sup>-1</sup>)</b>	0.3109	0.6217	3.109	6.217	12.434
<b>Mean predicted concentration (mg.L<sup>-1</sup>)</b>	0.3217	0.6275	3.174	6.145	12.527
<b>Relative bias (%)</b>	3.48	0.92	2.10	-1.15	0.75
<b>Recovery (%)</b>	103.47	100.93	102.09	98.84	100.75
<b>Repeatability standard deviation</b>	0.016	0.030	0.030	0.097	0.072
<b>Intermediate precision standard deviation</b>	0.019	0.030	0.080	0.185	0.149
<b>Repeatability RSD (%)</b>	5.15	4.83	0.96	1.56	0.58
<b>Intermediate precision RSD (%)</b>	5.97	4.83	2.56	2.97	1.20
<b>Relative tolerance interval at 95% (%)</b>	14.66	11.07	7.88	9.06	3.67
<b>Lower relative <math>\beta</math> tolerance limit (%)</b>	-11.18	-10.14	-5.78	-10.21	-2.92
<b>Upper relative <math>\beta</math> tolerance limit (%)</b>	18.13	11.99	9.98	7.90	4.41
<b>LOD (%)</b>	0.05 <sup>a</sup>				
<b>LOQ (%)</b>	0.05 <sup>b</sup>				
<b>Linearity</b> (m = 5; n = 3; p = 4)					
<b>Slope</b>	1.0045				
<b>y-intercept</b>	0.0002				
<b>r<sup>2</sup></b>	0.999				

m, number of concentration levels; n, number of replicates per concentration levels per series and p, number of series of experiments.

<sup>a</sup> = Based on signal-to-noise.

<sup>b</sup> = Estimated from accuracy profile.

**Table C.13:** Validation results for PN at impurity level using the L response function to back-calculate IVS amounts

<b>Validation criteria</b> (n = 3; p = 4)	<b>Level 1</b>	<b>Level 2</b>	<b>Level 3</b>	<b>Level 4</b>	<b>Level 5</b>
<b>Level (%)</b>	0.05	0.10	0.50	1.00	2.00
<b>Mean introduced concentration (mg.L<sup>-1</sup>)</b>	0.3369	0.6737	3.369	6.737	13.474
<b>Mean predicted concentration (mg.L<sup>-1</sup>)</b>	0.4019	0.7369	3.409	6.777	13.574
<b>Relative bias (%)</b>	19.30	9.39	1.21	0.59	0.74
<b>Recovery (%)</b>	119.29	109.38	101.19	100.59	100.74
<b>Repeatability standard deviation</b>	0.019	0.030	0.058	0.062	0.051
<b>Intermediate precision standard deviation</b>	0.047	0.040	0.124	0.282	0.122
<b>Repeatability RSD (%)</b>	5.64	4.45	1.72	0.92	0.38
<b>Intermediate precision RSD (%)</b>	13.82	5.90	3.68	4.19	0.90
<b>Relative tolerance interval at 95% (%)</b>	42.42	14.98	11.24	10.76	2.78
<b>Lower relative <math>\beta</math> tolerance limit (%)</b>	-23.13	-5.59	-10.04	-10.17	-2.04
<b>Upper relative <math>\beta</math> tolerance limit (%)</b>	61.72	24.36	12.45	11.35	3.51
<b>LOD (%)</b>	0.05 <sup>a</sup>				
<b>LOQ (%)</b>	0.28 <sup>b</sup>				
<b>Linearity</b> (m = 5; n = 3; p = 4)					
<b>Slope</b>	1.0025				
<b>y-intercept</b>	0.0494				
<b>r<sup>2</sup></b>	0.999				

m, number of concentration levels; n, number of replicates per concentration levels per series and p, number of series of experiments.

<sup>a</sup> = Based on signal-to-noise.

<sup>b</sup> = Estimated from accuracy profile.

**Table C.14:** Validation results for PN at impurity level using the  $L_0$  response function to back-calculate IVS amounts

<b>Validation criteria</b> (n = 3; p = 4)	<b>Level 1</b>	<b>Level 2</b>	<b>Level 3</b>	<b>Level 4</b>	<b>Level 5</b>
<b>Level (%)</b>	0.05	0.10	0.50	1.00	2.00
<b>Mean introduced concentration (mg.L<sup>-1</sup>)</b>	0.3369	0.6737	3.369	6.737	13.474
<b>Mean predicted concentration (mg.L<sup>-1</sup>)</b>	0.3543	0.6905	3.373	6.751	13.575
<b>Relative bias (%)</b>	5.17	2.48	0.14	0.21	0.75
<b>Recovery (%)</b>	105.16	102.49	100.12	100.21	100.75
<b>Repeatability standard deviation</b>	0.019	0.031	0.059	0.063	0.050
<b>Intermediate precision standard deviation</b>	0.026	0.043	0.124	0.264	0.180
<b>Repeatability RSD (%)</b>	5.64	4.60	1.75	0.94	0.37
<b>Intermediate precision RSD (%)</b>	7.84	6.44	3.68	3.92	1.33
<b>Relative tolerance interval at 95% (%)</b>	20.72	17.04	11.25	10.06	4.74
<b>Lower relative <math>\beta</math> tolerance limit (%)</b>	-15.55	-14.55	-11.11	-9.85	-3.99
<b>Upper relative <math>\beta</math> tolerance limit (%)</b>	25.88	19.52	11.38	10.26	5.49
<b>LOD (%)</b>	0.05 <sup>a</sup>				
<b>LOQ (%)</b>	0.10 <sup>b</sup>				
<b>Linearity</b> (m = 5; n = 3; p = 4)					
<b>Slope</b>	1.0062				
<b>y-intercept</b>	0.0003				
<b>r<sup>2</sup></b>	0.999				

m, number of concentration levels; n, number of replicates per concentration levels per series and p, number of series of experiments.

<sup>a</sup> = Based on signal-to-noise.

<sup>b</sup> = Estimated from accuracy profile.

**Table C.15:** Validation results for HC at impurity level using the L response function to back-calculate IVS amounts

<b>Validation criteria</b> (n = 3; p = 4)	<b>Level 1</b>	<b>Level 2</b>	<b>Level 3</b>	<b>Level 4</b>	<b>Level 5</b>
<b>Level (%)</b>	0.05	0.10	0.50	1.00	2.00
<b>Mean introduced concentration (mg.L<sup>-1</sup>)</b>	0.3453	0.6906	3.453	6.906	13.812
<b>Mean predicted concentration (mg.L<sup>-1</sup>)</b>	0.4097	0.7576	3.536	6.870	13.880
<b>Relative bias (%)</b>	18.66	9.70	2.41	-0.52	0.49
<b>Recovery (%)</b>	118.65	109.69	102.40	99.48	100.49
<b>Repeatability standard deviation</b>	0.023	0.045	0.091	0.075	0.101
<b>Intermediate precision standard deviation</b>	0.050	0.086	0.157	0.075	0.158
<b>Repeatability RSD (%)</b>	6.66	6.51	2.64	1.08	0.73
<b>Intermediate precision RSD (%)</b>	14.39	12.43	4.55	1.08	1.14
<b>Relative tolerance interval at 95% (%)</b>	44.05	37.85	12.79	2.48	3.19
<b>Lower relative <math>\beta</math> tolerance limit (%)</b>	-25.39	-28.15	-10.39	-3.00	-2.70
<b>Upper relative <math>\beta</math> tolerance limit (%)</b>	62.71	47.56	15.20	1.96	3.68
<b>LOD (%)</b>	0.05 <sup>a</sup>				
<b>LOQ (%)</b>	0.52 <sup>b</sup>				
<b>Linearity</b> (m = 5; n = 3; p = 4)					
<b>Slope</b>	0.9984				
<b>y-intercept</b>	0.0574				
<b>r<sup>2</sup></b>	0.999				

m, number of concentration levels; n, number of replicates per concentration levels per series and p, number of series of experiments.

<sup>a</sup> = Based on signal-to-noise.

<sup>b</sup> = Estimated from accuracy profile.

**Table C.16:** Validation results for HC at impurity level using the  $L_0$  response function to back-calculate IVS amounts

<b>Validation criteria</b> (n = 3; p = 4)	<b>Level 1</b>	<b>Level 2</b>	<b>Level 3</b>	<b>Level 4</b>	<b>Level 5</b>
<b>Level (%)</b>	0.05	0.10	0.50	1.00	2.00
<b>Mean introduced concentration (mg.L<sup>-1</sup>)</b>	0.3453	0.6906	3.453	6.906	13.812
<b>Mean predicted concentration (mg.L<sup>-1</sup>)</b>	0.3471	0.6972	3.492	6.846	13.897
<b>Relative bias (%)</b>	0.52	0.95	1.13	-0.88	0.61
<b>Recovery (%)</b>	100.52	100.96	101.13	99.13	100.62
<b>Repeatability standard deviation</b>	0.023	0.043	0.092	0.070	0.102
<b>Intermediate precision standard deviation</b>	0.035	0.043	0.134	0.070	0.168
<b>Repeatability RSD (%)</b>	6.60	6.30	2.66	1.02	0.74
<b>Intermediate precision RSD (%)</b>	10.12	6.30	3.88	1.02	1.21
<b>Relative tolerance interval at 95% (%)</b>	26.90	14.43	10.29	2.33	3.40
<b>Lower relative <math>\beta</math> tolerance limit (%)</b>	-26.38	-13.47	-9.15	-3.20	-2.79
<b>Upper relative <math>\beta</math> tolerance limit (%)</b>	27.42	15.38	11.42	1.45	4.01
<b>LOD (%)</b>	0.05 <sup>a</sup>				
<b>LOQ (%)</b>	0.08 <sup>b</sup>				
<b>Linearity</b> (m = 5; n = 3; p = 4)					
<b>Slope</b>	1.0043				
<b>y-intercept</b>	0.0072				
<b>r<sup>2</sup></b>	0.999				

m, number of concentration levels; n, number of replicates per concentration levels per series and p, number of series of experiments.

<sup>a</sup> = Based on signal-to-noise.

<sup>b</sup> = Estimated from accuracy profile.

**Table C.17:** Validation results for P at impurity level using the L response function to back-calculate IVS amounts

<b>Validation criteria</b> (n = 3; p = 4)	<b>Level 1</b>	<b>Level 2</b>	<b>Level 3</b>	<b>Level 4</b>	<b>Level 5</b>
<b>Level (%)</b>	0.05	0.10	0.50	1.00	2.00
<b>Mean introduced concentration (mg.L<sup>-1</sup>)</b>	0.2997	0.5993	2.997	5.993	11.986
<b>Mean predicted concentration (mg.L<sup>-1</sup>)</b>	0.3536	0.6419	3.043	6.022	12.141
<b>Relative bias (%)</b>	18.01	7.10	1.55	0.48	1.29
<b>Recovery (%)</b>	117.98	107.11	101.53	100.48	101.29
<b>Repeatability standard deviation</b>	0.011	0.022	0.100	0.071	0.062
<b>Intermediate precision standard deviation</b>	0.053	0.071	0.135	0.152	0.190
<b>Repeatability RSD (%)</b>	3.67	3.67	3.34	1.18	0.52
<b>Intermediate precision RSD (%)</b>	17.82	11.87	4.50	2.54	1.58
<b>Relative tolerance interval at 95% (%)</b>	63.20	41.97	11.45	6.22	5.59
<b>Lower relative <math>\beta</math> tolerance limit (%)</b>	-45.19	-34.87	-9.90	-5.75	-4.30
<b>Upper relative <math>\beta</math> tolerance limit (%)</b>	81.21	49.07	13.00	6.70	6.88
<b>LOD (%)</b>	0.05 <sup>a</sup>				
<b>LOQ (%)</b>	0.43 <sup>b</sup>				
<b>Linearity</b> (m = 5; n = 3; p = 4)					
<b>Slope</b>	1.0083				
<b>y-intercept</b>	0.0287				
<b>r<sup>2</sup></b>	0.999				

m, number of concentration levels; n, number of replicates per concentration levels per series and p, number of series of experiments.

<sup>a</sup> = Based on signal-to-noise.

<sup>b</sup> = Estimated from accuracy profile.

**Table C.18:** Validation results for P at impurity level using the  $L_0$  response function to back-calculate IVS amounts

<b>Validation criteria</b> (n = 3; p = 4)	<b>Level 1</b>	<b>Level 2</b>	<b>Level 3</b>	<b>Level 4</b>	<b>Level 5</b>
<b>Level (%)</b>	0.05	0.10	0.50	1.00	2.00
<b>Mean introduced concentration (mg.L<sup>-1</sup>)</b>	0.2997	0.5993	2.997	5.993	11.986
<b>Mean predicted concentration (mg.L<sup>-1</sup>)</b>	0.3082	0.5976	3.008	5.997	12.140
<b>Relative bias (%)</b>	2.86	-0.29	0.37	0.06	1.28
<b>Recovery (%)</b>	102.84	99.72	100.37	100.07	101.28
<b>Repeatability standard deviation</b>	0.012	0.022	0.101	0.072	0.063
<b>Intermediate precision standard deviation</b>	0.021	0.045	0.122	0.146	0.236
<b>Repeatability RSD (%)</b>	4.00	3.67	3.37	1.20	0.53
<b>Intermediate precision RSD (%)</b>	6.85	7.59	4.06	2.44	1.97
<b>Relative tolerance interval at 95% (%)</b>	19.28	23.19	9.97	7.46	6.97
<b>Lower relative <math>\beta</math> tolerance limit (%)</b>	-16.42	-23.48	-9.60	-7.40	-5.69
<b>Upper relative <math>\beta</math> tolerance limit (%)</b>	22.15	22.90	10.34	7.51	8.26
<b>LOD (%)</b>	0.05 <sup>a</sup>				
<b>LOQ (%)</b>	0.20 <sup>b</sup>				
<b>Linearity</b> (m = 5; n = 3; p = 4)					
<b>Slope</b>	1.0122				
<b>y-intercept</b>	0.0181				
<b>r<sup>2</sup></b>	0.999				

m, number of concentration levels; n, number of replicates per concentration levels per series and p, number of series of experiments.

<sup>a</sup> = Based on signal-to-noise.

<sup>b</sup> = Estimated from accuracy profile.

**Table C.19:** Validation results for 20(R) at impurity level using the L response function to back-calculate IVS amounts

<b>Validation criteria</b> (n = 3; p = 4)	<b>Level 1</b>	<b>Level 2</b>	<b>Level 3</b>	<b>Level 4</b>	<b>Level 5</b>
<b>Level (%)</b>	0.05	0.10	0.50	1.00	2.00
<b>Mean introduced concentration (mg.L<sup>-1</sup>)</b>	0.2942	0.5884	2.942	5.884	11.769
<b>Mean predicted concentration (mg.L<sup>-1</sup>)</b>	0.3350	0.6213	2.963	5.892	11.779
<b>Relative bias (%)</b>	13.86	5.58	0.71	0.12	0.08
<b>Recovery (%)</b>	113.87	105.59	100.71	100.14	100.08
<b>Repeatability standard deviation</b>	0.017	0.010	0.089	0.082	0.065
<b>Intermediate precision standard deviation</b>	0.051	0.053	0.123	0.129	0.101
<b>Repeatability RSD (%)</b>	5.78	1.73	2.80	1.39	0.55
<b>Intermediate precision RSD (%)</b>	17.48	9.03	4.17	2.19	0.86
<b>Relative tolerance interval at 95% (%)</b>	61.71	32.06	11.00	6.12	2.41
<b>Lower relative <math>\beta</math> tolerance limit (%)</b>	-47.85	-26.48	-10.29	-6.00	-2.32
<b>Upper relative <math>\beta</math> tolerance limit (%)</b>	75.57	37.63	11.71	6.24	2.49
<b>LOD (%)</b>	0.05 <sup>a</sup>				
<b>LOQ (%)</b>	0.37 <sup>b</sup>				
<b>Linearity</b> (m = 5; n = 3; p = 4)					
<b>Slope</b>	0.9975				
<b>y-intercept</b>	0.0332				
<b>r<sup>2</sup></b>	0.999				

m, number of concentration levels; n, number of replicates per concentration levels per series and p, number of series of experiments.

<sup>a</sup> = Based on signal-to-noise.

<sup>b</sup> = Estimated from accuracy profile.

**Table C.20:** Validation results for 20(R) at impurity level using the L<sub>0</sub> response function to back-calculate IVS amounts

<b>Validation criteria</b> (n = 3; p = 4)	<b>Level 1</b>	<b>Level 2</b>	<b>Level 3</b>	<b>Level 4</b>	<b>Level 5</b>
<b>Level (%)</b>	0.05	0.10	0.50	1.00	2.00
<b>Mean introduced concentration (mg.L<sup>-1</sup>)</b>	0.2942	0.5884	2.942	5.884	11.769
<b>Mean predicted concentration (mg.L<sup>-1</sup>)</b>	0.2973	0.5852	2.941	5.886	11.808
<b>Relative bias (%)</b>	1.04	-0.55	-0.04	0.02	0.34
<b>Recovery (%)</b>	101.05	99.46	99.97	100.03	100.33
<b>Repeatability standard deviation</b>	0.017	0.010	0.090	0.082	0.065
<b>Intermediate precision standard deviation</b>	0.020	0.032	0.108	0.134	0.115
<b>Repeatability RSD (%)</b>	5.78	1.70	3.06	1.39	0.55
<b>Intermediate precision RSD (%)</b>	6.88	5.45	3.69	2.28	0.98
<b>Relative tolerance interval at 95% (%)</b>	16.87	19.25	9.06	6.40	2.75
<b>Lower relative <math>\beta</math> tolerance limit (%)</b>	-15.83	-19.80	-9.10	-6.37	-2.41
<b>Upper relative <math>\beta</math> tolerance limit (%)</b>	17.91	18.70	9.02	6.42	3.08
<b>LOD (%)</b>	0.05 <sup>a</sup>				
<b>LOQ (%)</b>	0.05 <sup>b</sup>				
<b>Linearity</b> (m = 5; n = 3; p = 4)					
<b>Slope</b>	1.0033				
<b>y-intercept</b>	0.0064				
<b>r<sup>2</sup></b>	0.999				

m, number of concentration levels; n, number of replicates per concentration levels per series and p, number of series of experiments.

<sup>a</sup> = Based on signal-to-noise.

<sup>b</sup> = Estimated from accuracy profile.

**Table C.21:** Validation results for 20(S) at impurity level using the L response function to back-calculate IVS amounts

<b>Validation criteria</b> (n = 3; p = 4)	<b>Level 1</b>	<b>Level 2</b>	<b>Level 3</b>	<b>Level 4</b>	<b>Level 5</b>
<b>Level (%)</b>	0.05	0.10	0.50	1.00	2.00
<b>Mean introduced concentration (mg.L<sup>-1</sup>)</b>	0.2882	0.5763	2.882	5.763	11.526
<b>Mean predicted concentration (mg.L<sup>-1</sup>)</b>	0.3352	0.6083	2.931	5.799	11.549
<b>Relative bias (%)</b>	16.32	5.55	1.72	0.62	0.20
<b>Recovery (%)</b>	116.31	105.55	101.70	100.62	100.20
<b>Repeatability standard deviation</b>	0.018	0.013	0.092	0.072	0.063
<b>Intermediate precision standard deviation</b>	0.048	0.058	0.104	0.089	0.066
<b>Repeatability RSD (%)</b>	6.28	2.26	3.19	1.25	0.55
<b>Intermediate precision RSD (%)</b>	16.81	10.08	3.62	1.54	0.58
<b>Relative tolerance interval at 95% (%)</b>	51.68	36.75	8.67	3.81	1.34
<b>Lower relative <math>\beta</math> tolerance limit (%)</b>	-35.36	-30.19	-6.95	-3.19	-1.15
<b>Upper relative <math>\beta</math> tolerance limit (%)</b>	67.99	41.30	10.40	4.42	1.54
<b>LOD (%)</b>	0.05 <sup>a</sup>				
<b>LOQ (%)</b>	0.37 <sup>b</sup>				
<b>Linearity</b> (m = 5; n = 3; p = 4)					
<b>Slope</b>	0.9983				
<b>y-intercept</b>	0.0445				
<b>r<sup>2</sup></b>	0.999				

m, number of concentration levels; n, number of replicates per concentration levels per series and p, number of series of experiments.

<sup>a</sup> = Based on signal-to-noise.

<sup>b</sup> = Estimated from accuracy profile.

**Table C.22:** Validation results for 20(S) at impurity level using the  $L_0$  response function to back-calculate IVS amounts

<b>Validation criteria</b> (n = 3; p = 4)	<b>Level 1</b>	<b>Level 2</b>	<b>Level 3</b>	<b>Level 4</b>	<b>Level 5</b>
<b>Level (%)</b>	0.05	0.10	0.50	1.00	2.00
<b>Mean introduced concentration (mg.L<sup>-1</sup>)</b>	0.2882	0.5763	2.882	5.763	11.526
<b>Mean predicted concentration (mg.L<sup>-1</sup>)</b>	0.2984	0.5726	2.905	5.784	11.558
<b>Relative bias (%)</b>	3.54	-0.65	0.82	0.36	0.28
<b>Recovery (%)</b>	103.54	99.36	100.80	100.36	100.28
<b>Repeatability standard deviation</b>	0.018	0.013	0.092	0.072	0.063
<b>Intermediate precision standard deviation</b>	0.023	0.042	0.096	0.082	0.111
<b>Repeatability RSD (%)</b>	6.25	2.26	3.19	1.25	0.55
<b>Intermediate precision RSD (%)</b>	8.05	7.36	3.34	1.41	0.96
<b>Relative tolerance interval at 95% (%)</b>	20.39	26.00	7.79	3.39	2.70
<b>Lower relative <math>\beta</math> tolerance limit (%)</b>	-16.84	-26.65	-6.97	-3.03	-2.42
<b>Upper relative <math>\beta</math> tolerance limit (%)</b>	23.93	25.35	8.61	3.75	2.97
<b>LOD (%)</b>	0.05 <sup>a</sup>				
<b>LOQ (%)</b>	0.22 <sup>b</sup>				
<b>Linearity</b> (m = 5; n = 3; p = 4)					
<b>Slope</b>	1.0024				
<b>y-intercept</b>	0.0064				
<b>r<sup>2</sup></b>	0.999				

m, number of concentration levels; n, number of replicates per concentration levels per series and p, number of series of experiments.

<sup>a</sup> = Based on signal-to-noise.

<sup>b</sup> = Estimated from accuracy profile.

## Appendix D

### Accuracy profiles for UPSFC method

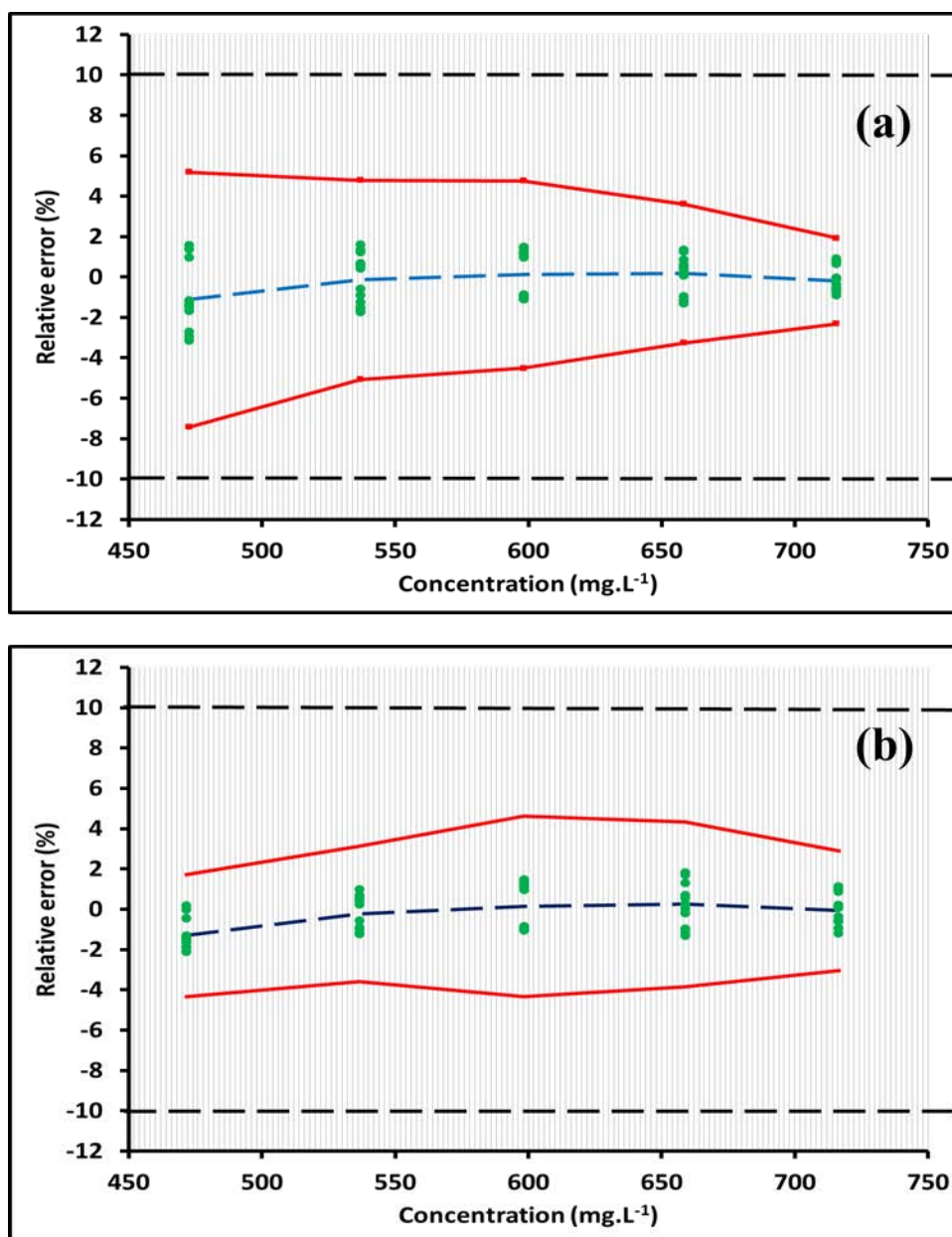


**Figure D.1:** PAC accuracy profile of the UPSFC method results when the simple L model (a) and the  $L_0$  model (b) is chosen as response function. The values of  $\beta$ -expectation tolerance limits (red lines) are set to 95%. The black dashed lines indicate the acceptance limits set at  $\pm 10\%$ . The blue dashed line is the mean relative bias of the procedure. The green dots are the individual relative bias at each concentration level. Chromatographic conditions as per Figure 4.14.

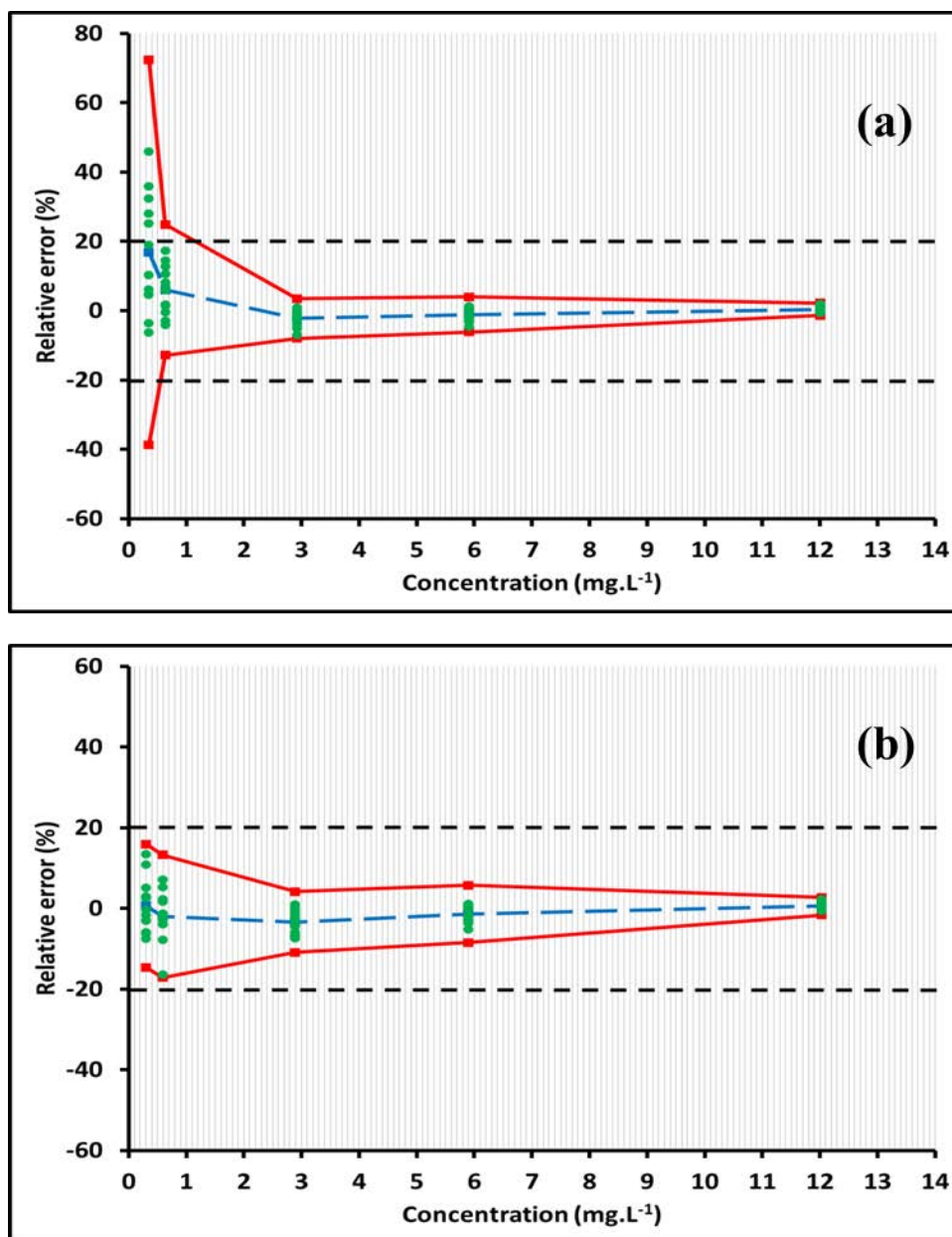


**Figure D.2:** Impurity level PAC accuracy profile of the UPSFC method results when the simple L model (a) and the  $L_0$  model (b) is chosen as response function. The values of  $\beta$ -expectation tolerance limits (red lines) are set to 95%. The black dashed lines indicate the acceptance limits set at  $\pm 20\%$ . The blue dashed line is the mean relative bias of the procedure. The green dots are the individual relative bias at each concentration level. The intersection between the  $\beta$ -expectation tolerance limits and the acceptance limits defines the LOQ. For (a) the LOQ is  $1.0 \text{ mg.L}^{-1}$  equivalent to  $0.17\%$ . For (b), there is no intersection, therefore the LOQ is  $0.2989 \text{ mg.L}^{-1}$  equivalent to  $0.05\%$ . Chromatographic conditions as per Figure 4.14.

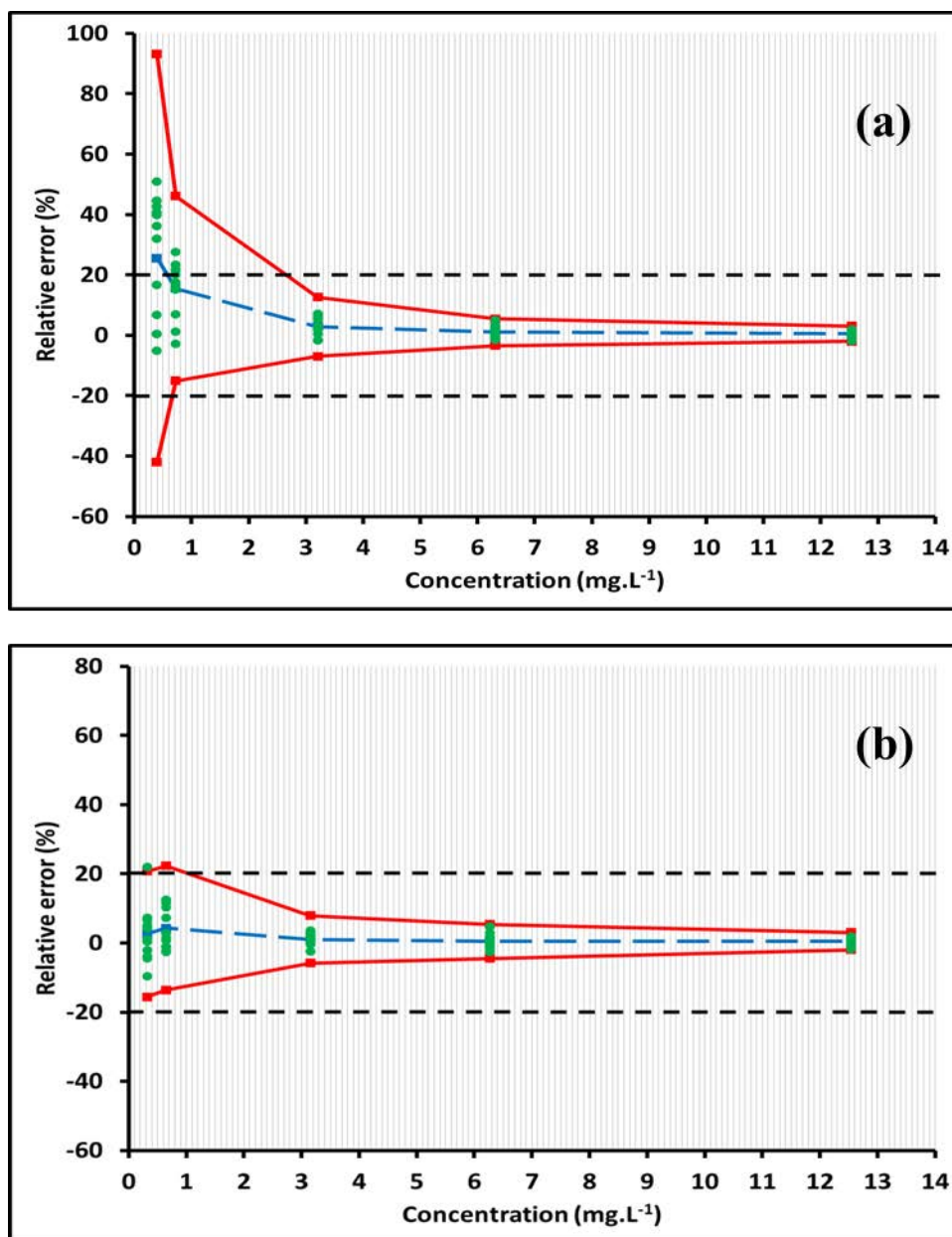


**Figure D.3:** *P-11,21D* accuracy profile of the UPSFC method results when the simple  $L$  model (a) and the  $L_0$  model (b) is chosen as response function.  $\beta$ -expectation tolerance limits, acceptance limits and plot components as per Figure D.2. The intersection between the  $\beta$ -expectation tolerance limits and the acceptance limits defines the LOQ. For (a), the LOQ is  $2.6 \text{ mg.L}^{-1}$  equivalent to  $0.43\%$ . For (b), the LOQ is  $0.9 \text{ mg.L}^{-1}$  equivalent to  $0.15\%$ . Chromatographic conditions as per Figure 4.14.

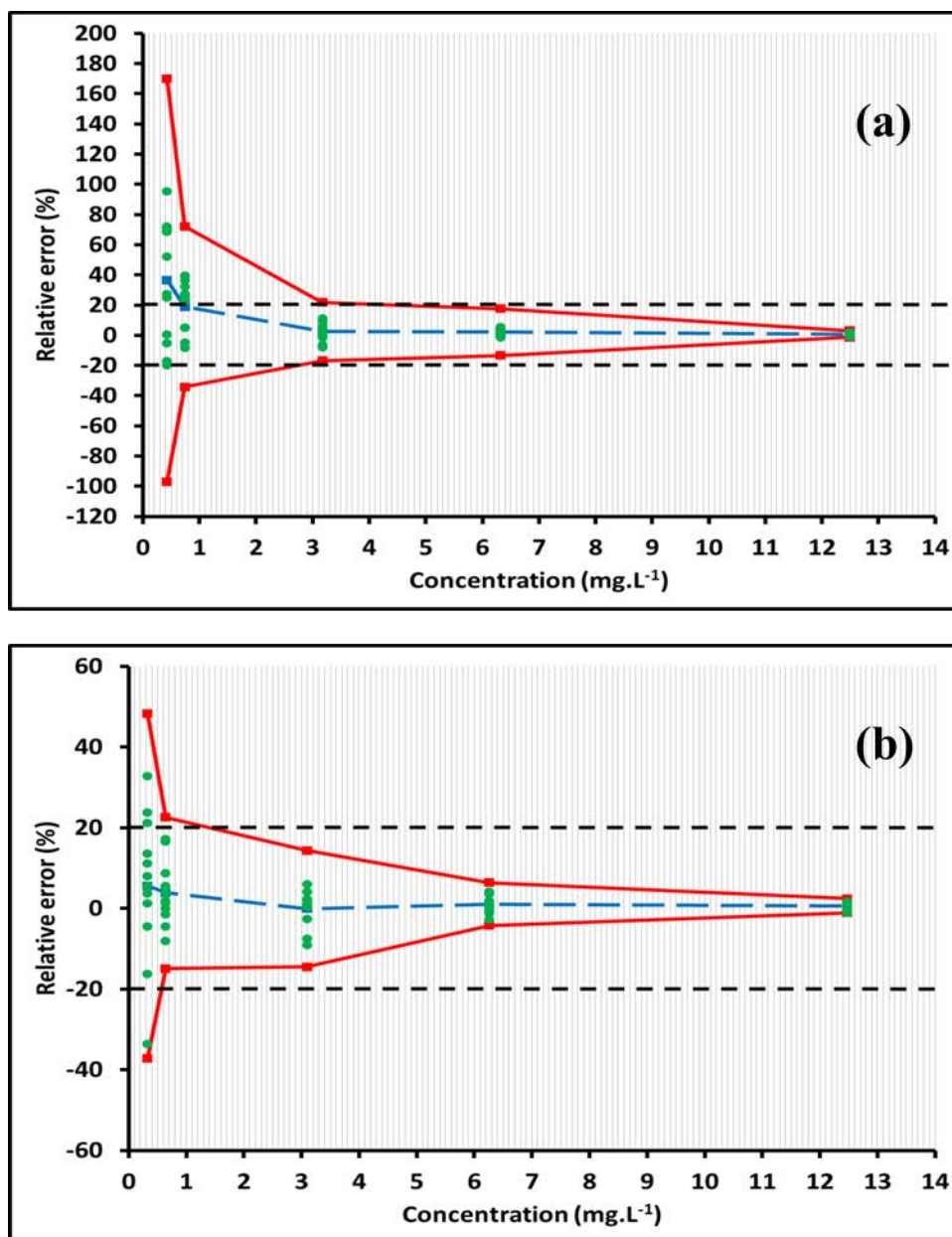


**Figure D.4:** HCA accuracy profile of the UPSFC method results when the simple L model (a) and the  $L_0$  model (b) is chosen as response function.  $\beta$ -expectation tolerance limits, acceptance limits and plot components as per Figure D.2. The intersection between the  $\beta$ -expectation tolerance limits and the acceptance limits defines the LOQ. For (a), the LOQ is  $3.7 \text{ mg.L}^{-1}$  equivalent to 0.62%. For (b), the LOQ is  $1.2 \text{ mg.L}^{-1}$  equivalent to 0.20%. Chromatographic conditions as per Figure 4.14.

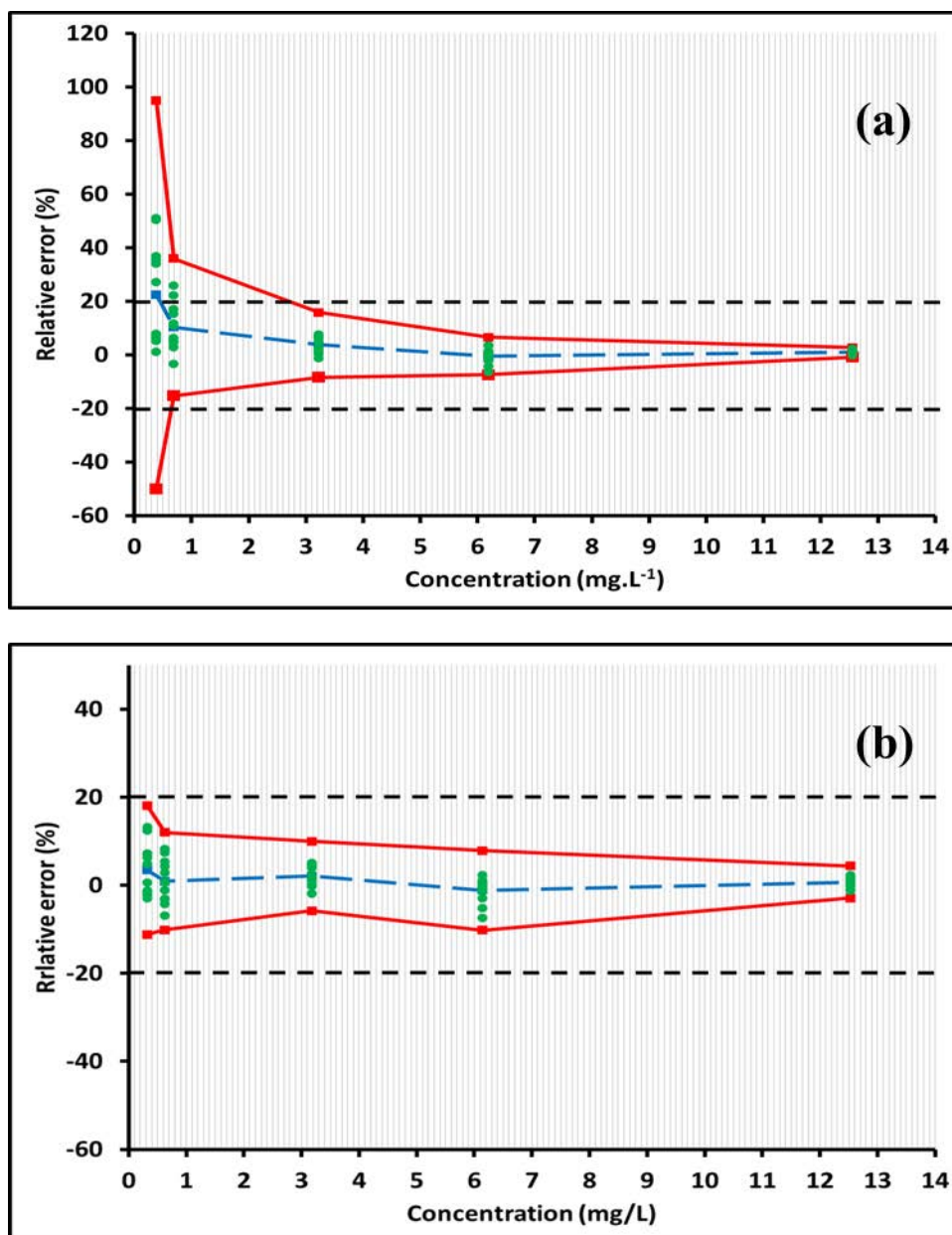


**Figure D.5:** *P-17A* accuracy profile of the UPSFC method results when the simple  $L$  model (a) and the  $L_0$  model (b) is chosen as response function.  $\beta$ -expectation tolerance limits, acceptance limits and plot components as per Figure D.2. The intersection between the  $\beta$ -expectation tolerance limits and the acceptance limits defines the LOQ. For (a), the LOQ is  $2.7 \text{ mg.L}^{-1}$  equivalent to 0.45%. For (b), there is no intersection; therefore the LOQ is  $0.310 \text{ mg.L}^{-1}$  equivalent to 0.05%. Chromatographic conditions as per Figure 4.14.

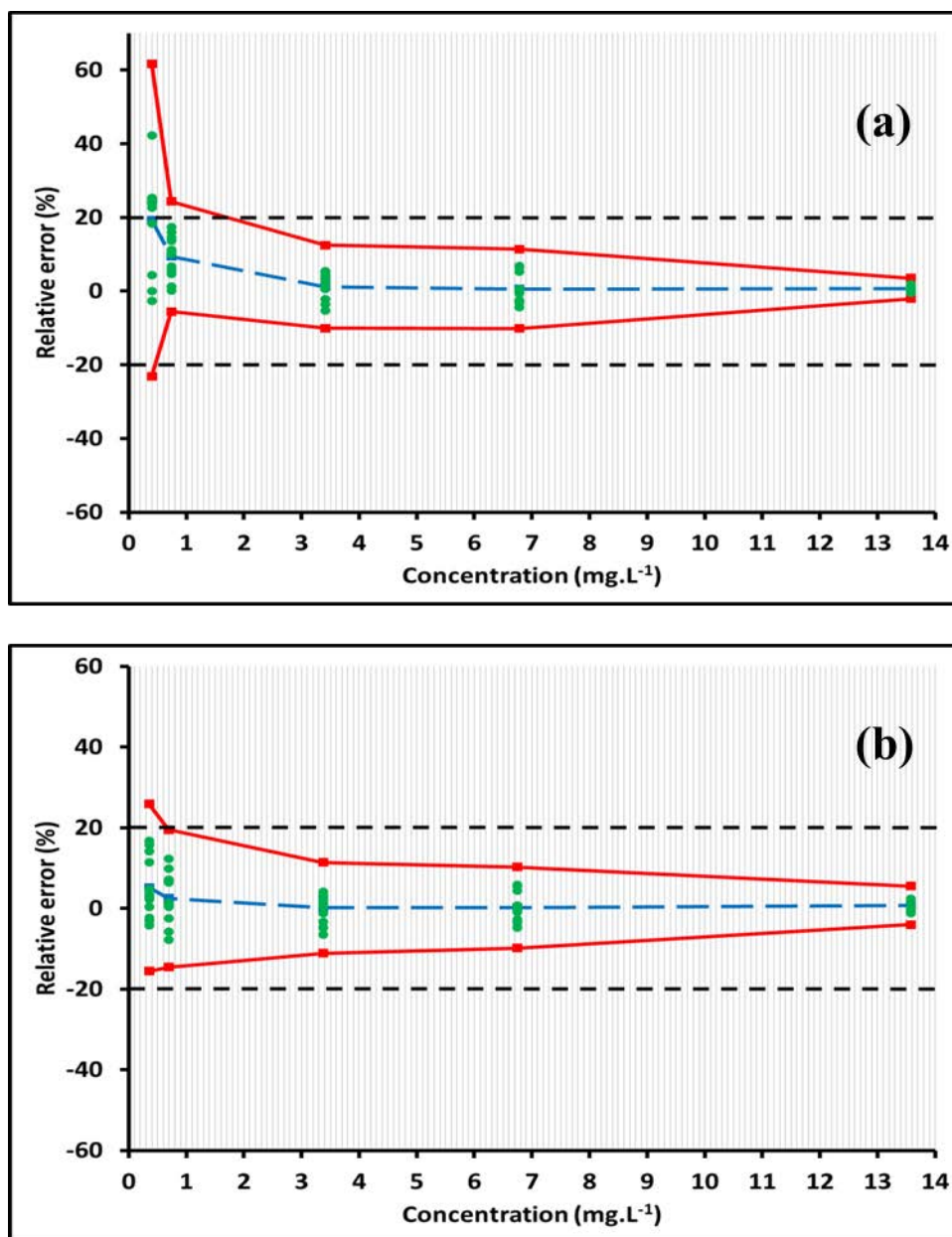


**Figure D.6:** PN accuracy profile of the UPSFC method results when the simple L model (a) and the L<sub>0</sub> model (b) is chosen as response function.  $\beta$ -expectation tolerance limits, acceptance limits and plot components as per Figure D.2. The intersection between the  $\beta$ -expectation tolerance limits and the acceptance limits defines the LOQ. For (a), the LOQ is 1.7 mg.L<sup>-1</sup> equivalent to 0.28%. For (b), the LOQ is 0.60 mg.L<sup>-1</sup> equivalent to 0.10%. Chromatographic conditions as per Figure 4.14.

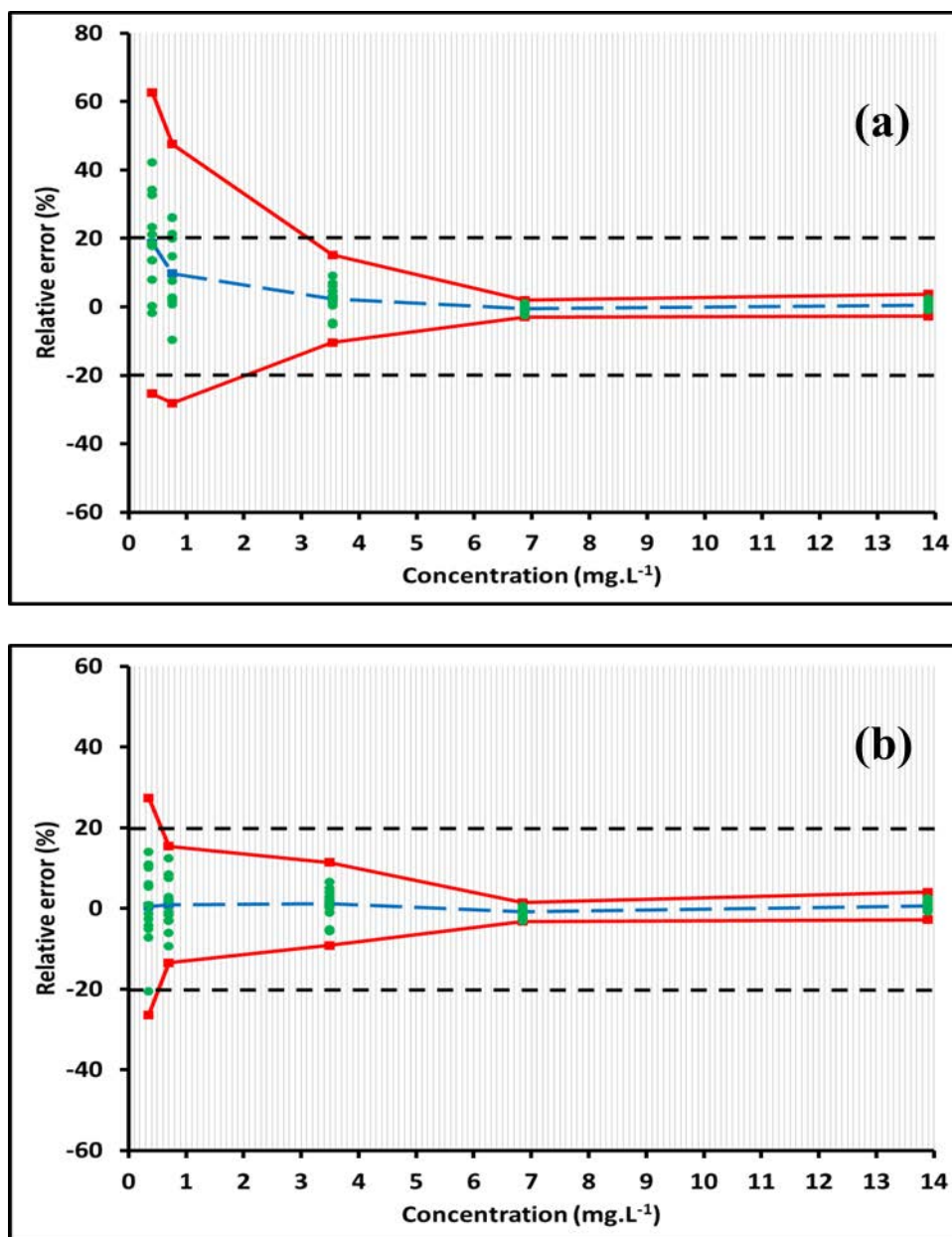


**Figure D.7:** HC accuracy profile of the UPSFC method results when the simple  $L$  model (a) and the  $L_0$  model (b) is chosen as response function.  $\beta$ -expectation tolerance limits, acceptance limits and plot components as per Figure D.2. The intersection between the  $\beta$ -expectation tolerance limits and the acceptance limits defines the LOQ. For (a), the LOQ is  $3.1 \text{ mg.L}^{-1}$  equivalent to  $0.52\%$ . For (b), the LOQ is  $0.50 \text{ mg.L}^{-1}$  equivalent to  $0.08\%$ . Chromatographic conditions as per Figure 4.14.

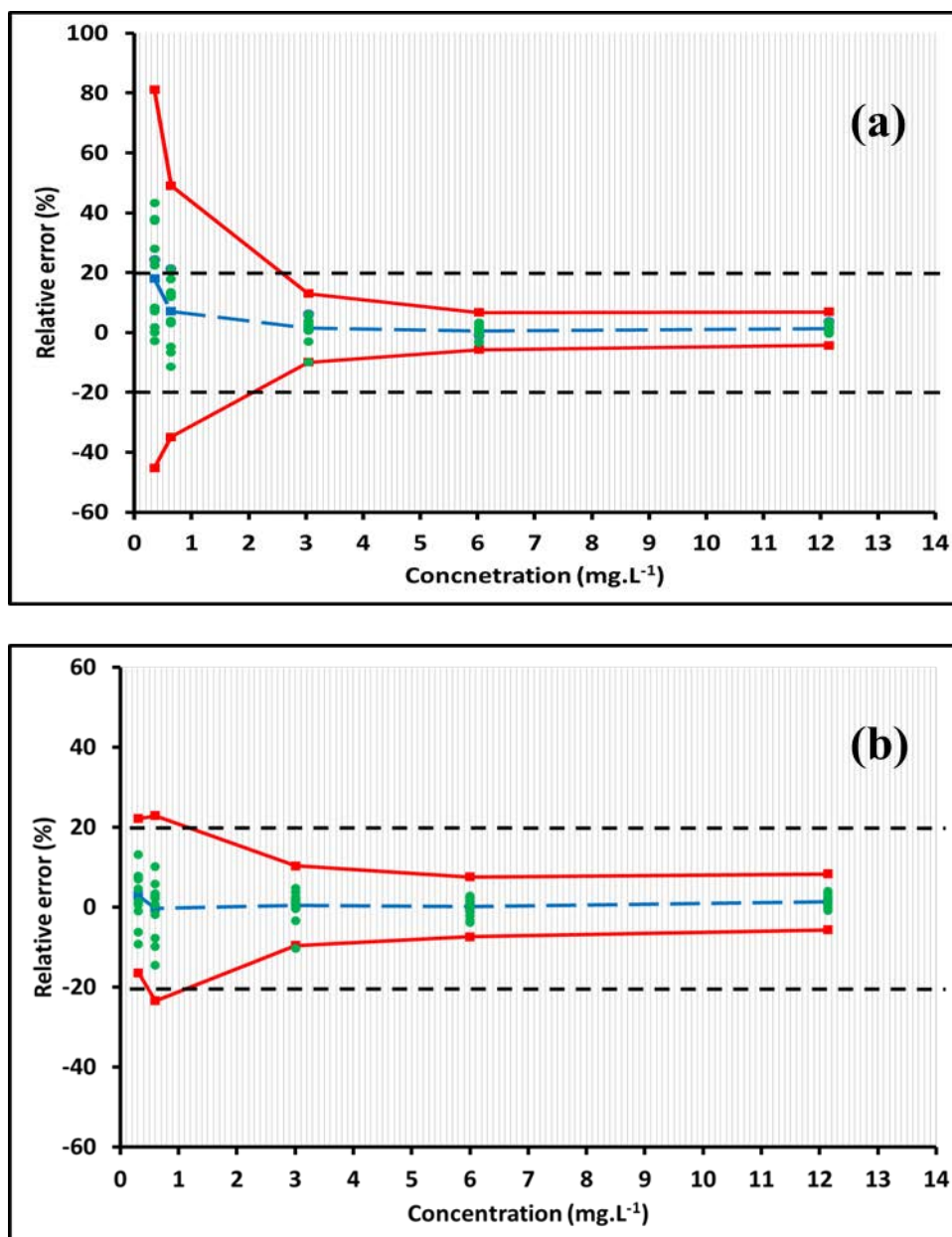


**Figure D.8:** *P* accuracy profile of the UPSFC method results when the simple  $L$  model (a) and the  $L_0$  model (b) is chosen as response function.  $\beta$ -expectation tolerance limits, acceptance limits and plot components as per Figure D.2. The intersection between the  $\beta$ -expectation tolerance limits and the acceptance limits defines the LOQ. For (a), the LOQ is  $2.6 \text{ mg.L}^{-1}$  equivalent to  $0.43\%$ . For (b), the LOQ is  $1.2 \text{ mg.L}^{-1}$  equivalent to  $0.20\%$ . Chromatographic conditions as per Figure 4.14.

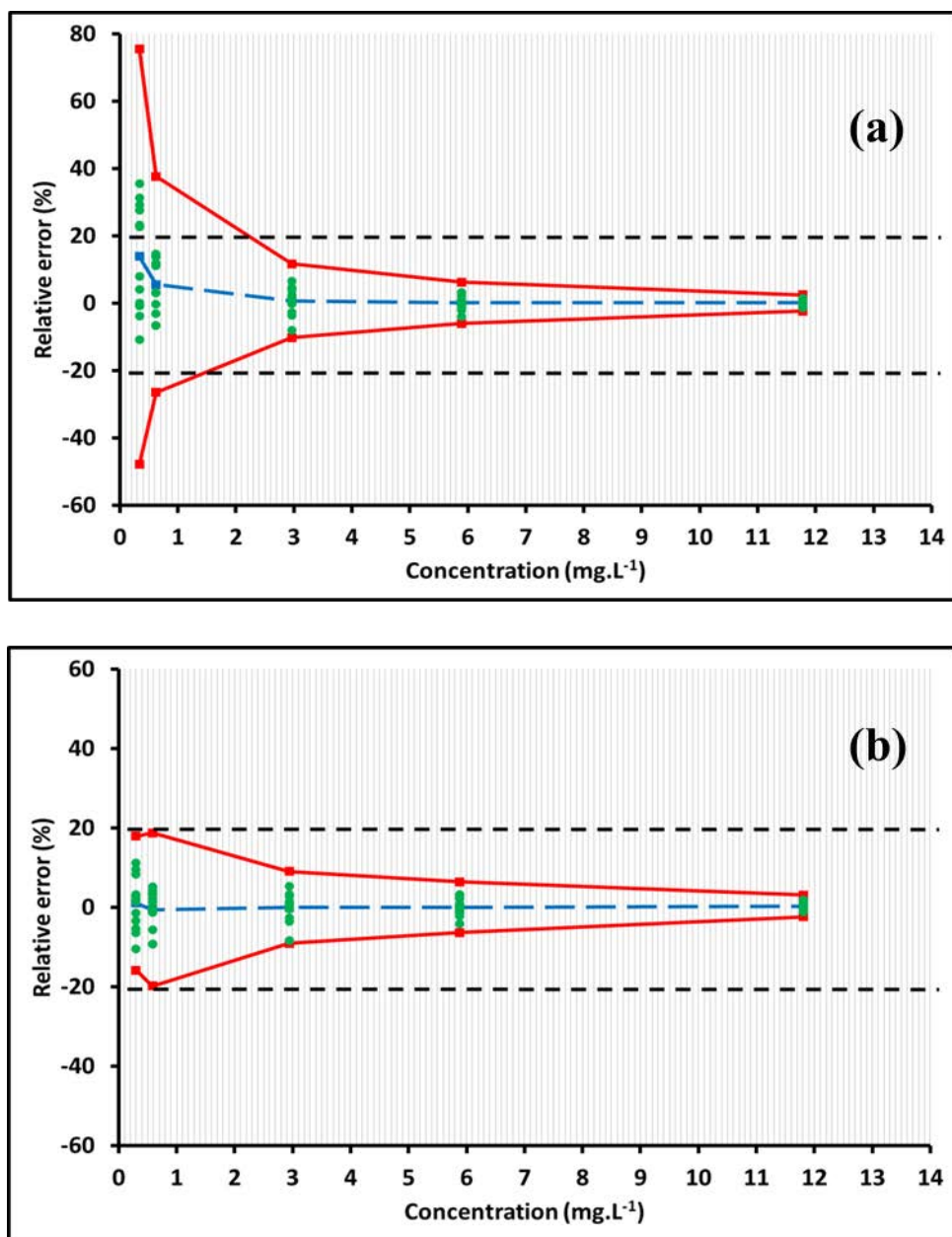


**Figure D.9:**  $20(R)$  accuracy profile of the UPSFC method results when the simple L model (a) and the  $L_0$  model (b) is chosen as response function.  $\beta$ -expectation tolerance limits, acceptance limits and plot components as per Figure D.2. The intersection between the  $\beta$ -expectation tolerance limits and the acceptance limits defines the LOQ. For (a), the LOQ is  $2.2 \text{ mg.L}^{-1}$  equivalent to 0.37%. For (b), there is no intersection; therefore the LOQ is  $0.294 \text{ mg.L}^{-1}$  equivalent to 0.05%. Chromatographic conditions as per Figure 4.14.

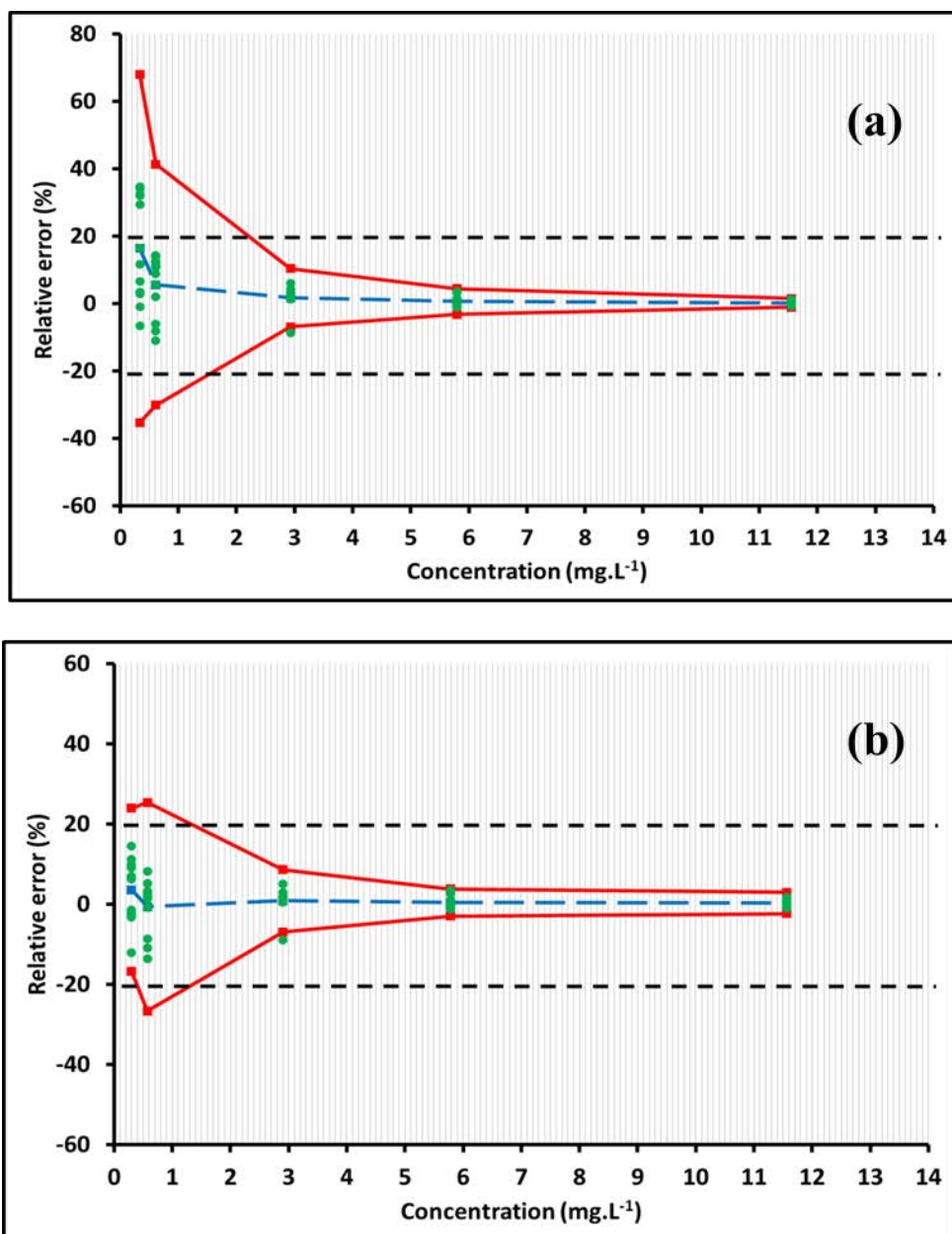


**Figure D.10:** 20(S) accuracy profile of the UPSFC method results when the simple L model (a) and the  $L_0$  model (b) is chosen as response function.  $\beta$ -expectation tolerance limits, acceptance limits and plot components as per Figure D.2. The intersection between the  $\beta$ -expectation tolerance limits and the acceptance limits defines the LOQ. For (a), the LOQ is 2.2 mg.L<sup>-1</sup> equivalent to 0.37%. For (b), the LOQ is 1.3 mg.L<sup>-1</sup> equivalent to 0.22%. Chromatographic conditions as per Figure 4.14.